Radiation Monitoring and Remediation Following
the Fukushima Daiichi Nuclear Power Plant Accident

Cooperation between Fukushima Prefecture and the IAEA

FINAL REPORT (2013 to 2022)

【Fukushima Prefecture Initiative Projects】

(Temporary translation)

March 2023

Fukushima Prefecture

Index

Introduction

The Great East Japan Earthquake occurred on 11 March 2011. It was followed by the accident of Tokyo Electric Power Company's Fukushima Daiichi Nuclear Power Plant[1], leaving a lot of damage to the Fukushima Prefecture. Radioactive materials have been released into the environment which contaminated the land. Due to the contamination of the land and other relevant reasons, more than 160,000 prefectural residents were forced to evacuate. About 29,000 residents have not been able to return home, as of 2022 September, about 11 years after the disaster[2].

In order for Fukushima Prefecture to recover from the severe and unprecedented nuclear disaster and create an environment where the residents can live with peace of mind in the future, the prefecture decided to cooperate with the International Atomic Energy Agency (hereinafter referred to as the "IAEA"), which owns high-level nuclear-related knowledge and world-wide experience. In December 2012, a memorandum for cooperation was signed between the prefecture and the IAEA.

Based on the memorandum, the Practical Arrangements (hereafter referred to as the "PA") relating to the fields of "radiation monitoring" and "decontamination" was signed between the parties on the same day (projects based on this PA are referred to as "FCPs; Fukushima Cooperative Project").

Subsequently in April and October 2013, PA were signed for five projects (hereinafter referred to as "FIPs; Fukushima Initiative Project") as described below in a new framework in which these projects would be supported by the IAEA for three years, and the FIPs started. In April 2016, they signed PAs for revising[3] the scope of cooperation and extending the duration of the FIPs. It continued until December 2017 (hereinafter referred to as "previous Project").

【Scope of cooperation for the previous Project (From April 2013 to December 2017)】

FIP1 Survey of radionuclide movement in river systems
FIP2 Survey of radionuclide movement with wildlife
FIP3 Countermeasures for radioactive materials in rivers and lakes
FIP4 Development of environmental mapping technology using GPS walking surveys
FIP5 Study of the proper treatment of waste containing radioactive materials at municipal solid waste incinerators

The outcomes of the previous Project were summarized in the report on "Cooperation between Fukushima Prefecture and the IAEA – SUMMARY REPORT (2013 to 2017) [Fukushima Prefecture

[1] The owner of the Fukushima Daiichi Nuclear Power Plant was renamed from Tokyo Electric Power Company to Tokyo Electric Power Company Holdings, Incorporated in April 1, 2016.

[2] Steps for Revitalization in Fukushima (ver.31.2; December 27, 2022).
(https://www.pref.fukushima.lg.jp/uploaded/attachment/547379.pdf)

[3] Revision of the scope of cooperation for FIP1~3, 5 and completion of FIP4.

Initiative Projects][4]" in March 2018.

However, remediation of the environment in the Prefecture was halfway and the accomplishment of the proposed projects required further support from the IAEA, the prefecture agreed with the IAEA to extend the PA[5] in December 2017 until December 2022 (hereinafter referred to as "this Project").

【Scope of cooperation for this Project (From January 2018 to December 2022)】

FIP1 Survey, and evaluation of the effect, of radocaesium dynamics in the aquatic systems based on the continuous monitoring
FIP2 Survey of radionuclide movement with wildlife
FIP3 Sustainable countermeasures to radioactive materials in freshwater system
FIP5 Study of proper treatment of waste containing radioactive material

The outcomes of the previous Project and this Project are summarized in this report.

[4] The previous report is available as printed material and also in the following website; (https://www.pref.fukushima.lg.jp/sec/298/iaeasummary2017.html)

[5] Revise the scope of cooperation for FIP1~3, 5.

1. FIP1: Survey, and evaluation of the effect, of radiocaesium dynamics in the aquatic systems based on the continuous monitoring

1.1. Abstract

As a result of the Fukushima Daiichi Nuclear Power Plant accident in March 2011, radioactive materials were released and deposited in the Fukushima Prefecture. It is important to provide information for the safe use of river water in the Prefecture. To investigate the dynamics of radioactive materials in river systems and to estimate the changes in radiocaesium concentrations in rivers over time by the model simulations, studies were conducted in the rivers of the Fukushima Prefecture. Surveys of the dynamics in suspended and dissolved radiocaesium were conducted in the Abukuma River system and in major rivers of the Hamadori area. The results obtained in March 2021 showed that the suspended and dissolved radiocaesium concentrations continue decreasing, even beyond ten years after the accident. In addition, it was shown that the migration of radiocaesium was affected by the presence of dams and decontamination activities in the catchment. Even though the radiocaesium concentrations tends to decrease over time, some suspended sediment samples showing an extremely high concentration were found. The investigation was carried out, and the presence of radiocaesium-bearing microparticles (CsMPs) was confirmed, however their contribution was suggested to be small. Model simulations were also performed to assess changes in the suspended and dissolved forms of radiocaesium under both base- and high-flow conditions. The estimated results showed good agreement with measured values, although some improvements are considered necessary. It was presumed that the load of suspended sediments due to riverbank erosion and resuspension of river sediment under high flow conditions contributed greatly to the increase in suspended radiocaesium transport.

1.2. Purpose

As a result of the accident in the Tokyo Electric Power's Fukushima Daiichi Nuclear Power Plant in March 2011, large amounts of radioactive materials were released into the environment, and their fallout and deposition in Fukushima Prefecture were confirmed. Therefore, it has been important to clarify the actual situation of radioactive materials (especially radiocaesium) in rivers and to provide the necessary information for future predictions and safe use of rivers and river water, considering that they are widely used for drinking water, agriculture, and industry. Radiocaesium in river water is found in suspended (adsorbed on fine particles) and dissolved (dissolved in water) forms. It is assumed that the dynamics in the environment differs depending on the difference in the form. Therefore, it is essential to understand the concentration of radiocaesium in the different forms, in order to comprehensively clarify the dynamics of both forms of radiocaesium in rivers. As there are many forested areas without decontamination in the upper catchment of rivers in Fukushima Prefecture, it is necessary to pay attention to the influences of these on the dynamics of radiocaesium in rivers in the surrounding area. Changes in social conditions (e.g. completion of the decontamination works, return of residents and resumption of farming following the lifting of evacuation orders) and the occurrence of

unexpected events (e.g. forest fires, large-scale floodings due to typhoons, heavy rainfalls, etc.) should be considered.

In this project, a long-term observation survey was conducted on the concentration of radiocaesium in rivers in Fukushima Prefecture, considering its different forms. The state of decline in the concentration of radiocaesium in rivers was assessed. The amount of radiocaesium fluxes in rivers were estimated from the monitoring results. The factors that could contribute to changes in the concentration and amount of flux in radiocaesium (e.g. decontamination works and the presence of CsMPs) were investigated.

In addition, to elucidate the dynamics of radiocaesium through rivers in more detail and be able to predict its future, model simulations reproduce the changes in the radiocaesium concentrations were carried out. And the source of suspended radiocaesium using characteristics of organic matter (total organic carbon and stable isotope composition) in suspended sediment was also estimated.

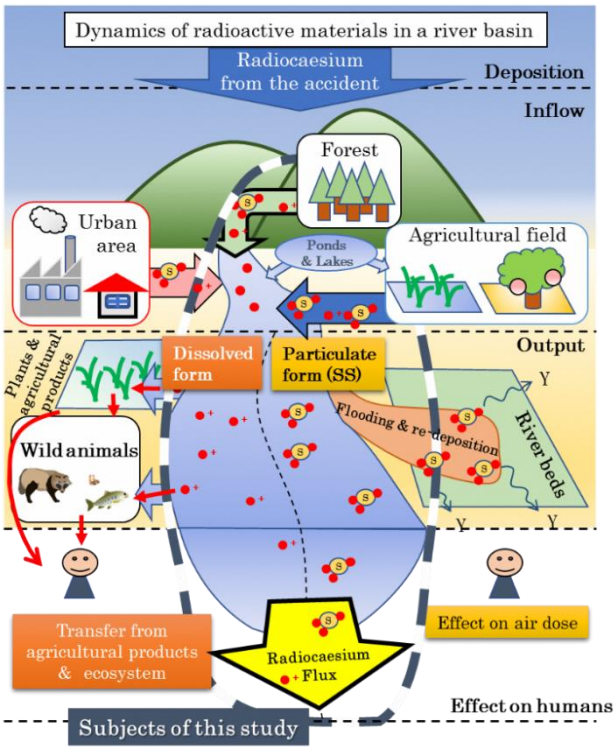

Figure 1. Schematic diagram describing dynamics of radiocaesium in a river basin.

1.3. Content of implementation

Figure 2 shows the monitoring points considered in this project. The background colour of the map indicates the deposition amount of radiocaesium on the ground surface as of July 2, 2011, which is assumed to be the initial deposition in this document. The monitoring points in the Abukuma River and major rivers in Hamadori area for the Wide-area Multipoint Survey are shown in Figure 2(b). The monitoring points in the Kuchibuto River Basin and the Hirose River Basin which are tributaries of the Abukuma River for a single basin survey, are shown in Figure 2(a) and 2(c), respectively.

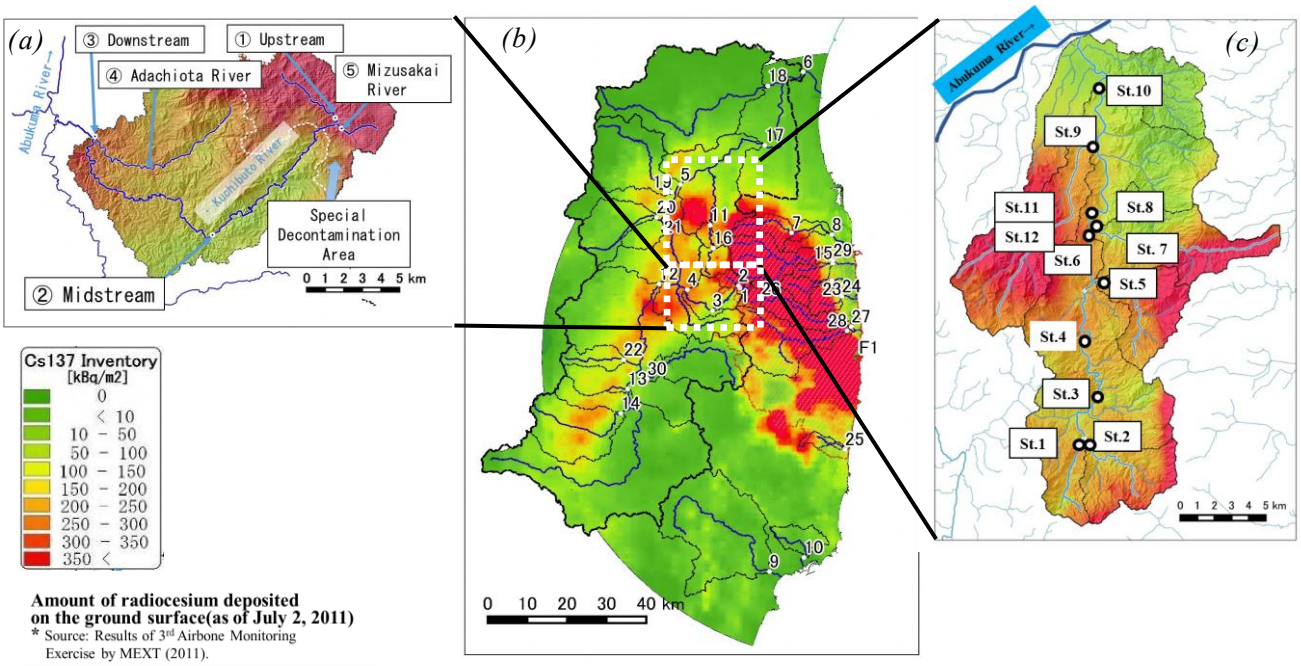

Figure 2. Monitoring points used in this study; (a) Single Basin Survey (Kuchibuto River Basin), (b) Wide-area Multipoint Survey, (c) Single Basin Survey (Hirose River Basin)

1.3.1. Wide-area Multipoint Survey

1.3.1.1. Wide-area Multipoint Survey

1.3.1.1.1. Purpose

From the fiscal year 2015, a Wide-area Multipoint Survey of the Abukuma River Basin and eight water systems in the Hamadori area was performed. Figure 2(b) shows the caesium-137-deposition in the study area and the positions of the monitoring points. Samples were taken regularly - following the same procedure - to explore the time-dependence of the caesium-137 activity concentration and to identify relationships with the basin characteristics. This survey was a continuation of a survey carried out by the University of Tsukuba from fiscal year 2011 to 2014 as a project on behalf of the Ministry of Education, Culture, Sports, Science and Technology and the Nuclear Regulation Authority. The results including the past survey conducted by the University of Tsukuba are also provided.

1.3.1.1.2. Method

At each monitoring point, the monitoring has been continued by installing and operating the equipment (including a suspended sediment (SS) sampler, a turbidity meter, and a water level gauge). The suspended sediments were collected with samplers at intervals of 1 to 3-month, dried in a vacuum freeze-dryer, and caesium-137 concentrations were measured using a germanium semiconductor detector. Turbidity and water level data were obtained at 10-minute intervals, and the concentration of suspended sediment (mg L^{-1}) and the flow rate (m^3 s^{-1}) were calculated applying the equations elaborated in the FIP Summary Report (2013-2017). The flux of suspended

caesium-137 was estimated by multiplying the concentration of suspended sediments, the river flow rate, and the caesium-137 concentrations in the suspended sediments.

To quantify the concentration of suspended and dissolved forms of radiocaesium, 40 to 100 L of river water were collected approximately twice a year. Dissolved and suspended radiocaesium forms were separated using a multi-stage filtration system (Figure 3). The samples were measured with a germanium semiconductor detector, and the suspended and dissolved caesium-137 concentrations in the river water were evaluated.

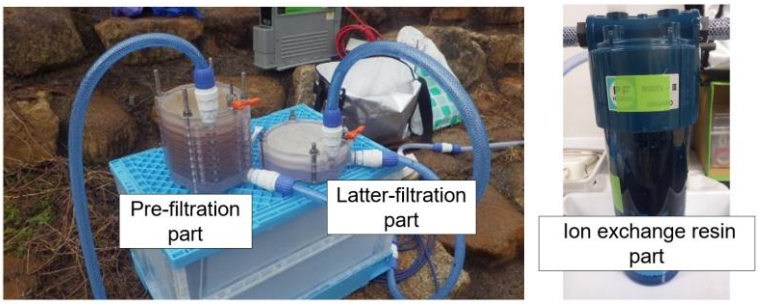

Figure 3. Radiocaesium collecting devices; Multi-stage Filtration System.

1.3.1.2. Survey of radiocaesium-bearing microparticles in suspended sediment samples

1.3.1.2.1. Purpose

In the SS samples collected during the Wide-area Multipoint Surveys, several samples with extremely higher than normal radiocaesium concentrations were found. An example is shown in Figure 4. While the concentration of radiocaesium tends to decrease with time, it is important to clarify the factors that specifically increased the concentration of radiocaesium in SS samples in order to understand the dynamics of radiocaesium transport through rivers.

Previous studies have reported the presence of radiocaesium-bearing microparticles (CsMPs), released during nuclear power plant accident [1), 2), 3)]. In this study, it was hypothesized that this may be due to the inflow of CsMPs into the river and their subsequent mixing with the SS.

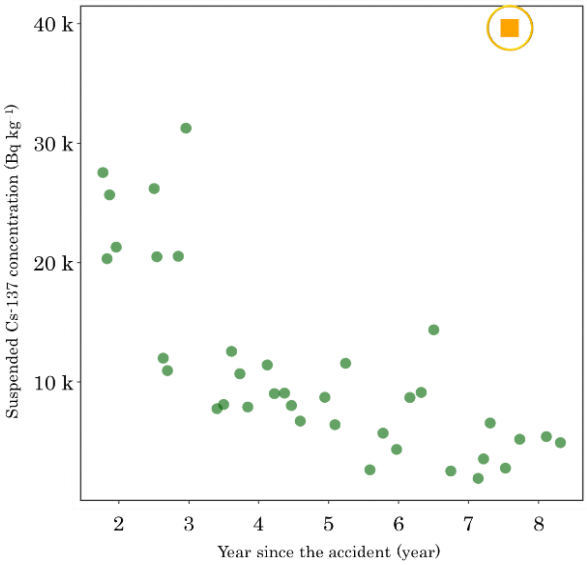

Figure 4. Temporal changes of suspended caesium-137 concentrations at one of the monitoring points of the Wide-area Multipoint Survey in Hamadori area (In the sample collected in October 2018, a higher concentration of caesium-137 was detected, significantly deviating from the trend of gradual decrease in concentration.)

1.3.1.2.2. Method

To clarify the influence of CsMPs on the suspended caesium-137 concentrations, the SS samples collected by the SS sampler that showed much higher radiocaesium concentrations compared to other samples were used. The radioactive particles in SS samples with high caesium-137 concentrations were investigated. The radioactivity of the particles was measured by germanium semiconductor detectors and imaging plate (IP) autoradiographic techniques, and the particle size and elemental analysis of the particles were measured by Scanning Electron Microscopy-energy dispersive X-ray spectroscopy (SEM) and Electron Probe Micro Analyzer (EPMA). In addition, a simple method for determining the presence or absence of CsMPs in the presence of such samples was investigated.

1.3.2. Single basin survey

1.3.2.1. Simulation of radiocaesium dynamics in river by TODAM[1] model

1.3.2.1.1. Purpose

The purpose of this study is to examine the future effects of radioactive caesium migration and redeposition via rivers. In this study, a numerical model was applied for the Hirose River and the Kuchibuto River, tributaries of the Abukuma River, and simulations of the dynamics of radiocaesium were performed. In the areas near the southeast boundary of the Hirose River Basin,

[1] Time-dependent One-dimensional Degradation And Migration Model [4,5], The TODAM model was provided by Prof. Yasuo Onishi, an IAEA specialist, in fiscal year 2015. For this simulation, technical support from Prof. Onishi was received.

a relatively large amount of radiocaesium was deposited (Figure 2(c)). The depositions were also high in the catchments of the tributaries, the Nuno River and the Oguni River (Table 1).

Table 1. Catchment area and initial caesium-137 deposition within the Hirose River Basin.

	River basin area [km^2]	Average Cs-137 deposition [kBq m^{-2}]
Hirose River	267.9	231
Takane River	19.2	270
Nuno River	18.6	343
Ishida River	30.1	290
Oguni River	40.4	343

To simulate the dynamics of radiocaesium in river water in these catchments, monitoring was carried out at twelve sites, as shown in Figure 2(c), from 2013 to 2021.An additional monitoring point was established along the main river channel of the Hirose River in 2019 (St. 4). For the Kuchibuto River Basin, the monitoring was carried out at five monitoring points, from 2017 to 2021, mainly those that were already included in the Wide-area Multipoint Survey. The initial deposition of radiocaesium in the catchment at each monitoring point was calculated and shown in Table 2.

Table 2. Catchment area and initial caesium-137 deposition within the Kuchibuto River Basin

	River basin area [km^2]	Average Cs-137deposition [kBq m^{-2}]
Mizusakai River	7.52	587
Kuchibuto River Upstream	21.4	408
Kuchibuto River Midstream	62.8	304
Adachiota River	17.6	235
Kuchibuto River Downstream	135.2	247

1.3.2.1.2. Method

At each monitoring point, approximately 100 L of river water were collected at base-flow levels (every 2 to 3 months) and at high-flow levels (7 samples/1 high-flow event, for 24 hours). Water quality (pH, electrical conductivity (EC), oxidation–reduction potential (ORP)) and SS concentrations were measured at the time of collection. Suspended and dissolved forms of radiocaesium were collected from river water samples in a cartridge filter [6] for caesium

monitoring using a radiocaesium monitoring device (Figue 5) [7]. Each form of radiocaesium was then measured with a germanium semiconductor detector. In addition, investigations of activity concentrations in the cross-section of the riverbed, and samplings of riverbank soil and sediment were carried out. Based on these data, the radiocaesium concentrations and their changes in the river were estimated under base flow and high flow conditions using the TODAM model. The TODAM model can simulate temporal changes of radionuclide concentrations in waters and sediments. For example, the TODAM model makes it possible to estimate the amount of radionuclides transported to the Pacific Ocean in rivers, to predict the locations in rivers where sediments are preferentially deposited, and to evaluate the influence of decontamination measures on the dislocation of sediments in rivers. In this survey, the TODAM model was used to estimate the radiocaesium activity and their changes under base flow and high flow conditions.

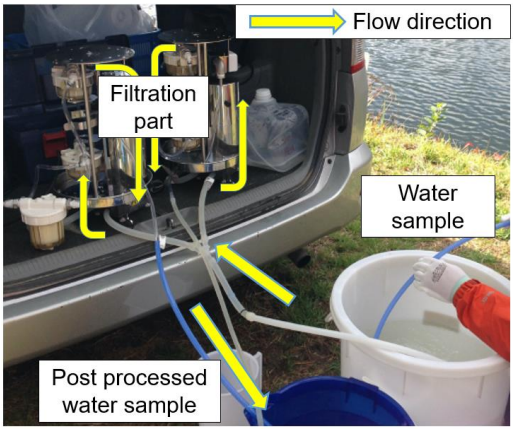

Figure 5. Radiocaesium monitoring device [7].

1.3.2.2. Estimation of the source of SS loads

1.3.2.2.1. Purpose

Suspended sediments (SS) play a significant role in the transition of caesium-137 as a particulate form through rivers. The concentration of SS in river water generally increases during high-flow events, resulting in quite a lot of caesium-137 transportation even in a single high-flow event. In order to clarify the relative contributions of the potential SS sources in a watershed to the amount and concentrations of fluvial SS both under high- and base-flow conditions, caesium-137 radioactivities, total organic carbon (TOC) concentrations, and stable carbon isotope composition ($\delta^{13}C$) in SS were employed for a simulation using a Bayesian isotopic mixing model, Stable Isotope Analysis in R (SIAR ver. 4.2).

1.3.2.2.2. Method

For measurements of TOC and $\delta^{13}C$ in SS, about 0.5 or 1.0 L river waters sampled at the same time as for caesium-137 measurements were filtrated by glass fiber filters (GF/F) which had been precombusted at 450 ℃ for 4 hours. Four potential SS sources were determined in this project (forest soils and litters, riverbank soils, and river sediments). Forest soils and litters were sampled in adjacent forests at the headwater region of the Hirose River. Riverbank soils and river sediments were sampled along the mainstream and tributaries of the

Hirose River. These source materials were air-dried at 40℃ for more than 48 hours. The samples were measured using an elemental analyzer coupled to an isotope ratio mass spectrometer using an interface. The detail procedures were shown in a study of Arai et al. (2021) [8].

1.4. Results

1.4.1. Wide-area Multipoint Survey

1.4.1.1. Wide-area Multipoint Survey

Figures 6(a) and 6(b) show the variations in suspended and dissolved caesium-137 concentrations over time (as of March 2021) obtained from the Wide-area Multipoint Survey. The data include results from the University of Tsukuba until the end of FY2014. The concentration of suspended caesium-137 at each monitoring point showed a tendency to decrease over time after the start of this project, but the decline observed immediately after the accident was the fastest [9), 10)]. As of March 2021, the concentration of dissolved and suspended caesium-137 was generally less than 1/10 of the value observed immediately after the accident (Figure 6(a)). The concentration of dissolved and suspended caesium-137 showed a similar time-dependence (Figure 6(b)). There was a period of missing data for dissolved caesium-137, however, the overall pattern suggests that the concentration of dissolved caesium-137 in the rivers of Fukushima Prefecture gradually decreased over time.

Based on data obtained from 2012-2021, the effective half-lives of suspended and dissolved caesium-137 were estimated to be approximately 3.2 and 2.8 years, respectively (Figure 7). Comparing Chornobyl and Fukushima, the of effective half-lives of caesium-137 in river water were similar just after the accident (0.24 year in Abukuma River vs 0.31 year in Pripyat River) [11)]. In the second year and beyond, the effective half-lives of the concentration of suspended caesium-137 in rivers of the Fukushima prefecture are in the range of 1 to 4 years; similar observations were made for European rivers.[11)].

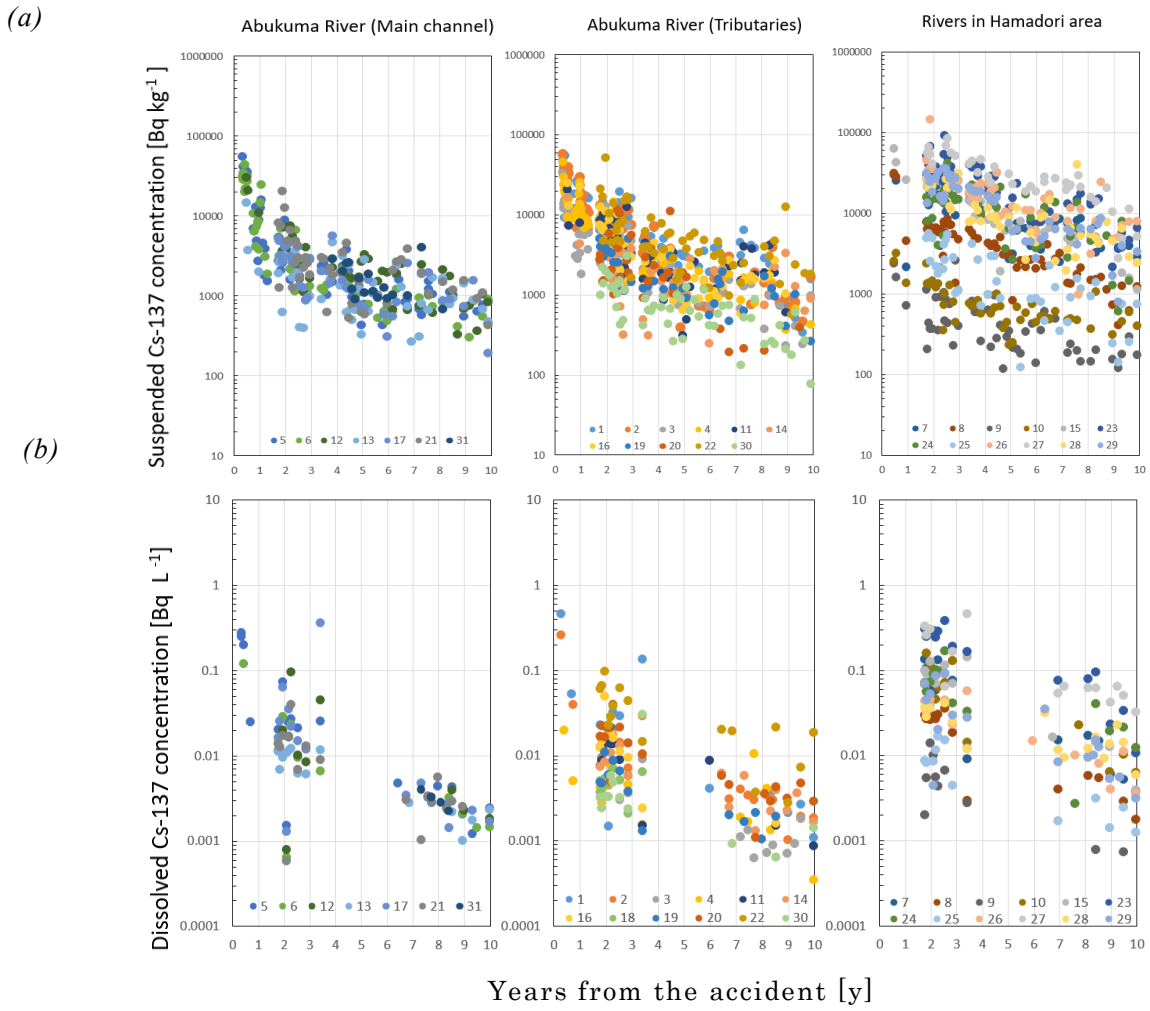

Figure 6. Caesium-137 concentrations in river water.
(a) Suspended caesium-137, (b) Dissolved caesium-137.

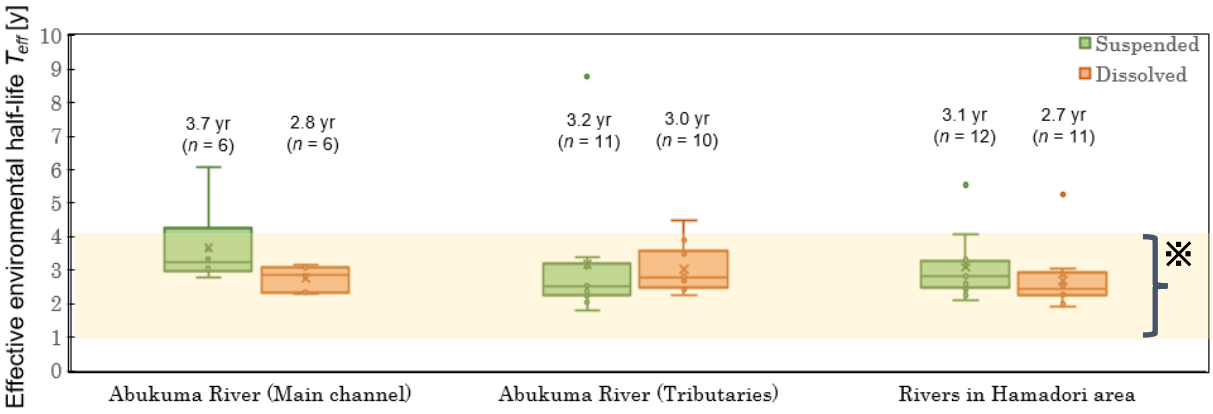

Figure 7. Effective environmental half-life of caesium-137 concentrations in river water in each region (data from 2012-2021). The asterisk indicates the range in the effective environmental half-life reported for European rivers after the Chornobyl Nuclear Power Plant Accident).

Figure 8 shows the average monthly flux of suspended caesium-137 at six monitoring points from 2011 to December 2018. The caesium-137 fluxes do not show a clear trend due to the strong temporal fluctuations of the flow rate of the river and the caesium-137 concentrations of suspended sediments. At the two monitoring points along the Abukuma River, 3.0-4.0% of the caesium-137-inventory of the catchment was displaced and located with suspended sediments, while at the four monitoring points along its tributaries the flux was 0.6-2.2% of the catchment's caesium-137 inventories.

The upper part of Figure 9 shows the flux of suspended caesium-137 integrated from October 2012 to October 2014. The lower part of Figure 9 shows the ratio of the area of a reservoir to the total catchment area (excluding No.12, 17, 18 due to several problems during the monitoring period - lower graph). Low caesium-137 fluxes were observed at the points where the area of the dam covers a large area of the catchment (red hatched part in the graph).

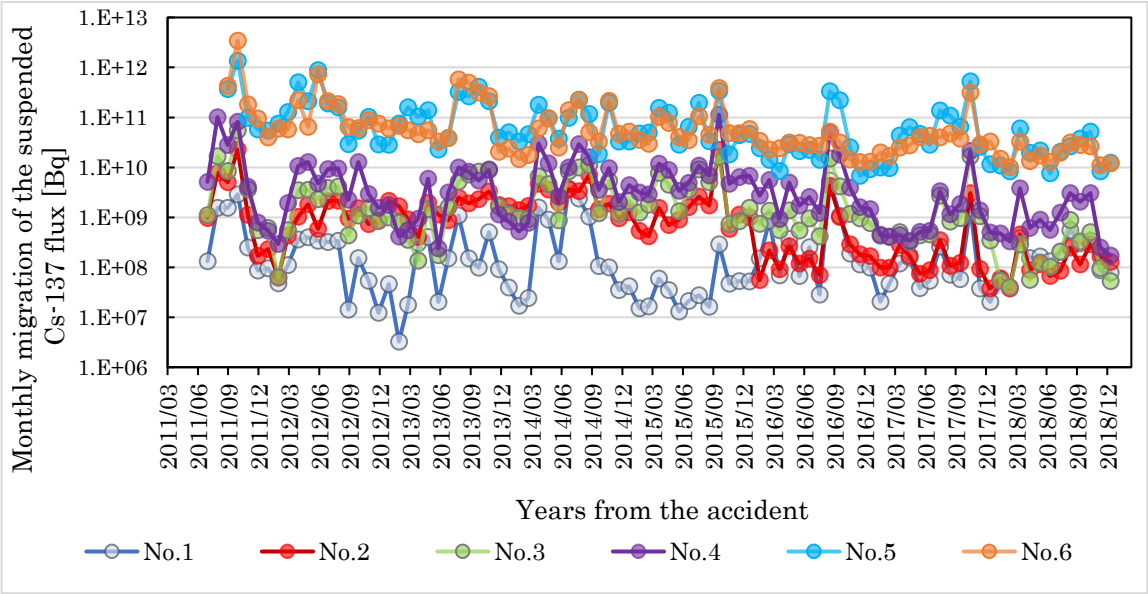

Figure 8. Monthly migration of the suspended caesium-137 at monitoring points (No.1-6) from May 2011 to December 2018.

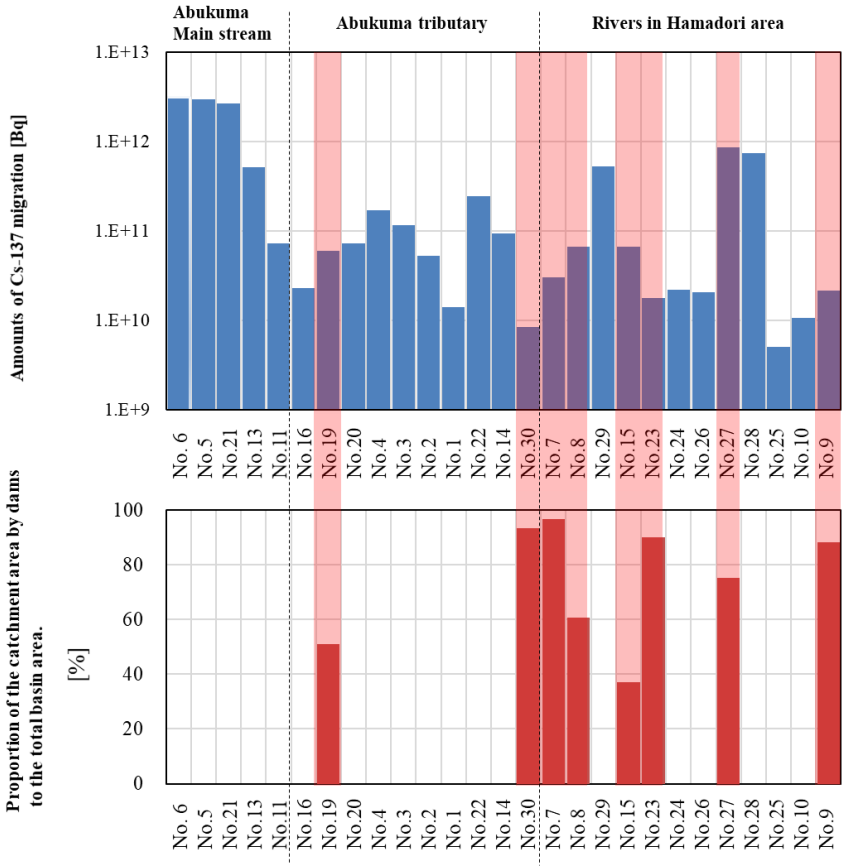

Figure 9. Total flux of suspended caesium-137 from Oct. 2012 to Oct. 2014. Red hatched bars indicate the monitoring point with higher proportion of the watershed area for dams to the total catchment area.

In addition, the impact of the surface decontamination measures implemented by the national government and the municipalities on the caesium-137 concentrations in river waters was assessed. The observed decreases in caesium-137 concentrations were similar to the trends observed in European rivers after the Chornobyl accident (Figure 6). However, it is difficult to determine the effect of surface decontamination measures on the caesium-137 concentrations in rivers because the area decontaminated is very small in relation to the area of the catchment. Therefore, it is assumed that the decrease observed in areas where decontamination measures were implemented is largely caused by natural attenuation processes [11)]

Subsequently, the data for the Kuchibuto River Basin were analyzed to investigate the effect of decontamination on suspended radiocaesium in river water. The data focused on the variations of the caesium-137 concentrations in suspended sediments during the decontamination works. The basin to decontaminate farmland was fully designated as a special decontamination area; work in the basin was planned in August 2012, it started in March 2013, and it was completed in December 2015 [2]. Figure 10 shows the progress of the decontamination of farmland. Decontamination started

[2] Decontamination Information website, Ministry of the Environment, http://josen.env.go.jp/area/details/kawamata.html

in March 2013, but only little progress was made until March 2014. Intensive farmland decontamination was carried out from April 2014 and decontamination was completed in December 2015. Thus, the period before February 2013 was defined as “Pre-decontamination”, the period from March 2013 to March 2014, when progress was very slow, was defined as “Decontamination in progress ①”, and the period from April 2014 to December 2015, when rapid progress was made, was defined as “Decontamination in progress ②”. Finally, the interval after January 2016, when decontamination was completed, was defined as “Post decontamination”.

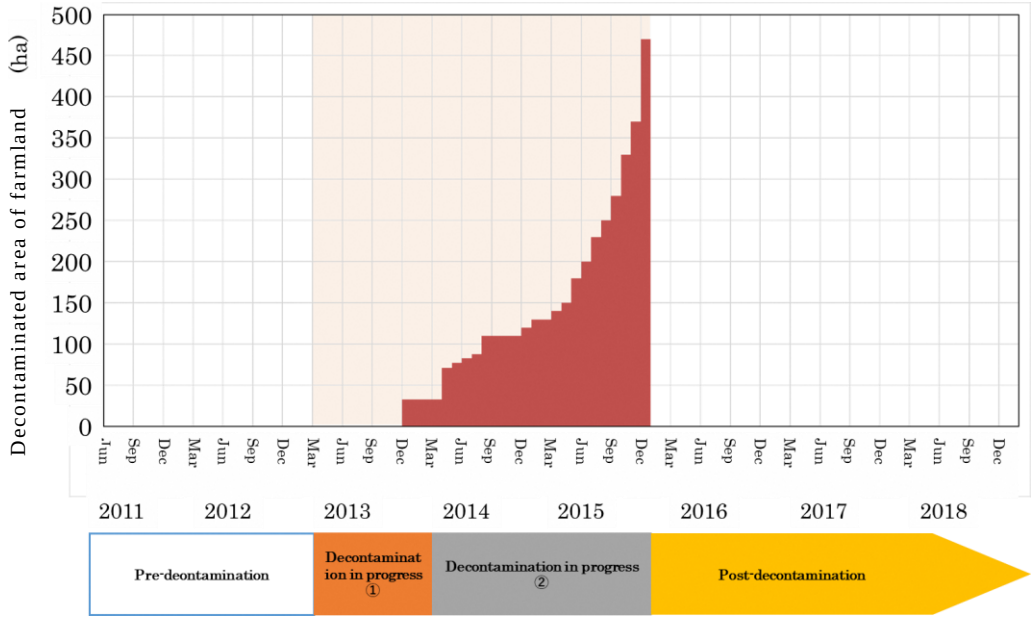

Figure 10. Progress in farmland decontamination

The time-dependence of caesium-137 concentrations in suspended sediments at three monitoring points (upstream, midstream, and downstream; Figure 2(a)) is shown in Figure 11. The effective half-lives for these periods are shown in Table 3. The results showed a faster decrease in suspended caesium-137 concentration in the upstream and midstream sites of the special decontamination area during “Decontamination in progress ②”. However, the decrease was slower in the downstream sites, and it slowed down in the second half of the “Decontamination in progress ②” period (about 4 years after the accident). In addition, the amount of suspended sediment in surface water runoff as a function of precipitation and catchment area showed a tendency to increase after the start of farmland decontamination, and a significant increase was observed during the “decontamination in progress ②” period. In the “post-decontamination” period, the amount of sediment in runoff decreased, but it was still higher than in the “pre-decontamination” period (Figure 12). This shows the same trend as the results of the analysis in the Niida River flowing through the Hamadori area, following decontamination, reported in the previous study [12].

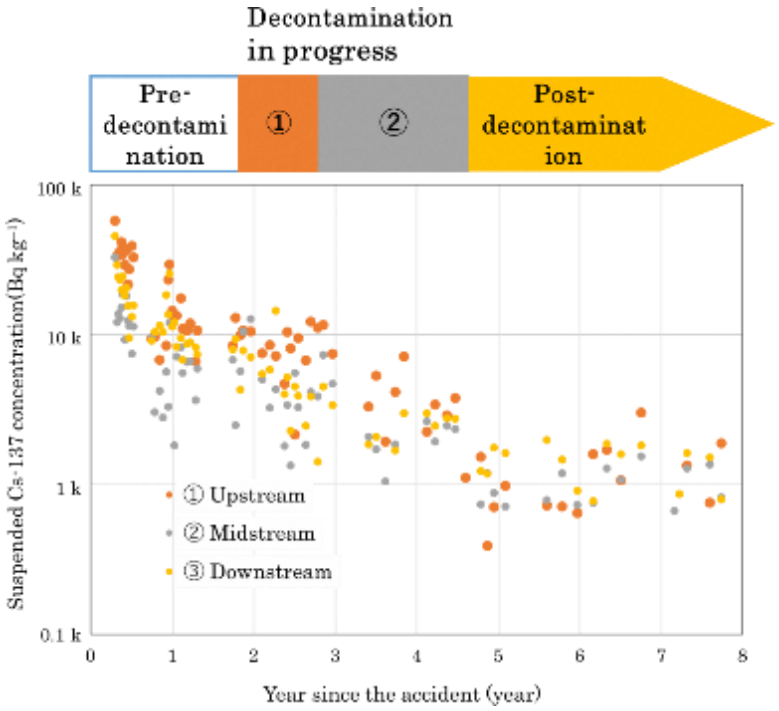

Figure 11. Change in suspended caesium-137 concentration over the course of decontamination.

Table 3. Effective environmental half-life for each period (years)

Monitoring point	Pre-decontamination	In progress ①	In progress ②	Post-decontamination
① Upstream	0.77	*n.s.*	0.98	*n.s.*
② Midstream	1.2	*n.s.*	1.6	*n.s.*
③ Downstream	0.86	0.59	4.2	4.8

n.s. indicates that suspended caesium-137 concentration did not change significantly during each period.

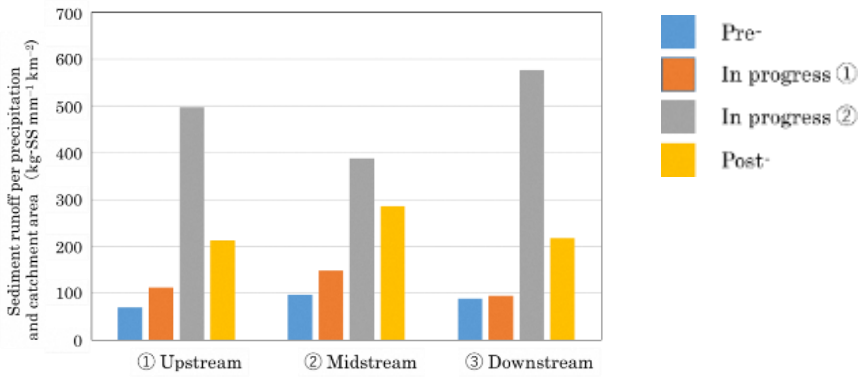

Figure 12. Relationship between decontamination progress and the amount of sediment runoff.

1.4.1.2. Survey of CsMPs in SS samples

Two spherical CsMP particles (A and B) were found in the suspended sediment samples (Table 4). The radioactivity of caesium-137 in those two particles was estimated to be approximately 13% of the total radioactivity of the sample.

Table 4. Characteristics of CsMPs identified in SS samples

Sample name	Particle size (μm)	Cs-137 (Bq)	Detected Element
A	4.2	14±0.1	O, Si, Cl, Fe, Zn, Sn, Cs
B	1.0	0.25±0.01	O, Si, Cl, Fe, Zn, Cs

When suspended sediments with extremely high caesium-137 concentration were found, a simple method to determine the presence or absence of CsMPs was investigated. Dry methods [2), 3)] and wet methods [1)] have been reported as methods for searching and separating a single CsMP from a sample. On the other hand, a simple method for determining the radioactivity and number of CsMPs without separating a single particle from the sample has been reported [1), 13)]. Applying this simple method to CsMPs with known radioactivity, we developed an equation relating radioactivity and IP brightness and attempted to determine the presence or absence of CsMPs in suspended sediment samples. The threshold of radioactivity for CsMP was set as the maximum radioactivity value of a particle different from CsMP (0.189 Bq) [14)], and particles above this radioactivity were classified CsMPs. Table 5 shows the results obtained: the presence of CsMPs in five suspended sediment samples collected in 2018-2019 was investigated and nine CsMPs were estimated to be present. The results indicated the presence of CsMPs in suspended sediment samples, but their contribution was very small.

Table 5. IP measurement results and radioactivity contribution of the SS samples

Sample name	Cs-137 concentration in the sample (Bq/g)	Weight of SS (g)	Cs-137 in the sample (Bq)	The number of CsMPs	Cs-137 in CsMP (Bq)			Cs-137 in CsMPs in total (%)
1-NZ1910	3.2±0.07	2.7	8.7	0				N/A
2-SU1910	18±0.3	1.4	23	2	0.48	0.22		3.0
3-SD1910	23±0.3	1.4	32	6	0.41 0.30	0.36 0.23	0.32 0.19	5.7
4-NR1810	2.1±0.03	3.2	6.7	0				N/A
5-TR1907	4.9±0.12	3.0	15	1	0.46			3.1

1.4.2. Single basin survey

1.4.2.1. Simulation of radiocaesium dynamics in river by TODAM model

Figure 13 shows riverbed cross sections at the monitoring points of St.3 and St.10 of the Hirose River (Figure 2a). Both points are about 24 km apart. Although the water depth was similar, the

river width at St.10, including the floodplains, was about twice as large as that at the St.3. During the monitoring, high flow events caused the riverbed and bank to be eroded, and fresh sediment deposited on the riverbed, but the riverbed cross-section at each monitoring point did not change significantly.

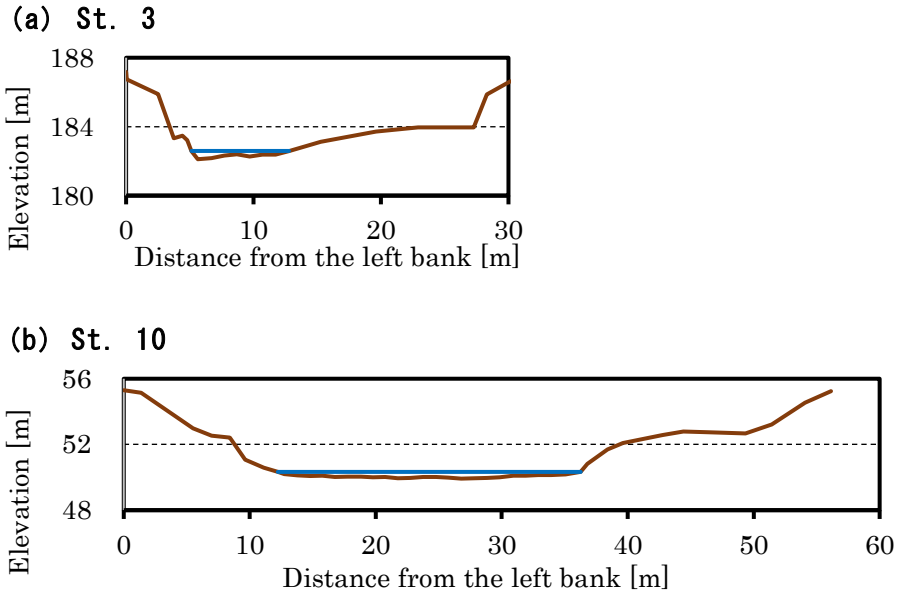

Figure 13. The cross sections at the monitoring points in the Hirose River Basin (St. 3 and St. 10).

Figure 14 shows the variations in suspended caesium-137 and suspended sediment concentrations in water at each monitoring point along the Hirose River in April 2016 at base flow levels. The concentration of suspended caesium-137 was high in the some of the tributaries. The caesium-137 concentrations are strongly influenced by the initial deposition in the catchment. The results varied between monitoring points, irrespective of the monitoring points and items (suspended caesium-137 and suspended sediment concentrations).

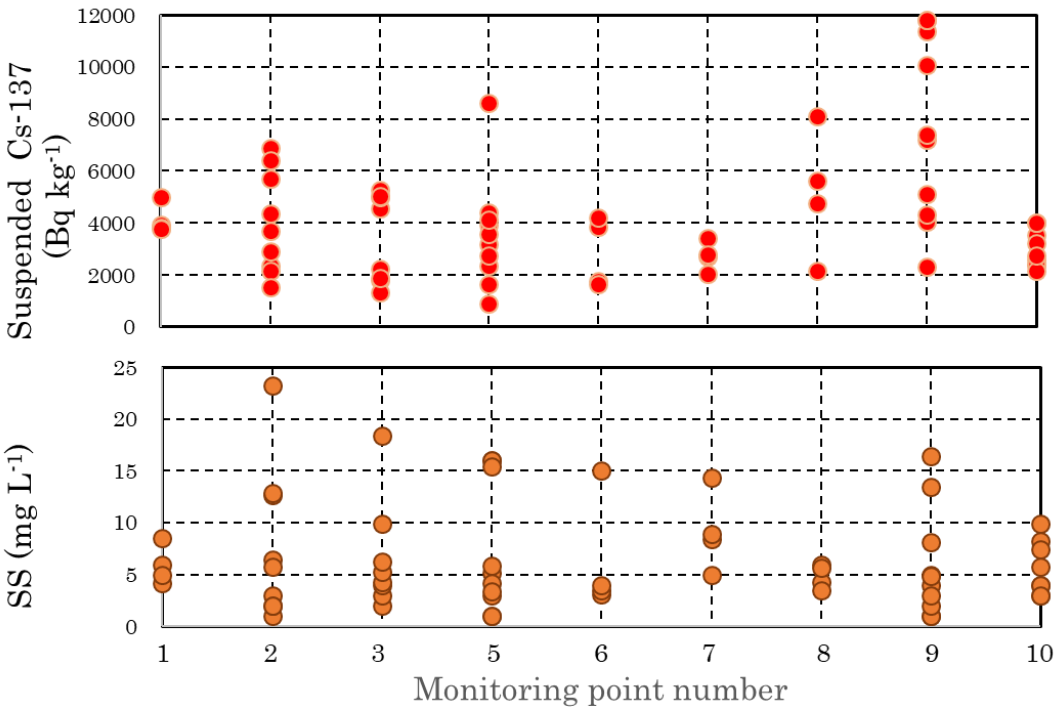

Figure 14. Suspended caesium-137, and SS concentrations at each monitoring point in April 2016

Figure 15 shows a scheme of the monitoring network considered in the application of the TODAM model to the Hirose River. The distance from the confluence of the Hirose River with the Abukuma River to the confluence of the Takane River with the Hirose River is 31,732 m. In the simulation, the inflows were considered from the Takane River, Nuno River, Ishida River, and Oguni River, main tributaries of the Hirose River. For the Hirose River, the simulation was performed every 200 m in the direction of the flow channel, and 150 calculation points were set in the Hirose River Basin. The dynamics of radiocaesium were simulated in the Hirose River based on the monitoring data.

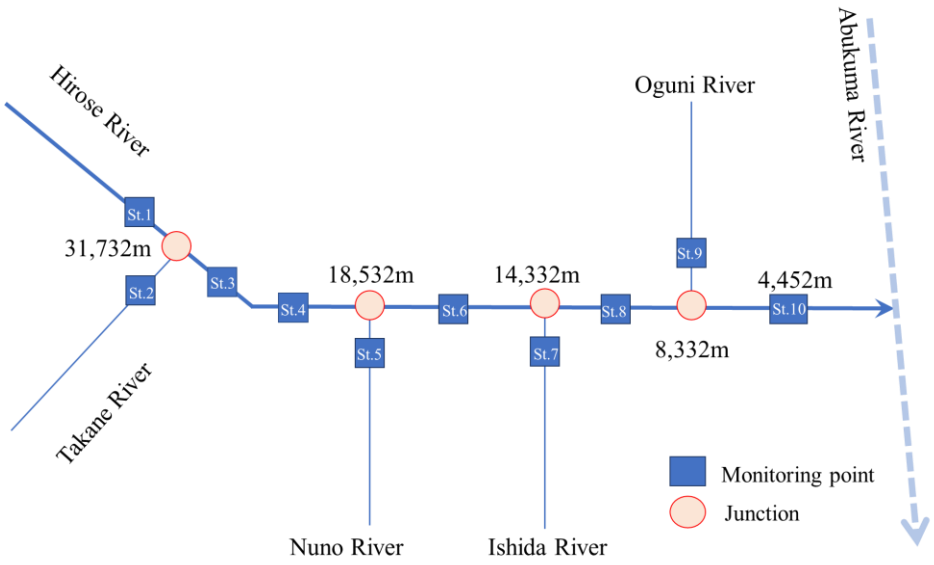

Figure 15. A schematic representation of the monitoring network in the Hirose River Basin.

Figure 16 shows the calculated and measured concentrations of suspended and dissolved caesium-137 concentrations along the Hirose River using the TODAM model under base flow conditions. The solid line represents the values estimated by the TODAM model, and the boxplot represents the actual measurement values obtained at six monitoring points along the main river channel of the Hirose River. It was possible to reproduce the data obtained at six monitoring points along the mainstream of the Hirose River using the TODAM model. The results obtained by the model simulation were in relatively good agreement with the measured values.

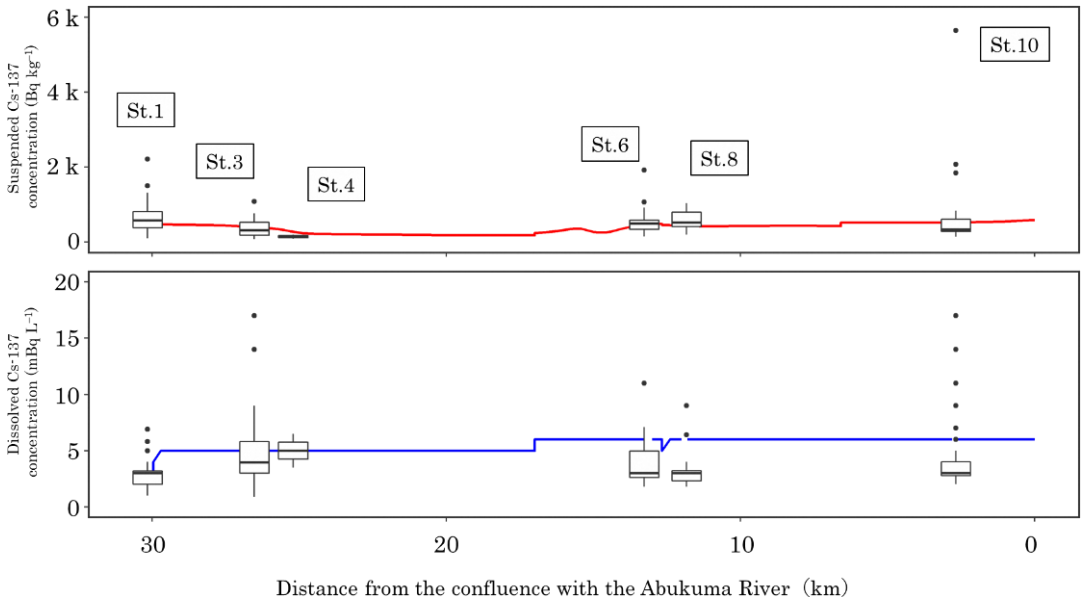

Figure 16. Simulation results of changes of caesium-137 concentration at base flow levels water estimated using the TODAM model (Hirose River).

A simulation of the concentration of caesium-137 in river water during the high flows from August 16 to 19, 2016 (total precipitation 67 mm; Japan Meteorological Agency, Yanagawa, Fukushima Prefecture) [15] is shown in Figure 17. The results also show a good agreement between measured and calculated values at the four monitoring points (St. 3, 6, 8, and 10) under high flow conditions.

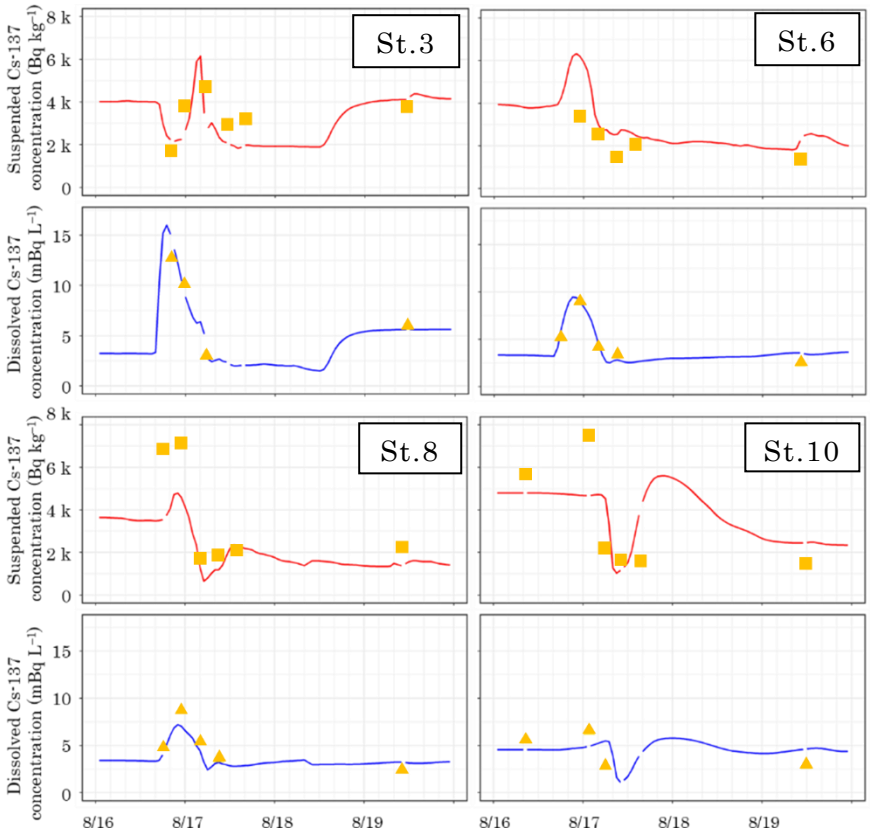

Figure 17. Simulation results of changes in caesium-137 concentrations during high flow events estimated using the TODAM model (Hirose River). [Upper rows: Suspended caesium-137 concentration, lower rows: Dissolved caesium-137 concentration] (High flow events from 16 August 2016 to 19 August 2016)

Monitoring data collected from 2017 at the Kuchibuto River Basin (Figure 2(a)) was used to simulate of the suspended and dissolved caesium-137 concentrations in river waters by the TODAM model. The results of the model simulation of the Kuchibuto River Basin are shown in Figure 18 and 19. In the results of the application along the flow path during base flow conditions, the characteristics of low caesium-137 concentrations in both dissolved and suspended forms in ②Midstream were generally reproduced (Figure 18). The simulation results at ③Downstream based on the data from the outflow on 5-6 July 2018 (total precipitation 36 mm; Japan Meteorological Agency, Tsushima, Fukushima Prefecture)[15], were also able to reproduce temporal changes in suspended sediment and both suspended and dissolved caesium-137 concentrations.

Through this cooperative project, it was possible to simulate the dynamics of caesium-137 using

the TODAM model for two rivers. In addition to predicting the dynamics of caesium-137 in these rivers, future applications to other rivers and to the dynamics of other contaminants are possible.

The accuracy of the simulation predictions can be improved through the calibration with site-specific information and data. In particular, hydrological data are required, such as the relationships between water level and flow rate in the target river, and between the flow rate and suspended sediment concentrations with particle size distributions. It is considered necessary to obtain these data in advance when performing preliminary impact assessments in preparation for an eventual nuclear disaster.

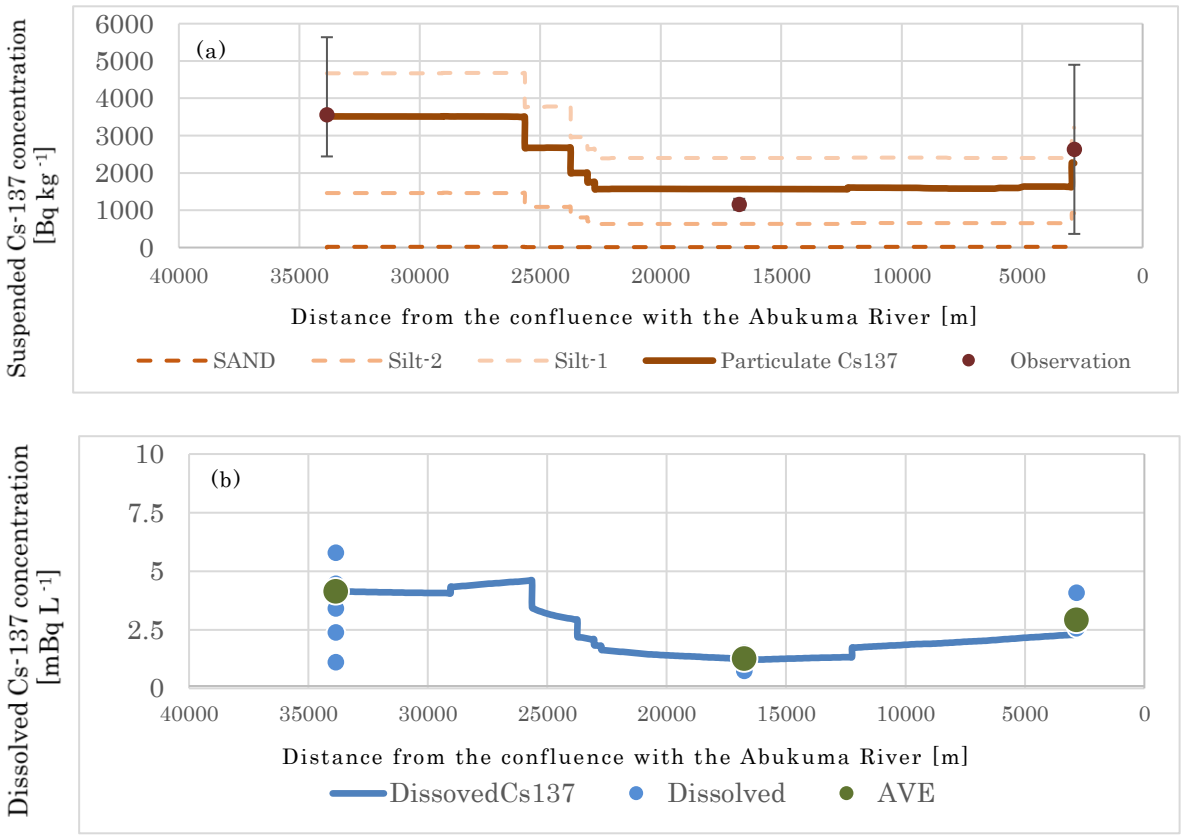

Figure 18. Simulation results of changes of caesium-137 concentration at base flow levels water estimated using the TODAM model (Kuchibuto River).
(a) Suspended caesium-137 concentration, (b) Dissolved caesium-137 concentration.

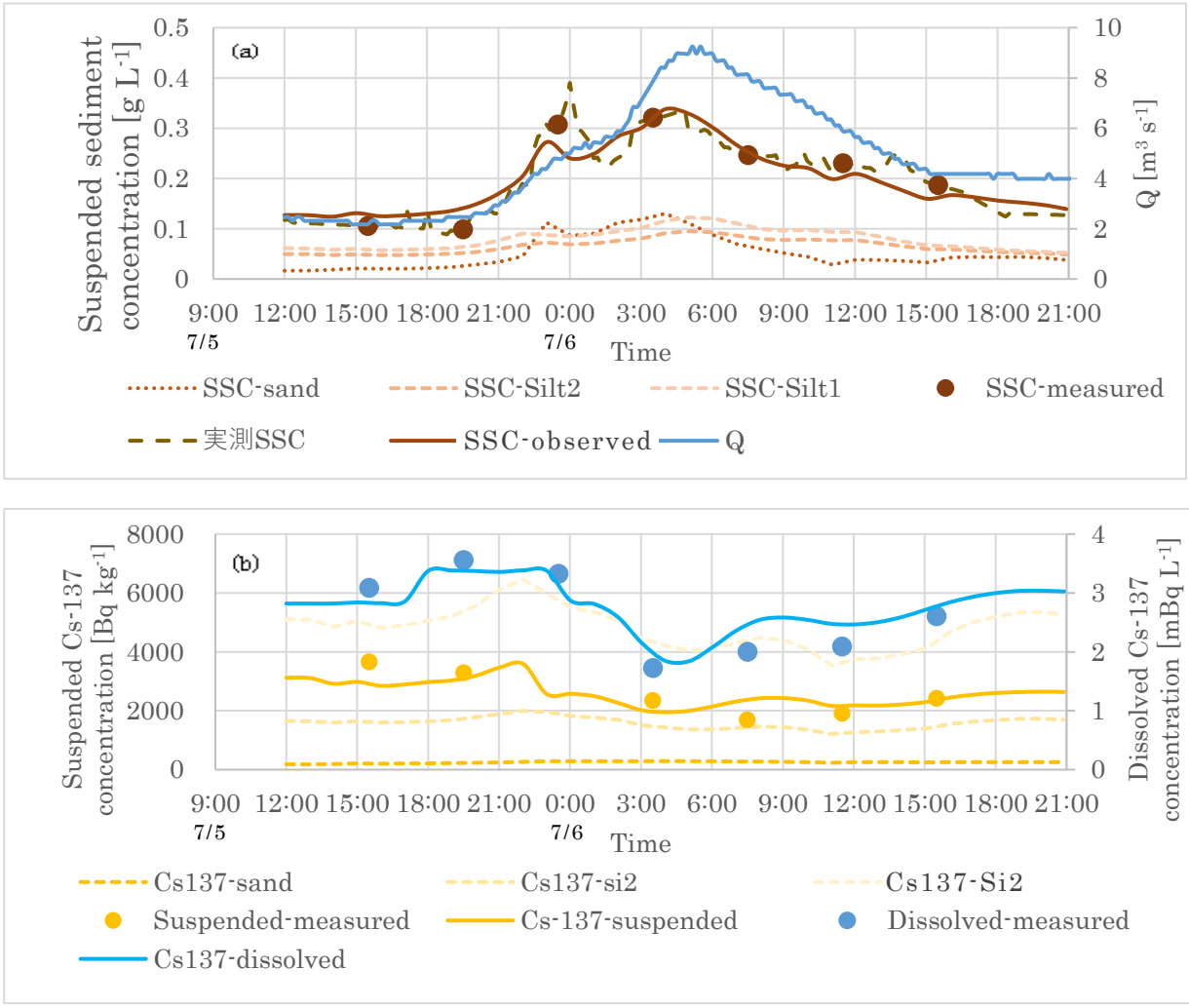

Figure 19. Simulation results of changes in caesium-137 concentrations during high flow events estimated using the TODAM model (Kuchibuto River). [Upper rows: Suspended caesium-137 concentration, lower rows: Dissolved caesium-137 concentration] (High flow events from 5 July 2018 to 6 July 2018)

1.4.2.2. Estimation of the source of SS loads

It was found that contents of caesium-137 and organic carbon in river water were increased with increasing SS concentration in river water (Figure 20). These results confirmed that both caesium-137 and organic carbon were move together with SS. On the other hand, there were no significant relationships between SS concentrations and both caesium-137 and TOC concentrations in SS (Figure 20). However, the average values of both caesium-137 and TOC concentrations in SS at the base-flow condition tended to be larger than those at the high-flow condition, indicating that the additional SS supplied during high-flow events had lower concentrations of caesium-137 and TOC than SS at the base-flow condition. In other words, during high-flow events, caesium-137 and TOC in SS were diluted by an input of mineral materials with low caesium-137 concentrations. The $\delta^{13}C$ values in SS showed a gradual decreasing trend with increasing SS concentration (Figure 20), which suggested a gradual change of organic carbon source in SS with increasing SS concentration in river water.

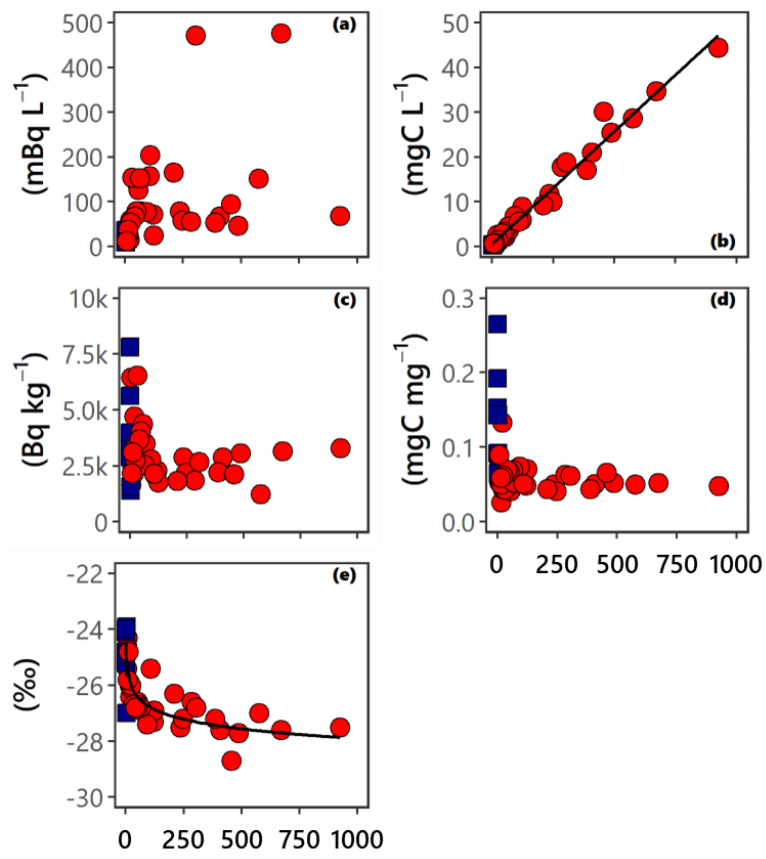

Figure 20. Changes of both contents in river water ((a) particulate caesium-137 and (b) particulate organic carbon) and properties in SS ((c) caesium-137, (d) TOC, and (e) $\delta^{13}C$) with SS concentrations are shown. Blue squares indicate the data at base-flow, while red circles indicate the data at high-flow river.

The results of caesium-137, TOC, and $\delta^{13}C$ in four potential sources of SS are shown in Table 6. As expected, forest soils showed the highest caesium-137 concentrations due to the lack of decontamination practices. Forest litters showed the highest TOC concentration and the most depleted $\delta^{13}C$ value, and riverbank soils and river sediments showed relatively low caesium-137 and TOC concentrations. The result of simulation by SIAR using these data revealed that forest soil is the predominant source of fluvial SS during base-flow condition, and the contributions of other sources remained at low levels (Figure 20). At the high-flow condition, on the other hand, the contribution of forest soils reduced significantly, although the contribution was still high. These results led to the conclusion that erosion of riverbank and resuspension of river sediments at high-flow events promoted additional inputs of SS materials with low caesium-137 concentrations, resulting in dilution effects of total SS in high-flow river water. It is suggested that it is better to clarify the formation process of SS during high-flow events and to assess the simulation results, using additional tracers and fingerprinting properties in future works.

Table 6. Properties of four potential SS sources. Averages are shown with the standard deviations (S.D.).

Type	^{137}Cs	n	δ^{13}C	n	TOC	n
	Bq kg^{-1}		‰		mgC mg^{-1}	
Forest Soils	5400 ± 1600	12	−26.9 ± 0.6	12	0.105 ± 0.021	12
Forest litters	240 ± 150	16	−30.0 ± 0.5	16	0.468 ± 0.011	16
Riverbank soils	470 ± 530	46	−26.4 ± 0.8	15	0.018 ± 0.015	15
River sediments	110 ± 110	175	−25.4 ± 0.8	21	0.001 ± 0.001	21
p value *	<0.001		<0.001		<0.001	

*Results of the Kruskal−Wallis H test.

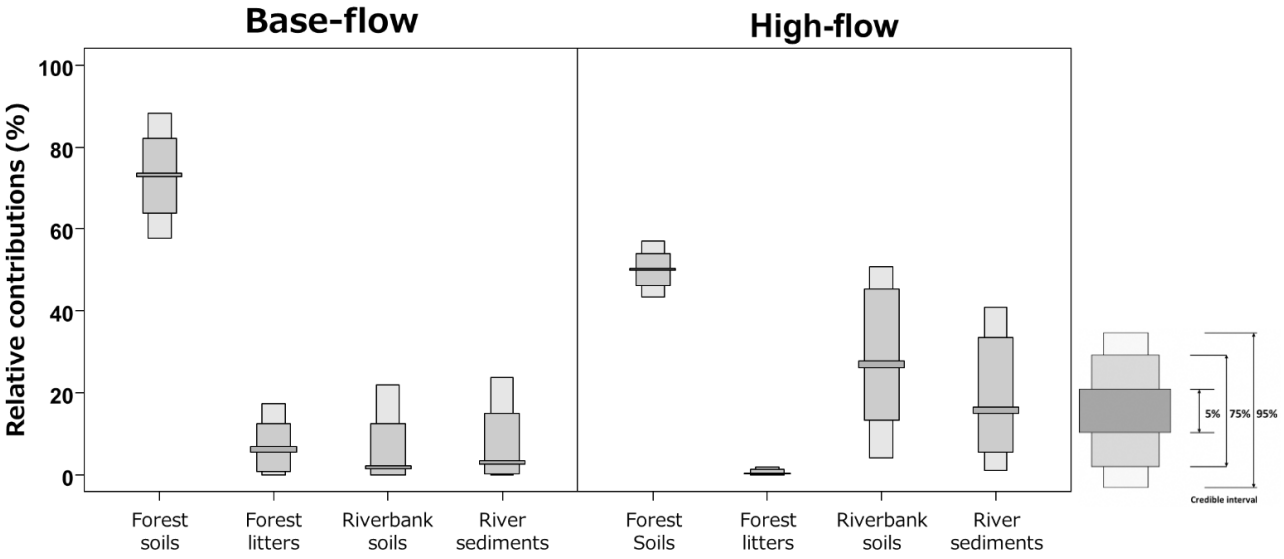

Figure 21. Simulation results for the relative contributions of each four potential source to SS under base- and high-flow conditions. The data were shown as the credible interval.

1.5. Conclusions

In the Wide-area Multipoint Survey of the Abukuma River system and major rivers in the Hamadori area, it was confirmed the presence of both suspended and dissolved radiocaesium concentrations, with a decreasing trend over time just after the accident in 2011. It was clarified that the amount of suspended radiocaesium fluxes decreased at the monitoring point with dams in the catchment area, and the decontamination works in the catchment clearly impacted on suspended radiocaesium-137 concentrations. The presence and the contribution of CsMPs were investigated for suspended sediment samples with greater radiocaesium concentrations. Although

the presence of CsMPs was confirmed in the samples, it was suggested that their contribution to the radioactivity in these samples was small.

TODAM model simulations were carried out for two rivers during base and high flow conditions, and the results were well reproduced the monitoring analysis results. In addition, riverbank erosion and resuspension of river sediments play significant roles in the increase of SS concentrations in river waters under high flow conditions.

References

1) Hikaru Miura, Yuichi Kurihara, Aya Sakaguchi, Kazuya Tanaka, Noriko Yamaguchi, Shogo Higaki, Yoshio Takahashi. 2018. Discovery of radiocesium-bearing microparticles in river water and their influence on the solid-water distribution coefficient (Kd) of radiocesium in the Kuchibuto River in Fukushima. 2018. Geochem. J. 52. (2). 145–154.
2) Yukihiko Satou, Keisuke Sueki, Kimikazu Sasa, Hideki Yoshikawa, Shigeo Nakama, Haruka Minowa, Yoshinari Abe, Izumi Nakai, Takahiro Ono, Kouji Adachi, Yasuhito Igarashi. 2018. Analysis of two forms of radioactive particles emitted during the early stages of the Fukushima Dai-ichi Nuclear Power Station accident. 2018. Geochem. J. 52. (2). 137–143.
3) Yasuhito Igarashi, Toshihiro Kogure, Yuichi Kurihara, Hikaru Miura, Taiga Okumura, Yukihito Satou, Yoshito Takahashi, Noriko Yamaguchi. 2019. A review of Cs-bearing microparticles in the environment emitted by the Fukushima Dai-ichi Nuclear Power Plant accident. J. Environ. Radioact. 205–206.101–118.
4) Onishi, Y., and Perkins, W.A. 1994. TODAM One–dimentional Sediment and Contaminant Transport Model with Multiply Connected Networks. Theory and Numerical Methods, vol. 1, Pacific Northwest National Laboratory, Richland, Washington.
5) Perkins, W., and Onishi, Y. 1994. TODAM One–dimentional Sediment and Contaminant Transport Model with Multiply Connected Networks User's Guide, vol. 2, Pacific Northwest National Laboratory, Richland, Washington.
6) Tsuji, H., Kondo, Y., and Suzuki, Y., Yasutaka,T., 2014. Development of a method for rapid and simultaneous monitoring of particulate and dissolved radiocesium in water with nonwoven fabric cartridge filters, Journal of Radioanalytical and Nuclear Chemistry, Volume 299, Issue 1, 139-147.
7) Radioactive Caesium Monitoring Consortium for Environmental water Technical Report Revision WG. 2021. Technical Report: A Comparison of the Radio Caesium Pretreatment and analytical methods in Environmental Water (2nd edition) February 2021. https://staff.aist.go.jp/t.yasutaka/MoniCons/MoniCons_index.html
8) Arai, H., Fujita, K., Yoshita, H., Taniguchi, K., Differences in the Proportional Contributions of Particulate Radiocesium Sources under Base- and High-Flow River Conditions: A Case Study in the Central Region of Fukushima, Water 2021, 13(21), 3021.
9) Taniguchi, K., Onda, Y., Smith, H, G., Blake, W, H., Yoshimura, K., Yamashiki, Y., Kuramoto, T., Saito, K. 2019. Transport and redistribution of radiocaesium in Fukushima fallout through rivers. 2019. Environ. Sci. Technol. 53, 12339–12347.

10) The Nuclear Regulatory Agency (2015), Fiscal 2014 Project Report about Integration of Radioactive Material Distribution Data and Development of Migration Model Accompanying Disaster at Tokyo Electric Power's Fukushima Daiichi Nuclear Power Plant - Part 2 "Radiocaesium migration status survey on river water systems" at http://radioactivity.nsr.go.jp/ja/list/560/list-1.html
11) Smith, J.T., Voitsekhovitch, O. V., Konoplev, A. V., Kudelsky, A. V. 2005. Radioactivity in aquatic systems, in: Smith, J.T., Beresford, N.A. (Eds.), Chernobyl - Catastrophe and Consequences. Praxis Publishing, 139–190.
12) Feng, B., Onda, Y., Wakiyama, Y., Taniguchi, K., Hashimoto, A. and Yupan Zhang, 2022. Persistent impact of Fukushima decontamination on soil erosion and suspended sediment. Nat Sustain (2022). 1-11.
13) Ryohei Ikehara, Mizuki Suetake, Tatsuki Komiya, Genki Furuki, Asumi Ochiai, Shinya Yamasaki, William R. Bower, Gareth T. W. Law, Toshihiko Ohnuki, Bernd Grambow, Rodney C. Ewing, and Satoshi Utsunomiya. 2018. Novel Method of Quantifying Radioactive Cesium-Rich Microparticles (CsMPs) in the Environment from the Fukushima Daiichi Nuclear Power Plant, Environ. Sci. Technol. 2018, 52, 6390−6398.
14) Taiga Okumura, Noriko Yamaguchi, and Toshihiro Kogure. 2019. Finding Radiocesium-bearing Microparticles More Minute than Previously Reported, Emitted by the Fukushima Nuclear Accident, Chemistry Letters, 2019, 48, 1336–1338.
15) Japan Meteorological Agency: Meteorological data (in Japanese) http://www.jma.go.jp/jma/menu/menureport.html. (Retrieved on 29th of July, 2022).

2. FIP2：Survey of Radionuclide Movements in Wildlife

2.1. Abstract

Fukushima Prefecture is conducting surveys and studies on the migrations of radionuclides to wild animals that constitute a part of the ecosystem to understand the movements of radionuclides in the ecosystem.

The present survey has measured the activity concentration of radio caesium contained in the bodies of wild animals, and investigated its fluctuation over time and differences among species. As the activity concentration is deeply related to wild animals' behaviour. For example, there is a possibility that wild animals with high radio caesium activity concentrations in their body have been moving into areas where wild animals with relatively low radio caesium activity concentration s inhabit. Therefore, the movements and dispersion of animal populations were investigated.

2.2. Purpose

The accident at the Fukushima Daiichi Nuclear Power Plant caused a widespread environmental contamination by radioactive materials. Radionuclides have been detected in many wild animals inhabiting the natural environment there because they ingested radioactive materials from the environment through food and water.

In order to ensure the safety and security of environment that citizens of Fukushima prefecture live, the Prefectural government, since immediately after the accident in 2011, has been monitoring radionuclide activity concentrations in the muscles of game animals whose meat is generally consumed by people. As a result of monitoring, mainly caesium -134 and 137, which are gamma-ray emitting nuclides, have been detected from the muscles of wild animals. However, it hasn't been studied enough how the radio caesium has been accumulated from the environment into their flesh. So in order to lift the distribution and consumption restrictions of the meat, and to ensure the local people's safety and security, surveys and studies on radio caesium movements in the ecosystem have been launched.

The migration of caesium-137 from the environment to the wild animals seems to be strongly affected by their ecology such as food habits and behavioral patterns. From 2013 to 2017, radio caesium activity concentrations in the bodies of wild animals were measured and their fluctuations with time and differences by animal species were investigated. In addition, wild animals' food habits and behavioral patterns deemed to be closely related to radionuclide movements into their bodies were also investigated. There is a positive relationship between the caesium-137 activity concentrations in the muscle and the stomach contents[1)].

The relationship between radio caesium and the existing form fraction[2)] was clarified by the survey from 2013 to 2017. Presently, a food habit survey by the deoxyribonucleic acid (DNA) analysis of stomach contents has started, and radio caesium accumulation in the bodies of wild animals according to their food habits has been investigated in detail. A behavioral survey regarding the home ranges of wild boars and Asian black bears using global positioning system

(GPS) collars has been also carried out, however, the amount of surveying has been inadequate to draw any firm conclusions. To show their behavioral characteristics, the behavioral survey using GPS collars was carried out concurrently with the food habit survey.

In addition, using the survey results starting from 2018, analyses using linear models were performed to clarify the long-term fluctuations of caesium-137 activity concentrations in the muscles of wild animals which took account of the seasonal fluctuations in the diet.

DNA analyses were carried out in order to show the structure of wild animal populations, which of the populations are increasing and which are moving into other areas as a result of the long-term abandonment of humans in the evacuation zones (zones where the evacuees still cannot return) and in the residence-restricted zones.

2.3. Investigation results made from 2013 to 2017

2.3.1. Content of implementation

We selected wild boars which inhabit wide areas of the prefecture as the main subjects of this research, because even studies assessing the impact of the Chernobyl disaster did not show any clear tendency of decrease in the time-series changes of radio caesium taken into animals.

2.3.1.1. Radionuclide dynamics in wild animals

2.3.1.1.1. Measurement of gamma-ray emitting radionuclide activity concentrations in wild animals

We measured gamma-ray emitting nuclides (wet weight) contained in the muscles of game species (wild boars, Asian black bear, copper pheasant, green pheasant, spot-billed duck, and mallard) captured by nuisance kill or by hunting. Figure 1 shows the measuring procedure. By using the measurement results, we investigated the variation of caesium-137 contained in the muscles of wild boars and other animals between individuals, and the tendency of fluctuation with the passage of time after the accident. We also measured gamma-ray emitting radionuclide activity concentrations in stomach contents and of various organs in the same way to check radionuclide distributions in wild boars.

We checked the caesium-137 soil ground deposition at the capture points of target wild animals from their capture information, and analyzed relationships between caesium-137 soil ground deposition and caesium-137 activity concentration in muscle. As to the soil ground deposition, we used the results of UAV surveys carried out by the Japan Atomic Energy Agency.

Example of sample (Muscle) Cell U-8 Measurement of radionuclide activity concentration (Germanium semiconductor detector)

Figure 1. Measurement of radionuclides in wild animals

2.3.1.1.2. Radionuclide migration from the environment into wild animals

To investigate the effect of diet on caesium-137 activity concentrations in the muscles of wild animals, we measured caesium-137 activity concentrations in the stomach contents of wild boars captured in Nihonmatsu Cityfrom fiscal 2013 to 2015. Then, we investigated relationships between caesium-137 activity concentrations in stomach contents and in the muscles of the same individuals.

2.3.1.1.3. Physicochemical fractions of radiocaesium in stomach contents

There are three physicochemical fractions of radiocaesium in soil (Figure 2). In the case of plants, they mainly absorb radiocaesium of exchangeable fractions. However, for plants, radiocaesium of strongly bound fraction, for example strongly bound clay ores is difficult to absorb. In the case of wild boar, it is thought that they take in soil when eating foods or gaining minerals intentionally. Because of soil intake and the influence of physicochemical fractions of radiocaesium in soil, there is also possibility that caesium-137 activity concentration in the muscles of boars is higher than those in other wildlife. However, it remains unknown about the amounts of absorption and migration of caesium-137 from soil and foods eaten by boar into their bodies.

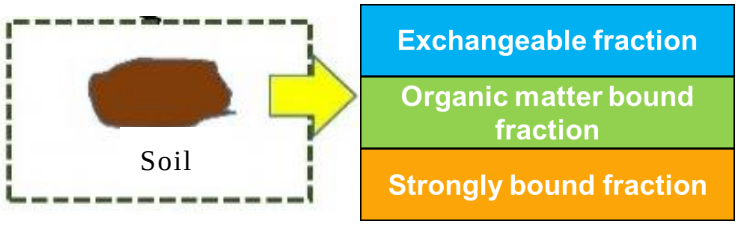

Figure 2. Physicochemical fractions of radiocaesium in soil
Exchangeable fraction: Comparatively, easily to elute.
Organic matter bound fraction: Coupled with organic matter.
Strongly bound fraction: Exist in soil particle.

In this study, we focus on about activity concentrations and ratios of physicochemical fractions of caesium-137 in stomach contents, and research about the relationships between physicochemical fractions of caesium-137 in stomach contents and migration into their body.

The physicochemical fractions of radio caesium is related to the absorption of the radio caesium from soil to plants. In collaboration with the Institute of Environmental Radioactivity at Fukushima University, we are verifying the possibility that the physicochemical fractions of radio caesium in stomach contents affects radio caesium migration into wild boars.

2.3.1.2. Investigating the home ranges of wild animals

We attached GPS data loggers (hereinafter, GPS collars) (Figure 3) to wild boars and investigated their behaviors. We set the GPS fix schedule of GPS collars as 1 GPS fix / 15 minutes, and recorded wild boar behaviors for more than one month. We investigated wild boar behaviors inside and outside the evacuation order zone (Figure 4).

Figure 3. GPS collar.

Figure 4. Attaching a GPS collar to an anethesized wild boar captured with the cooperation of a harmful bird and animal capture team.

2.3.2. Results

2.3.2.1. Dynamics of radionuclides in wild animals

2.3.2.1.1. Results of measuring gamma-ray emitting radionuclide activity concentrations in wild animals

Figure 5 shows the caesium-137 activity concentration in the muscles of wild boars captured throughout Fukushima Prefecture from May 2011 until March 2017.

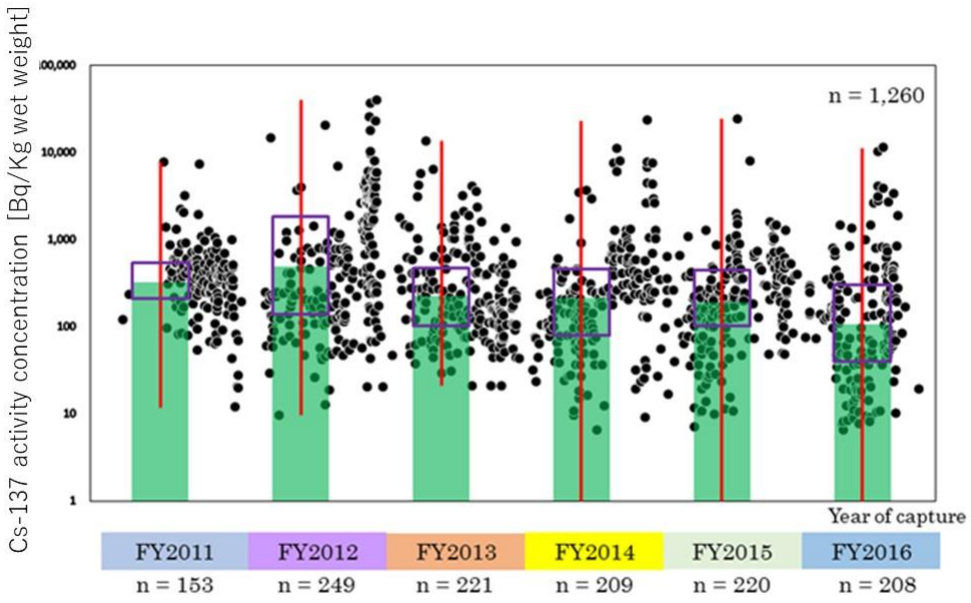

Figure 5. Results of monitoring caesium-137 activity concentration in wild boar muscles.
The X-axis indicates wild boar capture timing, and the Y-axis indicates logarithmically transformed caesium-137 activity concentration. The black dots indicate the measured values for individuals. The bar graph shows the geometric mean value of caesium-137 activity concentration in each year. Each box indicates the reliability section from 75% at the top and 25% at the bottom. The bars indicate the maximum and minimum values (May 2011 to March 2017).

From figure 5, any clear tendency was not shown because the variation in activity concentrations between individuals was great.

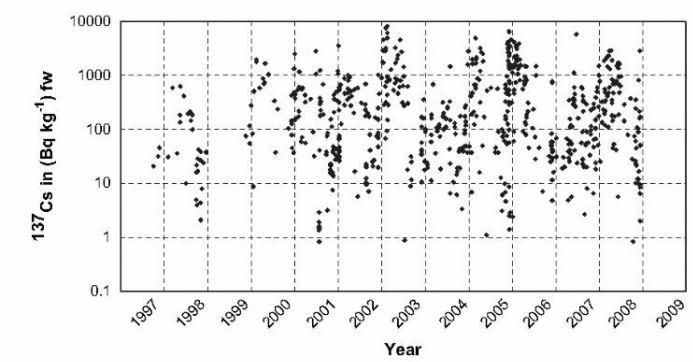

Figure 6. Temporal trends of caesium-137 in the muscle of boars (Regensburg, Southern Germany)[1].

For comparison with wild boars captured in Fukushima Prefecture, we investigated the annual changes of radio caesium activity concentrations in wild boars captured in Europe after the Chernobyl disaster. Figure 6 shows the case of Regensburg in South Germany[1]. Also in the case of Regensburg, caesium-137 activity concentration varied greatly between individuals and did not show any clear tendency of decrease. Since wild boars in Fukushima Prefecture also showed a similar tendency, we should continue to monitor the contamination trends in wild boars captured in Fukushima Prefecture.

Figure 7 shows caesium-137 activity concentrations in the muscles of Asian black bears that inhabit the forest ecosystem like wild boars. In Asian black bears, caesium-137 activity concentrations decreased with the passage of years confirmed by a statistical analysis of the data. This indicates that the annual change of caesium-137 activity concentration in muscles differs depending on the animal species.

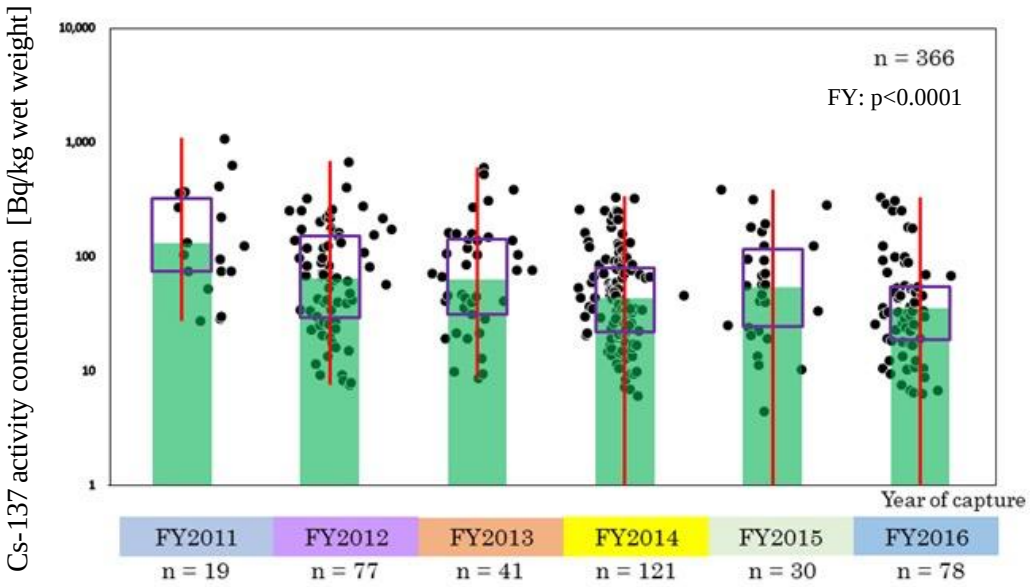

Figure 7. Results of monitoring caesium-137 activity concentration in Asian black bear muscles.
The X-axis indicates Asian black bear capture timing, and the Y-axis indicates logarithmically transformed caesium-137 activity concentration. The black dots indicate the measured values for individuals. The bar graph shows the geometric mean value of caesium-137 activity concentration in each year. Each box indicates the reliability section from 75% at the top and 25% at the bottom. The bars indicate the maximum and minimum values (May 2011 to March 2017).

Figure 8 shows relationships between caesium-137 soil ground deposition at the wild boar and Asian black bear capture points, and caesium-137 activity concentrations in muscles. Both wild boars and Asian black bears showed positive relationships between caesium-137 soil ground deposition at the capture points and caesium-137 activity concentrations in muscles. Wild boars and Asian black bears captured at points of greater caesium-137 in-soil deposition amounts showed higher caesium-137 activity concentrations in muscles. From the regression line in the figure, wild boars showed higher activity concentrations in muscles than Asian black bears captured at points with the same soil ground deposition.

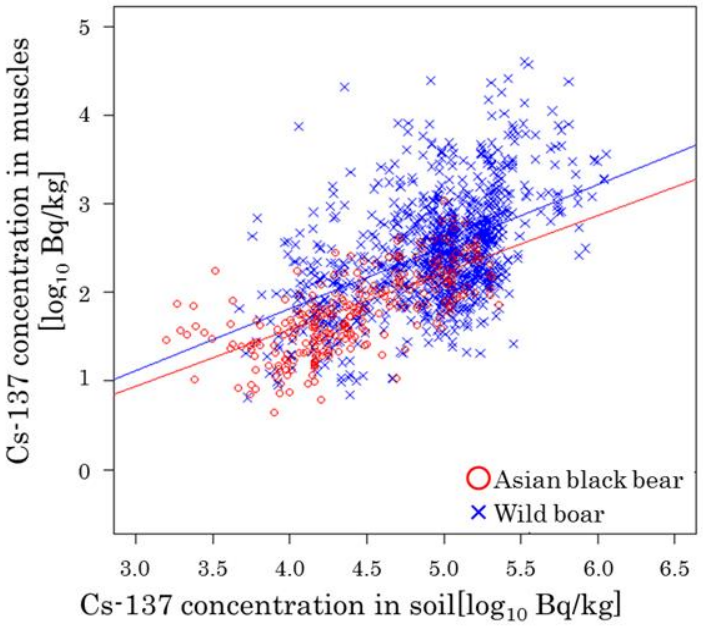

Figure 8. Relationships between caesium-137 activity concentrations in Asian black bear and wild boar muscles, and the amount of caesium-137 deposition to soil at the capture points.

Figure 9 shows wild boar and Asian black bear monitoring results by coloring depending on the area of capture. Individuals with high caesium-137 activity concentrations in muscles were frequently captured in the Hamadori region where the caesium-137 soil ground deposition is comparatively high. Individuals with low caesium-137 activity concentrations in muscles were frequently captured in the Aizu region where the caesium-137 soil ground deposition is comparatively low.

It has also been confirmed with birds that caesium-137 activity concentration in muscles of birds differs between species.

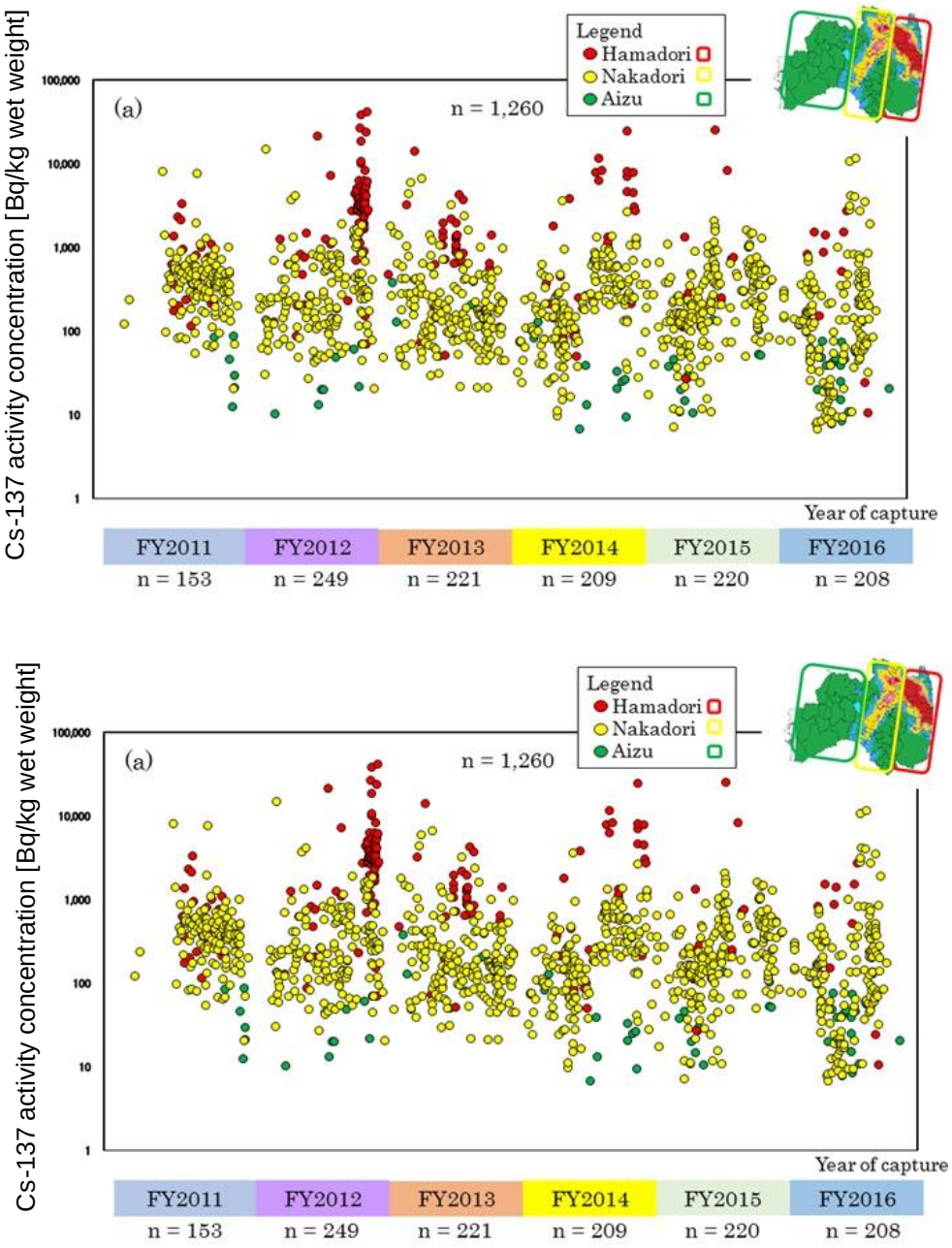

Figure 9. Monitoring results of caesium-137 activity concentration in the muscles of wild boars and Asian black bear (by the captured area).
The X-axis indicate the capture timing of wild boar and black bear and the Y-axis indicates logarithmically transformed caesium-137 activity concentration. The dots indicate the measured value for individuals that captured Hamadori (red dot), Nakadori (yellow dot), and Aizu (green dot). (May 2011 to March 2017)

Figure 10 shows caesium-137 activity concentrations in the muscles of copper pheasant, green pheasant, spot-billed duck, and mallard captured in the period from October 2011 until February 2017. When including N.D. values, the caesium-137 activity concentration in the copper pheasant muscles was higher than in the other species. The copper pheasant is not a migratory bird and inhabits a forest ecosystem.[2)]

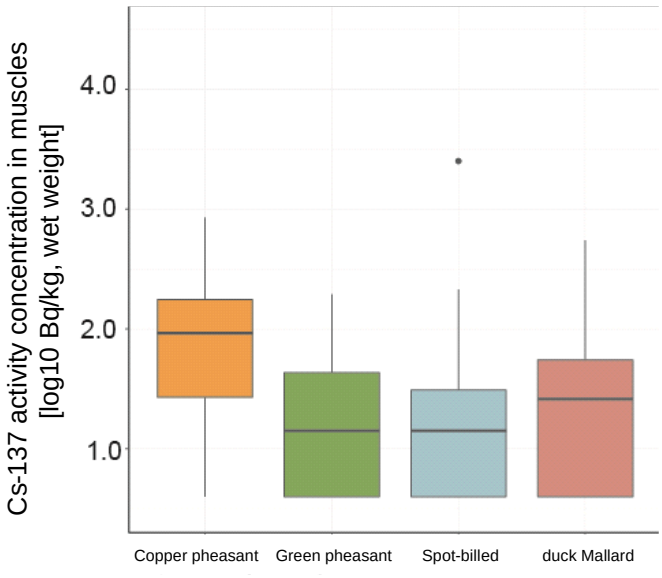

Figure 10. Monitoring results of caesium-137 activity concentrations in the muscle for copper pheasants, green pheasants, spot-billed ducks and mallards (data period: October 2011 - November 2017)
The activity concentration of caesium-137 in an individual that was below the detection limit was set at 4 Bq/kg (wet weight)[2].

Figure 11 shows the temporal change of caesium-137 activity concentration in muscle of copper pheasant and green pheasant. Caesium-137 activity concentration in muscle decreased gradually in the green pheasant, but no clear trend was observed in the copper pheasant where a large variation between individual birds was observed, similarly to the situation seen for wild boars. The reason for the difference between bird species is probably because of difference of food habitat and/or the condition of the accumulation of radionuclides in their environmental habitat; copper pheasant mainly inhabits forests, while green pheasant mainly inhabits the Satoyama ecosystem.[2]

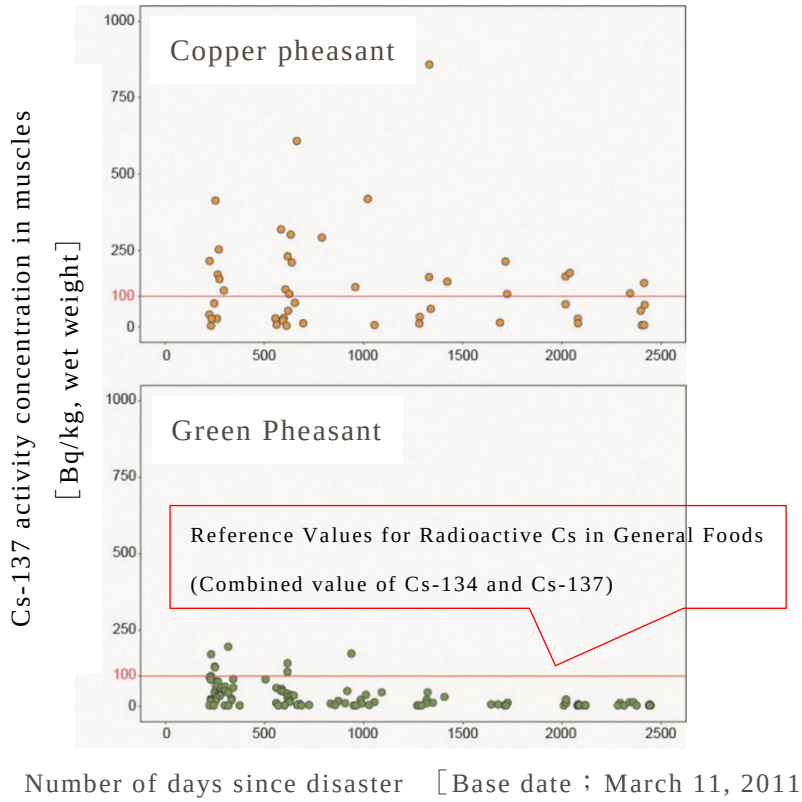

Figure 11. Monitoring results of caesium-137 activity concentration in the muscle of copper pheasants and green pheasants (October 2011 - November 2017)
The activity concentration of caesium-137 in individuals that was below the detection limit is set as 4 Bq/kg (wet weight)[2)]

2.3.2.1.2. Radionuclide migration from the environment into wild animals

Figure 12 shows relationships between caesium-137 activity concentrations in the muscles and stomach contents of the same wild boars. The caesium-137 activity concentrations in the muscles and stomach contents showed positive relationships. These relationships indicate the strong effect of intake of caesium-137 such as food items and soil on caesium-137 activity concentrations in wild boars.

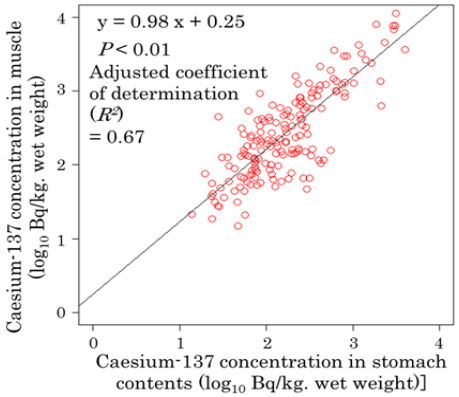

Figure 12. Relationship between caesium-137 activity concentration in muscle and in stomach contents of wild boar.

According to research on the impact of the Chernobyl disaster, caesium-137 activity

concentrations in the muscles of wild animals vary with the seasons because of such biological factors as food habits and habitat use. Thus, we analyzed relationships between caesium-137 activity concentrations in the muscles of wild boars and Asian black bears, and the months in which the animals were captured. Figure 13 shows the results.

Both species of wild boar and Asian black bear showed seasonal variation of caesium-137 activity concentration in muscles.

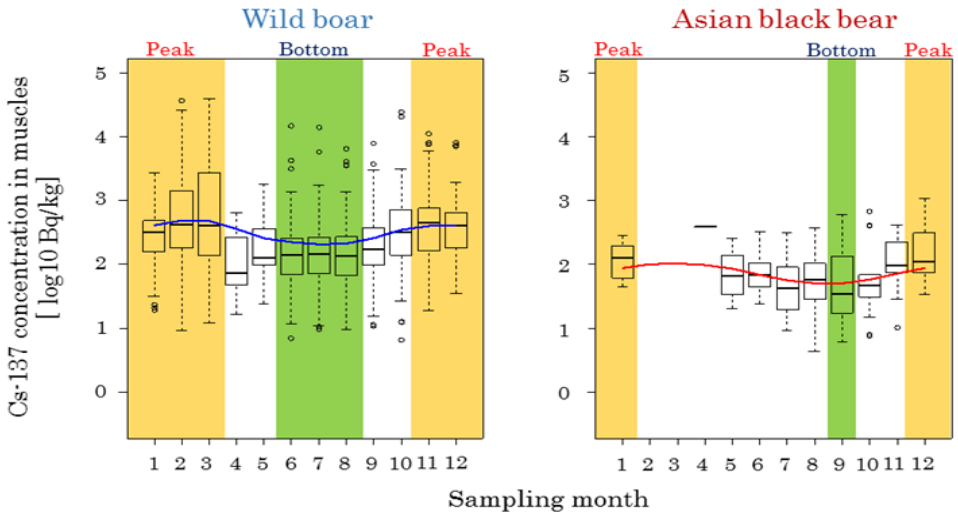

Figure 13. Seasonal variation of caesium-137 activity concentration in wild boar and Asian black bear muscles.

However, the variation pattern differs between the species. Caesium-137 activity concentrations in the muscles of wild boars were low in May to August, and high in November to March. Caesium-137 activity concentrations in the muscles of Asian black bears decreased from May to September, then increased until January.

2.3.2.1.3. Physicochemical fractions of radio caesium contained in stomach contents

Figure 14 shows correlations between caesium-137 activity concentrations in muscles of wild boars captured in the prefecture in 2015, and caesium-137 activity concentrations of each fraction in stomach contents. Caesium-137 activity concentrations in muscles showed significant correlations with activity concentrations in exchangeable fractions, and activity concentrations summed of exchangeable fractions and organic matter-bound fractions in the stomach contents. However, caesium-137 activity concentrations in muscles did not show significant correlations with activity concentrations of strongly bound fractions. Therefore, there is a possibility that exchangeable fractions and organic matter-bound fractions contained in (partially) ingested food item and soil are strongly related to caesium-137 migration into the bodies of wild boars.[3,4)]

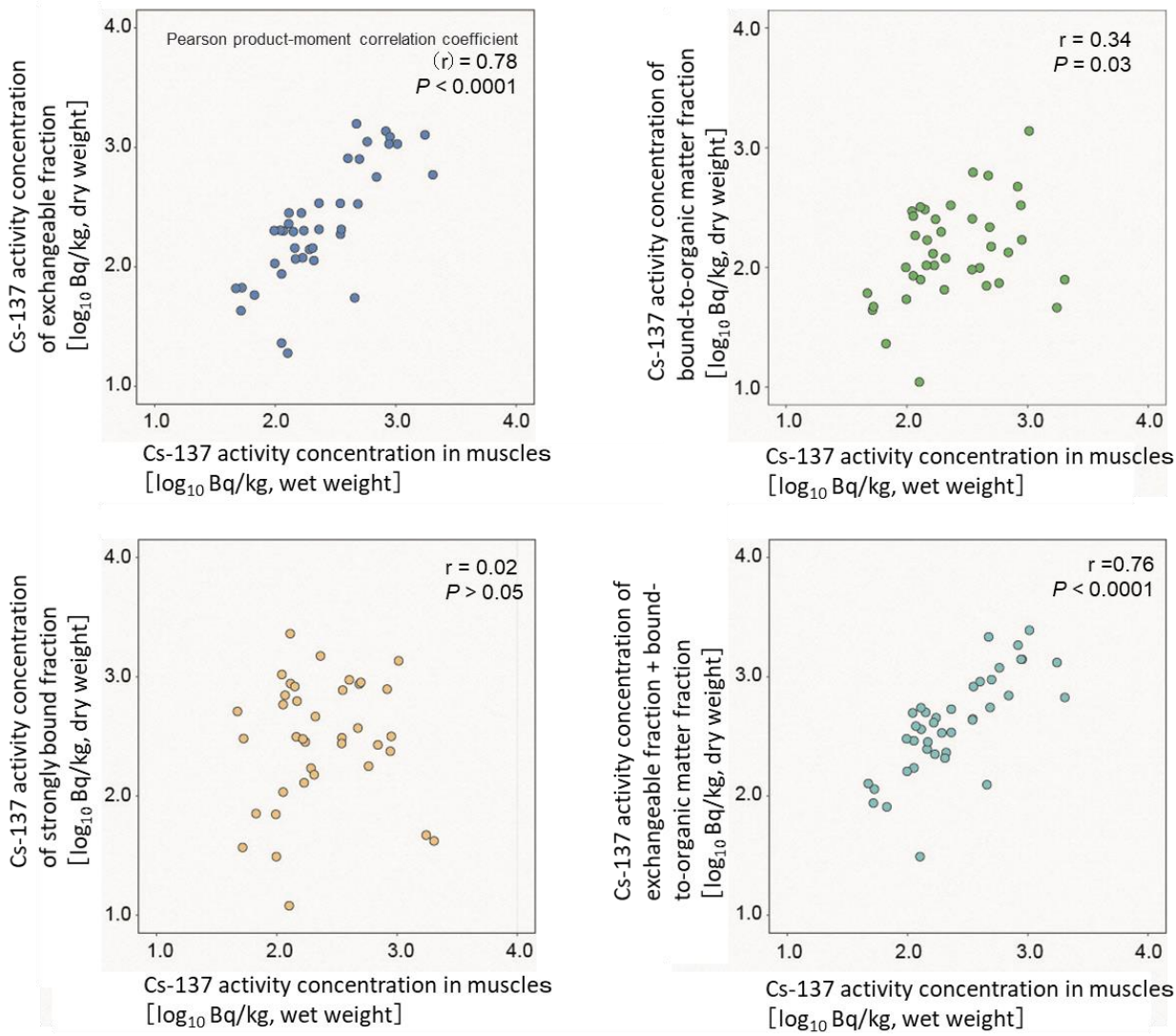

Figure 14. Correlation of the physicochemical fractions of caesium-137 activity concentrations between muscle tissue and stomach contents of wild boars

2.3.2.2. Investigating the home ranges of wild animals

We tracked boar behaviors by using a GPS collar, and could define the spatial range covered by the boar (home range) from 2013 to 2016 as shown in Figure 15. The home range was separated into a core area of a high activity concentration of measurement points (area containing almost 95% of points by activity concentration analysis) i.e. where the boar spent most of their time, and a larger roaming area containing all points (outermost area). The results of the analysis showed that the boars have two residential zones, the core area is approximately 37 ha, and the total area of their home range is 244 ha.

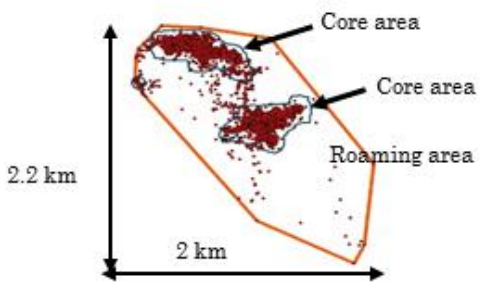

Figure 15. Example of sample structure of home range area.

We carried out wild boar home range surveys in Fukushima City (2 boars tracked for 50 and 99 days) and Tazawa, Iwashiro-chiku, Nihonmatsu City (4 boars, tracked for 9 to 110 days) outside the evacuation order zone. Figure 16 shows the survey results on the same scale (one-kilometer mesh in the figure). Fukushima City has urban and suburban environments, while Tazawa, Iwashiro-chiku, Nihonmatsu City is located between plains and mountains. The wild boars surveyed on this occasion had a core area of about 20 to 50 ha and home ranges of about 100 to 250 ha.

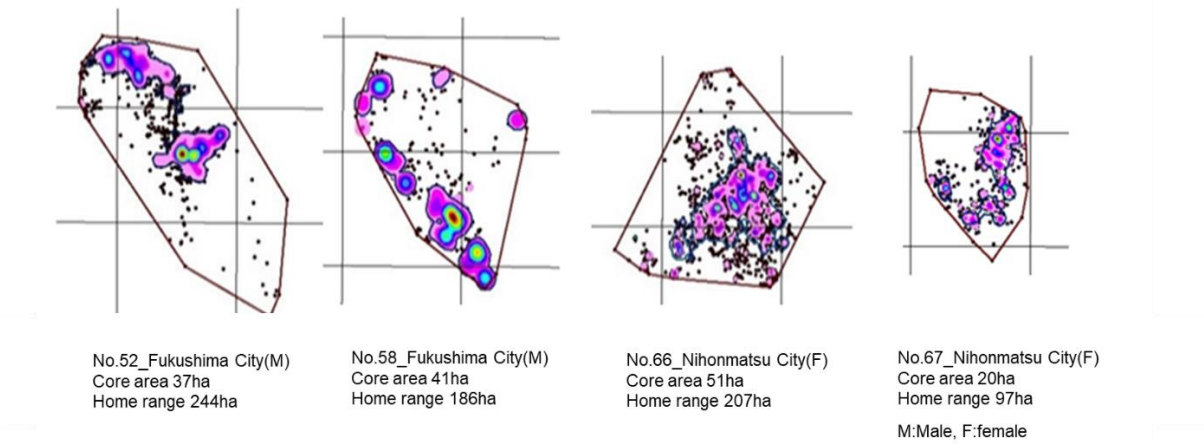

Figure 16. Size of wild boar home range outside the evacuation order zone.

We investigated wild boar home ranges in Tomioka-town, inside the evacuation order zone, to see how the ranges would change in the situation where there were fewer human activities. Figure 17 shows the core area and home range areas of 7 individuals tracked inside and outside the evacuation order zone. No. 50, 85, and 208 are in the evacuation order zone. No. 52 and 58 are in an environment around cities outside the evacuation order zone. No. 66 and 67 are in mountainous areas outside the evacuation order zone.

In the current survey, the number of animals that have been tracked is small and the sex, weight and duration of GPS collar attachment differ between individuals (Table 1). However, from the available data, the increase of human presence appears to be reducing the home ranges of wild boar.

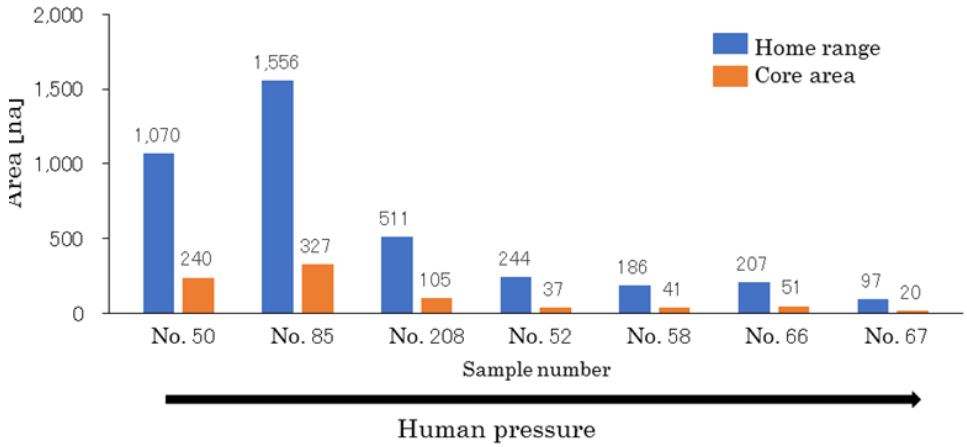

Figure 17. Comparison of home range and core area.

Table 1. Sexes, weights, and numbers of days with GPS collar

ID	No.50	No.85	No.208	No.52	No.58	No.66	No.67
Sex	M	F	F	M	M	F	F
Weight (kg)	37	48	51	44	70	35	37
Numbers of days with GPS collar	81	99	117	99	50	110	34

Wild boar home ranges may change depending on the timing of survey. Therefore, we compared the home range sizes of eight individuals (the inside of the evacuation order zone: three females and two males, the outside of the evacuation order zone: one male and two females) whose data could be acquired for one month or longer in November to December (winter), and January to February (the breeding season) in 2013 and 2014. Although the number of samples was small, the home ranges tended to be larger inside the evacuation order zone than outside (Figure 18).

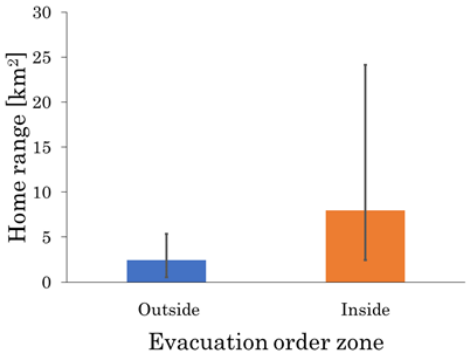

Figure 18. Average of home range size of wild boars inside and outside the evacuation zone. The error bars indicate the minimum and maximum values.

We investigated habitat type in the home ranges of individuals. In home ranges of individuals inside the evacuation order zone, farmland occupied a high percentage of the area and the results suggest that the home ranges of individuals inside the evacuation order zone includes roaming on farmland (Figure 19).

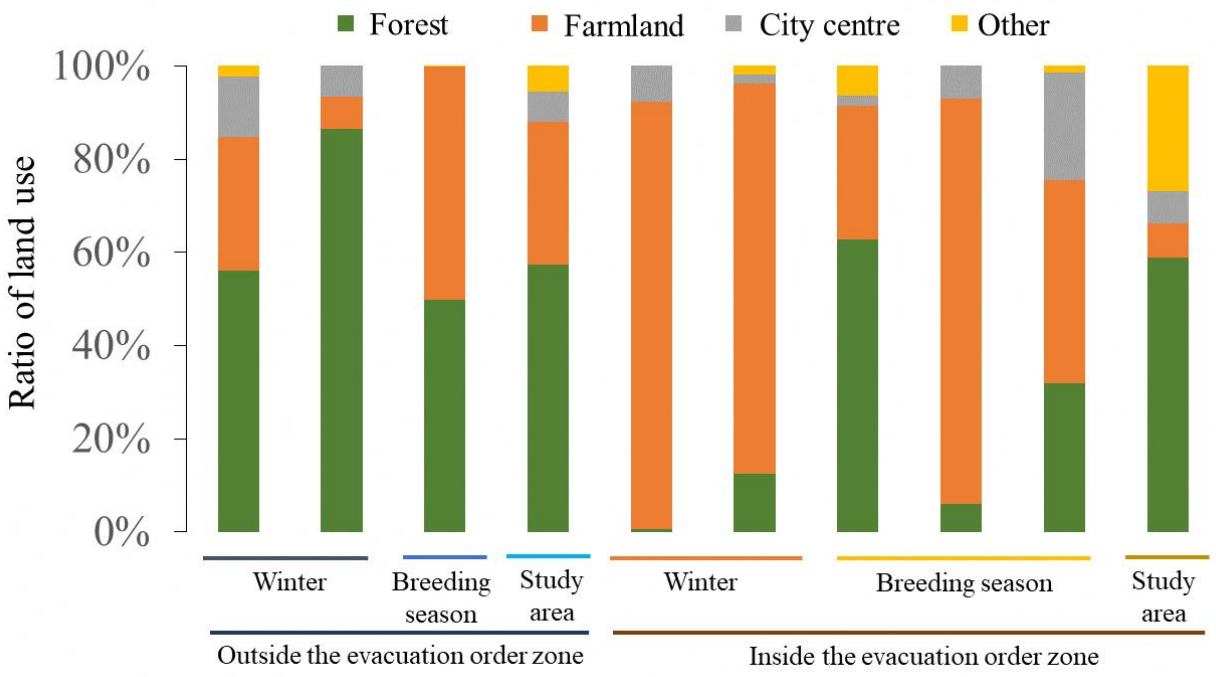

Figure 19. Ratio of land use in the home ranges of wild boars inside and outside the evacuation order zone (each bar indicates the value for an individual). Study areas showed the city where the wild boars were captured (Outside the evacuation order zone: Fukushima city and Nihonmatsu city, inside the evacuation order zone: Tomioka town).

2.4. Investigation results made from 2018 to 2022

Just as in the 2013 to 2017 period, the present survey has mainly targeted wild boars, whose radio caesium activity concentrations have been higher than those of other wild animals, and Asian black bears inhabiting the same forestry ecosystem as wild boars.

2.4.1. Content of implementation

2.4.1.1. Fluctuation of radiocaesium activity concentrations in wild animal's flesh

Regarding radionuclide activity concentrations in the muscles of wild animals inhabiting the prefecture, the Nature Conservation Division is monitoring game species such as wild boars, Asian black bears, copper pheasants, Japanese pheasants, spot-billed ducks and mallards captured for the culling by management program or for hunting, thereby identifying the caesium-134 and 137 activity concentrations in their muscles. Using the measurement results, the variations of caesium-137 in the muscles of wild boars and other animals and the fluctuations over time after the accident were also investigated.

The survey conducted from 2013 to 2017 clarified seasonal fluctuations in caesium-137 activity concentration in the muscles of wild animals (see 2.3.2.1.2. Figure 13)[5]. Based on the seasonal fluctuation patterns, the data were divided into the low-activity concentration period of April to August and the high-activity concentration period of December to March for wild boars and the

low-activity concentration period of July to September and the high-activity concentration period of November to January for Asian black bears. The long-term fluctuations of caesium-137 activity concentrations in the muscle after the accident was analyzed with a linear model that used the $\log_{10}$ conversion of the caesium-137 activity concentrations in their muscles as objective variable and the dates when they were captured and the $\log_{10}$ conversion of caesium-137 deposition density on soils at the locations where they were captured as explanatory variables. The linear model was applied in each of the low-activity concentration periods, high-activity concentration periods and the entire period.

2.4.1.1.1. Relationship with the animals' feeding habit

Previous studies (see Section 2.3.2.1.2.) showed a positive relationship between caesium-137 activity concentrations in boar muscle tissue and stomach contents, suggesting that caesium-137 activity concentrations in boar bodies are strongly influenced by ingestion of caesium-137 in food and soil (Figure 12). Therefore, with the aim of investigating factors that cause the extremely wide variations in measured values among individual wild boars and the factors that cause seasonal fluctuations and migration of high caesium-137 activity concentrations, we attempted to investigate the relationship between wild boar feeding habits and caesium-137 activity concentrations in their muscle tissues. This was carried out by (i) analyzing feeding habits based on metabarcoding methods (DNA analysis) and (ii) measuring caesium-137 activity concentrations in their main foods. DNA extracted from thoroughly agitated and crushed wild boar stomach contents was used to analyze wild boar feeding habits and the nuclear DNA ITS-2 region was analyzed to estimate herbivorous feeding habits[6].

In addition to food, wild boars are thought to ingest a large amount of soil from digging up and eating roots and stems that grow underground, but the transfer of caesium-137 into the bodies of wild boars through soil ingestion and its levels were unknown. Therefore, we considered a survey methodology to investigate the transfer of caesium-137 by soil ingestion.

Samples of main food species were collected in Nihonmatsu City and in the Adatara and Azuma Mountain ranges from 2016 to 2019. Samples of herbaceous plants (e.g., white clover, tsukushi-hagi, etc.), nuts (e.g., konara oak, Japanese oak, chestnuts, etc.), and Berry fruits (e.g., *Padus grayana*, etc.) were collected and measured for caesium-137.

2.4.1.1.2. Relationship with the animals' habitat

It has been reported that caesium-137 activity concentrations in the muscle tissues of wild animals are positively correlated with caesium-137 activity concentrations in food, and that these activity concentrations are positively correlated with caesium-137 soil deposition in the environment[7]. One possible reason for the seasonal variation in muscle caesium-137 activity concentrations could be seasonal use of locations for foraging with varying levels of caesium-137 contamination. In this study, therefore, we used behavioral data of Asian black bears wearing GPS collars in Fukushima Prefecture to examine the relationship between seasonal changes in habitat use and levels of caesium-137 contamination in these locations.

To assess the exposure dose rates of Asian black bears and wild boars in the study site, the activity concentration of caesium-137 in muscle (Bq/kg in wet weight) of Asian black bears and wild boars in the aforementioned Radiation Monitoring Survey for Wild Birds and Animals conducted by Fukushima Prefecture and caesium-137 soil deposition (Bq/m^2) at the capture location of each sample animal[8] were used to estimate the exposure dose rate (μGy/h) by ERICA tool[9].

2.4.1.2. Management of wild animals in the area contaminated by radionuclides

2.4.1.2.1. Monitoring

Caesium-134 and caesium-137 activity concentrations were measured in the muscle of pheasants captured throughout Fukushima Prefecture between October 2011 and March 2022.

2.4.1.2.2. Investigations of wild animals around the Evacuation-Designated Zone (EDZ)

We surveyed the population structure of wild boars in Fukusuhima prefecture using by multiplexed ISSR Genotyping by sequencing (MIG-seq) analysis. DNA extracted from the muscle tissue of wild boars captured widely in Fukushima prefecture and those captured in part areas in Kumamoto Prefecture that were treated as an out-group population. Single-nucleotide polymorphisms (SNPs) were obtained from genome-wide regions by MIG-seq method[10] for clarifying genetic structures of wild boars. We conducted STRUCTURE[11] and cluster analysis using the derived SNPs information. This survey was conducted in collaboration with the Fukushima Prefectural Center for Environment Creation and the National Institute for Environmental Studies.

2.4.1.2.3. Strategy to lift restrictions for distribution and consumption

History of consumption and distribution restrictions since the incident

① History of restrictions on consumption and distribution due to the nuclear incident

In response to the spread of radioactive materials from the nuclear power plant incident following the Great East Japan Earthquake on March 11, 2011, the government established on April 4, 2011 provisional regulation values for radioactive materials based on the Food Sanitation Act, and compiled the "Concepts of Inspection Planning and the Establishment and Cancellation of Items and Areas to which Restriction of Distribution and/or Consumption of Foods Concerned Applies." (hereinafter referred to as “guidelines”)

Subsequently, on April 1, 2012, the national government set the standard value for radioactive caesium in general foods at 100 becquerels/kg based on the results of previous inspections and other factors.

In this prefecture, a private research institute conducted a private survey on activity concentrations of radionuclides in muscle tissue in conjunction with the survey commissioned by the Ministry of the Environment. Since the results of the private survey were provided to the prefecture, they were made public. Since some samples from meat were found to exceed

the provisional regulation value of 500 becquerels per kilogram for radioactive materials, we reached out to prefectural residents through hunting groups and municipalities to refrain from private consumption.

Since October of the same year, the prefecture has announced and conducted surveys to measure activity concentrations of radionuclides in the meat of edible wild game in the prefecture, including wild boars, black bears, Japanese deer, pheasants, copper pheasants, and mallard ducks in seven areas of the prefecture to ensure the safety and security of the living environment.

As a result of this investigation, radioactive caesium exceeding 5,000 Bq/kg was found in wild boars in Soma City in November of the same year. Based on this, the national government (Nuclear Emergency Response Headquarters) issued a temporary order to refrain from consumption and distribution of wild boar meat originating in the Soso district, in accordance with Article 20, paragraph 3 of the Act on Special Measures concerning Nuclear Emergency Preparedness.

Subsequently, samples exceeding the standard values were detected in other areas of the prefecture, so distribution restrictions were placed on wild game including wild boars in all prefectures in July 2013. In the Kenpoku and Soso districts, the consumption restrictions still continue.

② Changes in populations of wild game (wild boars) caught in Fukushima Prefecture

Changes in numbers of wild boars caught in the prefecture since 2010 are shown in Figure 20.

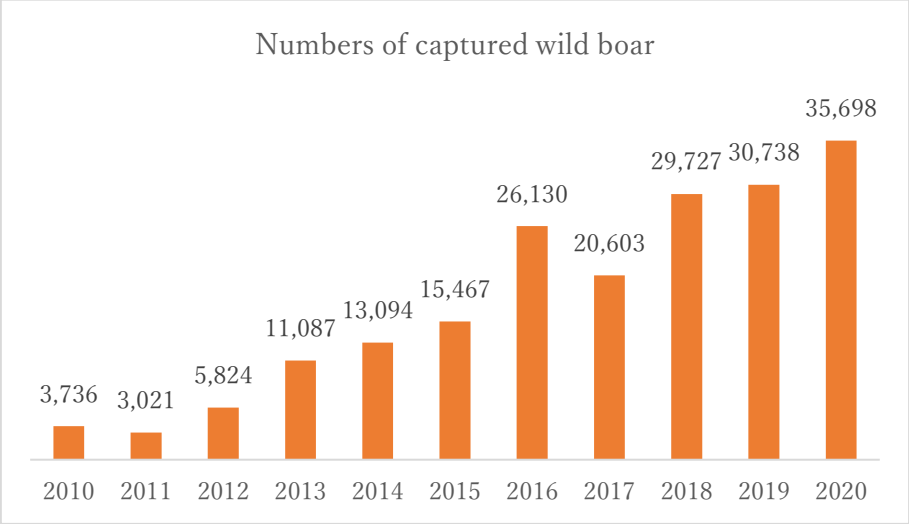

Figure 20. Numbers of captured wild boar (2010FY～)

③ Changes in the amount of damage caused by wild boar in Fukushima Prefecture

Changes in the amount of agricultural damage caused by wild boar in the prefecture since FY 2010 expressed in terms of monetary costs, are shown below in Figure 21.

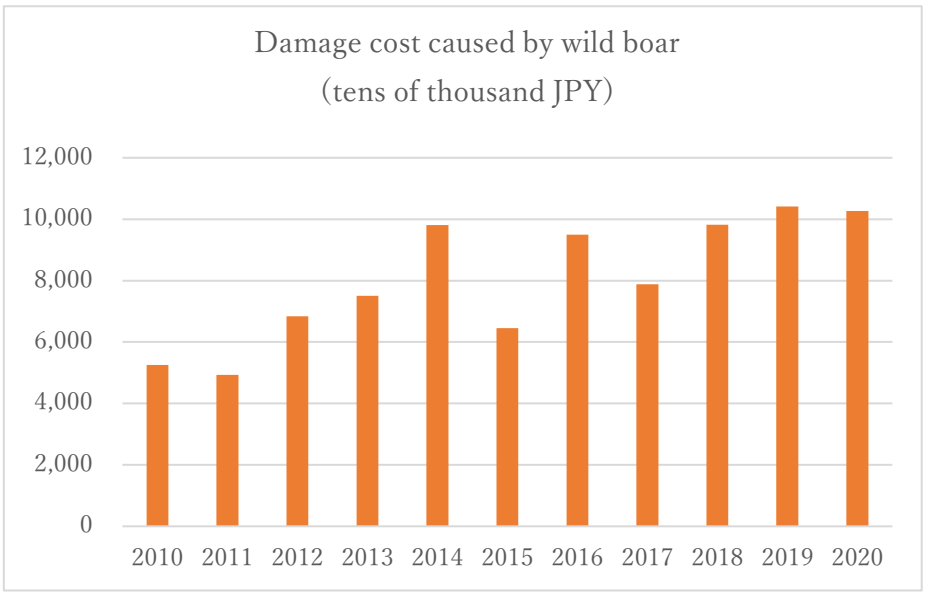

Figure 21. Damage cost caused by wild boar (2010FY～)

Management framework of radioactive material after the accident

① Issues arising from consumption and distribution restrictions

Due to national consumption and distribution restrictions, the meat of wild birds and beasts captured in Fukushima Prefecture was no longer available, limiting their capture for private consumption and sale. This made it impossible to apply sufficient trapping pressure, and the wild boar population was expected to increase and their habitat to expand, which would also cause serious damage to agricultural crops.

Therefore, Fukushima Prefecture greatly increased the number of wild boars captured to prevent an increase in the wild boar population and expansion of their habitat area, and to control damage to crops.

② The need to consider lifting the distribution restrictions for addressing challenges

Since the earthquake, in order to reduce damage caused by wild game to the living environment and agriculture, forestry and fishery industries in the prefecture, the prefecture has continued to implement measures such as habitat management and damage control by installing electric fences, etc. Direct captures were done by the prefecture workers and experts dispatched to local communities to conduct environmental research according to local conditions.

However, where the government has imposed consumption and distribution restrictions on meat from wild game, it is not possible to utilize them captured for Gibier, etc., and this has led to a decline in hunters' motivation to hunt wild animals.

③ Requirements for lifting distribution restrictions set by the government (partial excerpts from the guidelines)

【Lifting】

Area

In principle, the whole prefecture shall be covered. However, if some areas in the prefecture meet the conditions for restriction lifting and can be managed by the prefecture, municipalities, etc. so that only game caught in those areas are distributed, easing of restrictions may be made in units that clearly define the geographical range (i.e., municipalities).

Conditions for lifting restrictions

In areas where the restrictions will be lifted, inspections shall be conducted while ensuring a sufficient number of samples in consideration of the mobility, individual differences, seasonal variations, and the period of capture of wild game, and the results shall be below the standard values.

【Partial lifting】

If a system is in place to properly control and inspect the meat of wild game according to the distribution and inspection policy established by the prefecture, meat testing below the standard value may be distributed.

※Excerpt from the guidelines.

④ Current prefectural initiatives against national requirement

The prefectural government conducts radiation monitoring surveys of wild game meat for the safety and security of prefectural residents, and publishes the survey results.

The wild game covered in this survey are wild boars, black bears, pheasants, copper pheasants, spot-billed ducks, mallard ducks, common teals, Japanese deer, and hares.

An overview of the survey results (wild boars) to date is shown below.

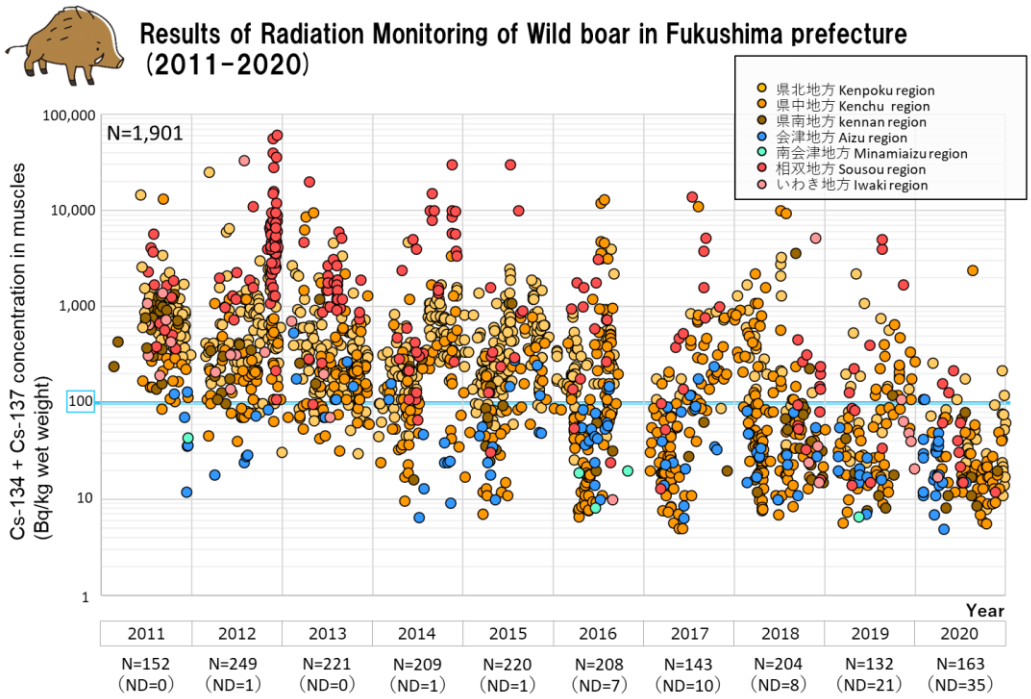

Figure 22. Monitoring result of caesium-134 + caesium-137 activity concentration in the flesh of wild animal (wild boar; 2011FY～2020FY)

In response to the situation, with the cooperation of the IAEA, we discussed, among other things, what methods should be used to meet the requirements indicated by the national government to lift consumption and distribution restrictions for wild game meat.

As the requirements for lifting restrictions are indicated in the guidelines, “ensuring a sufficient number of samples” is required. However, there is no specific number of samples nor relationship between the location where the samples were captured and the area where the restrictions will be lifted.

2.4.2. Results

2.4.2.1. Fluctuation and its reasons of radionuclides’ activity concentration in wild animal’s flesh

Figure 23 shows the caesium-134+137 activity concentrations in the muscles of wild boars and Asian black bears captured in Fukushima Prefecture in May 2011 to March 2022.

a)

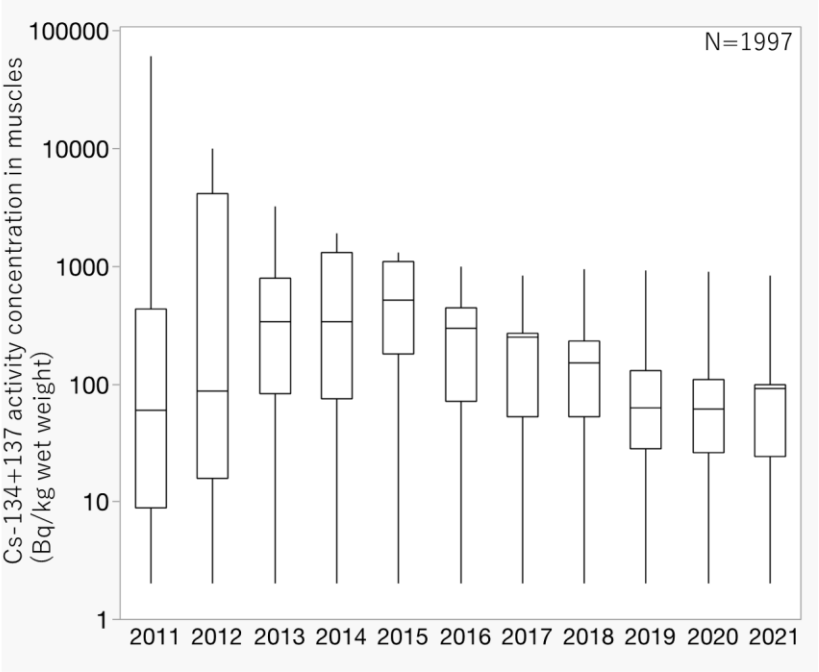

b)

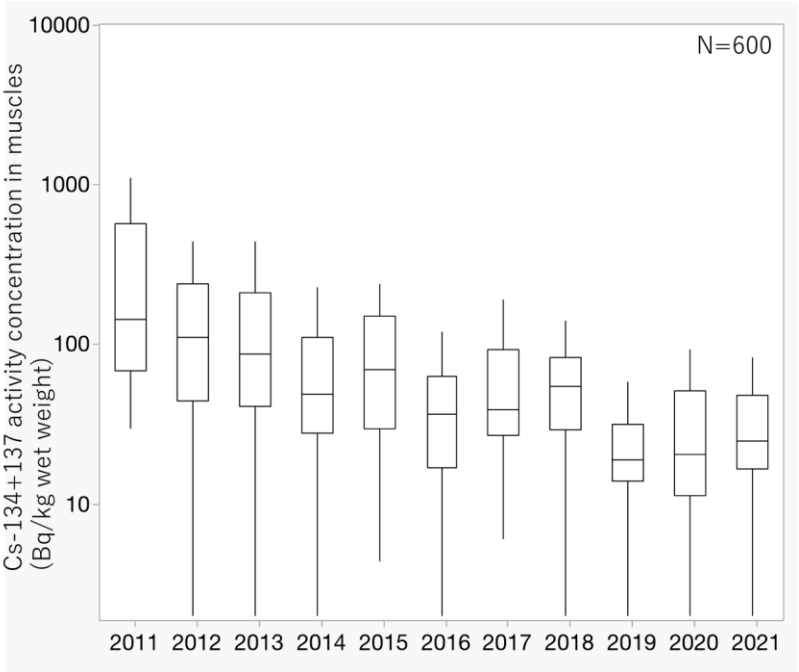

Figure 23. Results of measuring the caesium-134+137 activity concentrations in the muscles of (a) wild boars and (b) Asian black bears

* The 1st quartile (25%) and the 3rd quartile (75%) are indicated by the upper and lower ends of each box respectively, and maximum and minimum values are indicated by bars (those less than lower detection limit excluded).

The caesium-134+137 activity concentrations in the muscles of wild boars showed large variation among individuals. Some of them showed activity concentrations lower than the detection limit

although others shown higher activity concentrations than 10 times of the standard value of activity concentration. Asian black bears showed caesium-134+137 activity concentrations exceeding 100 Bq/kg[*1], which is the limit for general foodstuffs in Japan, were also found in FY 2021 ([*1]Sum of caesium-134 and -137).

Figure 24 shows the color-coded results of monitoring caesium-137 activity concentrations in the muscles of wild boars and Asian black bears in the regions of Fukushima prefecture.

a)

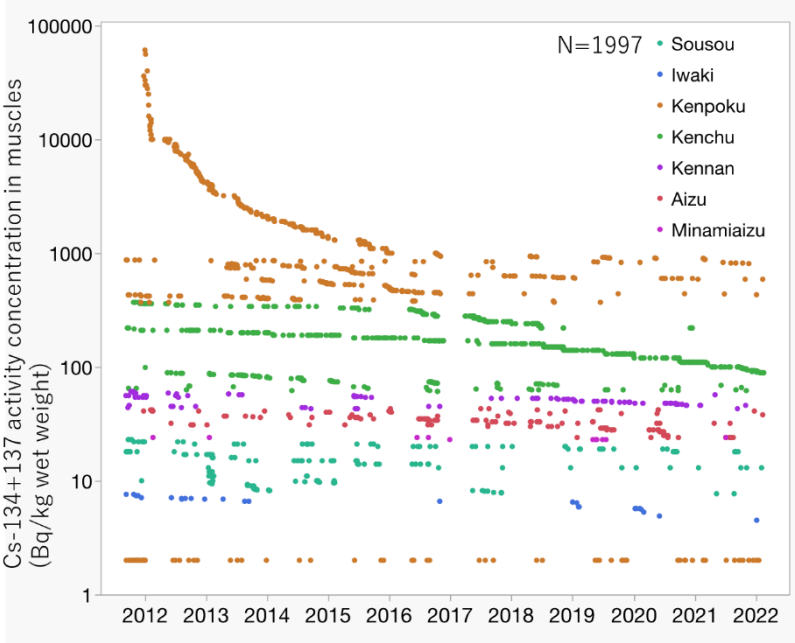

b)

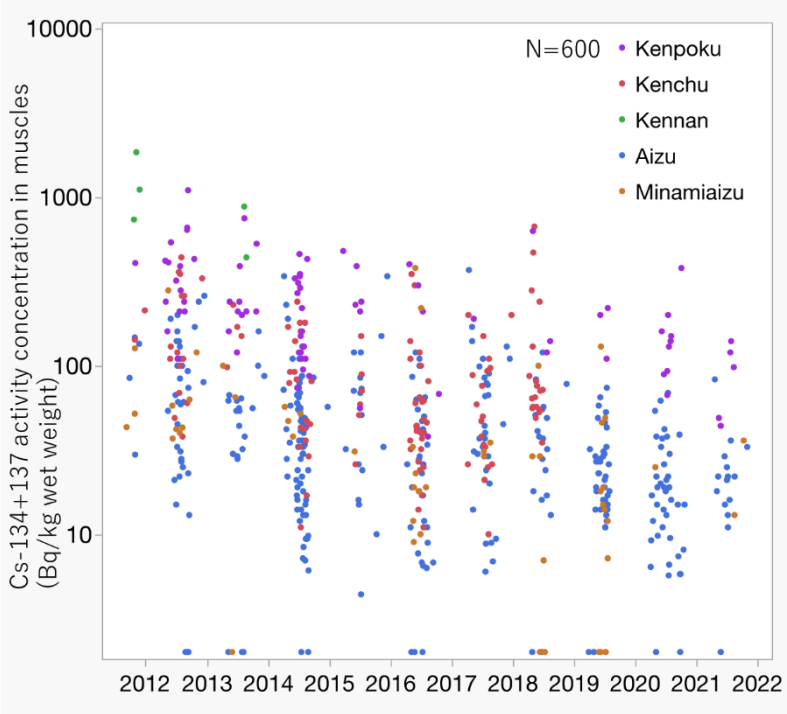

Figure 24. Caesium-137 activity concentrations in the muscles of (a) wild boars and (b) Asian black bears (in regions where they were captured)

* Each dot indicates the measured value for each wild animal.

The survey conducted from 2013 until 2017 revealed that the caesium-137 activity concentrations in the muscles of wild boars and Asian black bears were positively affected by the caesium-137 deposition density on the soils of locations where they were captured (see 2.3.2.1.1. Fig.8)[7]. In the Soso District, Ken-poku District and Ken-chu District, where the caesium-137 deposition density on soils was relatively high, many wild boars and Asian black bears with high caesium-137 activity concentrations were captured. In the Aizu District and Minami-Aizu District, where the caesium-137 deposition density on soils was relatively low, many wild boars and Asian black bears with low caesium-137 activity concentrations were captured.

Long-term variations in radio caesium activity concentrations in Asian black bear and wild boar muscle tissues

To understand long-term variations in the activity concentration of radionuclides in Asian black bear and wild boar muscle tissues, we analyzed the long-term variations of caesium-137 activity concentrations in the muscle of both species. Data collected from May 2011 to March 2016 from the Radiation Monitoring Survey for Wild Birds and Animals conducted by Fukushima Prefecture were used. Since seasonal variations were already known for Asian black bears and wild boars[5], based on that report, both data were used with divisions between low activity concentration periods (Asian black bear: July-September, wild boar: April-August) and high activity concentration periods (Asian black bear: November-January, wild boar: December-March). Using data from the low-activity concentration periods, the high-activity concentration periods, and all periods combined, a linear model was estimated with log10-transformed caesium-137 activity concentrations in muscle tissues (Bq/kg wet weight) as the objective variable and the capture date of each individual and log10-transformed caesium-137 soil deposition (Bq/m^2)[8] as explanatory variables. The estimated linear model was selected by Akaike's information criterion (AIC).

As a result, a model that included capture dates and log10-transformed caesium-137 soil depositions as explanatory variables was selected for Asian black bears in the low-activity concentration period, the high-activity concentration period, and all periods combined (Table 2). The long-term variation showed a decreasing trend in each period, while the 95% confidence interval of the estimated value tended to increase with time in the high activity concentration period (Figure 25). This is attributed to a limited amount of data.

Table 2. Model of long-term variation of caesium-137 activity concentration in muscle of Asian black bears

Period	AIC	Delta AIC	Intercept	Explanatory variables	
				Capture date	log10 (Cs-137 soil deposition)
Entire period	151.6	0.00*	7.729	-0.0002	0.6189
(n=271)	168.6	16.92	-1.057		0.6394
	319.7	168.03	13.930	-0.0002	
	337.6	186.00	1.768		
Low activity	57.2	0.00*	6.819	-0.0002	0.7111
concentration	68.8	11.59	-1.497		0.7226
period	222.7	165.47	12.520	-0.0002	
(n=191)	230.5	173.25	1.706		
High activity	20.9	0.00*	-0.4854		0.5785
concentration	22.8	1.90*	1.2520	$-4.036*10^{-5}$	0.5631
period	35.5	14.52	12.3400	$-2.486*10^{-4}$	
(n=28)	36.0	15.07	2.0570		

*: Valid model（Delta AIC<2.0）

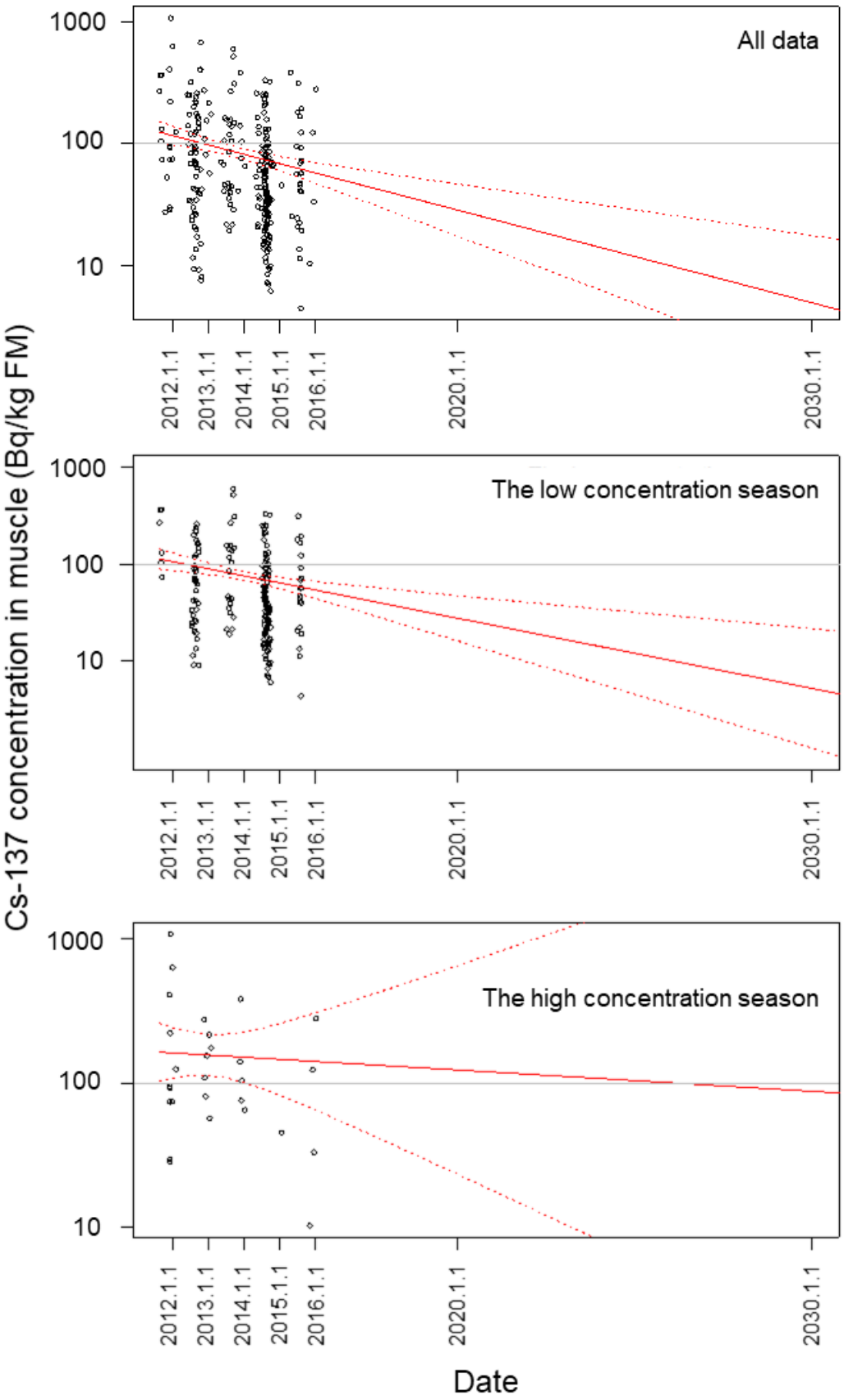

Figure 25. Long-term variation of caesium-137 activity concentration in muscle of Asian black bears

For wild boars, a model which included capture date and log10-transformed caesium-137 soil deposition as explanatory variables for the low-activity concentration period, the high-activity concentration period, and the entire period was also selected (Table 3). In each period, a decreasing trend was observed over time, but the degree of the decrease was small. This trend was similar to that observed in wild boars in Europe[12].

Table 3. Model of long-term variation of caesium-137 activity concentration in muscle of wild boars

Period	AIC	Delta AIC	Intercept	Explanatory variables	
				Capture date	log10 (Cs-137soil deposition)
Entire period	1514.0	0.00*	7.656	-0.0002	0.7409
(n=1031)	1578.9	37.87	-1.200		0.7377
	1865.6	324.62	10.960	-0.0002	
	1890.5	349.53	2.444		
Low activity	338.6	0.00*	14.140	-0.0004	0.7353
concentration	367.6	28.98	-1.425		0.7342
period	438.9	100.30	17.660	-0.0004	
(n=285)	458.7	120.10	2.168		
High activity	720.9	0.00*	2.738	$-9.061*10^{-5}$	0.7308
concentration	722.1	1.12*	-1.033		0.7320
period	838.1	117.18	6.631	$-9.671*10^{-5}$	
(n=456)	838.9	117.92	2.612		

*: Valid model（Delta AIC<2.0）

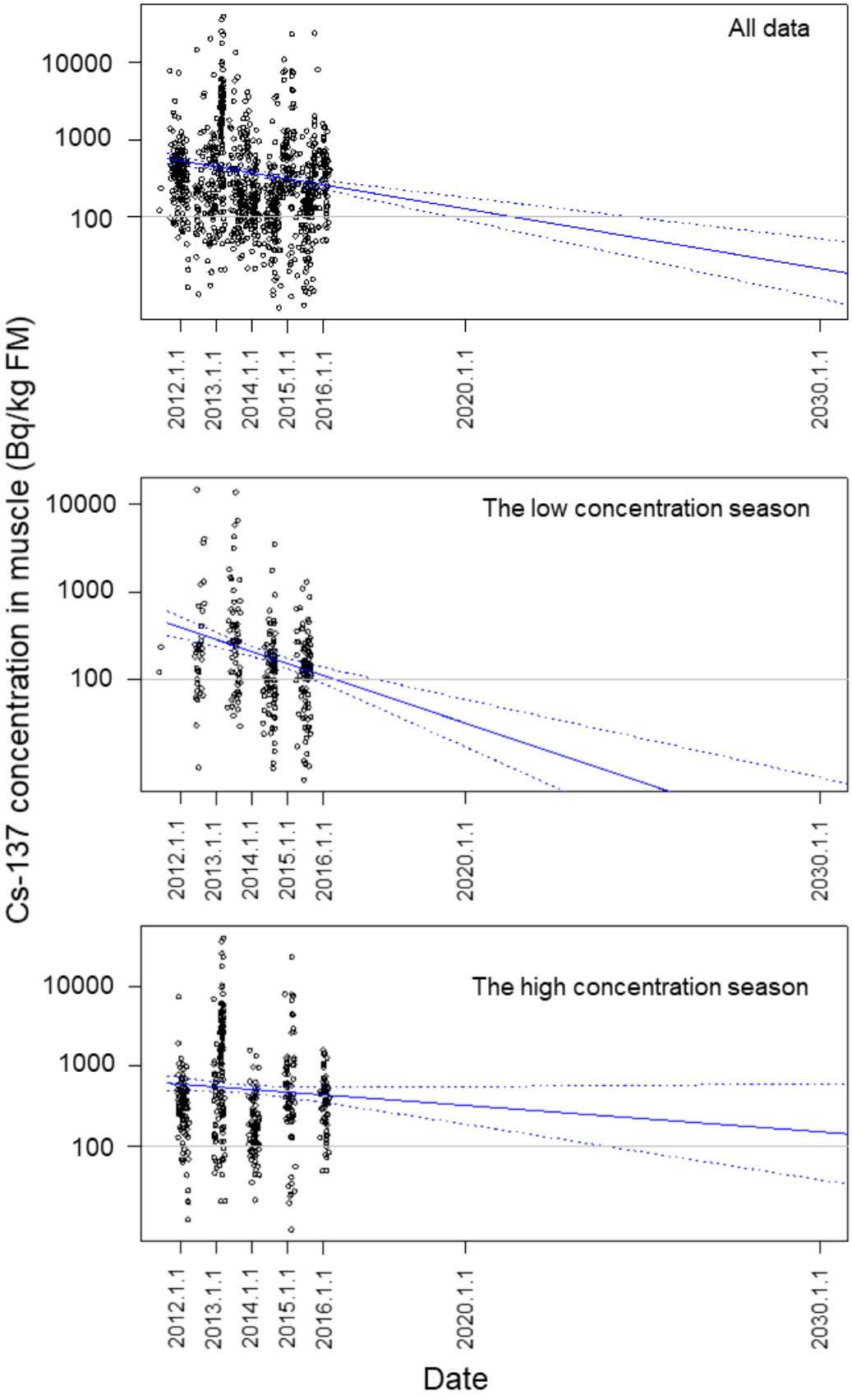

Figure 26. Long-term variation of caesium-137 activity concentration in muscle of wild boars

Differences in radio caesium activity concentrations in muscle tissues of Asian black bears and wild boars based on sex

To clarify the differences in the degree of radionuclide transfers from the environment to the bodies of Asian black bears and wild boars (depending on sex), we conducted analyses using monitoring data from the Radiation Monitoring Survey for Wild Birds and Animals by Fukushima Prefecture, in the same as 1) Long-term variation of radio caesium activity concentration in muscle tissues of Asian black bears and wild boars (hereinafter referred to as 1). Data used were divided into low and high activity concentration periods as in 1). In the low and high activity concentration periods, a linear mixed model was estimated with log10-transformed caesium-137 activity concentration s in muscle tissues (Bq/kg wet weight) as the objective variable, log10-transformed caesium-137 soil deposition (Bq/m^2)[8] at the capture location of each sample animal as the explanatory variable, sex as the interaction term for the explanatory variable, and the capture year of each animal as a random effect, to examine the effect of sex on the relationship between caesium-137 activity concentrations in muscle tissues and caesium-137 activity concentrations at capture locations. Subsequently the model selection was performed by AIC.

As result, for both Asian black bears and wild boars, only log10-transformed caesium-137 soil deposition (Bq/m^2) was included as an explanatory variable in the models selected for each period, but not sex (Tables 4 and 5). This result indicates that there is no difference between sexes in the extent of radionuclide transfer from the environment to the body for both species (Figures 27 and 28). Sexual dimorphism (i.e., body size) has been reported to be an important variable in ecological factors in wild animals[13, 14]. It is known that there are regional differences of Asian black bears and wild boars regarding sexual dimorphism in home range size, habitat selection, and behavioral patterns[15-18]. In this study, it is possible that there are no differences in sexual dimorphism and associated ecological factors in Asian black bears and wild boars in the region compared to other regions. Future studies of ecological factors such as behavior and sexual dimorphism, such as in body size, may shed light on these factors.

Table 4. Linear mixed model estimating the effect of sex on the relationship of caesium-137 activity concentration between in muscle and at the capture location of Asian black bears

Period	AIC	Delta AIC	Intercept	Explanatory variables
Low activity concentration period (n=191)	69.1	0.0*	-1.372	0.7076*log10 (Cs-137soil deposition)
	78.5	9.4	-1.370	log10 (Cs-137soil deposition) * Sex Female: 0.7064 Male: 0.7076
	229.3	160.2	-1.804	
High activity concentration period (n=28)	29.1	0.0*	-0.485	0.5785*log10 (Cs-137soil deposition)
	34.5	5.4	-0.275	log10 (Cs-137 soil deposition) * Sex Female: 0.5535 Male: 0.5146
	41.2	12.1	2.057	

*: Valid model（Delta AIC<2.0）

Table 5. Linear mixed model estimating the effect of sex on the relationship of caesium-137 activity concentration between in muscle and at the capture location of wild boars

Period	AIC	Delta AIC	Intercept	Explanatory variables
Low activity concentration period (n=285)	350.2	0.0*	-1.300	0.7192*log10 (Cs-137soil deposition)
	356.9	6.7	-1.344	log10 (Cs-137soil deposition) * Sex Female: 0.7178 Male: 0.7349
	442.4	92.2	2.211	
High activity concentration period (n=456)	650.7	0.0*	-0.776	0.5785*log10 (Cs-137soil deposition)
	659.0	8.3	-0.794	log10 (Cs-137soil deposition) * Sex Female: 0.5535 Male: 0.5146
	762.6	111.9	2.561	

*: Valid model（Delta AIC<2.0）

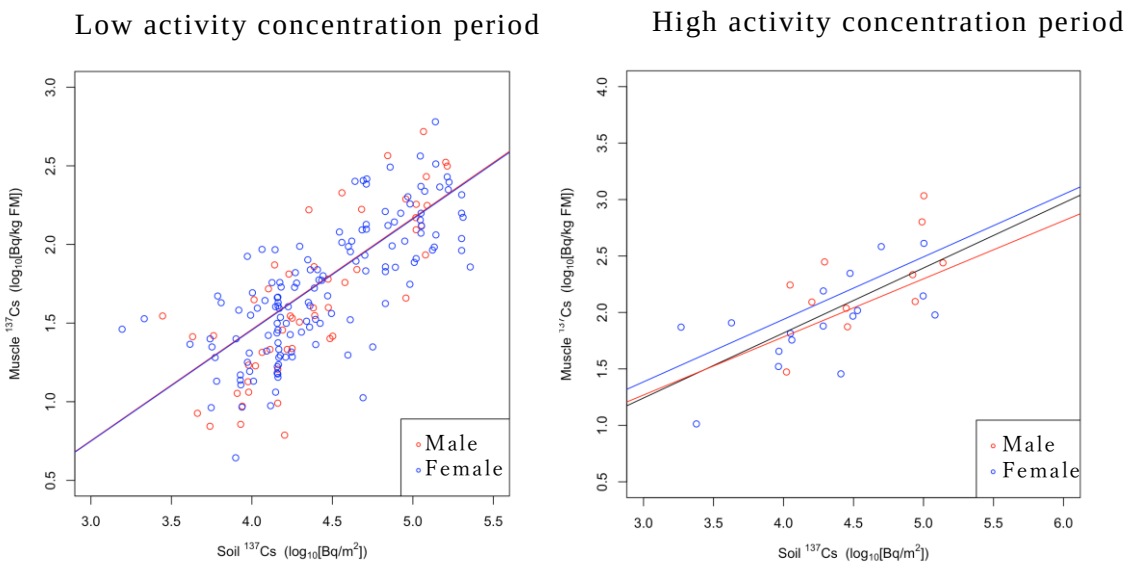

Figure 27. Relationship of caesium-137 activity concentration between in muscle and at the capture location by each sex of Asian black bears

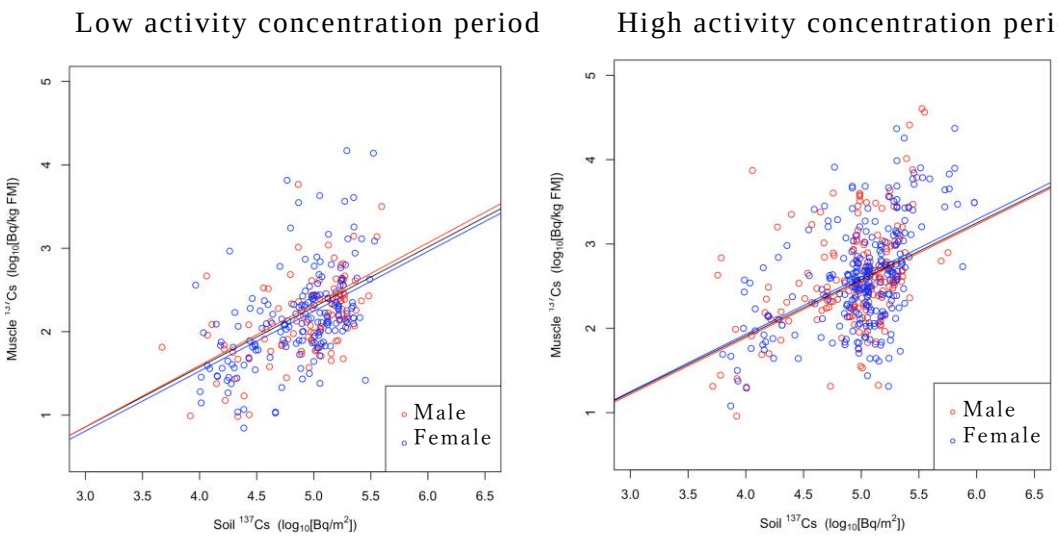

Figure 28. Relationship of caesium-137 activity concentration between in muscle and at the capture location by each sex of wild boars

2.4.2.1.1. Relationship with the animals' feeding habit

In the results of feeding habits analysis for wild boars captured in Nihonmatsu City in FY 2017, many individuals that fed on nuts (e.g., Japanese oaks and chestnuts) were found during the activity concentration increasing period (September to November) and the high activity concentration period (December to March). The results of caesium-137 activity concentrations in food are shown in Figure 29. Nuts tended to have higher caesium-137 activity concentrations than herbaceous and berry fruits. The relationship between the feeding habits of wild boars and the activity concentration of caesium-137 in their muscle tissues will be investigated in the future using DNA analysis and other methods, with researchers taking the lead in cooperative studies.

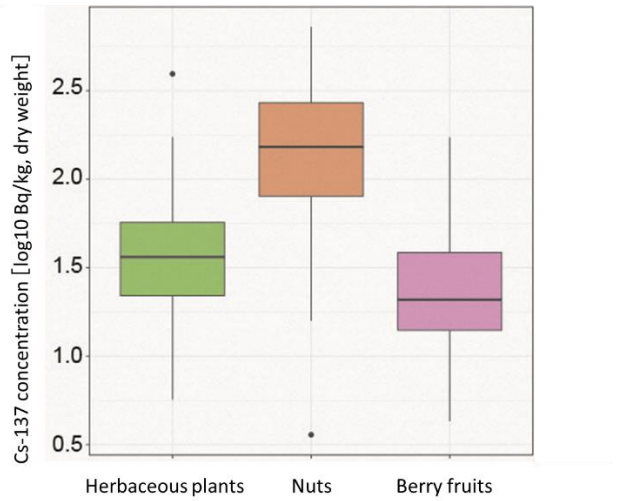

Figure 29. Caesium-137 activity concentrations in herbaceous plants, nuts and berry fruits

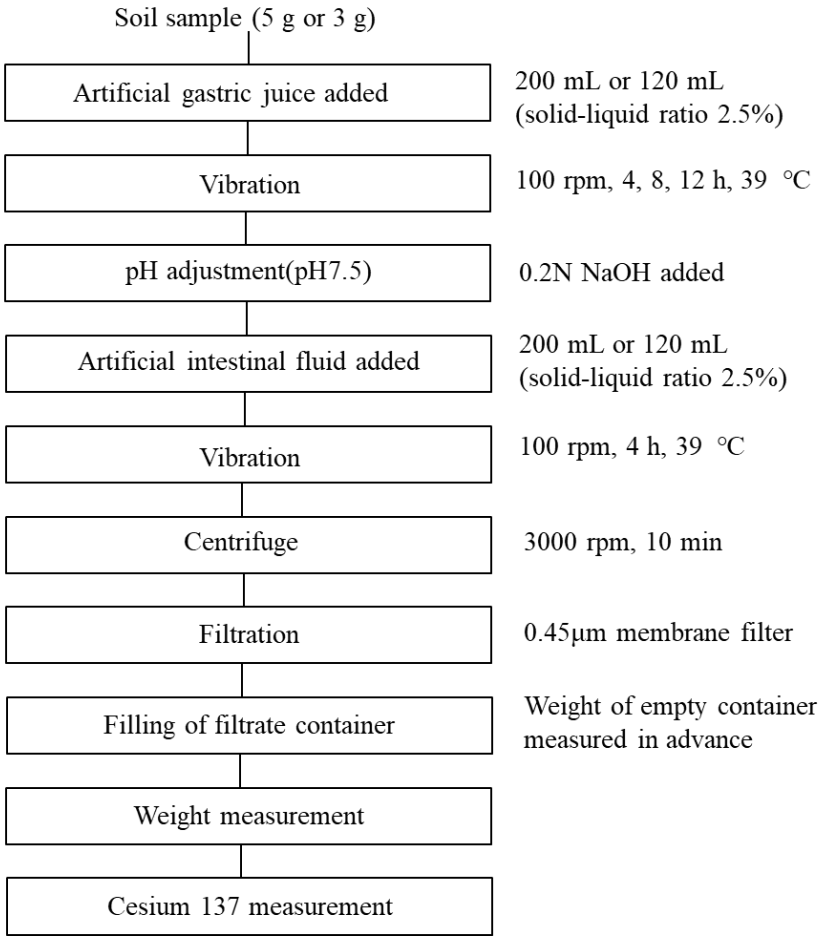

Artificial gastric juice :2.0 g/L pepsin solution prepared with 0.075 NHCl
Artificial gastric juice: 1.5 g/L pancreatin solution prepared using 0.2M phosphate buffer

Figure 30. Experimental methodology for leaching of radiocaesium from soil in the stomach and small intestine of wild boar

In evaluating the transfer of caesium-137 by soil ingestion of wild boars, we devised a method for soil radio caesium leaching in the stomach and small intestine of wild boars (Figure 30), based on the "artificial digestion test method mimicking digestion in the stomach and small intestine of pigs[19)]" as shown below. Data collection by this method, using soil collected in Fukushima Prefecture, will be conducted in the future with researchers taking the lead in the cooperative study.

2.4.2.1.2. Relationship with the animals' habitat

Changes in wildlife habitat use and radio caesium contamination of use locations

It has been reported that caesium-137 activity concentrations in the muscle tissues of wild animals are positively correlated with caesium-137 activity concentrations in food, and that caesium-137 these activity concentrations are positively correlated with caesium-137 soil deposition in the environment[7)]. One possible reason for the seasonal variation in muscle caesium-137 activity concentrations could be seasonal use of locations for foraging with varying degrees of caesium-137 contamination. In this study, therefore, we used behavioral data of Asian black bears wearing GPS collars in Fukushima Prefecture to examine the relationship between seasonal

changes in habitat use and degrees of caesium-137 contamination in these locations.

In 2018, bear traps were set in national forests in Otama Village (Figure 31) and three sample animals that were captured in the forests of Koriyama City by the Koriyama City Hunting Club were anesthetized, fitted with GPS collars and released. Date on the captured bears are shown in Table 6. Age estimates were taken by sectioning extracted the first premolars and counting the annual growth rings at the roots in cross section. The home ranges shown in Table 5 were estimated using the 100% Minimum Convex Polygon (hereafter referred to as 100% MCP) (Figure 32). The GPS collars worn were set to record one GPS location point every hour.

Figure 31. Capture locations: Traps for bears were set up in the national forests enclosed by light blue lines.

Table 6. Information on captured individuals which are obtained by behavioral data from GPS collars

Individuals' ID	Sex	Age	Weight (kg)	Data period	Home range size (km^2; 100% MCP)
AM01	Male	9	74	2018/7/23-2019/8/30	74
AM02	Male	10	114	2018/8/14-2019/7/30	104
AM03	Male	4	53	2018/10/28-2019/7/30	269

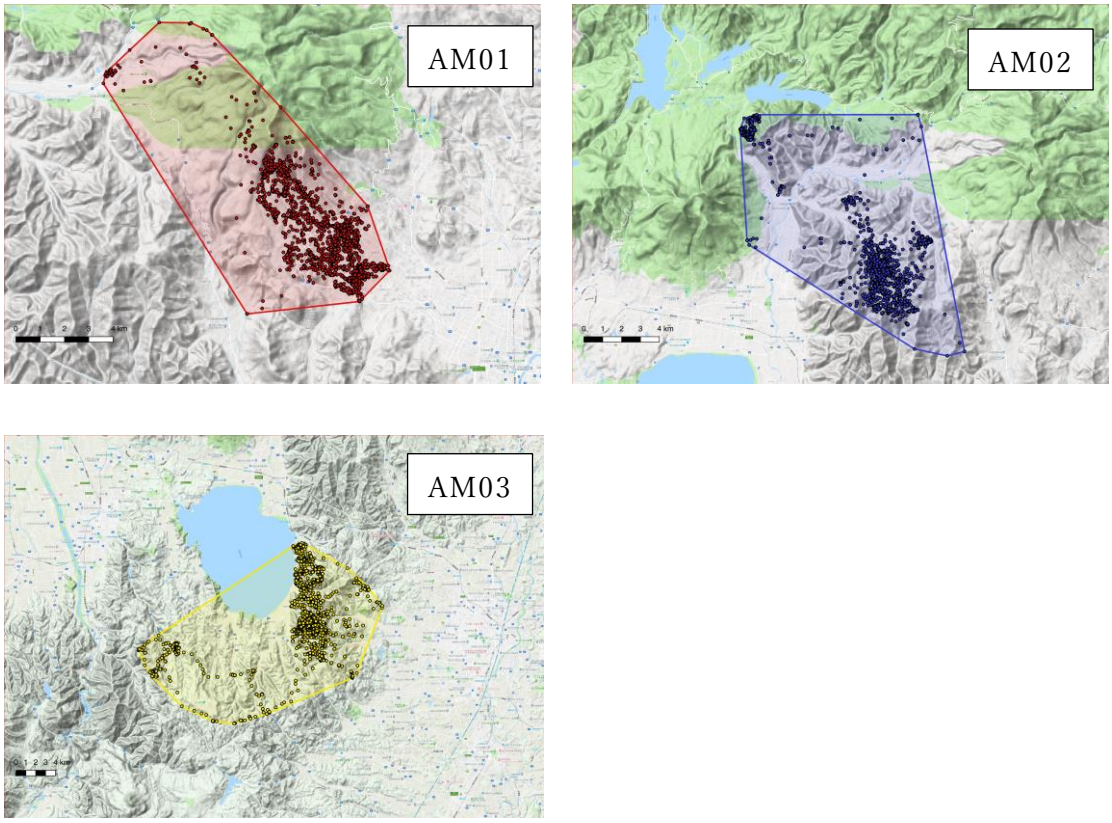

Figure 32. Home ranges of each individual estimated by 100% MCP

Using the behavioral data from these GPS collars, we first analyzed seasonal changes in caesium-137 soil deposition (Bq/m^2)[8] at the use location. As use locations, the 95% Brownian Bridge Movement Model[20] (hereafter referred to as BBMM) and 50% BBMM were used for each sample animal and each month using the obtained GPS points to estimate its home range and intensive use area. Random points were then created at a density of 100 points/km^2 in each home range and intensive use area. Caesium-137 soil deposition (Bq/m^2) at each random point was obtained from a caesium-137 soil deposition map[8]. A generalized Additive Mixed Model (hereinafter referred to as GAMM) assuming gamma distribution was estimated to estimate the seasonal variation of caesium-137 soil deposition within the home ranges and intensive use area by using the caesium-

137 soil deposition at the obtained random points as the objective variable, months in the home ranges and intensive use areas where the random points were generated as explanatory variables, and individual IDs as random variables. The estimate models were selected by AIC.

Next, to analyze relationships between caesium-137 soil depositions and environmental factors, we created an outer contour of GPS points for all individuals and generated 100 random points/km^2 within the contour.

Then, environmental factors (i.e., elevation, distance from urban land, distance from farmland, vegetation [beech (*Fagus crenata*) forest, Japanese oak (*Quercus crispula*) forest, berried fruit (e.g. *Malus toringo* and *Cerasus* sp.) forest, planted forest, conifer forest, broadleaf forest, mixed forest, shrub forest, grassland, naked land]) and the caesium-137 soil deposition at each random point were obtained. Linear models were estimated using caesium-137 the soil deposition at each random point as the objective variable and each environmental factor as explanatory variables. The estimated models were selected by AIC.

In addition, to clarify the seasonal variation pattern of each environmental factor at its use location, we obtained environmental factors at random points generated in the home ranges and intensive use area as described above, and then estimated its GAMM with each environmental factor as the objective variable, the month in which the home ranges and intensive use area were used as explanatory variables, and individual IDs as random variables.

To further clarify habitat selection for each month, the Generalized Linear Mixed Model (hereafter referred to as GLMM) assuming a binomial distribution was estimated using environmental factors obtained at random points generated in each of the above-mentioned home ranges and intensive use areas, with the binary variable set to 0 if each random point was in the home ranges and 1 if it was in the intensive use area as the objective variable, each environmental factor as the explanatory variable, and individual IDs as random variables. The estimated models were selected by AIC.

The results showed that caesium-137 soil deposition within the home ranges did not change seasonally, while caesium-137 soil deposition within the intensive use area did. However, such a seasonal variation pattern differed from the radio caesium activity concentration patterns in muscle tissues which decreases from spring to summer and then increases during winter[5], showing a decrease from April to June, and a sharp increase in July, and then a decrease during winter.

Table 7. GAMM which estimated monthly variation of caesium-137 soil deposition within the home ranges and intensive use area

Use location	AIC	Delta AIC	Intercept	Explanatory variables
Home ranges	-316853.3	0*	$2.29*10^{-5}$	
	-316631.4	221.89	$2.30*10^{-5}$	Month
Intensive use area	-32344.5	0*	$2.55*10^{-5}$	Month
	-32240.4	104.16	$2.55*10^{-5}$	

*: Valid model（Delta AIC<2.0）

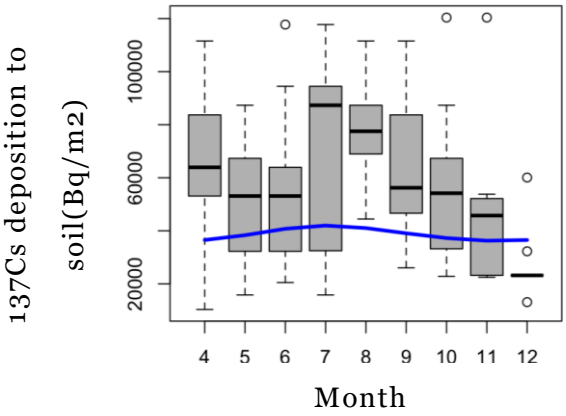

Figure 33. Seasonal variation of caesium-137 soil deposition within the intensive use area

The center horizontal line indicates the mean, the box indicates 75% of the data, and the bar indicates 95% of the data.

The blue line shows the regression curve estimated by GAMM.

The results of the relationship between caesium-137 soil deposition and environmental factors in the study site are shown in Table 8. Locations closer to the farm and urban lands as well as lower elevations, caesium-137 soil deposition tended to be higher. Caesium-137 soil depositions tended to be higher in the locations proportionate to higher activity concentrations of beech forests, broadleaf forests, coniferous forests, planted forests, mixed forests, scrub forests, grassland, or naked land. On the other hand, caesium-137 soil depositions tended to be lower in locations with a higher proportion of Japanese oak and Berry fruit forests.

Seasonal variations of environmental factors in the home ranges and intensive use areas are described in Figures 34-37 (based on the above results of the relationship between caesium-137 soil deposition and environmental factors in the study site), which are divided into negative and positive relationships with caesium-137 soil deposition. Regarding the environmental factors that were negatively related to caesium-137 soil deposition, a similar pattern of seasonal variations in muscle tissue caesium-137 activity concentrations was observed for all environmental factors

except for berry fruit forests in both the home ranges and intensive use areas. This seasonal use pattern of environmental factors may be account for the inconsistency of seasonal pattern of caesium-137 soil depositions within the home ranges and why the seasonal pattern of caesium-137 soil deposition within the intensive use area does not follow the seasonal pattern of caesium-137 activity concentration in muscle tissue. On the other hand, environmental factors that were positively related to caesium-137 soil deposition showed a pattern of seasonal variation similarly to the seasonal variation of caesium-137 activity concentrations in muscle tissues in beech forests, both in the home ranges and in the intensive use area. Therefore, it is likely that seasonal variations in beech forest use affects seasonal variations in caesium-137 activity concentrations in muscle. The seasonal variation in use locations pattern revealed that the Asian black bears in the study area gradually increase their use of broadleaf forests, planted forests, and berry fruit forests at lower elevations from spring to summer, (resulting in closer proximity to farm and urban lands), while gradually increasing their use of Japanese oak forests and beech forests at higher elevations from autumn to winter.

Table 8. Relationship between caesium-137 soil deposition and environmental factors in the study site

Environmental factor	Regression coefficient	Standard error	t value	Pr (>|t|)
Distance from the farmland	-1533.49	93.85	-16.34	<2e-16
Distance from the urban land	-1820.86	87.26	-20.87	<2e-16
Elevation	-5415.76	102.71	-52.73	<2e-16
Beech forests	22147.57	185.73	119.25	<2e-16
Japanese oak forests	-9347.18	171.6	-54.47	<2e-16
Berry fruits forests	-8170.12	111.73	-73.12	<2e-16
Broadleaf forests	10521.41	94.93	110.83	<2e-16
Coniferous forests	1514.94	81.96	18.48	<2e-16
Planted forests	9818.76	103.88	94.52	<2e-16
Mixed forests	1573.31	82.4	19.09	<2e-16
Scrub forests	1901.41	82.66	23	<2e-16
Grassland or naked land	4363.89	88.4	49.37	<2e-16

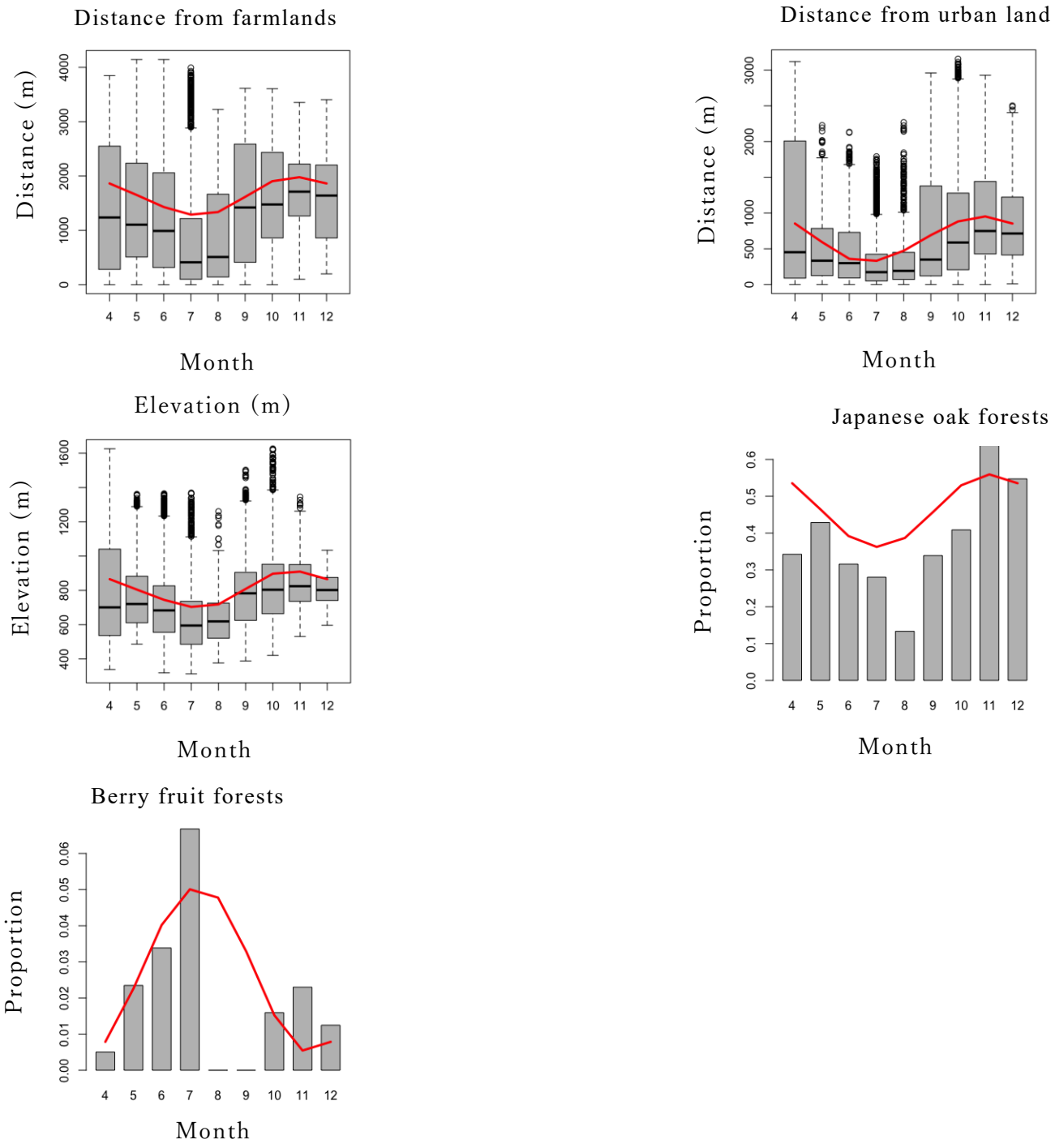

Figure 34. Seasonal variation of environmental factors negatively related to caesium-137 soil deposition within the home ranges

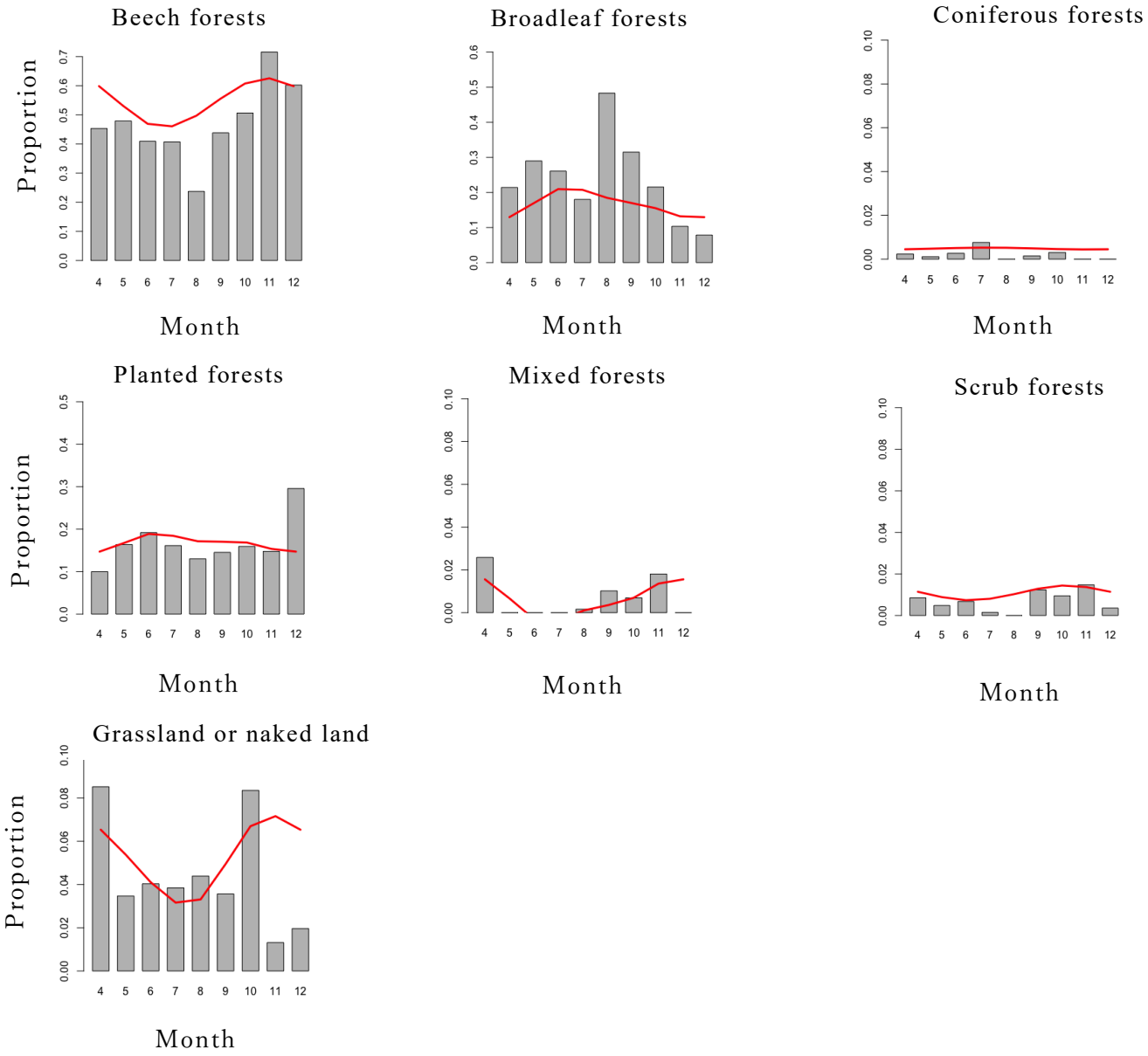

Figure 35. Seasonal variation of environmental factors positively related to caesium-137 soil in home range

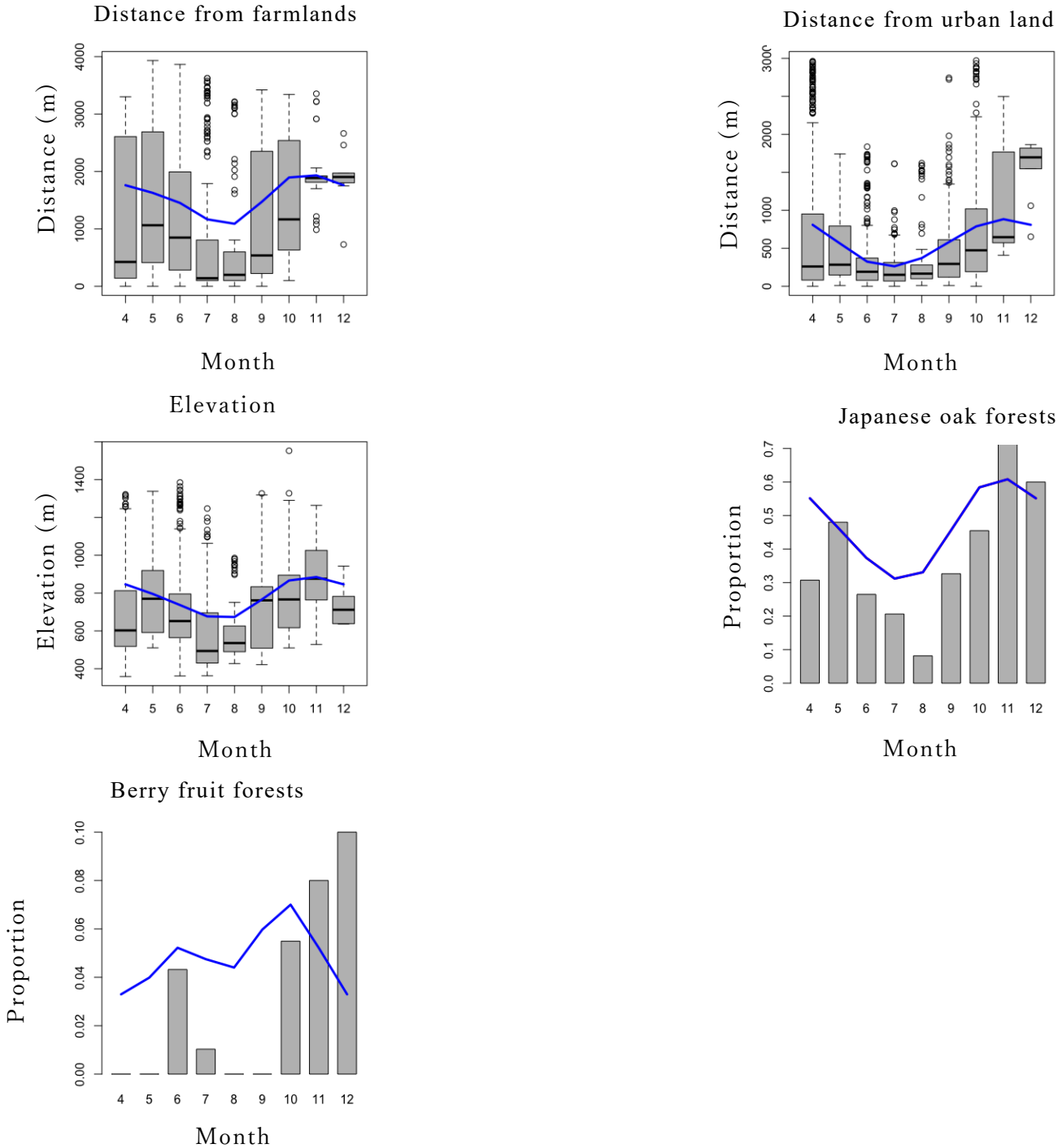

Figure 36. Seasonal variation of environmental factors negatively related to caesium-137 soil deposition within the intensive use area

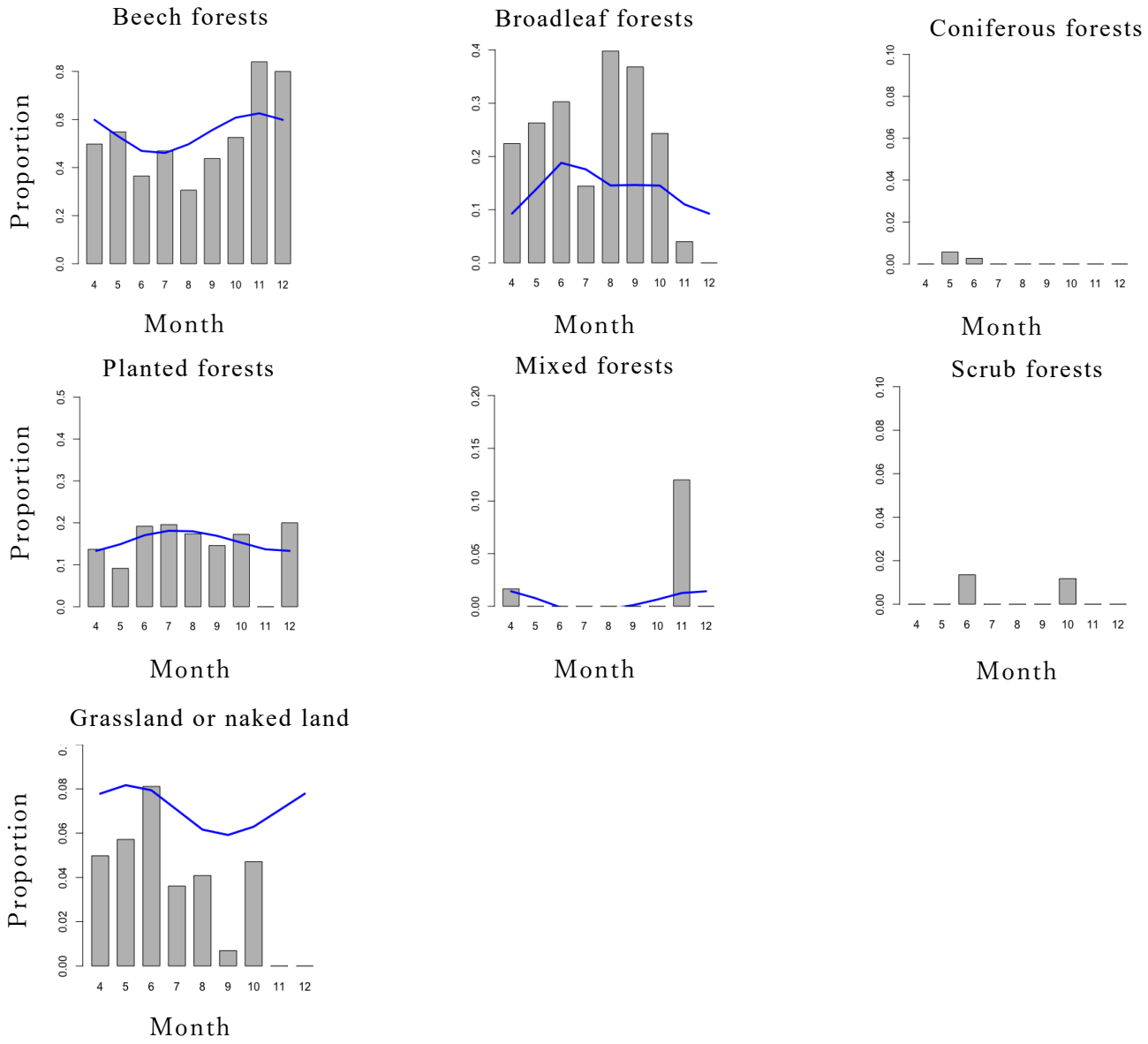

Figure 37. Seasonal variation of environmental factors positively related to caesium-137 soil deposition within the intensive use area

For the results of the habitat selection analysis, each environmental factor is noted in Figure 38 for environmental factors negatively related to caesium-137 soil deposition, and in Figure 39 for environmental factors positively related to caesium-137 soil deposition, based on the results of the relationship between caesium-137 soil deposition and environmental factors described above. For the negatively related environmental factors, locations far from farmlands were selected in October and December; in August, September, and December, locations far from urban lands were selected. The lower elevations were selected in April, June to October and December, while the higher elevations were selected in November. Japanese oak forests were selected in June, October, and December, but avoided in May and July. Berry fruit forests were selected in June and October, but avoided in December. For environmental factors positively related to caesium-137 soil deposition, a variety of vegetation types were selected in April, June, and July, i.e., beech forests, broadleaf forests, planted forests, mixed forests, and scrub forests. The lack of a clear pattern of

seasonal variation in caesium-137 activity concentrations in muscle tissue for any of the environmental factors suggests that seasonal variation in caesium-137 activity concentrations may be affected by seasonal variations in habitat use, particularly the frequency of use of beech forests, as opposed to habitat selection.

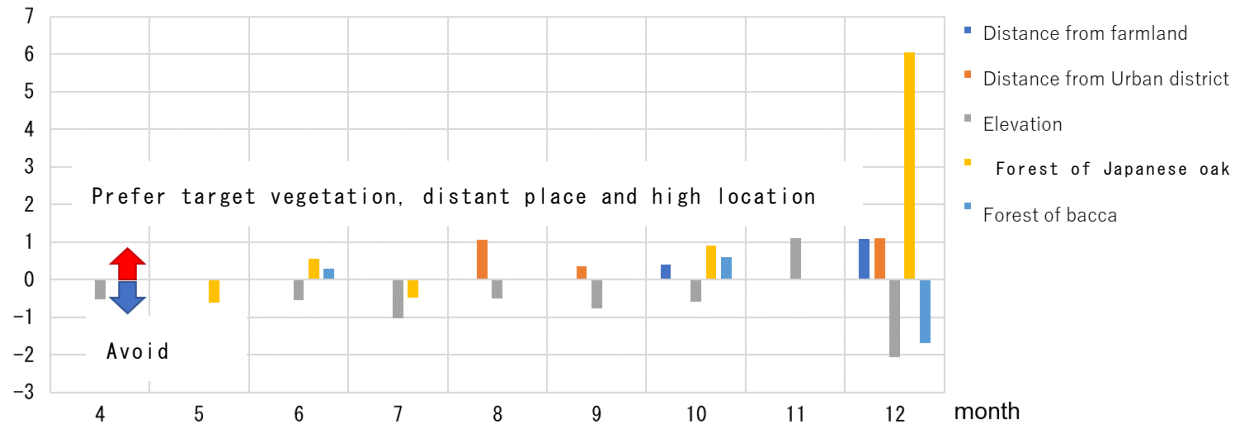

Figure 38. Habitat selectivity of environmental factors negatively related to caesium-137 soil deposition

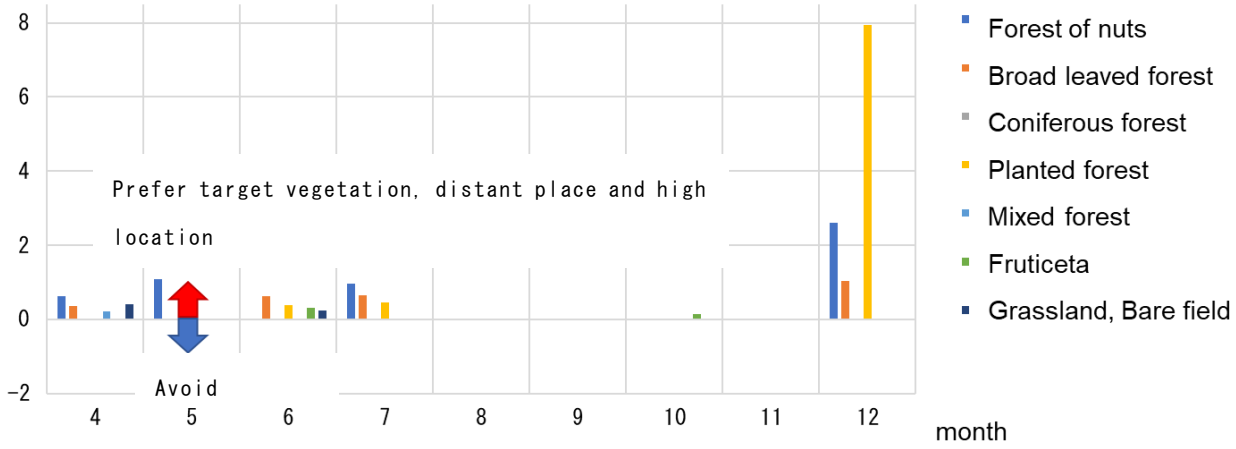

Figure 39. Habitat selectivity of environmental factors positively related to caesium-137 soil deposition

2.4.2.2. Management of wild animals in the area contaminated by radionuclides

2.4.2.2.1. Monitoring

Figure 40 shows the activity concentration of caesium 134+137 in the muscle of green pheasants captured throughout Fukushima Prefecture from October 2011 to March 2022. Since then, no individuals have been detected with caesium activity concentrations exceeding the food standard values. In recent years, caesium activity concentrations have remained below the detection limit in many individuals.

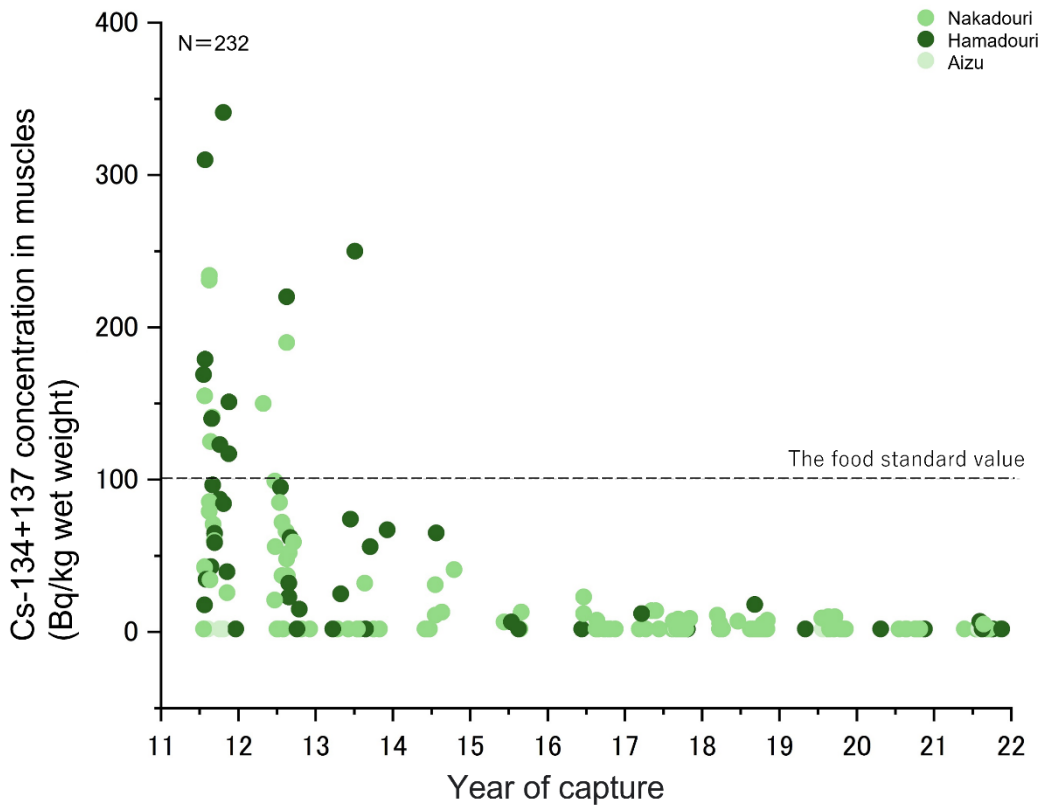

Figure 40. Monitoring results of caesium-137 concentrations in the muscles of pheasants

2.4.2.2.2. Investigations of wild animals around the Evacuation-Designated Zone (EDZ)

Genomic DNA of wild boars was extracted from 179 specimens in Fukushima Prefecture and 9 specimens in Kumamoto Prefecture*, and subjecting them to a MIG-seq analysis. As a result, in a total of 688 Single-nucleotide polymorphisms (SNPs) were extracted[24]. For confirming the geographical trends of population structure, the wild boars captured in Fukushima Prefecture were classified into seven groups based on their captured locations and those captured in Kumamoto Prefecture into one group (eight groups in total) (Figure 41).

A STRUCTURE[11] analysis and cluster analysis using the SNPs information was then carried out. According to ΔK value under STRUCTURE analysis data, the results for wild boars suggested that they were divided into two genetic lineages (Figure 42). Moreover, the results of cluster analysis revealed two clusters that can be divided into an eastern group inhabiting northern Soso District, southern Soso District, Iwaki District and Ken-nan District of Fukushima Prefecture, and a western group inhabiting Ken-poku District, Ken-chu District and Aizu District of Fukushima Prefecture and Kumamoto Prefecture (Figure 43). (*The meat specimens obtained in Kumamoto Prefecture are provided by Munemasa Kousan, a stock company.) BayesAss[25] estimated gene flow for the wild boar population distributed on the east side of the Abukuma River and the population on the west side. The results showed that the gene flow from the eastern population to the western

population (10.3%) was greater than that from the western population to the east population (3.3%). The results also indicated that gene exchange within the east and west populations was more significant than between the east and west populations (within the east population: 96.7%, within the west population: 89.7%). It was expected that the east and west populations would be maintained as separate populations across the Abukuma River and the urban area and that there would be little back and forth between each other's populations (Figure 44).

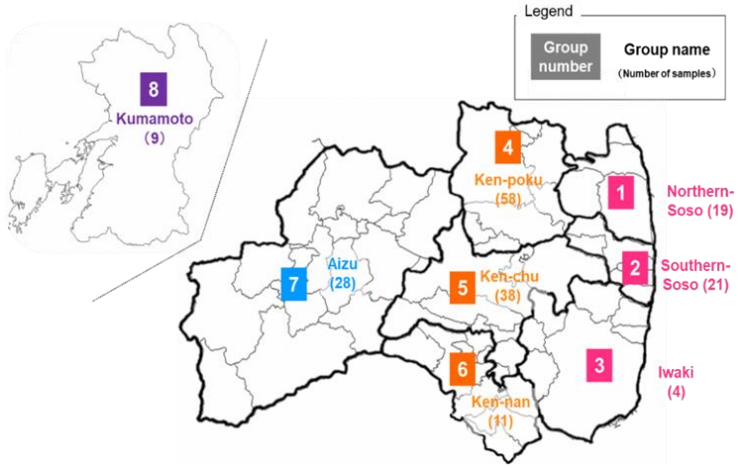

Figure 41. Grouping of specimens after their MIG-seq analyses and the number of analyses

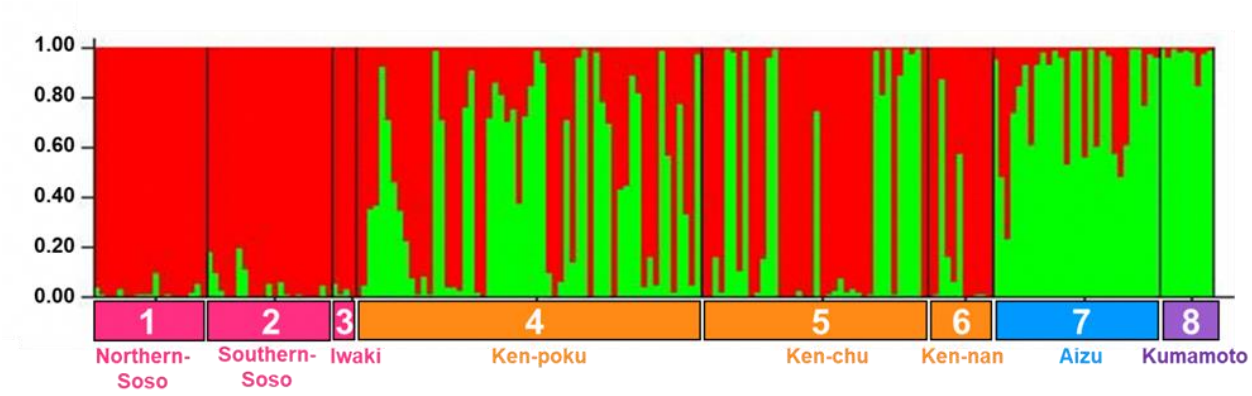

Figure 42. Results of STRUCTURE analysis based on wild boars DNA data
2 colors (red and green) represent genetic lineages suggested by the results of STRUCTURE analysis. Ratio of the colors are of the lineages in each sample shown by vertical column (0.00-1.00)

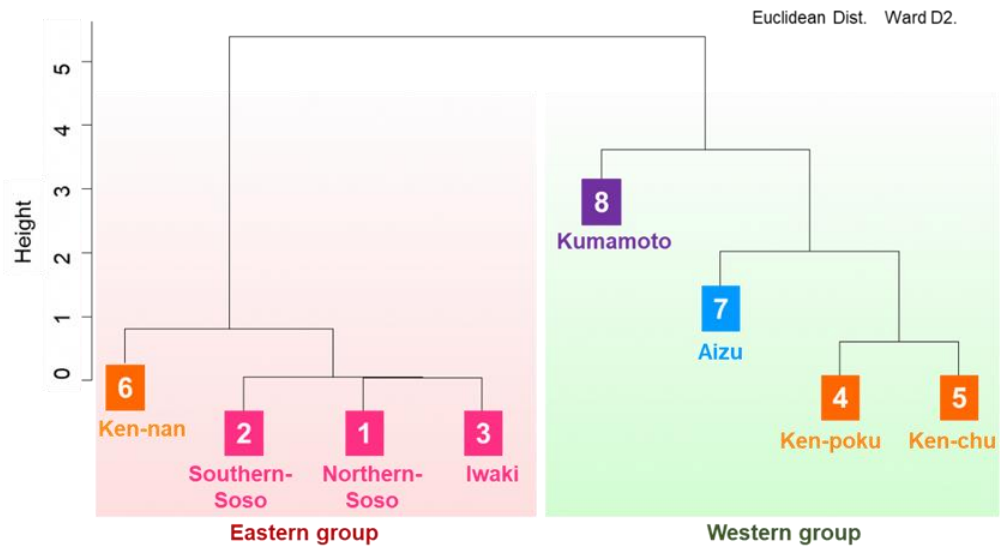

Figure 43. Results of cluster analysis based on wild boars' DNA data

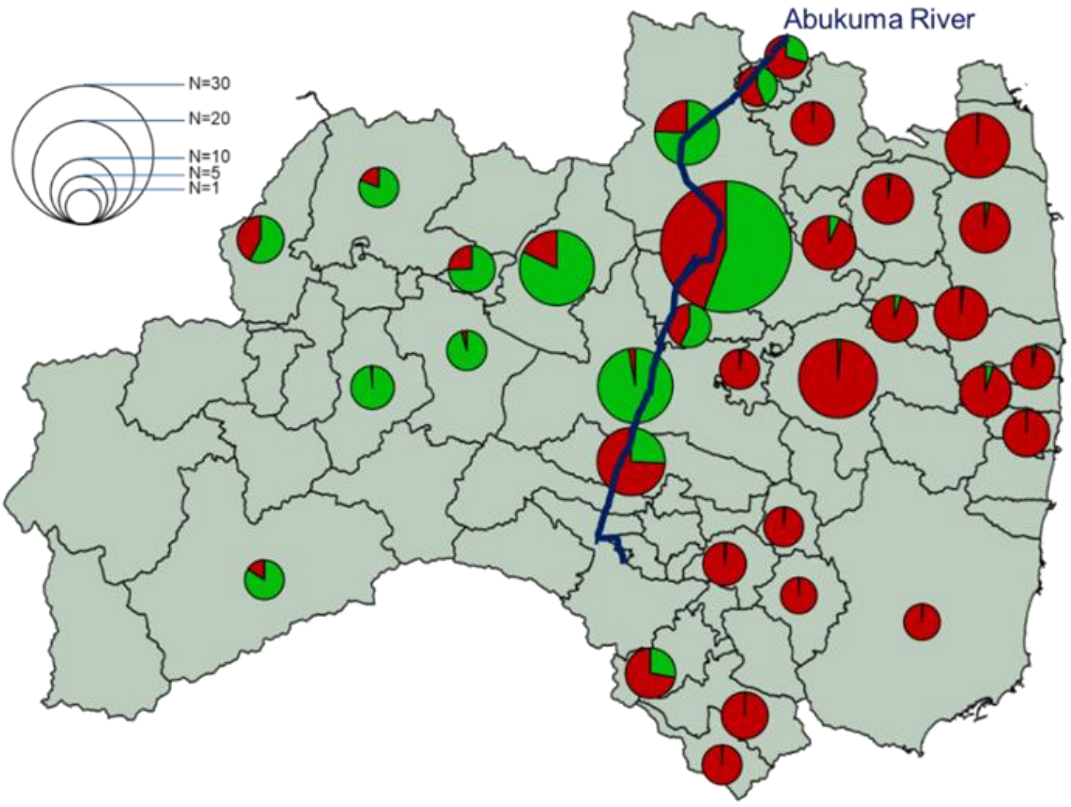

Figure 44. Geographical distribution of wild boars of two genetic lineages Ratio of genetic lineages shown by the STRUCTURE analysis (See Figure 42) in each municipality. Size of the circle represents the amount of samples.

2.4.2.2.3. Strategy to lift restrictions for distribution and consumption

IAEA's recommendations

Therefore, the Prefecture made a request to the IAEA's knowledge and received the following recommendations.

【Prior cases in overseas】

・Based on prior cases in overseas, it would likely be difficult deciding to lift distribution restrictions, etc, only when the monitoring result of samples in areas where lifted restrictions are found below the standard values. Rather, establishing a system to allow residents to directly monitor and self-consume or distribute only those samples that are below the standard values should be considered.

Considerations in response to recommendations

At present, the prefectural government, in cooperation with the Consumer Affairs Agency and the National Consumer Affairs Center of Japan, lends or transfers radioactive material inspection equipment to municipalities with which prefecture residents can inspect their vegetables and other food products for radioactive materials in their neighborhoods, and is working to enhance and strengthen the inspection system. However, the foods under consumption and distribution restrictions are not covered by such inspections.

On the other hand, regarding the distribution of wild game as commercial products, although the national government (Ministry of Agriculture, Forestry and Fisheries) has a system in place to subsidize municipalities for the construction of meat processing facilities to promote the utilization of wild game as Gibier, no municipalities in the prefecture have constructed or currently operate meat processing facilities because the government subsidizes only half of construction costs, the municipalities must bear the remaining costs and is thus unlikely to be commercially profitable.

In view of this, the prefecture continues to request the national government to prepare requirements for lifting restrictions in accordance with the actual conditions of the regions due to the considerable difficulties of conducting continuous monitoring and ensuring sufficient samples of wild game.

Creation of a brochure aimed at fostering understanding among hunters

To convey the importance of monitoring and ensuring sufficient sample numbers, a brochure for hunters was prepared in cooperation with the IAEA and 4,000 copies were distributed to hunters in the prefecture in October 2021.

2.5. Conclusions

Comparisons of the activity concentrations of caesium-137 in the muscle tissues of wild boars and Asian black bears revealed higher activity concentrations in wild boars, while comparisons between copper pheasant and green pheasants revealed higher levels in copper pheasant, revealing that trends differed depending on the species.

The activity concentrations of caesium-137 in the muscle tissues of wild boars were confirmed to be strongly affected by diet. Seasonal variations were also observed in both wild boars and Asian black bears (which were higher in winter season), although the patterns differed.

High caesium-137 activity concentrations of muscle were observed in wild boars and Asian black bears captured in areas where the caesium-137 deposition density was high, but the activity concentrations significantly varied among individuals in the areas. Even in recent years, those showing activity concentrations exceeding 10 times the standard limit for general foods in Japan have sometimes been captured. Regarding long-term fluctuations of caesium-137 activity concentrations in the muscles of wild boars and Asian black bears, they have decreased over time during the entire period and during times of the year with low-activity concentrations in muscle tissues observed. However, during times of the year where high-activity concentrations in muscle tissue are observed, the range of estimated values increased over time.

Compared to wild boars living outside the areas under evacuation orders, those living in the areas under evacuation orders tended to have wider home ranges that tended to shift to farmlands. In addition, the results of the studies suggested that the wild boars in Fukushima Prefecture are divided into two lineages, and these populations are situated in the east and west areas around the Abukuma River, with the river acting as the boundary that restricts the movement from east to west and vice versa.

Caesium-137 activity concentrations in muscles of wild boars and Asian black bears are on a decreasing trend, but they vary among individuals and are observed to fluctuate seasonally. Therefore, in order to precisely estimate their long-term fluctuations, further data expansion is necessary. Moreover, the movement and spatial range covered by the wild animals seems to be a factor contributing to the variation of caesium-137 activity concentrations observed even among those animals captured in the same region.

In the future, the monitoring of radio caesium activity concentrations in the bodies of wild boars and other wild animals and birds will be continued. The factors contributing to the high radio caesium activity concentrations in some wild animals will be investigated, and survey methods for the conservation and management of wild animals will be studied.

References

1) Semizhon, T., et al., Time-dependency of the 137Cs contamination of wild boar from a region in Southern Germany in the years 1998 to 2008. Journal of environmental radioactivity, 2009. 100 11: p. 988-92.
2) Saito, R., et al., Monitoring 137Cs activity concentrations in bird species occupying different ecological niches; game birds and raptors in Fukushima Prefecture. Journal of environmental radioactivity, 2019. 197: p. 67-73.
3) Saito, R., Y. Nemoto, and H. Tsukada, Relationship between radiocaesium in muscle and physicochemical fractions of radiocaesium in the stomach of wild boar. Sci Rep, 2020. 10(1): p. 6796.
4) Saito, R. and H. Tsukada, Physicochemical Fractions of Radiocesium in the Stomach Contents of Wild Boar and Its Transfer to Muscle Tissue, in Behavior of Radionuclides in the Environment III. 2022, Springer. p. 495-505.
5) Nemoto, Y., R. Saito, and H. Oomachi, Seasonal variation of Cesium-137 concentration in

Asian black bear (*Ursus thibetanus*) and wild boar *(Sus scrofa*) in Fukushima Prefecture, Japan. PLoS One, 2018. 13(7): p. e0200797.

6) SAITO, R., et al., The use of DNA metabarcoding to analyse wild boar diets: Reproducibility of plant diet analyses and effective blocking of boar DNA amplification when evaluating animal dietary components.Japanese Journal of Ecology, 2020. 70(3): p. 163.
7) Nemoto, Y., et al., Effects of (137)Cs contamination after the TEPCO Fukushima Dai-ichi Nuclear Power Station accident on food and habitat of wild boar in Fukushima Prefecture. J Environ Radioact, 2020. 225: p. 106342.
8) JAEA, Results of Deposition of Radioactive Cesium of the Fifth Airborne Monitoring Survey and Air- Borne Monitoring Survey outside 80 Km from the Fukushima Dai-Ichi NPP. 2012: p. 31.
9) Brown, J.E., et al., A new version of the ERICA tool to facilitate impact assessments of radioactivity on wild plants and animals. Journal of environmental radioactivity, 2016. 153: p. 141-148.
10) Suyama, Y. and Y. Matsuki, MIG-seq: an effective PCR-based method for genome-wide single-nucleotide polymorphism genotyping using the next-generation sequencing platform. Sci Rep, 2015. 5: p. 16963.
11) Evanno, G., S. Regnaut, and J. Goudet, Detecting the number of clusters of individuals using the software STRUCTURE: a simulation study. Mol Ecol, 2005. 14(8): p. 2611-20.
12) Strebl, F. and F. Tataruch, Time trends (1986–2003) of radiocesium transfer to roe deer and wild boar in two Austrian forest regions. Journal of environmental radioactivity, 2007. 98(1-2): p. 137-152.
13) Rode, K.D., S.D. Farley, and C.T. Robbins, Sexual dimorphism, reproductive strategy, and human activities determine resource use by brown bears. Ecology, 2006. 87(10): p. 2636-2646.
14) Ciarniello, L.M., et al., Grizzly bear habitat selection is scale dependent. Ecol Appl, 2007. 17(5): p. 1424-1440.
15) Massei, G., et al., Factors influencing home range and activity of wild boar (*Sus scrofa*) in a Mediterranean coastal area. Journal of Zoology, 1997. 242(3): p. 411-423.
16) Morelle, K., et al., Towards understanding wild boar Sus scrofa movement: a synthetic movement ecology approach. Mammal Review, 2014. 45: p. 15-29.
17) Takahata, C., et al., Habitat selection of a large carnivore along human-wildlife boundaries in a highly modified landscape. PloS one, 2014. 9(1): p. e86181.
18) Nemoto, Y.K., C. ; Yamazaki, K. ; Koike, S. ; Masaki, T. ; Kaji, K., Individual and sexual variation in the selection of hard mast forests and artificial land by Asian black bears in fall. Mammalian Science (Honyuryu Kagaku) 2018. 58(2): p. 205-219.
19) Reyes, J., E. Delgado, and J. Ly, Digestion of sweet potato (*Ipomoea batatas (L.) Lam*) foliage in pigs. Ileal and fecal in vitro digestibility. Cuban Journal of Agricultural Science, 2013. 47(3).
20) Horne, J.S., et al., Analyzing animal movements using Brownian bridges. Ecology, 2007. 88(9): p. 2354-2363.

21) Yamazaki, K., Ursus thibetanus G. Cubier, 1823. The Wild Mammals of Japan Second Edition ed. I.Y. Ohdachi S, Iwasa M, Fukui D. 2015, SHOUKADOH Book Sellers and the Mammalogical Society of Japan.
22) Kodera, Y., Sus scrofa Linnaeus, 1758. The wild mammals of Japan Second Edition. 2015. 312-313.
23) JAEA, Results of Airborne Monitoring in Fukushima Prefecture and neighboring prefectures and the Thirteenth Airborne Monitoring in the 80km zone from the Fukushima Daiichi NPP. 2019: p. 5.
24) Saito, R., et al., Genetic Population Structure of Wild Boars (*Sus scrofa*) in Fukushima Prefecture. Animals, 2022. 12(4): p. 491.
25) Wilson, G.A. and Rannala, B. Bayesian inference of recent migration rates using multilocus genotypes. Genetics, 2003. 163: pp.1177–1191.

3. FIP3：Sustainable countermeasures for radioactive materials in terrestrial and aquatic areas

3.1. Abstract

Decontamination methods were developed and tested in rivers designated for radiocaesium removal measures. Their effectiveness and sustainability were studied. The contamination situation in riverside areas used by the public in Fukushima Prefecture and the measures taken to deal with it were also considered. In addition, the contamination of riverbanks and changes in air dose rates following heavy rains were investigated.

3.2. Purpose

Radioactive substances, including radioactive caesium, were released into the environment following the accident in the Fukushima Daiichi Nuclear Power Plant. The aquatic environment was contaminated and this potentially affected the use and management of rivers, lakes and other freshwater bodies. In response, monitoring of water, sediments and aquatic products was conducted to understand the behaviour of radioactive substances in the aquatic environment, mainly by government authorities and research institutions. Decontamination measures were also promoted. In this project, countermeasures for radiocaesium applicable for use in Fukushima Prefecture were planned and implemented based on national and international knowledge. Tests were conducted for demonstrating the decontamination of rivers and to study the resulting reduction of external exposures in such areas. The persistence of the decontamination measures implemented was also tested. In addition, the contamination situation at riverside parks in the Fukushima Prefecture was investigated and the impact of the flood caused by Typhoon No.19 in 2019 (Hagibis) on the air dose rates at the studied sites was assessed.

3.3. Content of implementation

3.3.1. Identification of radiocaesium countermeasures considered applicable to Fukushima Prefecture

Among the measures taken against the diffusion of radioactive substances in the environment after the accident at the Fukushima Daiichi Nuclear Power Plant of the Tokyo Electric Power Company, the measures for radioactive substances deposited on inland water bodies (rivers, lakes, etc.) and their effectiveness have not been clarified. Therefore, at the start of this project, the focus was on studying measures that would enable the use of rivers, lakes and other freshwater bodies affected by the accident. The effectiveness of decontamination measures considered applicable in Fukushima Prefecture to reduce activity levels in rivers was studied.

3.3.2. Decontamination tests at riverside parks and sustainability of their effectiveness

3.3.2.1. Purpose

There are only few examples for countermeasures to reduce external exposure caused by the

contamination of riverbeds, riverbanks and flood plains of rivers. In the Fukushima Prefecture, as there are in many cases where non-decontaminated forested areas exist upstream, surface run-off water transports radiocaesium bearing material downstream into rivers. As a result, there may be thick deposits of soil and sediment containing radiocaesium in areas outside the embankments of rivers. Soil decontamination methods applied to agricultural land, forests, and residential areas assume that radiocaesium usually has accumulated in the surface layer of a few centimetres. However, it is not clear whether these methods are appropriate for flood plains outside the embankments of rivers where sediments may continuously deposit during floods, for example following typhoons.

Even after decontamination of the outside of the embankment, there is a concern that re-contamination may occur in these areas, due to the continuous input of surface run-off water containing contaminated suspended sediments. In particular, if vegetation thrives in the outer areas of the embankment, fine-grained sediment with a relatively high caesium-137-concentration may be retained by vegetation leading to a local increase of radiocaesium concentrations.

Therefore, an effective decontamination method for the outer areas of the embankment was expected to be sediment removal and this was carried out to investigate its effectiveness in reducing air dose rate. The thickness of the removed layer was defined by the depth distribution of radiocaesium in the sediments on the embankments. The sustainability of the decontamination effect was also investigated. The same species of vegetation continued to grow where the decontamination demonstration tests were carried out as had been growing before sediment removal. The air dose rate and the deposition of sediments were continuously monitored to investigate whether or not there was re-contamination due to the growth of the vegetation.

3.3.2.2. Method

The study site is located 55 km north-west of the Fukushima Daiichi Nuclear Power Plant of the Tokyo Electric Power Company Holdings, Inc., in the lowest reach of the Kami-Oguni River, a tertiary tributary of the Abukuma River (Figures 1(a) and 1(b)). The deposition of radiocaesium (caesium-134 and caesium-137) as of July 2011 ranged from 300 to 600 kBq/m^2.[1)] Most of the catchment is covered by forest, with farmland and residential areas located along the river (Figure 1(b)). The total decontamination area was 170 m long, with an average bank width of 15 m on both banks and a river channel width of 2-6 m during normal water (Figures 1(c) and 1(d)). The left bank of the river was used as school route to the primary school, the right bank was used by the arboretum, and the flood channel was used by the primary school for teaching and other purposes. The primary school and the school route were decontaminated before the test.

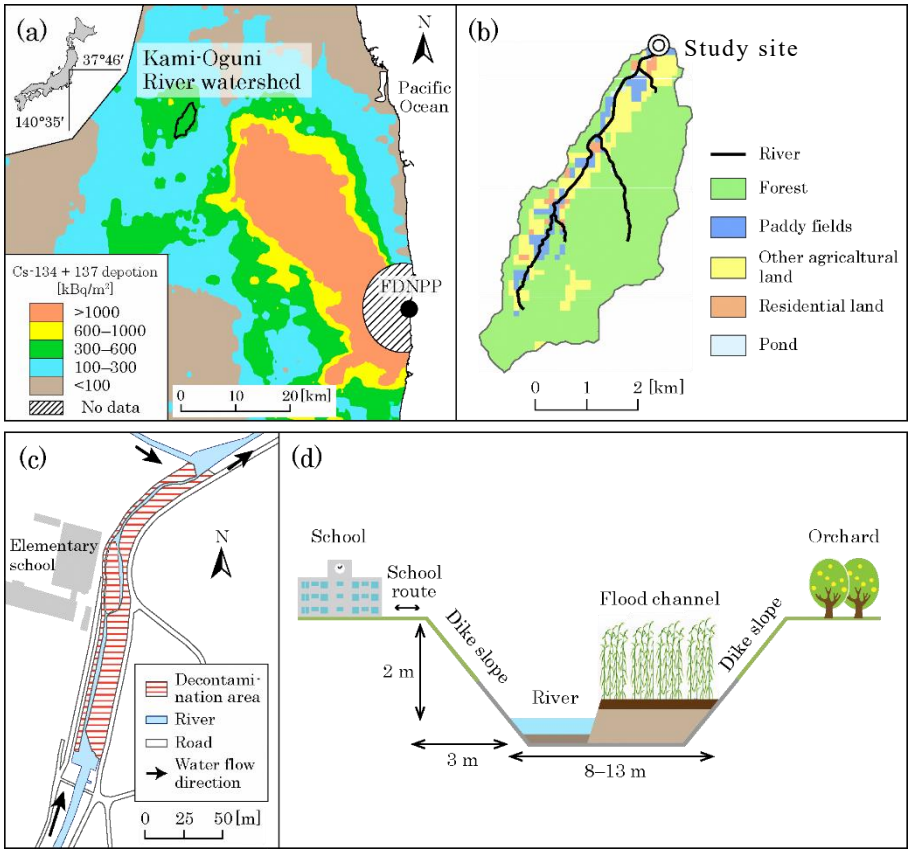

Figure 1. Outline of the study site
Radiocaesium deposition is based on the results of the third round of aircraft monitoring[1] (converted to 2 July 2011).

The decontamination demonstration of the outer embankment area was carried out in 2014 according to the procedure shown in Figure 2. First, the depth distribution of the radiocaesium concentration in the sediments outside the embankment was measured. The depth of sediment removal was set according to the radiocaesium distribution, and decontamination was carried out accordingly. Air dose rates were continuously measured after decontamination. From the decontamination in 2014 to the end of 2016, all vegetation in the outer bank area was mowed, and from 2017, vegetation was not mowed. In 2018, embankment works were carried out on the upstream side of the right bank for flood protection.

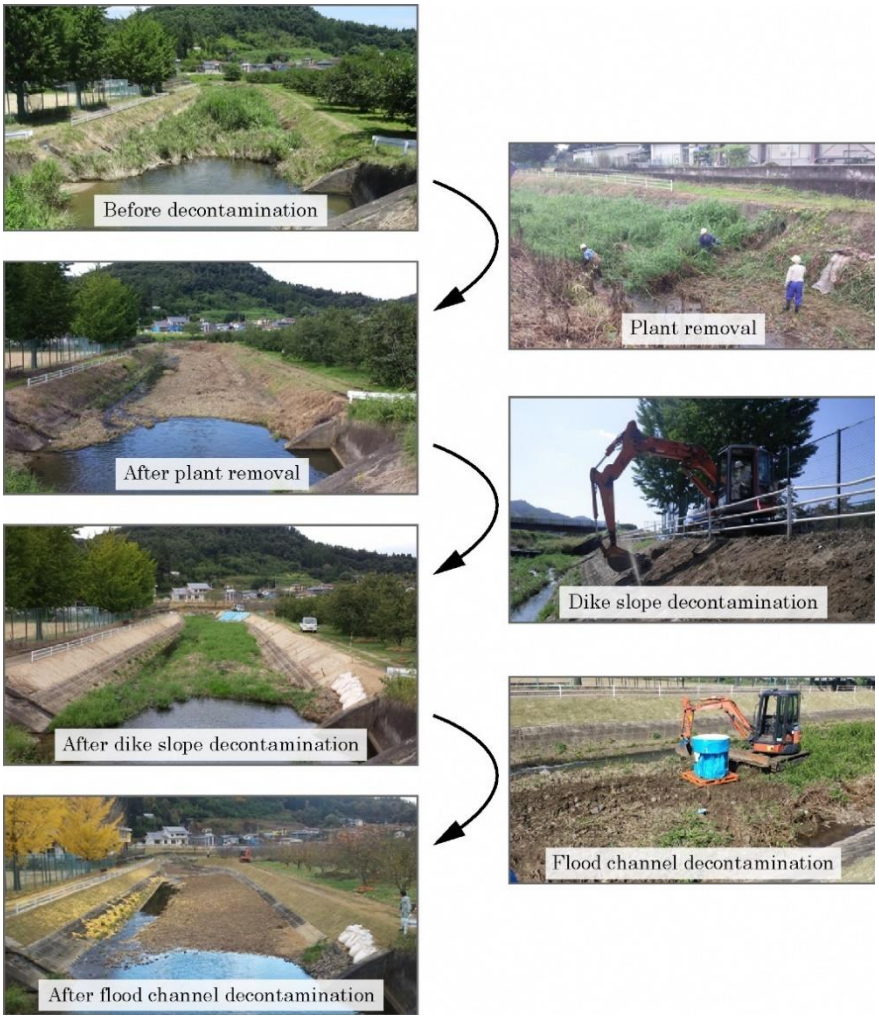

Figure 2. Photographs of the decontamination test procedures

Air dose rates at 1 m above the surface of the decontaminated area were measured during baseflow using a NaI scintillation survey meters. High waterbed and riverbed sediments were sampled from before the decontamination demonstration test (in 2014) up to 2016. Sediment samples in the high waterbed were divided into sediments that were newly deposited since the last measurement (new sediments) and sediments that had been deposited before (old sediments) at seven sites in 2017-2018 using the ring method (A method in which rings are placed on the ground surface in advance and the old and new sediments are separated according to their top and bottom. See Figure 7.). The sediments were measured for radiocaesium concentrations; gravel was removed before the measurement. The ratio of the mud fraction (silt and clay, particle size < 63 μm) to the total mass of the samples was determined.

The annual dose due to external exposure before and after decontamination was calculated in the following way. It was assumed that the time of use was 35 hours per year (10 minutes per day, 210 days per year) for walking to school on the left bank and 24 hours per year (2 hours per day, 12 days per year) for teaching and other activities on the high waterbed. This was multiplied by the average air dose rate at the study site minus the air dose rate before the nuclear accident (0.04 μSv/h).[2)]

3.3.3. Investigation of the distribution of radiocaesium in river parks and testing remedial measures

3.3.3.1. Purpose

As mentioned above, radiocaesium may deposit outside the embankment as a result of sedimentation during floods. In the Coastal region, the eastern part of the Fukushima Prefecture, there is a relatively high deposition in the upstream area, and it is very likely that downstream areas near the river outside the embankment are more contaminated than areas farther away from the riverbed. Therefore, the contamination situation was studied and countermeasures for river parks on high water beds in the Coastal region were investigated.

3.3.3.2. Method

The survey was conducted at two sites downstream of the Niida River, which flows through the coastal region (Figure 3). Park A is located along the mainstream of the Niida River and Park B is located along the Mizunashi River, a primary tributary of the Niida River. A dam is located 5 km upstream of Park B. Deposition of radiocaesium (caesium-134 and caesium-137) in the catchment as of July 2011 exceeds 1000 kBq/m^2 in the upper reaches, but it is less than 100 kBq/m^2 in the lowest reach. Deposition of radiocaesium in Park A is 490 kBq/m^2 and 210 kBq/m^2 in Park B.[3] The area of Park A is 2.7 ha and that of Park B is 1.6 ha.

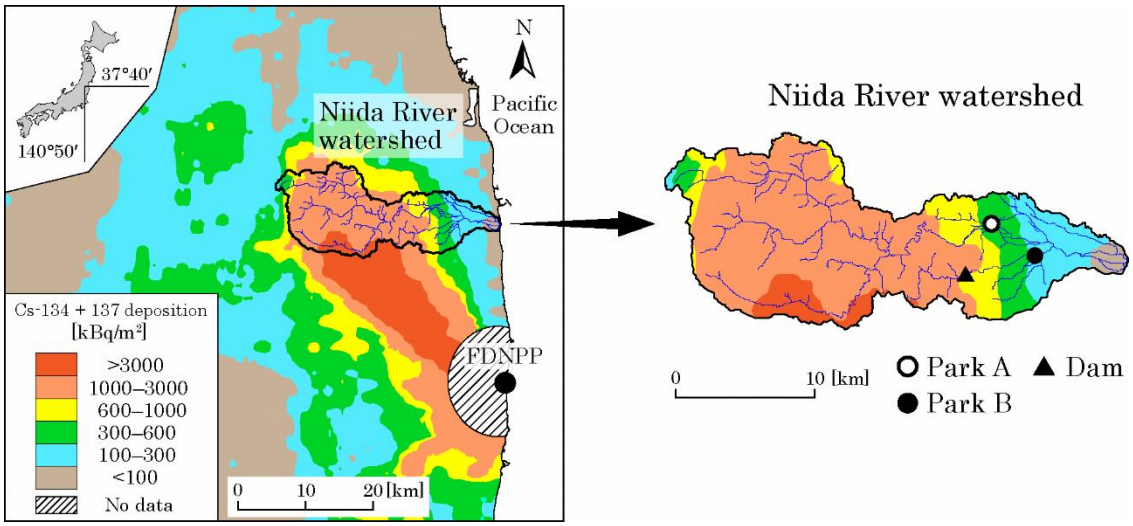

Figure 3. Location of study sites
The map of the radiocaesium deposition is based on the results of the third round of aircraft monitoring[1] (converted to 2 July 2011).

Air dose rates were measured in August 2015 in the study area at 1 m height above the ground using a portable gamma-dose rate meter (GAMMA Plotter H, Japan Radiation Engineering Co., Ltd.). Based on the data obtained, a map of the spatial distribution of radiocaesium was created

using the decontamination activity support system (RESET)[1] developed by Japan Atomic Energy Agency. Air dose rates were measured again on 28 September 2015, as a flood event occurred from 6-11 September 2015 (total precipitation during the period at the AMeDAS Haramachi station (6 km southeast of Park A) was 385 mm[5)]), when nearly half of the park was flooded. Soil cores were collected in December 2015 and the depth distribution of radiocaesium in soil in the study area was investigated.

External exposures for the parts of the parks, used for recreation, walking and maintenance, were estimated using a dosimeter that provides the integrated air dose rate over the measurement period (DOSE e nano, Fuji Electric Co., Ltd.). Based on a dosimeter reading for about 1 hour, external exposures were estimated assuming that both parks were used for 36 hours per year[2].

3.3.4. Exploring public concerns on the safety of freshwater bodies

3.3.4.1. Purpose

When considering future medium- and long-term measures to mitigate the consequences of the accident in the Fukushima Daiichi Nuclear Power Plant, it is important to understand the issues and trends related to the use of freshwater resources by various stakeholders in the Fukushima Prefecture. The aim of this study was to identify concerns related to the management of freshwater resources through interviews with relevant stakeholders, and to identify changes over time in the prefectural residents' views on the safety of the aquatic environment.

3.3.4.2. Method

From May to June 2016, administrative officials responsible for implementing measures to ensure the safe uses of water were interviewed to learn about the challenges they faced caused by radioactive substances in the aquatic environment. From the results of the interviews, the relevant issues were extracted and addressed. In addition, raw data from the prefectural public opinion survey conducted by Fukushima Prefecture[6)] every fiscal year from 2010 to 2015 was provided by the Public Consultation Unit of the Fukushima Prefectural Government. From this data, we focused on the question “Do you feel safe from pollution including water and air pollution in your living environment?” Trends and changes in the responses to this question over time by gender, age, and place of residence were examined, and an analysis was conducted to determine whether there was a relationship between this question and the question “Is your living space safe from radiation?” (radiation risk).

---

[1] Restoration Support System for Environment (RESET). The system can be used to simulate the percentage reduction in air dose rates due to decontamination and the changes in air dose rates after decontamination.[4)]

[2] Park A: 12 hours per year for recreation (2 hours per day, 6 days per year), 12 hours per year for walking (1 hour per day, 12 days per year), 12 hours per year for park maintenance such as flowerbeds (1 hour per day, 12 days per year)
Park B: 24 hours per year for recreation or playground equipment use (2 hours per day, 12 days per year); 12 hours per year for walking (1 hour per day, 12 days per year))

3.3.5. Changes of radiocaesium concentration in riverbanks during large-scale flooding

3.3.5.1. Purpose

Radioactive materials may accumulate in riverbanks as a result of sediment deposition. Resuspension of riverbank sediments and additional deposition of suspended sediments on riverbanks can also occur, especially during flood events caused by typhoons or heavy precipitation. These processes result in changes of the depth distribution of radiocaesium concentrations in bottom sediments.[7, 8] These processes can reduce air dose rates from riverbanks, and are generally referred to as natural attenuation.

Typhoon Hagibis, which passed through Fukushima Prefecture in October 2019, caused riverbank breaches and overflows in various rivers of the Fukushima Prefecture, causing significant damage along the rivers. To clarify whether there was recontamination due to erosion and sedimentation during the water run-off, and whether air dose rates decreased due to these processes, changes in air dose rates and contamination levels in riverbanks and river parks following the passage of Typhoon Hagibis were investigated.

3.3.5.2. Method

Surveys were conducted in two river parks in the Niida River catchment (Figure 3) and at the demonstration site on the Kami-Oguni River (Figure 1), as described in section 3.3.3. and 3.3.2..

Typhoon Hagibis passed through Fukushima Prefecture on 12-13 October 2019. At the AMeDAS Haramachi station, which is closest to Parks A and B, 274 mm of precipitation was observed as a result of a series of rainstorms.[5] In the Fukushima Prefecture, rivers in various areas, including the Abukuma River, a major river in the prefecture, suffered dike breaches and flood damage, and river dikes in the surveyed areas were overflowed. Air dose rates at a height of 1 m above the ground were measured using a portable gamma-dose rate meter in January 2018 before the typhoon and in October 2019 after the typhoon. In addition, the erosion and deposition of sediment in the riverbank and park were confirmed when walking at the site after the passage of the typhoon.

3.4. Results

3.4.1. Indentification of radiocaesium countermeasures considered applicable to Fukushima Prefecture

The exposure pathways and transfer processes and potential measures that can be implemented that are related to the use of rivers, lakes, etc. are addressed in the guidelines of the relevant ministries[9, 10] and in the report on the experience of the Chornobyl nuclear accident.[11] The most important contents are briefly summarised in Table 1.

Table 1. Issues and measures for specific purposes in rivers and lakes

Issue (Exposure pathways and environmental transfer)	Related media	Measures
Internal exposure due to use as drinking water	Rivers and lakes	Changing water sources
Transfer from irrigation water to agricultural products and external exposure during farming	Rivers and lakes	Reducing sediment inflow using silt fences
	Irrigation ponds	Reducing sediment outflow using silt fences Removal of bottom sediment
	Agricultural products	Application of enhanced levels of potassium fertilizer to reduce Cs-uptake from soil
Internal exposure from consuming freshwater fish	Rivers and lakes	Shipping restrictions Application of potassium (effective only in closed lakes)
External exposure from using watersides (Parks, roads, residences, etc.)	Rivers and lakes	Restricting access, soil decontamination Removing riverbed sediments to reduce sediment deposition onto riverbanks Building embankments for inundation control
	Irrigation ponds (at drainage)	Use restriction, removal of sediments, and covering of exposed bottom sediments
Common to all issues		Decontamination of sources and prevention of sediment discharge Risk communication to reduce anxieties

3.4.2. Decontamination tests at riverside parks and sustainability of their effectiveness

The depth distribution of radiocaesium concentrations in the sediments of the high waterbed before decontamination is shown in Figure 4. The samples were collected 3.5 years after the accident in the Fukushima Daiichi Nuclear Power Plant at 5 points as shown in Figure 4. The caesium-134 concentration was a few kBq/kg, but the caesium-137 concentration at points 1 and 2 exceeded 10 kBq/kg at depths greater than 10 cm. These layers had a relatively high mud fraction of 39-56% (Figure 4). As radiocaesium is strongly adsorbed by clay and silt,[12] it is unlikely that radiocaesium would penetrate downwards below the mud-rich layers. Therefore, these layers are considered to be the results of sediment deposition. On the other hand, points 3 to 5 had relatively low caesium-137 concentrations. Due to this heterogeneous distribution of radiocaesium, both in the vertical and planar direction, the depth to which sediments were removed in the

decontamination demonstration test was set at 15-35 cm. Similar depth distributions have been reported for flood beds,[7), 13)] so it is considered important to know the depth distribution in advance for decontamination of the areas outside the embankment.

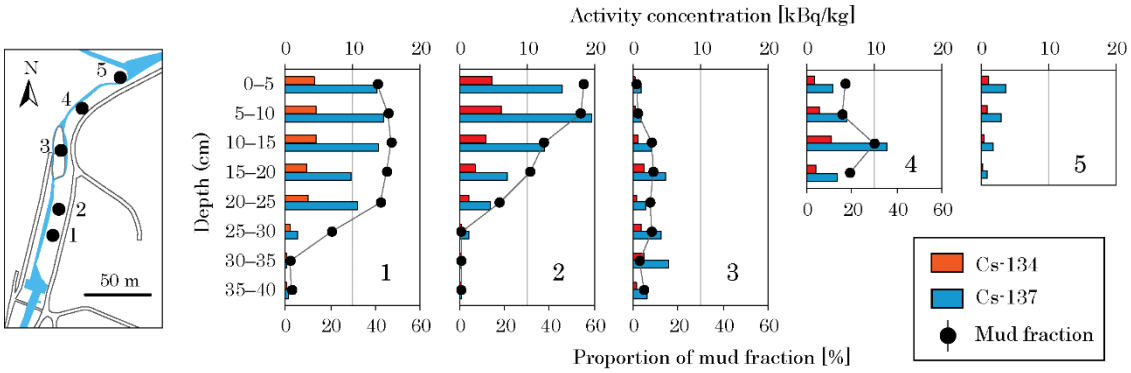

Figure 4. Depth profile of radiocaesium concentrations and the mud fractions in percent in high waterbed sediments before decontamination

The spatial distribution of air dose rates at 1 m above the ground surface before and after the decontamination demonstration test is shown in Figure 5. The mean value before decontamination was 0.66 μSv/h (standard deviation: 0.22 μSv/h), which was approximately halved to 0.34 μSv/h (standard deviation: 0.11 μSv/h) when decontamination by removing sediment was completed, confirming the effectiveness of this decontamination measure. The concentration of caesium-137 in the upper 5 cm layer of the sediment in the high waterbed (5 sites, Figure 4) was less than 3 kBq/kg in all cases after decontamination.

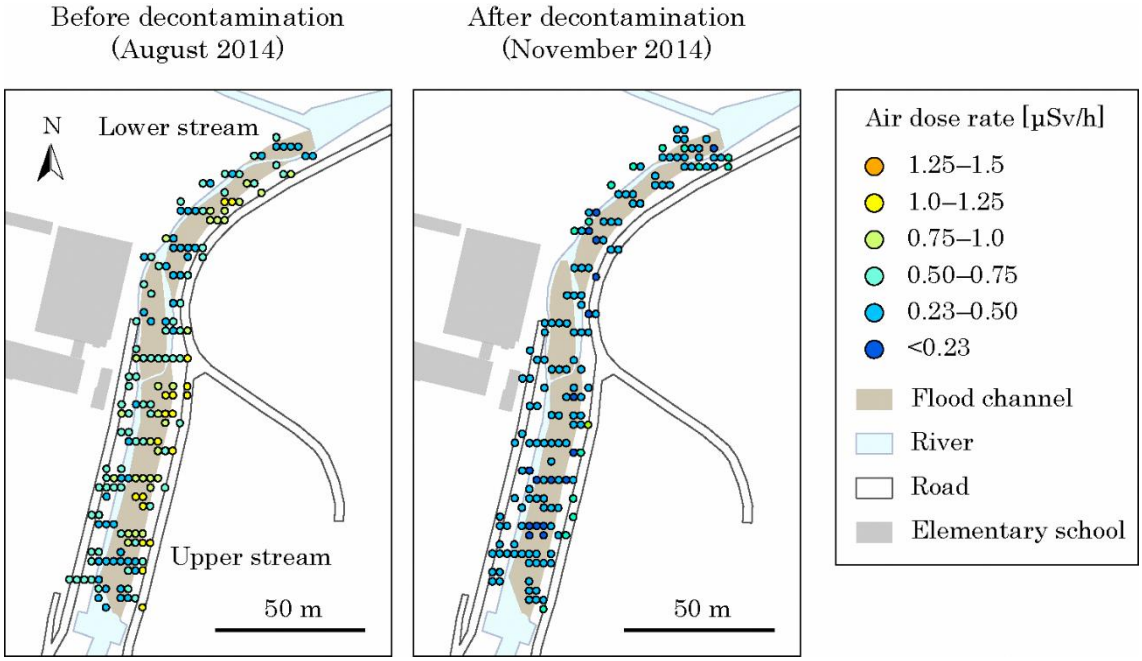

Figure 5. Distribution of air dose rates at 1 m above the ground surface before and after decontamination

The temporal changes in air dose rates at 1 m above the ground from 2014 (before decontamination) to the end of 2018 are shown in Figure 6. The figure also shows the measured values in the non-decontaminated section located 20 m upstream of the upstream edge of the decontaminated area. At the AMeDAS Yanagawa station (9 km north of the decontamination area), rainfall of 50 mm per day or more was observed four times during the two years after decontamination.[5] Therefore, it is assumed that the high waterbed was flooded several times, but the air dose rate there decreased as slowly as in the non-decontaminated area.

In the decontaminated sections, after the initial reduction of the air dose rate by about a factor of 2 following the decontamination test, the air dose rate decreased slightly faster than the physical decay of radiocaesium (considering caesium-134 and caesium-137). For the non-decontaminated sections, the air dose rate also decreased faster than physical decay only. The effective environmental half-life obtained by fitting an exponential function was shorter for the non-decontaminated section (5.9 years) than for the decontaminated section (8.1 years). The largest decrease in air dose rate occurred when Typhoon Etau passed in September 2015, which is considered to have been significantly affected by large-scale flooding.

After 2017, when the vegetation in the decontaminated sections was no longer cleared, the trend of declining air dose rates continued, and no re-contamination after the decontamination demonstration test has been observed.

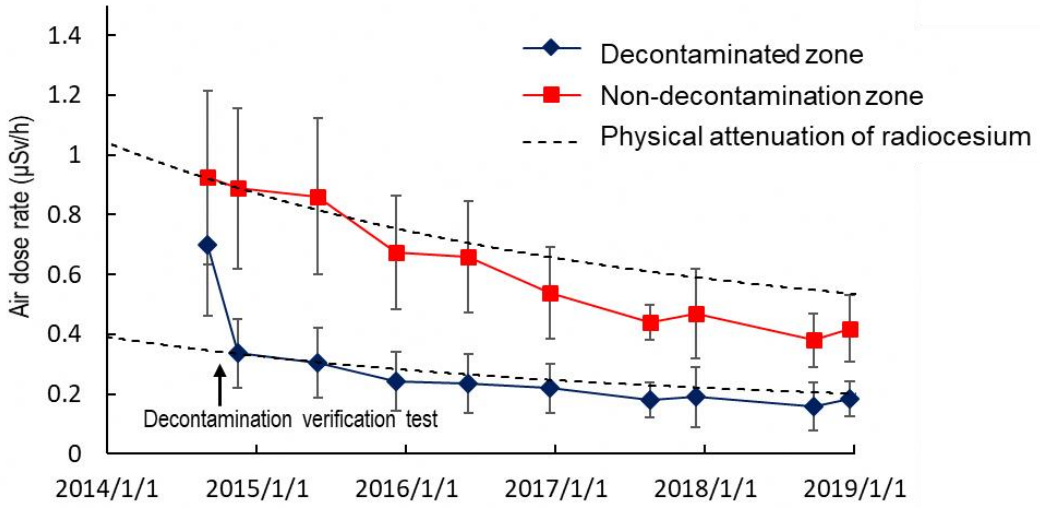

Figure 6. Changes over time in air dose rates at 1 m above the ground surface
The physical decay of caesium-134 and caesium-137 was calculated with the initial deposition ratio being 1:1. Initial values were fitted to the values measured on November 16, 2014 after the completion of the decontamination test.

Based on the assumption for the occupancy times of these areas, the annual additional external dose due to the school walk and the use of the flood bed was estimated to be 0.029 mSv per year before decontamination and 0.016 mSv per year after decontamination in 2014. In the vicinity of

the study site, based on measurements for adults using glass badges[3] from July 2013 to June 2014, the annual additional dose from external exposure was estimated to be 1.23 mSv per year.[14] Therefore, it was concluded that the doses due to external exposure received from the study sites represent a small proportion of the overall doses from external exposure in daily life (before decontamination: 2.3%, after decontamination: 1.3%).

Between the end of 2016 and August 2017, new sediments deposited on riverbanks where there was thriving vegetation showed higher radiocaesium concentrations than new sediments deposited on riverbanks without vegetation at the end of 2016 or the old sediments collected in August 2017 (Figure 7). These new sediments also had a relatively high clay and silt content, suggesting that vegetation facilitated trapping of fine-grained sediment. However, the radiocaesium concentration of this material was lower than that of the riverbank sediments before the decontamination test, and the mud content was smaller. It should be mentioned that the air dose rate did not increase during the August 2017 measurements because the overall amount of sediment was not large.

On the other hand, after the passage of Typhoon Lan in 2017, a sediment layer with a thickness of about 20 cm was deposited on the riverbank (Figure 7). However, the radiocaesium concentration of this material was lower than that of the riverbank sediments after the decontamination demonstration test, and the mud fraction was low. The amount of vegetation biomass on the riverbank as of summer 2017 was only 40% of that near the decontamination area (measured in 2019). During the recovery and re-growth of the vegetation during the year after heavy flooding such as typhoons, the retention effect of fine-grained sediment is likely to have been small. In 2018, there were fewer heavy rainfall events that could have resulted in sediment deposition, and the sediments had lower radiocaesium concentrations and a smaller mud content.

[3] A type of integrated dosimeter that uses a special glass that emits fluorescence when exposed to ultraviolet light after irradiation. The dosimeter is attached to the chest of the human body and measures 1 cm dose equivalent.

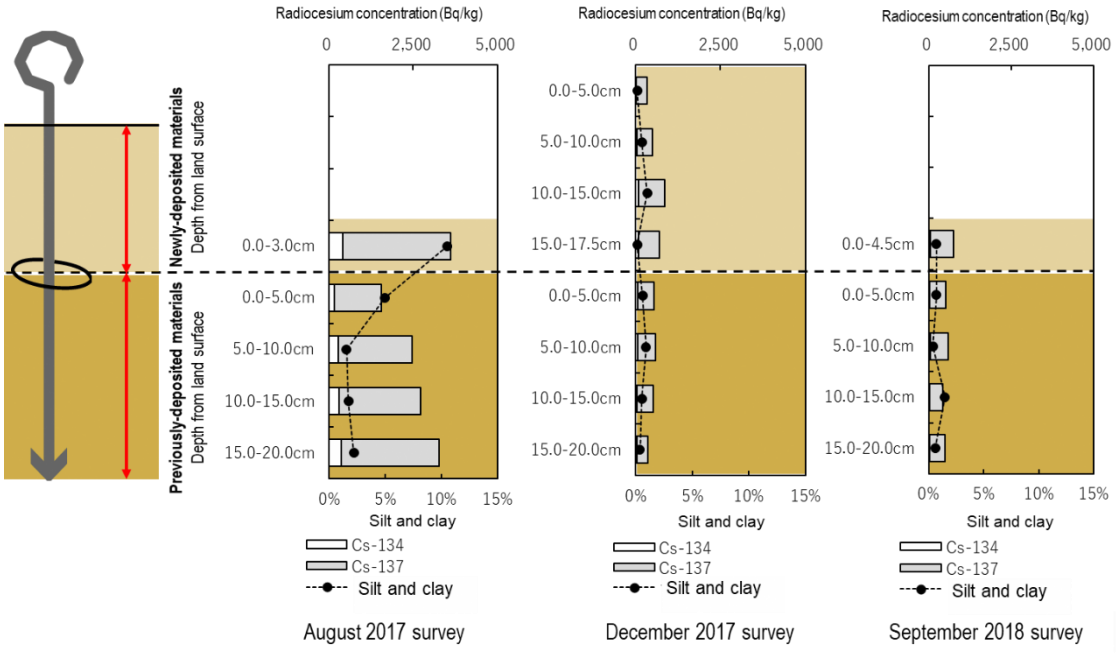

Figure 7. An example of depth distribution of radiocaesium concentrations in post-decontamination materials deposited in a riverside area (center of the survey area)

3.4.3. Investigation of the distribution of radiocaesium in river parks and testing remedial measures

Air dose rates at 1 m above the ground of Park A measured in August and September 2015 (before and after flooding following the passage of Typhoon Etau) are shown in Figure 8. Before the flood, the dose rates above 1.0 μSv/h were found along the river and in the north-eastern area. However, after the flood, at many of these sites gamma dose rate dropped to values of less than 1.0 μSv/h. In Park B, on the other hand, no notable changes were observed before and after the flood (Figure 9).

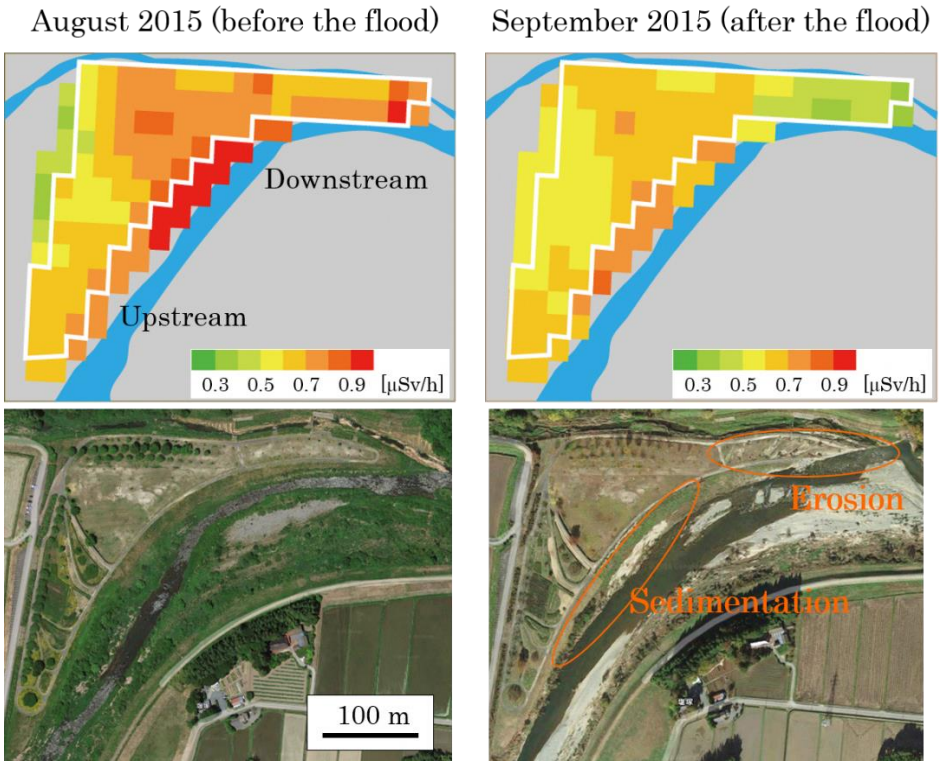

Figure 8. Distribution of air dose rates at 1 m above ground surface in Park A
The park is marked by white lines.

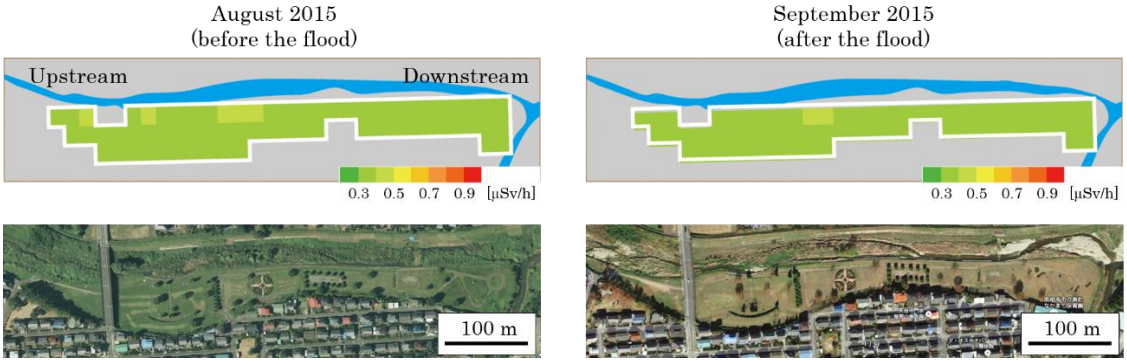

Figure 9. Distribution of air dose rates at 1 m above ground surface in Park B
The park is marked by white lines.

The deposition of caesium-137 in soil of Park A is shown in Figure 10. The total inventory of caesium-137 in the sampling depth ranged from 200 to 400 kBq/m^2 in lawns and flower beds, whereas the maximum caesium-137-inventory of up to 2400 kBq/m^2 was observed along the riverbanks, which was almost ten times higher. The high air dose rates along the riverbanks before the floods reflected this observation. In the lawn area, the caesium-137 concentration was highest in the surface layer (a few centimetres), while in the deeper layers the concentration was uniform and much lower than in the surface layer. In the flower beds, the distribution is quite uniform up to a depth of 15 cm due to homogenisation by cultivation. On the other hand, in the riverside area, low-concentrations were found to a depth of about 25-30 cm and the caesium-137 concentration peaked at a depth of about 40-50 cm. Observation of soil cross-sections at site 3 showed a clear

difference in colour tone and sediment grain size at a depth of around 30 cm, indicating that the 30 cm thick surface layer along the part of the riverbank is likely to consist of deposits from the September 2015 flood. Due to the formation of this low concentration layer and the erosion in the north-eastern part of the river bend (Figure 8), it was observed that the air dose rate decreased after the flood and so natural decontamination had occurred due to the flood. In the Niida River basin, it has been reported that significant erosion in the upper reach and deposition of sediments with low caesium-137 concentrations in the lower reach of this major flood have resulted in natural decontamination action along the riverbanks in various parts of the catchment.[15] The findings for Park A are consistent with this.

The situation was different in Park B, where the total inventory of caesium-137 up to the sampling depth of 20 cm was in the range of 130-220 kBq/m^2 in both flooded and unflooded areas. In both cases the high concentration layer remained within the surface layer of 10 cm. (Figure 11). Therefore, it can be assumed that only little sediment deposition occurred and this is why the air dose rates did not change noticeably (see Figure 9). These differences between the two sites in terms of sediment deposition and the tendency to accumulate caesium-137 are likely to be assumed for the following reasons based on the observations and measurements made.

- The riverbank of Park B is grassland, while in Park A there is thick vegetation of about 1 m height along the riverbank, which easily retains sediment;
- Upstream of Park B, sediment is retained in the reservoir, therefore, the sediment transport to Park B is low;
- The highly contaminated area (> 1000 kBq/m^2) is located upstream of the dam (Figure 3); therefore it is unlikely that sediments with high radiocaesium concentrations will reach Park B.

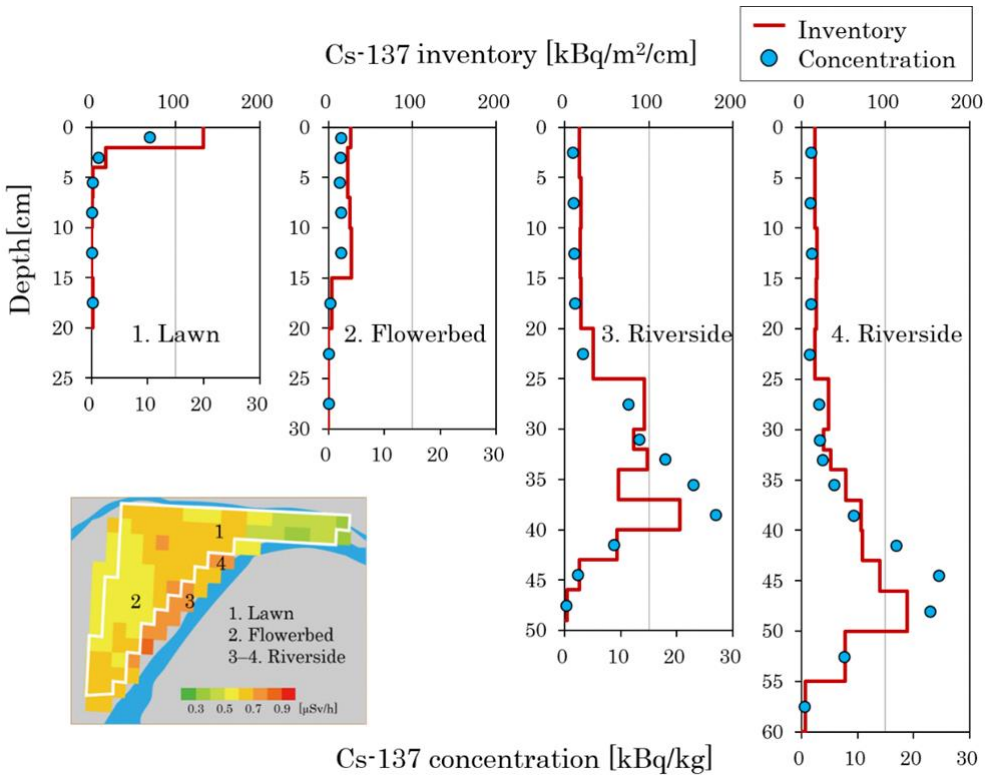

Figure 10. Depth distribution of radiocaesium in soil of Park A
Samples were collected after the extreme flood in September 2015.

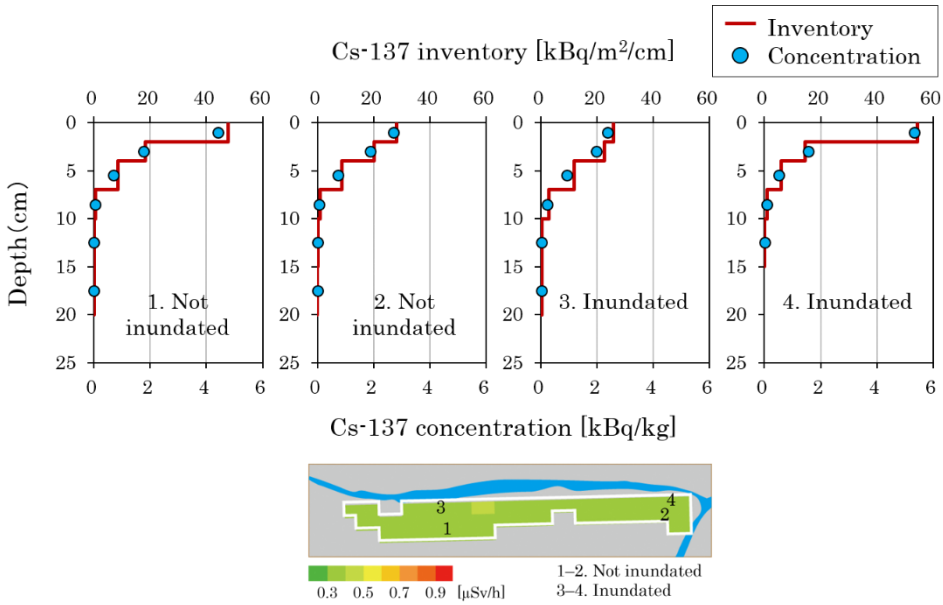

Figure 11. Depth distribution of radiocaesium in soil of Park B
Samples were collected after the extreme flood in September 2015.

The annual external doses due to the use of Parks A and B was estimated to be 0.018 mSv/year and 0.009 mSv/year respectively. The annual external dose estimated from measurements using glass badges in Minamisoma City where the parks are located, is 0.44 mSv/year (measurement period: July-September 2015; measured values were extrapolated to one year), [16] and the exposure

associated with park use is equivalent to 2-4% of this value. Therefore, the overall effect in terms of exposure reduction by decontamination of these parks is limited. Taking into account the results for the Kami-Oguni River in section 3.4 (2), it is considered that the importance of implementing decontamination measures along the riverbank is not high, as the time that people spend on the riverbank is generally limited and the radiation levels along the river decline due to natural processes[4].

3.4.4. Exploring public concerns on the safety of freshwater bodies

Five years after the accident, it was found that the challenges facing the administrative bodies in Fukushima Prefecture with regard to the aquatic environment due to radioactive substances and other factors are "*hindrance to activities carried out before the accident*", "*future impact of radioactive substances*" and "*continuation and maintenance of post-accident measures*". The results of the Fukushima Prefecture Public Opinion Survey also showed that there are regional differences in the change of Fukushima residents' views on safety for water, air and the environment. The change of view tends to be slower in the Central and Coastal Region than in Aizu Region (Figure 12). It was also found that perceptions of water and air and environment safety were significantly associated with the perception of radiation risks.

[4] Such processes include in particular i) migration of radionuclides to deeper layers => radionuclides in deeper layers are shielded by the overlying material, ii) deposition of sediment with lower radiocaesium activity on top of sediment with higher radiocaesium activity => shielding of the sediment with a high activity, iii) dislocation of sediment containing radionuclides due to erosion, iv) shielding effect due to vegetation

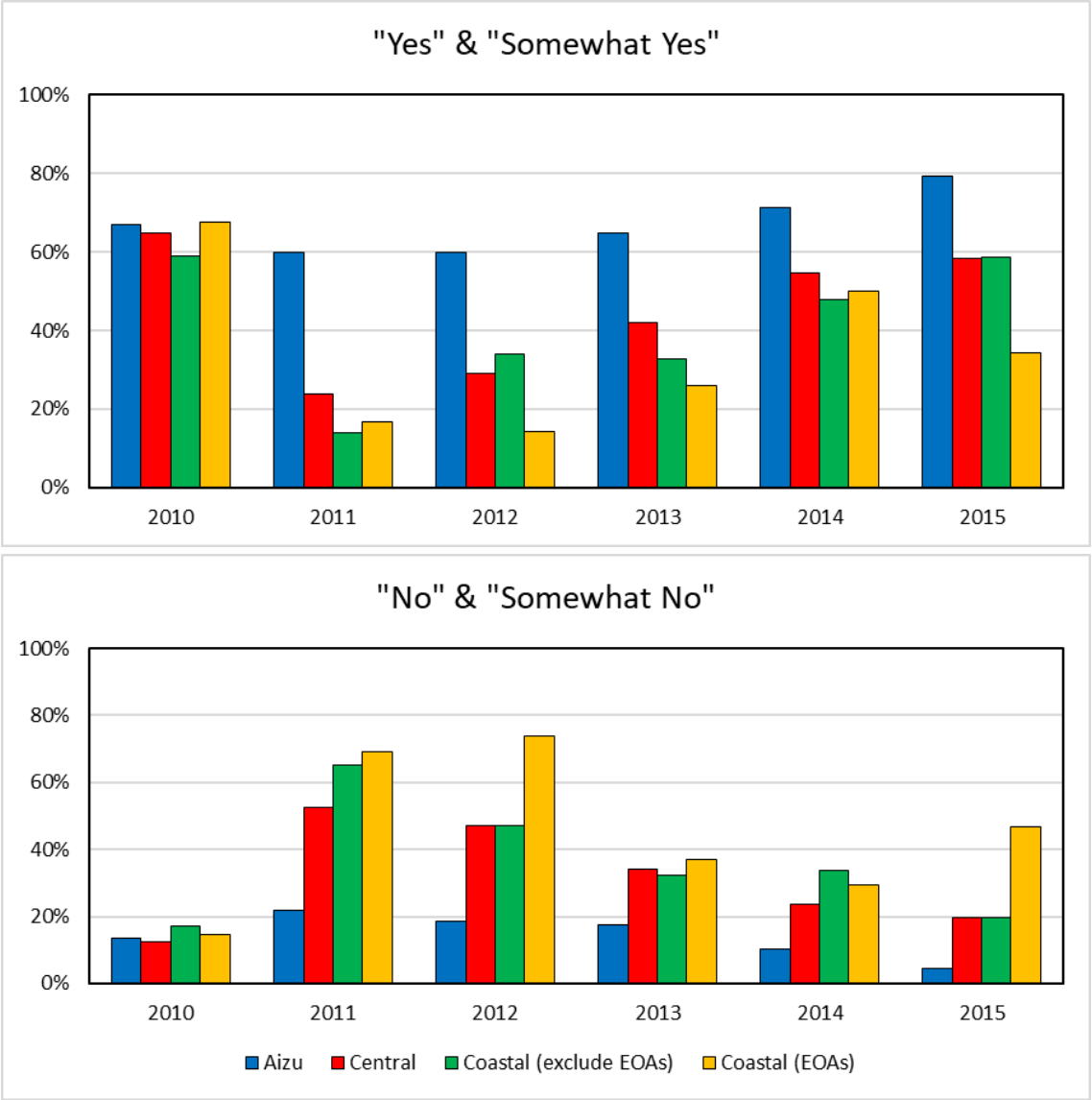

Figure 12. Changes over time in responses to question "Do you feel that your living environment is safe from environmental pollution including water and air pollution?"

EOAs represents Evacuation Order Areas.

3.4.5. Changes of radiocaesium concentration in riverbanks during large-scale flooding

The results of air dose rate measurements in Park A are shown in Figure 13: the average air dose rate before (31 January 2018) and after (17 October 2019) the passage of Typhoon Hagibis in 2019 was 0.30 μSv/h and 0.20 μSv/h respectively. Taking into account the 13% decrease in air dose rates due to physical decay between the measurements, this means that air dose rates have decreased by 23% due to erosion caused by rainfall events as typhoons. The impact of Typhoon Hagibis was stronger than that of previous typhoons, e.g., the air dose rate decreased by 14% after the passage of Typhoon Etau in September 2015. This difference in impact may be due to the different extent of erosion and sedimentation. After the passage of Typhoon Hagibis, a large amount of riverbank sediment was eroded along the Niida River as shown in the aerial photograph

of the park (Figure 13), e.g., the area with the highest air dose rate measured before the typhoon was washed away, exposing the park revetment (Figures 14(a) and 14(b)).

High radiocaesium inventories were observed in this area, but during the passage of Typhoon Etau in 2015, sediments with relatively low radiocaesium concentrations were deposited on the surface which caused a shielding effect, reducing the air dose rate (from the results in section 3.4.3.). However, as shown in Figure 14(b), sediment was deposited on the dike and vegetation continued to thrive after the passage of Typhoon Etau.

The main impact of Typhoon Hagibis on the reduction of air dose rates was caused by the loss of radiocaesium due to erosion of riverbank sediment. Therefore the effect of Typhoon Hagibis on the reduction of air dose rates was probably greater than the shielding effect due to deposition of sediments with low caesium activities that occurred during Typhoon Etau. On the other hand, the large amount of sand deposited around the Niida River inside the park and the branch river to the north of the park (Figures 14(c) and 14(d)) suggests that the reduction in air dose rates inside the park was due to shielding.

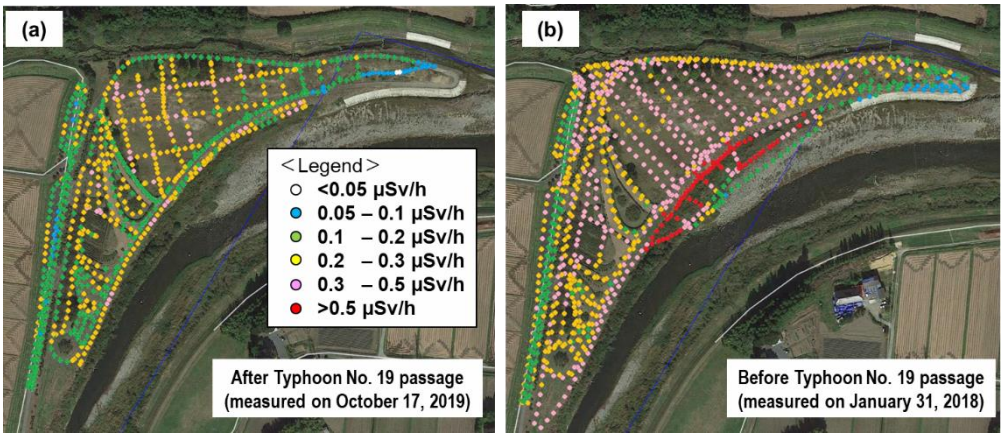

Figure 13. Air dose rate distribution at 1 m above ground surface in Park A (a) after the passage of Typhoon Hagibis, (b) before its passage

Background photographs (a) and (b) were obtained from Google Earth Pro[17] (date of the photo: October 21, 2018).

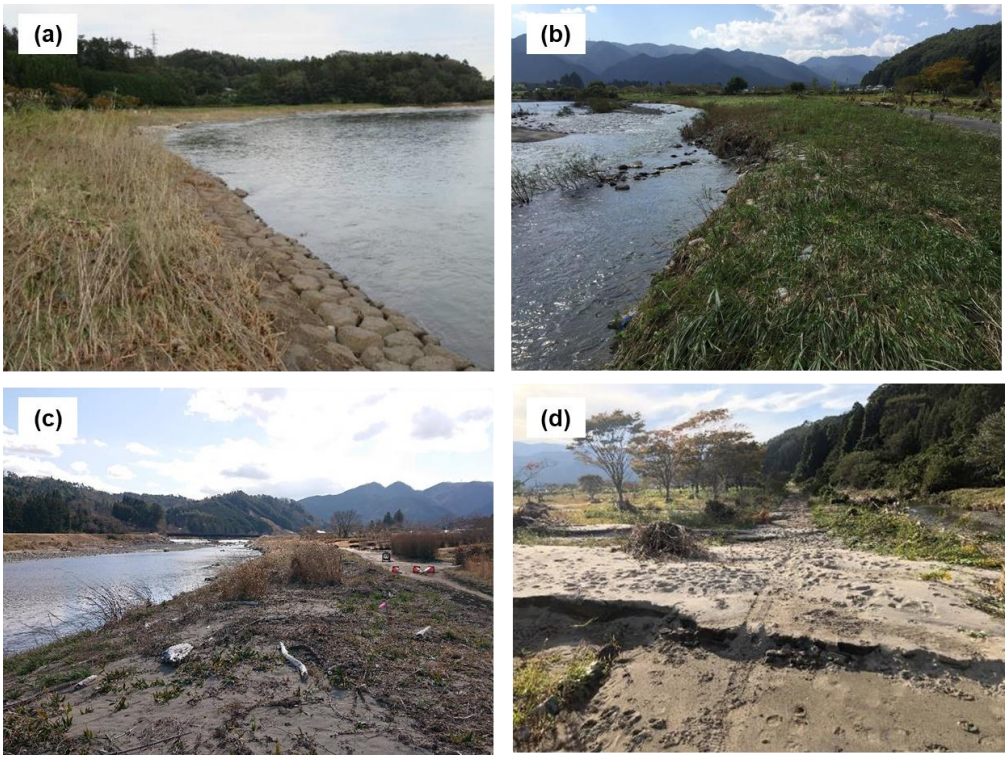

Figure 14. Photos showing the situations of riverside areas
(a) River revetment exposed due to river bank erosion caused by the passage of Typhoon Hagibis, (b) The same river revetment before being eroded (a photo taken from the opposite side on September 28, 2015), (c) Sediments deposited along the Niida River, (d) Sediment deposited along the branch river north of the park

For Park B, the mean air dose rate before and after the passage of Typhoon Hagibis in 2019 was 0.21 μSv/h and 0.16 μSv/h, respectively. When corrected for physical decay, this corresponds to a decrease of 12% due to erosion caused by events such as Typhoon Hagibis (Figure 15). Compared to a 5% decrease caused by Typhoon Etau in 2015, as in Park A, Typhoon Hagibis led to a larger decrease of air dose rates.

For Park B, only little erosion and sedimentation occurred during the passage of Typhoon Etau, but with the passage of Typhoon Hagibis, the entire park was flooded, causing changes in the river channel in the upstream area of the park. Large amounts of sand and gravel were deposited in the park, especially on upstream sides of the river channel. Considering the significant decrease of air dose rates in upstream areas, it is assumed that the reason that the air dose rates decreased was mainly due to shielding by deposited sediment.

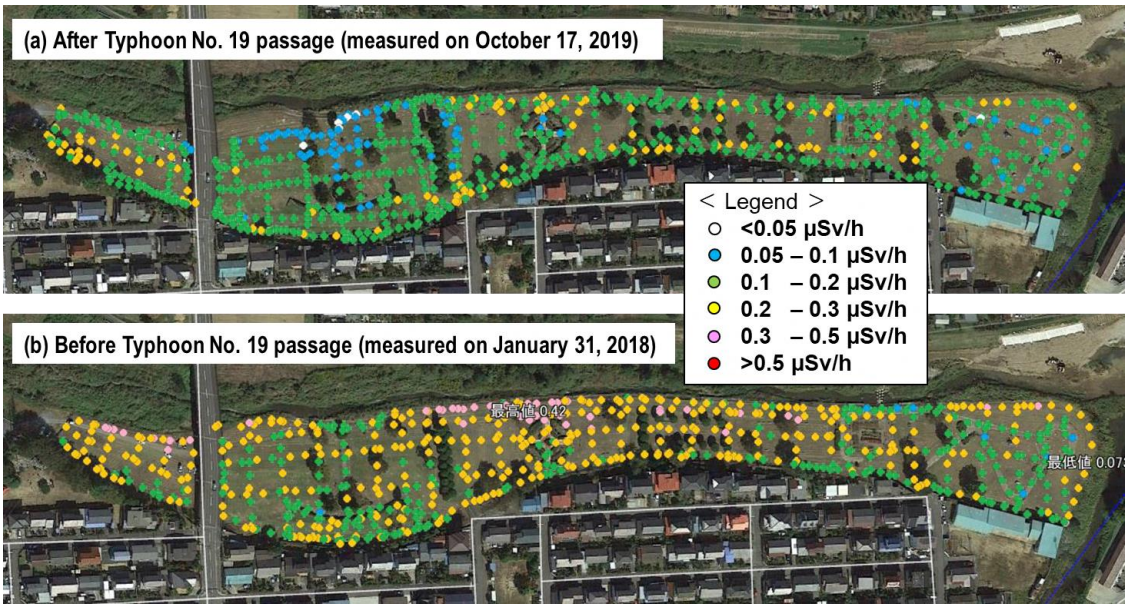

Figure 15. Spatial distribution of air dose rate at 1 m above ground surface in Park B

(a) After the passage of Typhoon Hagibis, (b) Before its passage

The background photographs were obtained from Google Earth Pro[17] (date of the photos: October 21, 2018).

In the Kami-Oguni River study site, air dose rates decreased not only in the river channel but also on the embankment around the river. Most of the sediment in the river channel had been removed due to the channel excavation work carried out immediately before the survey, but large amounts of newly deposited sediments (in particular sand and gravel) had accumulated in the river channel due to Typhoon Hagibis.

The results of this study confirm that Typhoon Hagibis in 2019 did not generally cause re-contamination at all sites investigated in this study, but rather reduced air dose rates through natural attenuation processes, such as removal of material with relatively high radiocaesium activities and sedimentation of material with low radiocaesium concentrations.

3.5. Conclusions

Firstly, the project tested countermeasures applicable for terrestrial and aquatic areas of the Fukushima Prefecture to mitigate the effects of radiocaesium deposition, based on existing knowledge. In addition, the effectiveness of decontamination methods based on the spatial distribution of radiocaesium was demonstrated at a study site set up in a riverbank, and the sustainability of the effectiveness after the decontamination test was verified. In addition, it was found that – although radiocaesium may accumulate in the riverbeds downstream – in the case of large-scale floods such as Typhoon Etau in 2015 and Typhoon Hagibis in 2019, there was no re-contamination due to sediment deposition, but rather that the natural 'decontamination' processes worked to reduce the air dose rate. External exposure at the riverbanks was therefore found to be low.

In addition, analysis of the results of public awareness surveys confirmed that there is still persistent concern about the safety of the aquatic environment in severely contaminated areas.

The results of this study were successively communicated to the relevant departments in Fukushima Prefecture. The methods for decontamination of the riverbeds were subsequently utilised as river maintenance measures.

References

1) Ministry of Education, Culture, Sports, Science and Technology (2011) Results of the 3rd round of aircraft monitoring measurements by the Ministry of Education, Culture, Sports, Science and Technology. (Japanese) https://radioactivity.nsr.go.jp/ja/contents/5000/4858/24/1305819_0708.pdf
2) Minato S. (2006) Distribution of Terrestrial Gamma Ray Dose Rates in Japan. Journal of Geography, 115, 87-95 (Japanese)
3) Japan Atomic Energy Agency, Database for Radioactive Substance Monitoring Data. https://emdb.jaea.go.jp/emdb/
4) Japan Atomic Energy Agency, Overview of Operations at Fukushima Environmental Safety Center (Advancement of Decontamination and Volume Reduction Technology) (Japanese), https://fukushima.jaea.go.jp/fukushima/work/work3.html
5) Japan Meteorological Agency, Data and Materials (Japanese), http://www.jma.go.jp/jma/menu/menureport.html.
6) Fukushima Prefecture, the prefectural public opinion survey (Japanese), https://www.pref.fukushima.lg.jp/sec/01010e/koucho1-439.html
7) Konoplev A., Golosov V., Wakiyama Y., Takase T., Yoschenko V., Yoshihara T., Parenyuk O., Cresswell A., Ivanov M., Carradine M., Nanba K., Onda Y. (2018) Natural attenuation of Fukushima-derived radiocesium in soils due to its vertical and lateral migration. Journal of Environmental Radioactivity, 186, 23-33.
8) Nakanishi T., Sato S., Matsumoto T. (2019) Temporal changes in radiocesium deposition on the Fukushima Floodplain. Radiation Protection Dosimetry, 184, 311-314.
9) Ministry of the Environment (2013) Decontamination Guidelines 2nd Edition (Japanese) http://josen.env.go.jp/material/pdf/josen-gl-full_ver2_supplement_1803.pdf, (Tentative Translation) http://josen.env.go.jp/en/policy_document/pdf/decontamination_guidelines_2nd.pdf
10) Ministry of Agriculture, Forestry and Fisheries (2016) Technical Manual for Countermeasures against Radioactive Materials in Reservoirs (Japanese), https://www.maff.go.jp/j/nousin/saigai/attach/pdf/tamemanu_zentai-3.pdf
11) IAEA (2006) Environmental consequences of the Chernobyl accident and their remediation: Twenty years of experience report of the Chernobyl forum expert group ‘environment’. Vienna.

12) Nakao, A., Funakawa, S., Tsukada, H., Kosaki, T. (2012) The fate of caesium-137 in a soil environment controlled by immobilization on clay minerals. SANSAI Environ. An Environmental Journal for the Global Community, 6, 17-29.
13) Tanaka, K., Kondo, H., Sakaguchi, A., Takahashi, Y. (2015) Cumulative history recorded in the depth distribution of radiocesium in sediments deposited on a sandbar. Journal of Environmental Radioactivity, 150, 213-219.
14) Date City, Fukushima Prefecture (2015) Date Recovery and Revitalization News (Vol. 22) (Japanese), https://www.city.fukushima-date.lg.jp/uploaded/attachment/16650.pdf
15) Konoplev, A., Golosov, V., Laptev, G., Nanba, K., Onda, Y., Takase, T., Wakiyama Y., Yoshimura, K. (2016) Behavior of accidentally released radiocesium in soil–water environment: Looking at Fukushima from a Chernobyl perspective. Journal of environmental radioactivity, 151, 568-578.
16) Minamisoma City, Fukushima Prefecture (2016) Results of the Indivisual Cumulative Dose Measurement (July – September 2015) (Japanese), https://www.city.minamisoma.lg.jp/portal/health/hoshasen_hibaku/3/1/3/4954.html
17) Google Earth Pro aerial photograph. https://www.google.co.jp/earth/

4. FIP4：Development of environmental mapping technology using GPS walking surveys

(Note: Reprint of the previous report with some wordings revised and update added since the theme ended in FY2015)

4.1. Abstract

Fukushima Prefecture developed environmental mapping technology with GPS walking surveys as a tool for surveying the regional distribution of air dose rates.

This report covers the results of parameter verification necessary for the development of this technology and the history of development.

4.2. Purpose

To understand the air dose rate (hereinafter simply referred to as the dose rate) in Fukushima Prefecture after the accident at the Fukushima Daiichi Nuclear Power Plant, we have conducted fixed-point measurements with monitoring posts and dose rate measurements in car-borne surveys using the GPS-linked dose rate measurement device KURAMA (Kyoto University RAdiation MApping System)-II, and have provided information to prefecture residents on the prefecture homepage (Figure 1 and 2).

(a)

(b)

Figure 1. Example of current monitoring
(a)：Example of a fixed-point measurement (using a real-time dose-rate measurement system)
(b)：Example of a car-borne survey (KURAMA-II installed on the back of a local bus)

Figure 2. Fukushima Prefecture radiation measurement map
(http://fukushima-radioactivity.jp/pc/)
(a): Example of a fixed-point measurement
(b): Example of a traveling survey

As of March 2016, measurements are being made at 3500 fixed points with monitoring posts in Fukushima Prefecture. Car-borne surveys using local buses are also being conducted with the purpose of interpolating the fixed-point measurements.

It is, however, difficult to conduct fixed-point measurements or car-borne surveys in some places, including parks, forests, and alleys near residential areas, and dose rates sometimes differ between fixed measuring points at the same facility or site (Figure 3). For these reasons, in addition to fixed-point measurements and car-borne surveys, we require measurement technology with which to understand a more detailed distribution of dose rates, and we need to present the measurement results in a format that is easy to understand.

Therefore, to employ interpolation to obtain dose rates for parks, forests, and alleys near residential areas where fixed-point measurements and car-borne surveys are difficult, we developed environmental mapping technology using GPS walking surveys together with unmanned aerial vehicles (UAVs) developed by the IAEA.

The prefecture and IAEA have shared the development of environmental mapping technology with GPS walking surveys (FIP4) and environmental mapping technology with unmanned aerial vehicles (FCP3), and by combining these technologies and visualizing measurement results, we were able to create dose distribution maps that are more detailed and effective.

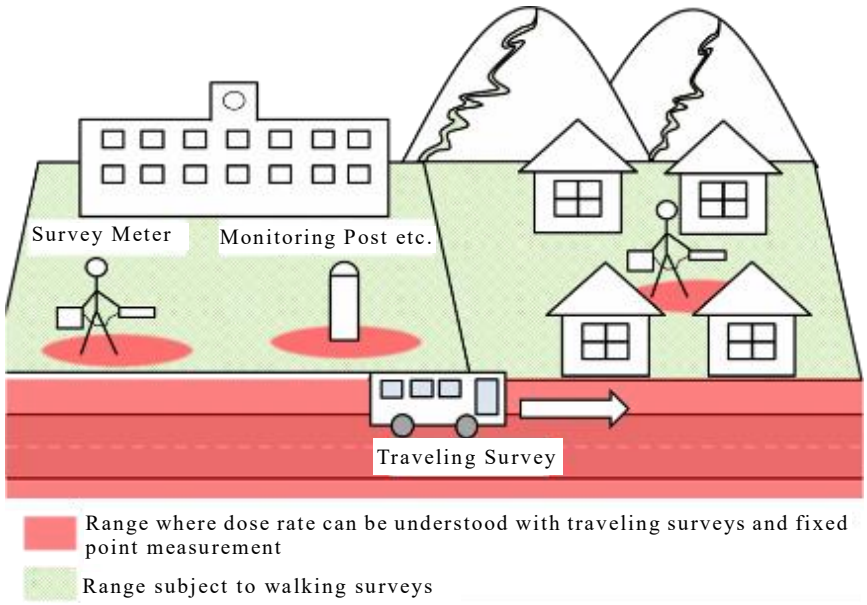

Figure 3. Measurement ranges of conventional measurement methods

4.3. Content of implementation

4.3.1. Development of equipment

We used the KURAMA-II, which was developed by Kyoto University, for walking surveys, and assembled five pieces of equipment in a way suited to walking surveys (Figure 4). The orange backpack contains a CsI (T1) scintillation detector, which is a low-dose-rate detector, and a high-precision GPS unit. The back packer measures the dose rate by walking on a transverse course while merging dose rate data from the low-dose CsI detector and position information from the high-precision GPS device.

Figure 4. Walking survey equipment
(a): Appearance of the devices
(b): Low-dose-rate CsI detector (Hamamatsu Photonics K.K. C12137-01) and high-precision GPS unit (SOKKIA GIR1600)

The measurement screen is shown in Figure 5. The measurement interval may be selected as 3 seconds, 5 seconds, and so on. At the start of the measurement, information such as the current position and dose rate are recorded to a notebook computer, and the position information, dose rate, trends, and mapping results are displayed on the computer screen.

Measurers can look at the screen to check the measurement position and dose rate while

conducting detailed measurements.

Figure 5. Display screen on a personal computer

4.3.2. Development of mapping technology using Geographic Information System (GIS)

We conducted a specification study and developed a GIS tool for capturing, combining, and mapping the dose rate and position information gained from walking surveys and UAVs. An overview of the tool is shown in Figure 6.

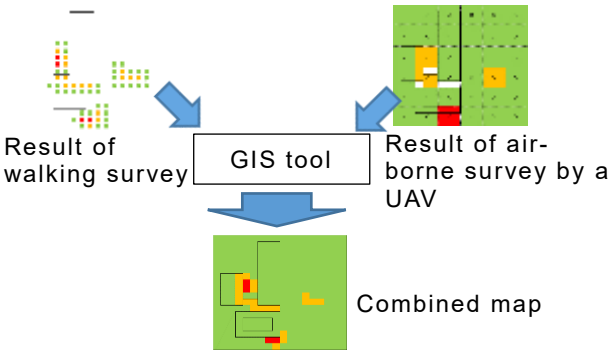

Figure 6. Overview of the GIS tool

年月日	時間	緯度	経度	標高	速度	方位	線量率	検出器温度
2015/3/15	12:17:05	37.47682	140.9572	25.8	0.5	98.95	1.71	15.51
2015/3/15	12:17:08	37.47679	140.9572	26.7	8.5	165.71	1.78	15.51
2015/3/15	12:17:11	37.47676	140.9572	27.5	8.5	193.67	1.83	15.53
2015/3/15	12:17:14	37.47672	140.9572	28.2	7.8	168.79	1.73	15.53
2015/3/15	12:17:17	37.47669	140.9572	28.6	9.6	187.57	1.76	15.53
2015/3/15	12:17:20	37.47666	140.9572	28.9	8.9	224.37	1.78	15.54
2015/3/15	12:17:23	37.47663	140.9571	29.2	11.4	229.71	2.01	15.54
2015/3/15	12:17:26	37.47661	140.9571	29.2	10.4	221.91	1.98	15.54
2015/3/15	12:17:29	37.47657	140.9571	29.2	9.2	196.46	1.91	15.56
2015/3/15	12:17:32	37.47654	140.9571	29.3	9.1	190.88	1.96	15.56
2015/3/15	12:17:35	37.4765	140.9571	29.3	11.6	183.68	2.03	15.56
2015/3/15	12:17:38	37.47646	140.9571	29.3	9.2	186.22	2.14	15.56
2015/3/15	12:17:41	37.47643	140.9571	29.3	10.5	186.58	2.14	15.58
2015/3/15	12:17:44	37.47639	140.9571	29.2	7.7	151.32	2.16	15.58
2015/3/15	12:17:47	37.47636	140.9571	29.3	7.8	174.76	2.09	15.58

Figure 7. Data including the dose rate

It is possible to produce a contour map using the GIS tool. Data in comma-separated-value format recorded in walking surveys are converted to Microsoft Excel file format (Figure 7), and point data with dose rate information are created from the latitudinal and longitudinal information contained in the data (Figure 8). With the GIS tool, it is possible to estimate the dose rate at unmeasured positions and to produce contour maps from the point data created using any interpolation algorithm, such as Inverse Distance Weighting (IDW) algorithm (Figure 9).

Figure 8. Map data and dose rate plotting

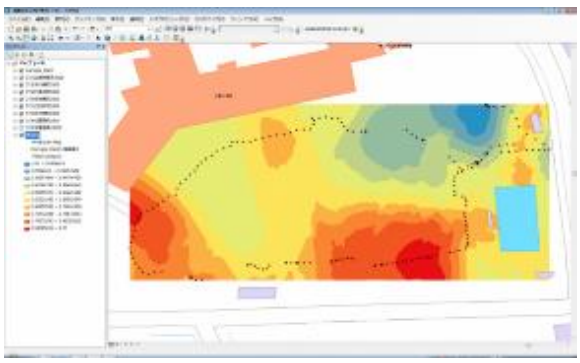

Figure 9. Interpolated dose map

4.3.3. Walking survey implementation

We collected parameters necessary for walking surveys, and carried out the survey in several areas.

4.3.4. Manual preparation

We created a manual surveying the walking survey method. Photos and sentences are combined in this manual for easy understanding.

4.4. Results

4.4.1. Gathering parameters necessary for walking surveys

We conducted a field test of walking surveys, and gathered data for evaluation and analysis (Figure 10). Data were gathered to check the direction characteristics and appropriate measurement density, as well as to determine correction factors.

Figure 10. View of a walking survey

4.4.1.1. Checking direction characteristics

Shielding from the measurers themselves affects the contribution from the radiation source depending on the walking direction in walking surveys (Figure 11). Walking surveys were therefore conducted by changing the walking speed and by walking back and forth so as to straddle the radiation source and check the effect of direction characteristics.

As a result, while shifts occurred in places where peaks appeared, they fell within a range of about 2 meters, and measurements showed that the maximum value of the dose rate was nearly the same during forward and reverse passes (Figure 12). We also confirmed that reducing the walking

speed caused the peaks of the dose rate distribution to grow sharply (Figures 13 and 14).Judging from the above result, the impact of direction characteristics on a measured value of a walk survey was considered small at a constant walking speed.

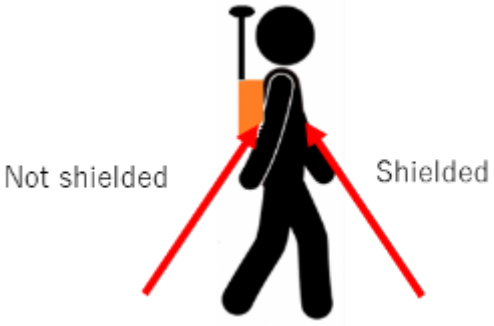

Figure 11. Measurement of direction characteristics

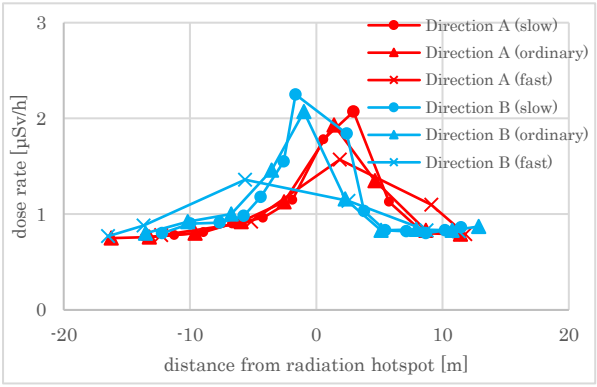

Figure 12. Measurements after changing speed and direction

Figure 13. Change in walking speed

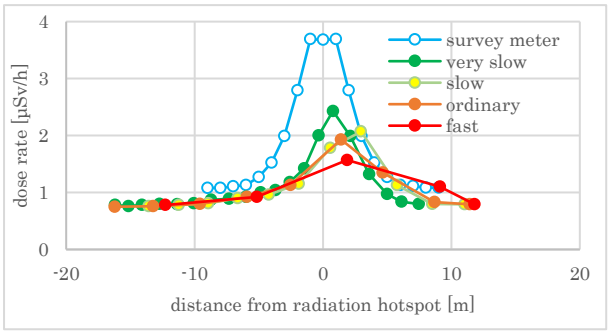

Figure 14. Change in measurements due to walking speed

4.4.1.2. Determination of correction factors in a comparison test with survey meters

We assumed measurements made with a NaI (Tl) scintillation survey meter (TCS-172B) at a height of 1m to be the most reliable, and the survey meter was calibrated with traceability. We compared measurements made using a survey meter with those obtained in a walking survey (Figure 15). A comparison was made at several points with differing dose rates. At each point, we faced north, south, east, and west and made measurements five times in each direction to mitigate direction characteristics. We then took the average value for all directions as the measurement for that point. We next plotted the measurements of walking surveys against the survey meter to determine the correction factor.

Figure 15. Images of measuring
(a): Measurement with a survey meter
(b): Measurement with a walking survey
Both measurements were made facing four directions.

The results of the comparison are shown in Figure 16(a). There was good linearity between the measurements of walking surveys and the survey meter below a survey meter measurement of 1 μSv/h, whereas the linearity deteriorated above approximately 1 μSv/h. This phenomenon is due to count loss caused by excessive radiation incidence on the low-dose CsI detector.

In light of the above results, we changed the detector to a high-dose-rate CsI detector (Figure 17) and compared the results obtained using the survey meter with measurement results of walking surveys again. The results are shown in Figure 16(b). We confirmed that as a result of changing the detector, the linearity of walking survey measurements against survey meter measurements is obtained even in the high dose range.

We also confirmed that the high-dose CsI detector can make better measurements than the low-dose rate CsI detector in the high dose range in field tests. This is also confirmed in Figure 18, which shows the walking survey results having changed detectors at the same geographic point. The maximum indicated value is higher for the high-dose-rate CsI detector than for the low-dose-rate CsI detector, and the high-dose-rate area represented by red markers appears, indicating that measurements are made without counting loss of radiation.

(a)

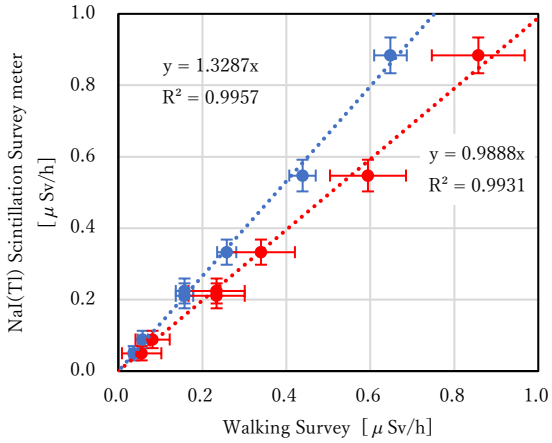

(b)

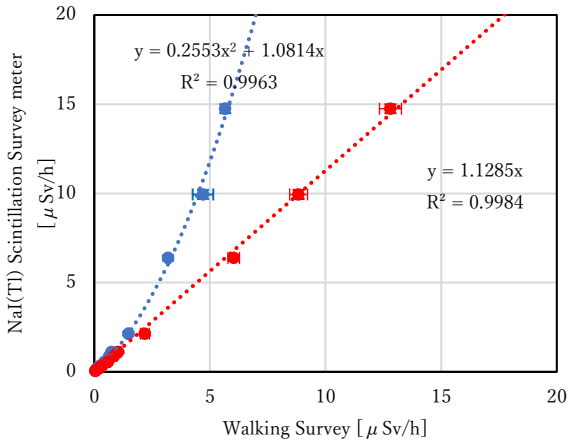

Figure 16. Comparison of measurements of the survey meter and walking survey

(a): Chart plotting data below 1 μSv/h

(b): Chart plotting all data

● Comparison of the measurements of the low-dose-rate CsI detector (caesium-137, 662keV measuring range: 0.001 to 10 μSv/h) and NaI survey meter.

● Comparison of the measurements of the high-dose-rate CsI detector (caesium-137, 662keV measuring range: 0.01 to 100 μSv/h) and NaI survey meter.

Note that the approximate curve is not affected by the self-dose from the measurement detector, with the intercept being zero.

Figure 17. High-dose CsI detector (Hamamatsu Photonics C12137)

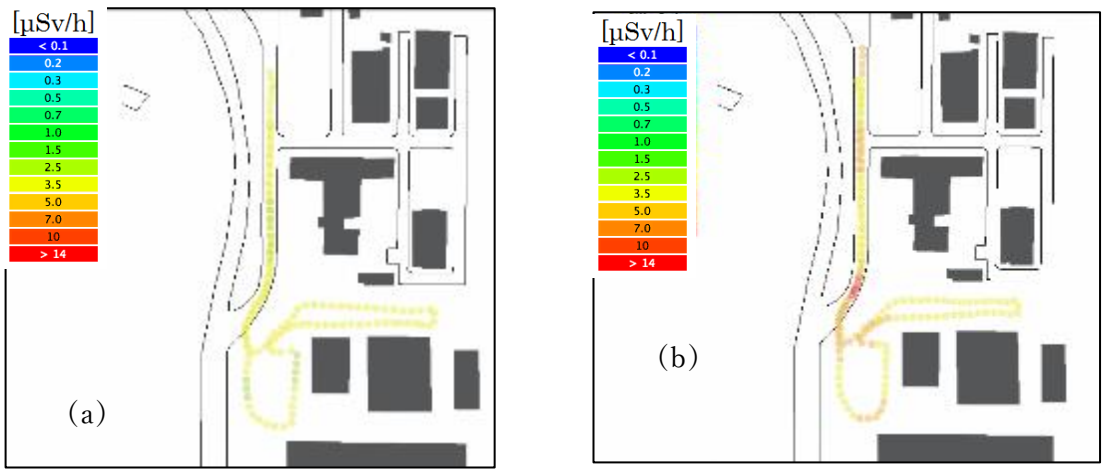

Figure 18. Walking surveys having changed the detector
(a): Walking survey with the low-dose-rate CsI detector.
The indicated value range is 2.77 to 5.99 μSv/h.
(b): Walking survey with the high-dose-rate CsI detector.
The indicated value range is 5.00 to 29.5 μSv/h.

According to the above comparisons, we set the correction factors of walking surveys to 1.3 when using the low-dose-rate CsI detector at points with a dose rate less than 1 μSv/h and 1.1 when using the high-dose-rate CsI detector.

4.4.1.3. Confirming variations in measurements

We conducted-fixed point measurements to confirm variations in measurements for a measurement time of 3 seconds in the low dose rate range. Fixed-point measurements were made with both the low-dose-rate CsI detector and the high-dose-rate CsI detector.

Results showed that the variation in measurement results was larger for the high-dose-rate CsI detector at points with a low dose rate (Figure 19). The variation coefficient obtained from dividing the standard deviation of measurements by the average value was 19.7% for the low-dose-rate CsI detector but 42.7% for the high-dose-rate detector. Error in measurements made with the low-dose-rate detector was small because of the high counting rate achieved with the large crystal while error in measurements made with the high-dose-rate detector was large because of the small counting rate achieved with the small crystal.

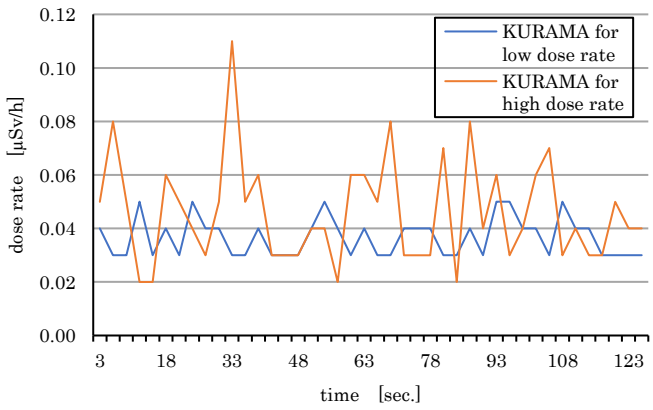

Figure 19. Measured value dispersion check

On this basis, we decided to use the low-dose-rate CsI detector, which has a small variation at low dose rates, at geographic points with a dose rate less than 1 μSv/h, and to use the high-dose-rate CsI detector at geographic points with a dose rate greater than 1 μSv/h.

4.4.2. Conducting walking surveys

With the purpose of studying the operation of walking surveys and acquiring basic data, we conducted walking surveys at places with differing conditions. Examples of such walking surveys are described below.

4.4.2.1. Walking survey in western Fukushima City

We conducted a walking survey on a trial basis in western Fukushima City. At the center of this geographic area is a surface paved with asphalt, with ditches along the edges. There were no obstructions on the outside of the asphalt surface, leaving the surface wide open and surrounded by grass.

Results of a walking survey conducted at this geographic point are shown in Figure 20. The paved surface at the center of the range of the walking survey had a low dose rate compared with that of the surroundings. It is considered that this low dose rate is due to the easy decontamination of the paved surface and the strong effect of weathering. In addition, the radiation dose in the vicinity of the ditch was higher than that of the surroundings. This is probably because there was an inflow of radioactive material from the surrounding area.

We conducted a high-density walking survey and tested interpolation with a GIS tool (Figure 21). Interpolation was conducted with IDW. The interpolated radiation dose rate in the paved area was low, and the dose rate in the vicinity of the ditch was high.

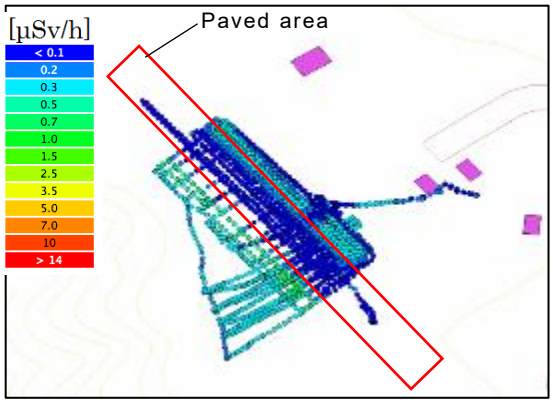

Figure 20. Results of a walking survey in western Fukushima City

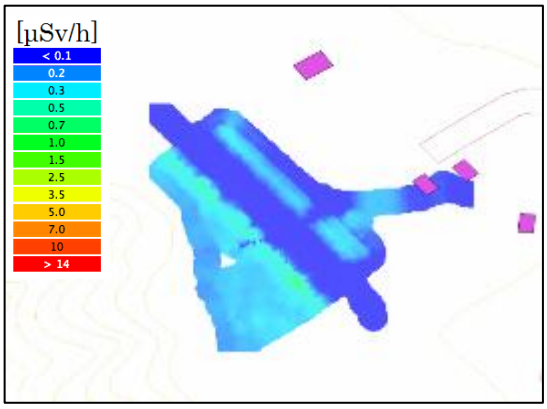

Figure 21. Results of interpolation with IDW

4.4.2.2. Walking survey in the periphery of a temporary storage site

We conducted a walking survey in a temporary storage site and its periphery in the Nakadori region of Fukushima Prefecture (Figure 22). The area inside the red frame in the figure is the temporary storage site. The dose rate near the temporary storage site was equal to or less than the dose rate in the periphery, and no effect on the outside on the outer side was seen in this temporary storage site.

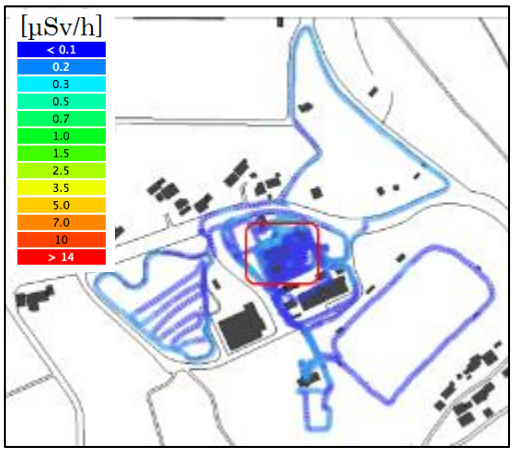

Figure 22. Dose map (with the temporary storage site indicated by the red frame.)

4.4.2.3. Walking survey in the Hamadori region (outside the evacuation zone)

We conducted a walking survey around rivers in the Hamadori region of Fukushima Prefecture (outside the evacuation zone) (Figures 23 and 24). There is a paved surface on the left side of the figure, with the rest of the study area being gravel or grassland. The dose rate was low on the paved surface and nearly uniform in other areas.

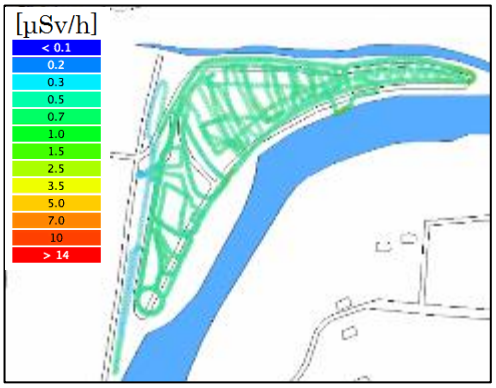

Figure 23. Dose map

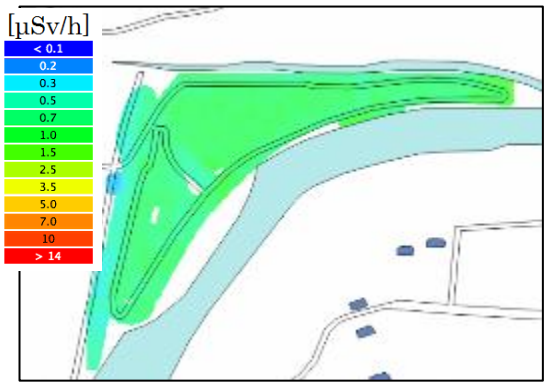

Figure 24. IDW interpolation result

4.4.2.4. Walking survey in a difficult-to-return evacuation zone

We conducted a walking survey in a difficult-to-return evacuation zone in Fukushima Prefecture (Figures 25 and 26). The area where the walking survey was conducted was nearly

uniform grassland. The dose rate was nearly uniform in the area, with no large deviation observed.

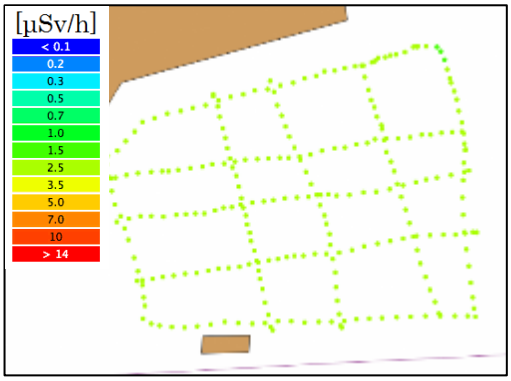

Figure 25. Dose map

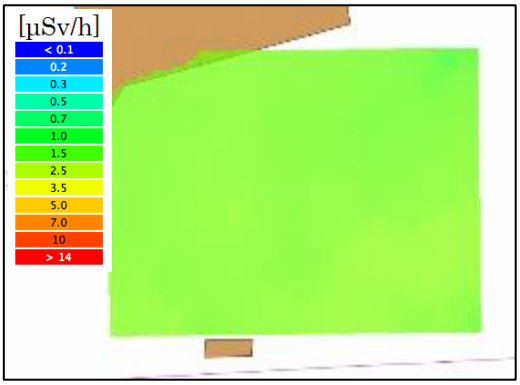

Figure 26. Results of interpolation by IDW

4.5. Conclusions

Results were obtained in developing walking surveys by 2015.

In terms of developed equipment, the walking survey system adopted KURAMA, which was designed by Kyoto University and has a structure suitable for a walking survey. Additionally, to analyze the obtained data or to work with other monitoring methods, such as a UAV survey, we prepared a GIS data processing system. Furthermore, by collecting data for the determination of direction characteristics and calibration constants, it has become possible to measure the dose rate in a walking survey.

We conducted walking surveys at several points and confirmed that it is possible to measure the air dose rate and to create a contour map with a GIS processing system.

We published a manual for walking surveys and made the manual available to the general public.

In fiscal 2016, we conducted walking surveys or lent the necessary equipment at the request of municipalities. In recent years, walking surveys have been utilized in the public projects for monitoring of the air dose rates (e.g., Satoyama Restration Model Project).

5. FIP5：Study of proper treatment of waste containing radioactive material

5.1. Abstract

Using incineration ash (bottom ash and fly ash) containing radiocaesium generated in Fukushima Prefecture, laboratory tests were conducted to investigate radiocaesium elution and the suppression of radiocaesium elution by acid clay and zeolite. Based on the results, experiments regarding the suppression of radiocaesium elution from fly ash using two different addition methods were carried out at actual municipal waste incineration facilities.

Moreover, each status of the landfill disposal sites was investigated, including the method of landfilling incineration ash and the concentration of radioactive caesium in leachate. While a study on landfill disposal sites was included in this project from FY 2018, Fukushima Prefecture had launched the same study on its own before that, so this report also includes the content of the study conducted by FY 2017.

5.2. Purpose

When municipal waste containing radioactive caesium scattered by the incident at TEPCO's Fukushima Daiichi Nuclear Power Station is incinerated, radioactive caesium moves and concentrates in the incineration ash. Although 10 years have passed since the accident and concentrations of radioactive caesium have decreased considerably, ash from the incineration of municipal waste contaminated with radioactive materials is still continuously produced, making the proper treatment and disposal of this ash a challenge. In particular, landfill sites, which are the final destination of waste containing radioactive caesium, are required to continue to provide safe (i.e., non-leaking) storage of radioactive caesium until it decays to an acceptable level. Therefore, Fukushima Prefecture has decided to compile actual cases on methods to prevent leakage of radioactive caesium from incineration fly ash (which contains particularly high levels of radioactive caesium), investigate leakage behavior of radioactive caesium from landfill sites, assess the safety of individual disposal sites and their management of monitoring after completion of landfill disposal, etc..

5.3. Radiocaesium distribution between bottom ash and fly ash

Incineration of waste generates two types of incineration ash: fly ash generated during the exhaust fumes treatment process and bottom ash discharged from the bottom of the furnace. Radiocaesium in fly ash has a high concentration and is easily dissolved in water, while radiocaesium in the bottom ash has a low concentration and is difficult to dissolve in water. Therefore, two methods to control the distribution of radiocaesium in fly ash or bottom ash were explored for the purpose of separation of radiocaesium; washing or the safe storage of bottom ash containing radiocaesium.

In addition, to confirm the safety of incinerating the waste filter cloth in the incineration facility, which was generated during the exchange of bag filters of equipment to collect fly ash in the exhaust fumes treatment process, incineration tests of waste filter cloth were conducted, and an

investigation of the exhaust fumes and incineration ash emitted during the incineration was conducted.

5.3.1. Investigations

5.3.1.1. Radiocaesium distribution between bottom ash and fly ash

Radiocaesium generally tends to evaporate during incineration and to transfer to fly ash rather than remaining in bottom ash. The distribution of radiocaesium in bottom ash and fly ash at incineration facilities in Fukushima Prefecture are given in Table 1. Approximately 60% of total radiocaesium is transferred to fly ash.

Table 1. Radiocaesium distribution between bottom ash (BA) and fly ash (FA) at MSW incineration facilities in Fukushima Prefecture.

Facilty	Capacity	Dust collection	Annual inicine-ration (2011FY)	Ash generation		Radiocaesium concentration		Radiocaesium distribution	
				BA	FA	BA	FA	BA	FA
	[t/d]		[t/y]	[t/y]		[Bq/kg]		[%]	
A	105	BF	16,035	2,053	632	12,220	49,400	45	55
B	120	BF	28,964	4,019	747	3,910	34,900	38	62
F	80	BF	20,230	2,190	1,076	16,640	33,900	50	50
G	100	EP	30,111	2,912	737	3,920	36,300	30	70
H	90	BF	16,948	1,392	681	1,494	6,640	31	69
J	60	BF	10,181	1,342	336	639	4,650	35	65
N	50	BF	837	93	41	3,140	13,110	35	65
P	50	BF	8,906	720	422	2,269	5,690	40	60
Q	150	EP	35,612	4,797	724	7,540	45,500	52	48
R	40	BF	12,401	2,190	262	2,200	17,360	51	49
S	30	BF	4,574	381	86	1,706	12,260	38	62

Note 1 Values in this table are not corrected for the amount of water and materials added.
Note 2 incinerators at all facilities are of the stoker furnace.
Note 3 Radiocaesium concentrations were measured in July 2011.
Note 4 Dust collection method, BF:bag filter; EP:electrostatic precipitator

We identified the following five main factors that have the potential to govern the transfer of radiocaesium: (a) combustion temperature, (b) air ratio, (c) waste composition, (d) addition of chemicals, and (e) particle size of ash.

Among these factors, (b) air ratio (air volume) affects various system parameters, including the flue gas velocity, which potentially disturbs the combustion balance and affects proper incineration, (c) waste composition cannot be controlled, and (e) ash particle size is technically difficult to control. We thus focused on the relationships between the migration behavior of radiocaesium and (a) combustion temperature and (d) addition of chemicals.

5.3.1.1.1. Effect of combustion temperature

Of the 16 municipally owned municipal solid waste incineration facilities in Fukushima Prefecture, we performed tests in cooperation with 4 incineration Facilities A to D. All facilities were equipped with stoker furnaces.

We compared the distribution of radiocaesium in bottom ash and fly ash when the temperature at the incineration chamber outlet was increased (or decreased) 50°C from the normal operating temperature range during normal operation.

To obtain a combustion chamber outlet temperature of 50°C higher or lower than that in normal operation, we changed the temperature of combustion air supplied to the combustion chamber (i.e., primary air) by approximately 50°C from the temperature maintained during normal operation. The amount of combustion air (i.e., primary air) was not changed which prevented changes in the production of bottom ash and fly ash due to ash blow up. Other operating conditions, such as those related to the furnace water spray and the amount of secondary air, differ among facilities.

The true combustion temperature (combustion temperature range in the incinerator) could not be measured directly. Therefore, we used the combustion chamber outlet temperature measured by the facility as an index of the combustion temperature and evaluated the impact of the chamber outlet temperature changes on radiocaesium migration. At Facility C, however, we inserted a thermocouple into the incineration chamber to measure the internal temperature as an index of the combustion temperature because the automatic control of secondary air flow could not be disengaged, and changes in the combustion chamber outlet temperature might not correspond to actual changes in the incinerator internal temperature.

The test operation was continued for 1 day (i.e., 24 h) under the same conditions based on the time needed to stabilize the combustion state and the long retention time of the bottom ash in the system.

We sampled fly ash and flue gas at least 1 h after the establishment of the test conditions.

For bottom ash, owing to the facility-specific retention time inside the incinerator and ash discharger, we predetermined for each facility a sampling time based on the retention times estimated in a simple model and a tracer test (where metal cans were thrown into the waste hopper and their arrival was observed at a planned sampling point).

Figure 1 shows sampling points for bottom ash, fly ash, and exhaust gas, and estimated retention times of bottom ash inside the system for Facility A. Incinerator ashes was collected every hour, but the start of bottom ash collection was delayed by two hours from the start of fly ash collection because the discharge of bottom ash is considered to be two hours later than fly ash due to differences in discharge routes.

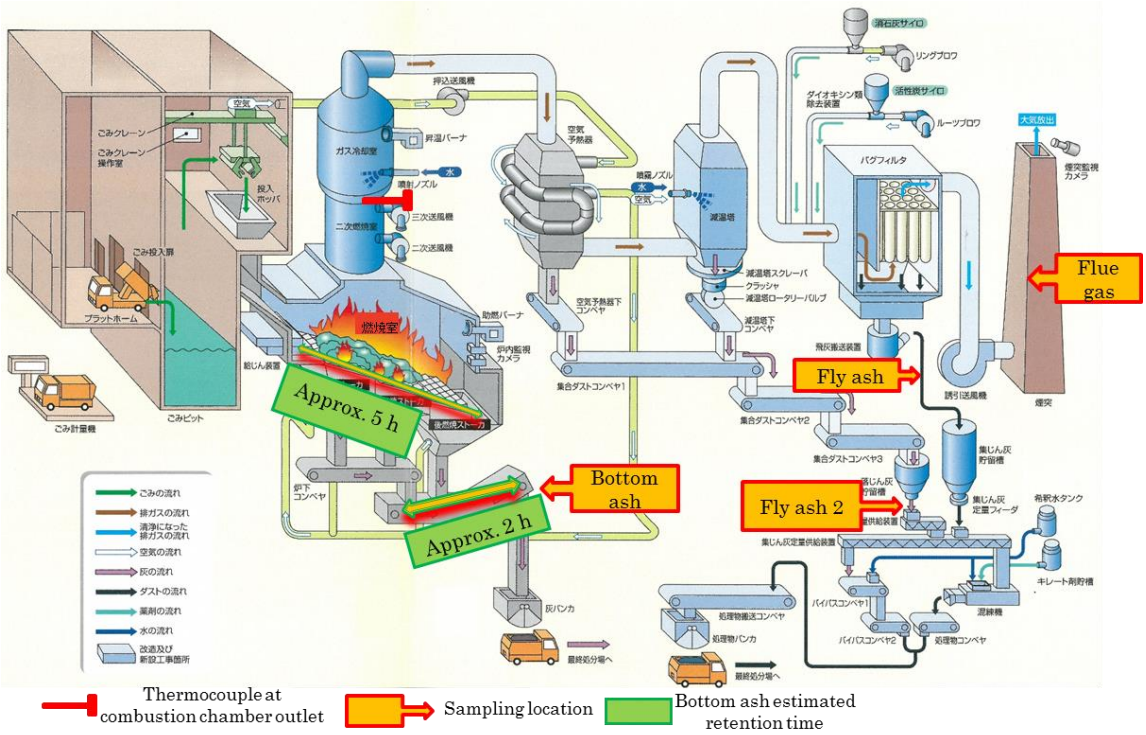

Figure 1. Sampling positions of bottom ash, fly ash, and exhaust gas and estimated residence times for bottom ash at incinerator Facility A.

The measurements and analysis procedures are shown in Table 2 for the bottom ash, fly ash, and flue gas sampled as described above.

Table 2. Samples and measurement items.

Waste Composition	Moisture content, Ash content, Combust content, Material composition, heating value、elemental analysis（C、H、N、O、
Bottom Ash	Radiocaesium concentration(Note 1), ignition loss(Note 2) elemental analysis（Cs、Na、K、Ca、Mg、Al、Si、P、Fe）
Fly Ash	Radiocaesium concentration(Note 1), elemental analysis（Cs、Na、K、Ca、Mg、Al、Si、P、Fe）
Flue Gas	Radiocaesium concentration(Note 3), Dioxins(Note 2)

Note 1 :4 samples of bottom ash and fly ash were collected every hour. Four were mixed and distributed for the analysis. Radiocaesium concentration of 4 samples before mixing were also subject to NaI gamma ray spectrometer.
Note 2 :Conducted to check that there is no incomplete combustion under low temperature operation.
Note 3 :Conducted to check that there is not increased radiocaesium under high temperature operation and operation with radiocaesium evaporation promotoin agents added.

Analytical results for the waste composition are given in Table 3 and constitute the most basic information about waste. Compositional differences are thought to define the behavior of radiocaesium in the combustion process.

Table 3. Waste composition analysis.

Facility			A			B		C		D	
Collection date(2014)			6/26	6/27	10/15	7/9	7/10	7/29	7/30	11/25	11/28
Apparent specific gravity		[kg/m^3]	220	217	131	139	223	97	126	184	176
Moisture content		[%]	45.65	47.12	39.18	43.16	45.13	36.38	45.78	49.38	45.15
Ash content		[%]	9.72	6.32	10.16	8	7.36	5.54	6.14	8.15	6.86
Lower callorific value		[kJ/kg]	8,460	9,380	9,920	8,330	9,420	12,100	10,130	7,700	8,620
Compsition of dried waste	Paper/cloth	[%]	53	38.4	39.4	59.2	45.4	56.3	37.5	39	49.7
	Plastic/synthetic resin/rubber/leather	[%]	22.6	27.1	18.6	15.5	21.2	22.7	32.9	21.4	24.1
	Wood/bamboo/straw	[%]	13.7	10	24.8	8.1	11.2	6.7	12	14.1	8.3
	Kitchen waste	[%]	3.7	14.3	9.5	13.9	10.4	9.2	8.4	14.9	10
	Non-burnable	[%]	2.3	2.4	5.1	0.4	4.6	0.6	2.5	4.3	0.7
	Other(under 5mm)	[%]	4.7	7.8	2.6	2.9	7.2	4.5	6.7	6.3	7.2
Ash content of dried waste	Paper/cloth	[%]	5.6	4.4	5	7.7	2.9	4.9	4.3	3.7	4.5
	Plastic/synthetic resin/rubber/leather	[%]	1.9	1.2	1	0.9	1.4	1.2	1.6	1.9	2.7
	Wood/bamboo/straw	[%]	4.7	1.1	3.1	1.6	0.4	0.4	0.7	0.8	0.9
	Kitchen waste	[%]	0.7	1	1.1	2.5	1.5	0.6	0.6	3.1	1.7
	Non-burnable	[%]	2.3	2.4	5.1	0.4	4.6	0.6	2.5	4.3	0.7
	Other(under 5mm)	[%]	2.7	1.9	1.3	1.1	2.6	1	1.6	2.3	2
	Total	[%]	17.9	12	16.6	14.2	13.4	8.7	11.3	16.1	12.5
Elemental composition	Carbon	[%]	40.36	49.98	47.11	44.15	48.27	50.91	54.47	44.37	46.9
	Hydrogen	[%]	6.36	8.1	7.19	6.49	7.19	8.23	9.3	7.07	7.1
	Nitrogen	[%]	0.71	0.81	1.16	1.18	1.48	0.56	0.66	0.97	0.61
	Sulphur	[%]	0.08	0.07	0	0.07	0.08	0.06	0.07	0.06	0.07
	Chlorine	[%]	0.31	0.16	0.81	0.15	0.57	0.42	0.42	0.21	0.21
	Oxygen	[%]	36.2	31.07	31.48	34.2	33.19	31.68	26	34.97	33.17

We did not observe a clear relation between the composition of waste and the area or season in which the waste was generated. The waste incinerated at Facilities A and B had calorific values of 8,330 to 9,920 kJ/kg, while all values exceeded 10,000 kJ/kg at Facility C, which had higher caloric value for waste in summer. Meanwhile, although Facility D received autumn waste at the end of November, it had the lowest calorific value.

5.3.1.1.2. Continuous sampling test

We conducted a tests in order to understand the relationship between combustion temperature and radiocaesium distribution during normal furnace operation. Stoker furnace equipped facilities (B and F) had bottom and fly ash sampling every two hours continuously for 5 days. Ash samples were subject to radiocaesium concentration measurement by NaI spectroscopy.

The first four samples obtained each day were mixed together, divided and distributed for Ge measurements and an elemental (Cs, Na, K, Ca, Mg, Al, Si, P, and Fe) analysis. These data were used to examine the relationship between the combustion temperature during normal operation and migration behavior (distribution of bottom ash/fly ash) of radiocaesium.

Sampling points and times were determined according to the methods employed in subsection

5.3.1.1.1..

5.3.1.1.3. Effects of a radiocaesium evaporation accelerator and inhibitor

We examined the effects of adding hydrated lime ($Ca(OH)_2$), which is expected to promote the evaporation of radiocaesium, and bentonite (clay), which is expected to inhibit the evaporation of radiocaesium.

① Test of hydrated lime (2.4%) and bentonite (2.2%) addition at Facility A

② Test of hydrated lime (2.6%, 5.5%) addition at Facility A to determine the reproducibility of the effect observed in test ①.

③ Test of hydrated lime (2.2%) addition at Facility D to determine whether the results obtained in tests ① and ② are facility-specific.

④ The materials were sprayed on the surface of each crane of waste thrown into the hopper.

5.3.1.2. Proper treatment of used filter cloths of bag filters

We conducted three test runs at both Facility B using glass-fiber made filter cloths and at Facility E using Tefaire® filter cloths. In one run, ordinary incineration was performed without used filter cloths co-incineration (Run-1). In the other two runs, co-incineration of used filter cloths with MSW was performed, but the used filter cloth throw-in amount and interval differed between Run-2 and Run-3 (Table 4). At Facility B, two used filter cloth throw-in ratios were set according to a questionnaire survey of facilities having with actual experience with co-incineration treatment. These had a mean value of 0.20% and the maximum value of 0.40%. At Facility E, the throw-in ratio was set to 0.03% according to ‘Cleaning Technical Report, No. 8’ issued by the Clean Authority of Tokyo (2008) and other data. The incinerators at both facilities are stoker-type incinerators.

Table 4. Details of the used bag filter cloth co-incineration test.

Facility name			B (60 t/furnace·day)			E (75 t/furnace·day)		
Filter cloth material			Glass fiber			Tefaire®		
Run			RUN 1	RUN 2	RUN 3	RUN 1	RUN 2	RUN 3
Co-incineration ratio			Normal operation	0.2%	0.4%	Normal operation	0.03%	
Filter cloth input amount				6.4 kg/H	12.8 kg/H		0.90 kg/H	
Input amount and time interval, time continued				(1.5/0.5 H), 6 h	3/0.5 H, 6 H		0.5/1 H, 6 H	1.5/3H, 6 H
Measurement item	Used filter cloth	Radiocaesium	○			○		
	Flue gas	Radiocaesium	○	○	○	○	–	○
		Hydrogen chloride	–	○	○	–	○	○
		Sulphur oxide	–	○	○	–	○	○
		Nitrogen oxide	–	○	○	–	○	○
		Dioxins (*2)	–	–	○	–	–	○
		Fluorine compounds	–	–	–	○	○ (four times)	○ (four times)
	Bottom ash	Radiocaesium (*1)	○	○	○	○	○	○
		Ignition loss (*2)	–	–	○	–	–	○
	Fly ash	Radiocaesium (*1)	○	○	○	○	○	○
*1) Radiocaesium samples were collected once per hour for NaI measurements, for a total of five samples, four of which were mixed into one sample and then divided for Ge measurements. *2) Conducted in the RUN under the most severe conditions.			Filter cloth dimensions: φ164 mm · 5250 mm (L). The manufacturer's standard value was used for weight: 2.38 kg each, calculated from a density of 880 g/m^2.			Filter cloth dimensions: φ140 mm · 6000 mm (L). The manufacturer's standard value for weight was used: 2.0 kg each measured value at the facility.		

The effects of co-incineration on the migration behavior of radiocaesium due to fly ash that contains radiocaesium adhering to the filter cloth was studied. For used cloths with glass fiber, combustion is difficult in the established conditions, and for the cloths made of Tefaire, there is an increase in the concentration of fluorine compounds due to their combustion. We collected and analyzed bottom ash, fly ash, and flue gas before and during the test or collected measurements obtained by the facility. For these items, we then compared the data obtained before inputting the filter cloth and during the test and surveyed the effects on the migration of radiocaesium. Sampling points and times were set according to the methods described in subsection 5.3.1.1.1..

5.3.2. Results

5.3.2.1. Radiocaesium distribution between bottom ash and fly ash

5.3.2.1.1. Effect of combustion temperature

Data on the migration and distribution of radiocaesium are given in Table 5.

Ordinary untouched operation is regarded as a standard test.

The tests were conducted at four facilities, but we were unable to obtain a combustion chamber outlet temperature that was higher than that of standard operation during high-temperature operation at Facility C. Additionally, at Facility D, we were unable to obtain a combustion chamber outlet temperature that was lower than that of standard operation in low-temperature operation.

Table 5. Combustion temperature and migration of radiocaesium for each facility and each test.

Facility	Test date	Test	Primary air temp	Combustion chamber outlet temp	Radiocaesium concentration[Bq/kg] (measurement value)		Radiocaesium concentration[Bq/kg] (corrected value(※2))		Distribution ratio % of radiocaesium to fly ash	Fly ash/bottom ash radiocaesium concentration ratio(※3)
			[℃]	[℃]	Bottom ash	Fly ash	Bottom ash	Fly ash		
A	6/23	Standard1	125	904	1,580	8,300	1,900	13,000	60	6.8
	6/24	Standard2	121	912	1,750	10,300	2,100	16,000	63	7.6
	6/26	High temp1	183	964	2,020	10,800	2,500	17,000	61	6.8
	6/27	High temp2	189	950	1,460	13,500	1,900	21,000	72	11.1
	7/2	Hydrated lime2.4%	119	923	840	14,800	1,100	23,000	84	20.9
	7/3	Bentonite 2.2%	123	940	1,990	14,600	2,400	23,000	69	9.6
A Add	10/14	Standard	121	904	1,260	14,500	1,400	20,000	76	14.3
	10/16	Hydrated lime2.6%	116	891	920	15,700	1,200	22,000	83	18.3
	10/17	Hydrated lime5.5%	116	904	540	10,400	650	15,000	84	23.1
B	7/8	Low temp1	101	855	1,020	5,700	1,200	6,800	68	5.7
	7/9	Low temp2	103	842	900	4,600	980	5,500	67	5.6
	7/10	High temp1	200	946	940	5,100	1,000	6,100	68	6.1
	7/11	High temp2	194	956	590	4,700	630	5,600	76	8.9
C	7/28	Standard1	52	933 (1043)※1	930	7,800	1,100	12,000	71	10.9
	7/29	High temp1	100	931 (984)※1	1,110	6,400	1,300	9,900	64	7.6
	7/30	High temp2	100	924 (1040)※1	1,740	9,600	1,800	15,000	63	8.3
	7/31	Standard2	52	937 (1075)※1	1,490	9,500	1,700	15,000	64	8.8
D	11/25	Standard1	178	880	480	1,590	430	2,900	54	6.7
	11/26	Low temp1	129	867	480	1,450	430	2,600	52	6
	11/27	Low temp2	134	873	453	1,470	400	2,600	54	6.5
	11/28	Standard2	177	883	530	1,250	470	2,200	46	4.7
	11/29	Hydrated lime2.2%	178	893	410	1,280	360	2,300	53	6.4

(※1) In-core farnace tempreture measured with a provisionally installed thermocouple
(※2) Measured values were corrected for flue gas treatment agents and water added during the process.
(※3) Corrected values were used.

At Facilities A and B, where high-temperature runs produced high combustion chamber outlet temperatures, the distribution of radiocaesium in fly ash increased on the second day of the high-temperature run. We obtained a rise of 2.6% in the distribution rates at Facility A and a rise of 0.8% at Facility B per 10°C combustion temperature by linear approximation, excluding data obtained on the first day (Figures 2 and 3).

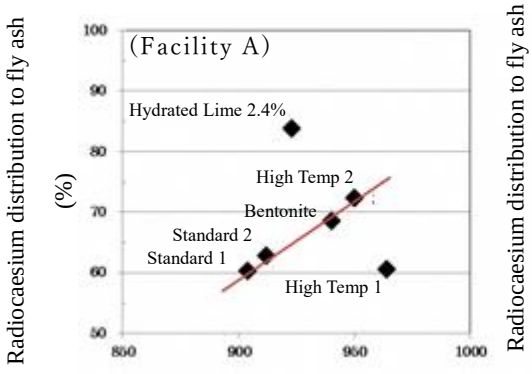

Figure 2. Rate of the distribution of radiocaesium to fly ash versus the combustion chamber outlet temperature (Facility A).

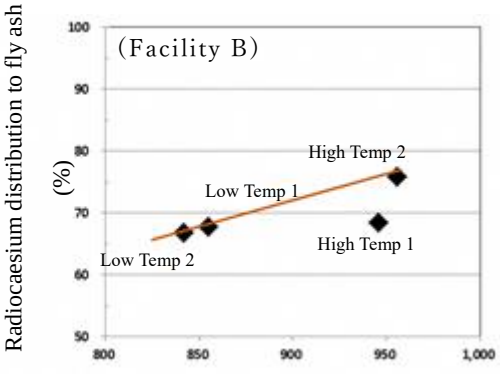

Figure 3. Rate of the distribution of radiocaesium to fly ash versus the combustion chamber outlet temperature (Facility B).

To examine variation in the temperature and migration status of radiocaesium before and after changing the combustion temperature conditions from standard to high-temperature operation, we sampled bottom ash and fly ash every 2 h for 2 days at Facility B, and measured by a NaI detector. In response to the change in operation mode from low-temperature operation to high-temperature operation, the combustion chamber outlet temperature increased approximately 100°C, from 850°C to 950°C, and the ratio of fly ash/bottom ash radiocaesium concentration increased along with the increasing temperature (Figure 4).

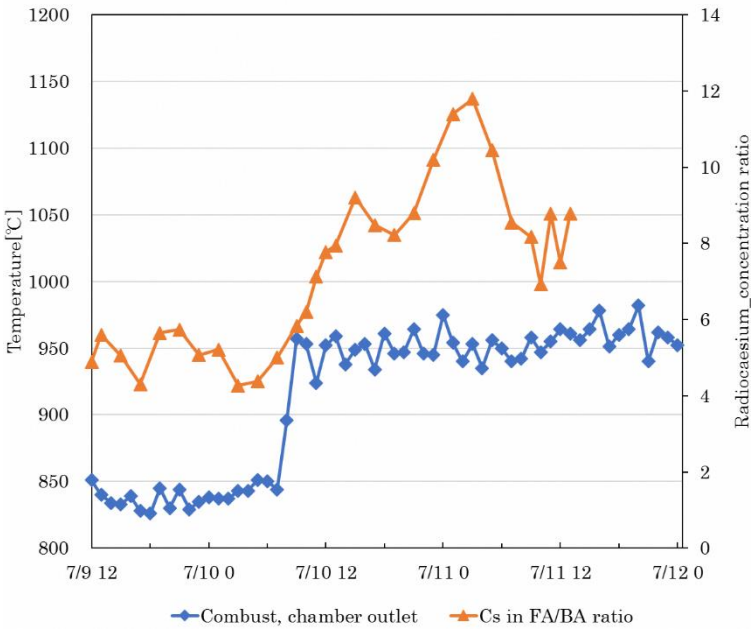

Figure 4. Combustionchamber outlet temperature and radiocaesium concentration ratio (Facility B).

5.3.2.1.2. Continuous sampling test

Figure 5 (Facility B) and 6 (Facility F) show the combustion chamber outlet temperature, NaI-detector-based radiocaesium concentration in bottom ash and fly ash, the radiocaesium distribution to fly ash based on NaI measurements, and the radiocaesium distribution ratio to fly ash based on Ge measurements.

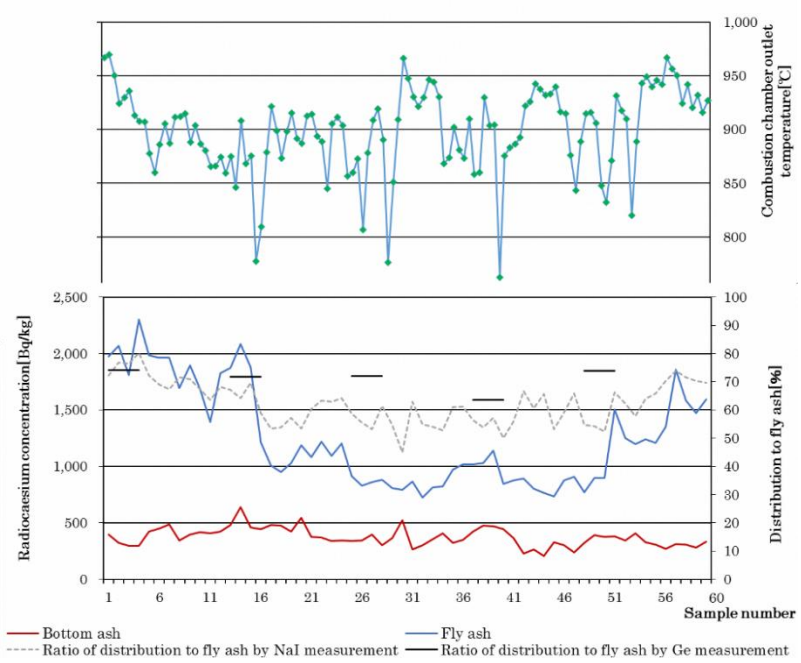

Figure 5. Radiocaesium concentrations in bottom ash and fly ash, radiocaesium distribution based on NaI and Ge measurements, and combustion chamber outlet temperature (dry ash at Facility B).

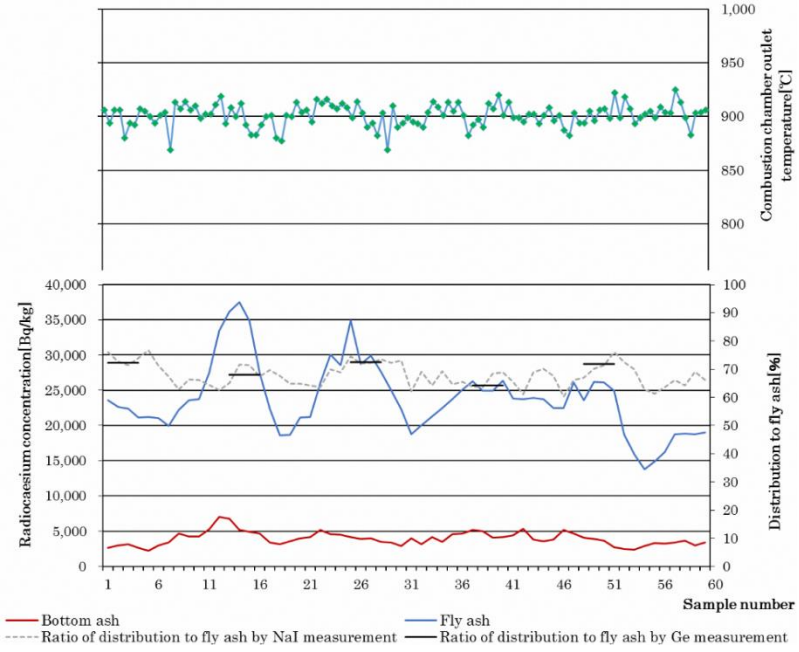

Figure 6. Radiocaesium concentrations in bottom ash and fly ash, radiocaesium distribution based on NaI and Ge measurements, and combustion chamber outlet temperature (dry ash at Facility F).

It is difficult to detect a clear relationship between the combustion chamber outlet temperature and the distribution of radiocaesium to fly ash.

As shown in the plots of the temperature against the radiocaesium distribution to fly ash based on NaI measurements (Figures 7 and 8), the increase in the combustion chamber outlet temperature at Facility B was accompanied by an increase in the ratio of the radiocaesium distribution to fly ash. Sudden drops in temperature may correspond to the inputs of sewage sludge, and it should be noted that the waste composition also changed substantially. The range of outlet temperatures for the combustion chamber of Facility F was small, and no clear relationship between the radiocaesium distribution ratio and combustion chamber outlet temperature was observed.

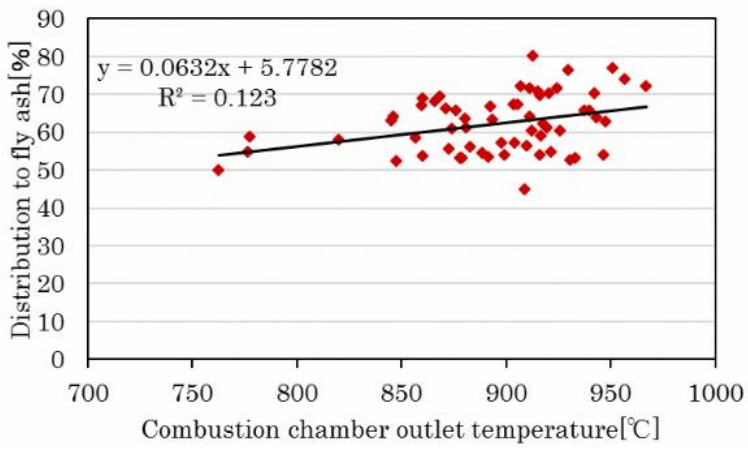

Figure 7. Combustion chamber outlet temperature and radiocaesium distribution to fly ash (Facility B); the radiocaesium concentration was measured by NaI.

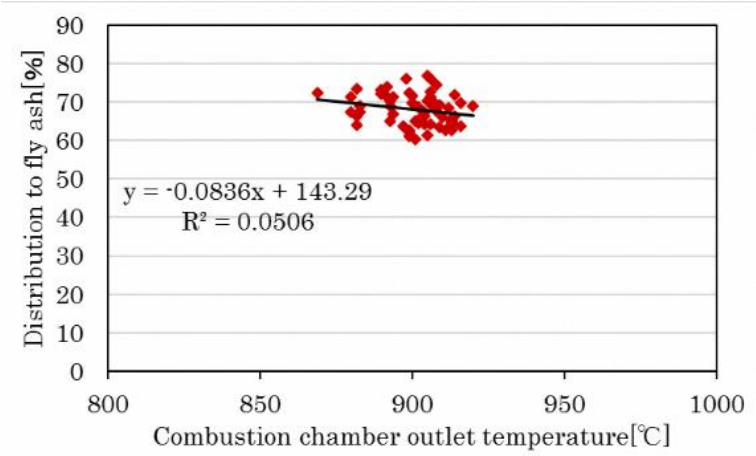

Figure 8. Combustion chamber outlet temperature and radiocaesium distribution to fly ash (Facility F); radiocaesium concentration was measured by NaI.

Regarding the relationship between basicity and radiocaesium distribution, at Facilities F, we detected positive correlations between the basicity of the waste calculated from the chemical composition of ash sampled during the 5-day continuous sampling test and the radiocaesium

distribution to fly ash (Figure 10). However, we found no positive correlations at the Facility B (Figure 9).

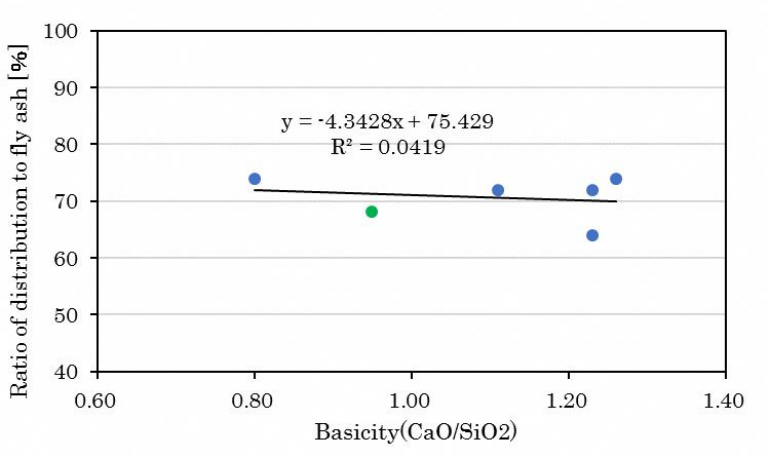

Figure 9. Basicity and radiocaesium distribution to fly ash calculated from the ash composition (Facility B).

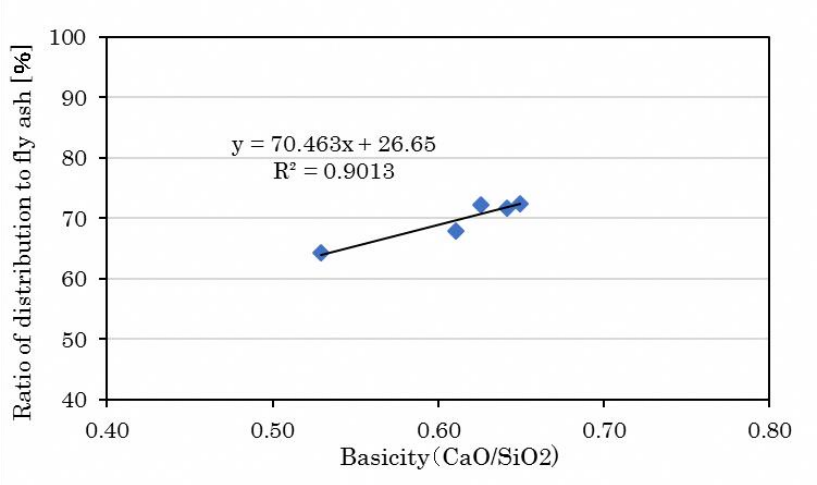

Figure 10. Basicity and radiocaesium distribution to fly ash calculated from the ash composition (Facility F).

5.3.2.1.3. Effects of a radiocaesium evaporation accelerator and inhibitor

The addition of hydrated lime $Ca(OH)_2$, (subsection 5.3.1.1.3.①) at Facility A increased the ratio of radiocaesium distribution to fly ash remarkably (9.3% increase per 1% addition). However, the inhibitory effect of bentonite could not be confirmed (Figure 11).

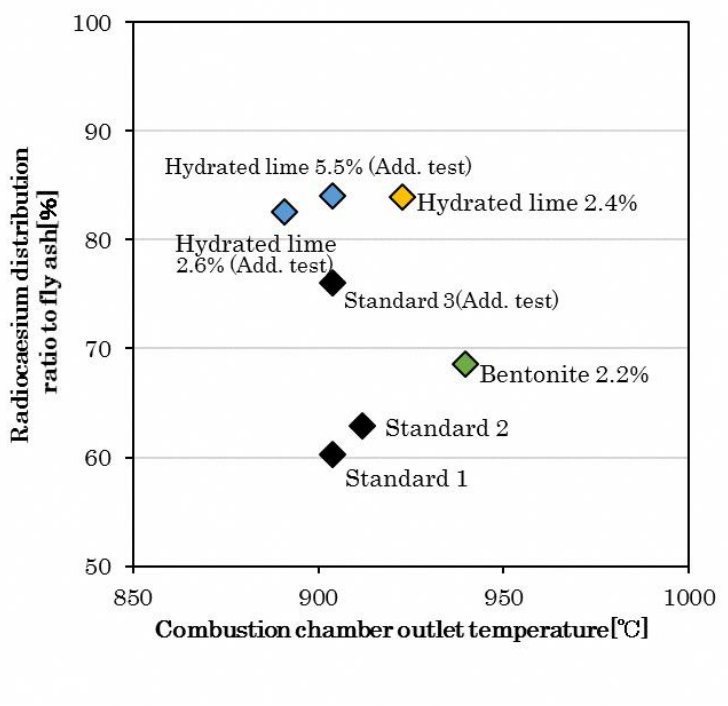

Figure 11. Effect of additives on the radiocaesium distribution to fly ash (Facility A).

We conducted additional tests to determine the general effects of hydrated lime; an effect was confirmed at Facility A, but it was weaker than that observed in the first test. Additionally, hydrated lime had no effect at Facility D (Figure 12).

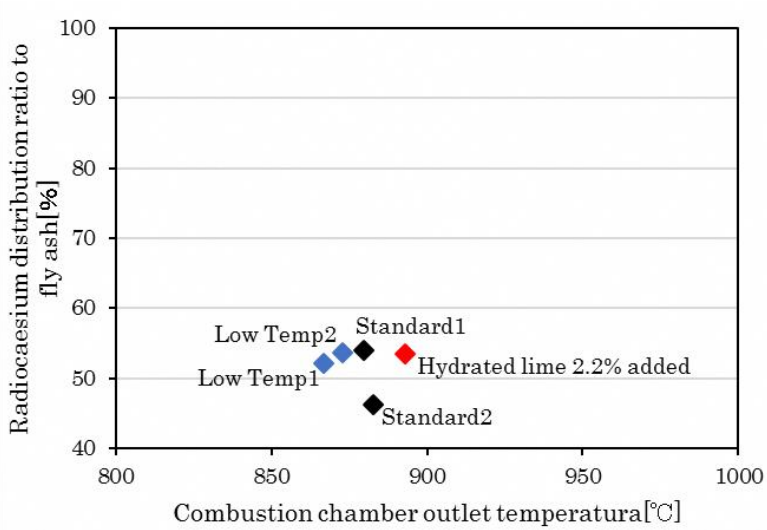

Figure 12. Effect of hydrated lime on the radiocaesium distribution to fly ash (Facility D).

The higher basicity of incinerated waste of Facility D is expected to accelerate the evaporation of radiocaesium[1]. The basicity of the waste, based on the chemical analysis of bottom ash and fly ash conducted at Facilities A to D, is given in Table 6. The basicity of waste at Facility A was lower than that at other facilities. It is probable that the obvious effect observed at Facility A was

due to the addition of the basicity-increasing material, hydrated lime, to low-basicity waste. In the case of Facility D, it is possible that the basicity-increasing material was added to waste whose basicity was already somewhat high, and the hydrated lime thus did not promote the evaporation of radiocaesium.

Table 6. Basicity of waste calculated from the chemical compositions of BA and FA.

Facility	A						B		C		D		
Ash sampling date(2014)	6/23	6/26	7/2	10/14	10/16	10/17	7/8	7/10	7/28	7/29	11/25	11/26	11/29
Hydrated lime added[%]	-	-	2.4	-	2.6	5.5	-	-	-	-	-	-	2.2
CaO/SiO_2	0.44	0.55	1.03※1	0.65	1.02※2	1.42※2	0.82	1.11	0.96	0.62	0.67	0.75	1.42※3
	0.49						0.95		0.77		0.71		
$(CaO+MgO+Al_2O_3)/SiO_2$	0.81	0.97	1.43※1	1.07	1.46※2	1.89※2	1.38	1.79	1.58	1.13	1.11	1.22	1.89※3
	0.88						1.56		1.33		1.16		
Radiocaesium distribution to FA[%]	60	61	84	76	83	84	68	68	71	64	54	52	53

Calculation of basisity for days that hydrated lime was added: We used the average of analyzed chemical composition values and added hydrated lime quantity of 6/24 and 7/2(※1), the analyzed value of 10/14 for 10/16 and 10/17(※2), and the average of analyzed value and added hydrated lime quantity of 11/25 and 11/26 for 11/29(※3).

In this test, strict operating conditions were used that differ from typical operating conditions, and it was thought that these conditions increased the radiocaesium concentration in flue gas. We therefore conducted measurements of flue gas and dioxins. We did not detect radiocaesium in the flue gas. Furthermore, the dioxin concentration in the flue gas and ignition loss values of bottom ash met relevant regulations (Table 7).

Table 7. DXNs concentration in flue gas and ignition loss of bottom ash.

Facility	Operating condition	Measurement date		DXNs in flue [ng-TEQ/m^3_N]		IL of BA [%]	
				Measured	Criteria	Measured	Criteria
B	Low-T	2014	July 8	0.032	5	5.9	10
	Low-T		July 8	0.019		6.0	
C	Low-T	2014	Nov. 26	0.0004	0.1	<0.1	10
	Low-T		Nov. 27	0.00038		0.2	

5.3.2.2. Proper treatment of used filter cloths of bag filters

The co-incineration of used filter cloth with MSW was confirmed to be safe and feasible under the proper management of the co-incineration amount.

Based on many measurements, used filter cloth co-incineration did not affect the measurements, but increased the concentration of radiocaesium in bottom and fly ash (Table 8).

Table 8. Radiocaesium concentration in bottom ash and fly ash.

Facility		B			E		
Test RUN No.		RUN 1	RUN 2	RUN 3	RUN 1	RUN 2	RUN 3
Used filter cloths input(pieces)		-	1.5/0.5H	3.0/0.5H	-	0.5/1.0H	1.5/3.0H
Radiocaesium concentration (Cs-134＋Cs-137) [Bq/kg]	Used filter cloths	600			1,260		
	Bottom ash	318	400	800	266	157	105
	Fly ash	2,400	3,260	3,640	1,400	1,210	1,220

An increase was observed at Facility B and no increase was observed at Facility E. The increase is thought to be caused by a change in the radiocaesium concentration in co-incinerated MSW, rather than the input of used filter cloth. This is supported by two pieces of evidence. First, the increase was higher than the value calculated from the radiocaesium concentration of the input filter cloth. Second, the increased values remained within the range of variation of the measurements obtained by the facility in 2015. No radiocaesium was detected in flue gas and no effects of co-incineration on flue gas were observed. Table 9 presents the results for Facility E.

Table 9. Radiocaesium concentration in flue gas during bag filter cloth co-incineration tests.

Facility			B			E		
Sampling point			Bag Filter outlet			Bag filter outlet		
Sampling date(2015)			7/28	7/29	7/30	10/26	10/27	10/28
RUN no. and used filter cloth input rate(pieces)			RUN1	RUN2	RUN3	RUN 1	RUN 2	RUN 3
			-	1.5/0.5H	3.0/0.5H	-	0.5/H	1.5/H
Radiocaesium concentration in flue gas [Bq/m^{3}N]	Filter	Cs-134	<0.3	<0.3	<0.3	<0.3	<0.3	<0.3
		Cs-137	<0.3	<0.3	<0.3	<0.3	<0.3	<0.3
	Drain	Cs-134	<0.3	<0.3	<0.3	<0.3	<0.3	<0.3
		Cs-137	<0.3	<0.3	<0.3	<0.3	<0.3	<0.3
Wet flue gas		[m^{3}N/h]	56,000	63,900	64,600	37,600	38,500	35,300
Dry flue gas		[m^{3}N/h]	44,400	54,700	52,200	26,100	27,100	25,600
Moisture content		[%]	20.8	14.5	19.1	30.2	29.6	27.1
Gas composition	CO_2	[%]	2.9	2.5	3.2	5.6	6.7	6.3
	O_2	[%]	17.6	17.9	17.1	14.7	13.5	13.8
	CO	[%]	<0.1	<0.1	<0.1	<0.01	<0.01	<0.01
	N_2	[%]	79.5	79.6	79.7	79.7	79.8	79.9

Regarding concerned fluorine gas when Tefaire cloths were co-incinerated (Facilities B and E), measured values of HF were less than approximately 1 mg/m^{3}N (Table 10).

There were no changes in the ignition loss of bottom ash, harmful acidic substances, and dioxins in flue gas at either facility. These parameters are conceivably changed when combustion

conditions deteriorate (Table 10).

Table 10. Harmful acidic substances and dioxins in flue gas, and ignition loss of bottom ash.

Facility			B			E		
RUN No.			RUN2	RUN3	Past figure	RUN2	RUN3	Past figure
Flue gas	SOx	[m^3N/h]	<5	<5	<10 (2015)	<5	<5	<3.5～80 (2015)
	NOx	[ppm]	140	160	140～150 (2015)	150	170	99～180 (2015)
	HCl	[mg/m^3N]	<10	<10	27～32 (2015)	120	150	<5～310 (2015)
	HF	[mg/m^3N]	-	-	-	<1.1	<1	<1 (2015)
	Dioxins	[ng-TEQ /m^3N]	-	0.01	0.046～0.072 (2015)	-	0.0028	0.060～0.099 (2015)
Bottom ash	Ignition loss	[%]	-	5.1	5.0～8.1 (2015)	-	5.1	1.3～6.2 (2015)

5.3.3. Conclusions

It is generally known that radiocaesium volatilizes upon its combustion and tends to migrate to fly ash rather than to bottom ash. Five factors that influence the migration of radiocaesium were classified, i.e. combustion temperature, air ratio, waste quality, chemical addition and ash particle diameter. Among these factors, the correlation between “combustion temperature and chemical addition,” which are relatively easy to control and “radiocaesium migration behavior” were investigated through verification tests at actual facilities. As a result, it was found that it is difficult to change the combustion temperature in an operating incinerator because maintenance and management standards stipulating an allowable combustion temperature range have been established by laws relating to Waste Management and Public Cleaning Act. As for a chemical addition method, the addition of hydrated lime to incinerated waste somewhat promoted radiocaesium migration to fly ash at some facilities, but the reproducibility of such a phenomenon was scarce.

At each of the facilities B (filter cloth: glass fiber) and E (filter cloth: Teflon), a normal operation without the co-combustion of waste filter cloths and municipal waste and another operation with the co-combustion of radiocaesium-containing waste filter cloths and municipal waste by changing the input ratio and input time interval of the radiocaesium-containing waste filter cloths were carried out. The results revealed that the co-combustion of bag-filter waste cloths with municipal waste at the facilities is safe and appropriate as long as the co-combustion ratio is managed properly.

5.4. Radiocaesium elution tests from ashes

Incineration ash generated at a municipal waste incineration facility in Fukushima Prefecture was collected and elution tests of radiocaesium were conducted. At the same time, laboratory experiments were conducted to test methods to reduce the elution rate of radiocaesium by using zeolite and other materials. The effect of radiocaesium on the rate of insolubility and heavy metal efflux inhibitors was also investigated.

In addition, a zeolite addition test was conducted at a waste incineration facility actually in use in Fukushima Prefecture. In two systems (exhaust treatment system and chelate adding system) of an actual municipal waste incineration facility, investigations were carried out on the ability of zeolite to suppress radioactive caesium elution, the effect on exhaust gas treatment, and the effect on heavy metal insolubilization.

5.4.1. Investigations

5.4.1.1. Radiocaesium elution tests from ashes

5.4.1.1.1. Data acquisition of radiocaesium leaching characteristics

We sampled bottom ash, fly ash and limited number of boiler ash from 15 incineration facilities in Fukushima Prefecture and performed radiocaesium leaching tests for a total of 64 samples to acquire radiocaesium leaching data. For some facilities, we sampled and tested summer and winter ash to evaluate seasonal changes in radiocaesium leaching properties. Leaching tests were performed in accordance with 'JIS K0058-1, As-is Agitation Test'; each sample was placed in a container as is, pure water was added at a volume that was 10 times greater than the amount of ash (L/kg), and the top liquid phase was agitated with a propeller.

5.4.1.1.2. Laboratory radiocaesium immobilisation test

As zeolite, bentonite, and sewage sludge are expected to reduce radiocaesium leaching from incineration ash, we used these three materials as additives to the sampled incineration ash. The test procedure simulates the actual fly ash kneading process. We added the materials to bottom ash, fly ash, and treated fly ash obtained from Facility K at various amount (20% and 5% of dry ash weight) and added water (30%). The water-supplemented samples were thoroughly mixed and kept at various temperatures (25°C and 80°C) for different periods (one week and one month). Then, each sample was subjected to leaching tests.

5.4.1.2. Tests on radiocaesium elution suppression

5.4.1.2.1. Tactical agitation tests using a germanium semiconductor detector

Using a germanium semiconductor detector, radiocaesium concentrations in bottom ash, humidified bottom ash (treated bottom ash), fly ash, and fly ash provided with a heavy metal elution prevention treatment (treated fly ash) sampled from municipal waste incineration facilities in Fukushima Prefecture were measured. Next, an elution test to investigate the elution property of radiocaesium was performed using 2.5 L of ultrapure water for about 250 g of incineration ash, in accordance with JIS K 0058-1. A radiocaesium elution rate (%) was determined by the

following:

[radiocaesium concentration (Bq/kg) in the eluate] x [the weight of ultrapure water used in the elution test (kg)] ÷ [radiocaesium concentration in incineration ash (Bq/kg)] x [the weight of incineration ash used in as-is agitation test (kg)] x 100.

5.4.1.2.2. A test on radiocaesium elution suppression (long-term as-is agitation test)

In order to find a method of suppressing radiocaesium elution from incineration ash having been exposed to rain water during its storage or after a landfill (elution-suppressing method), an acid clay was added to an incineration ash by 5% in weight, they were mixed with water until the water content reached 30% and then were subjected to a radiocaesium measurement using a germanium semiconductor detector as a long-term as-is agitation test. The durations of agitation were set at 6 hours, 24 hours, 7 days, 14 days, and 30 days. Radiocaesium elution rates were determined and the radiocaesium elution-suppressing effect of an acid clay was investigated by mixing or not mixing it into the incineration ash.

5.4.1.2.3. A test on radiocaesium elution suppression (MP-AES / ion chromatography test)

In order to investigate the effect of mixing acid clay into incineration ash on the metal elution from the ash, an elution test was carried out using incineration ash mixed with acid clay and one not mixed with it. Concentrations of elements in the eluates were measured using an MP-AEA spectroscopic analyzer and an ion chromatography device.

5.4.1.3. Tests on radiocaesium elution suppression in incineration ash at municipal waste incineration facilities

Regarding zeolite, which was found to be effective in the suppression of radiocaesium elution as described in 5.4.1.1.2., zeolite addition tests were performed at two systems of an actual municipal waste incineration facility to verify the feasibility of a radiocaesium elution countermeasure using zeolite at an incineration facility.

5.4.1.3.1. A test during normal operation

This test was performed for three days in total during a normal operation period. Bottom ash, fly ash and treated fly ash were sampled at 11:00 and 14:00 each day, and tests were performed to determine radiocaesium concentrations and elution properties.

5.4.1.3.1.1. Germanium semiconductor detector test, a JIS K 0058-1 elution test and the Environment Agency's Notice No. 13 elution test

Using the methods shown in Table 11, tests were conducted to investigate the radiocaesium concentration of each sample and the elution properties of radiocaesium and heavy metals.

Table 11. Test Conditions and Others

Sample		Test Methods	Used Equipment	Minimum Determination Limit
Radiocesium Concentration	Contain	Gamma-ray Spectrometry by Germanium Semiconductor Detector, Radioactivity Measurement Method Series No. 7 by MEXT	Germanium Semiconductor Detector (ORTEC GEM20P4-70)	Fill U8 container up to a height of 5 cm and measure for 3,600 seconds
	Elution			Fill a 2L Marinelli container up to a height of 12 cm and measure for 20,000 seconds
pH		JIS K 0058-1	GST-5741C, DKK-TOA CORPORATION	-
EC			CM-30R, DKK-TOA CORPORATION	-
Hg		JIS K 0058-1 or Environment Agency's Notice No. 13 (Notice No. 13)	RA-3A, Nippon Instruments Corporation	0.0005mg/L
Cd			Agilent Technologies 7500ce ICP-MS or 7800 ICP-MS	0.009mg/L
Pb				0.03mg/L
As				0.01mg/L
Se				
Cr				0.02mg/L
Cl-			Thermofisher Scientific ICS-1100	0.1mg/L

5.4.1.3.1.2. Repetitive elution tests (JIS K 0058-1)

In order to investigate the quantities of repetitive elution of radiocaesium and heavy metals, the JIS K 0058-1 elution test shown in Table 11 was repeated four times (each sample used for an elution test was subjected to another elution test by putting it into a new solvent) using bottom ash and treated fly ash sampled at the same time when the radiocaesium concentration in fly ash was the highest during a normal operation period. An eluate obtained from each test was examined for radiocaesium concentration, heavy metal concentrations, pH and EC.

5.4.1.3.1.3. Zeolite addition test in laboratory

To study zeolite addition ratios in zeolite addition tests at actual facilities, zeolite was added from 5 to 20% (in 5% increments) to the fly ash and treated fly ash that that contained the highest radiocaesium concentrationsampled during a normal operation test period, and then water was mixed with the fly ash and treated fly ash until their water content reached 30%. The test shown in table 11 was performed on each mixed sample to check the presence or absence of a radiocaesium elution suppression effect and an effect on heavy metals and others.

5.4.1.3.2. Tests on zeolite addition to an exhaust gas treatment agent at actual facilities

At the municipal waste facilities mentioned in 5.4.1.3.1., exhaust gas treatment using an exhaust gas treatment agent mixed with zeolite was performed for five consecutive days. During the treatment period, the treated fly ash was sampled at 14:00 each day. The samples were tested to determine radiocaesium concentrations and elution property.

5.4.1.3.2.1. Exhaust gas composition analysis tests

To investigate the effect of the blow injection of chemical mixture on exhaust gas, a test was performed only for one day during the chemical mixture addition test period, using methods described in the Waste Management Division's Notification No. 95, Exhibit 3, II and the Ministry

of the Environment's 2011 Notification, No. 111.

5.4.1.3.2.2. Germanium semiconductor detector test, JIS K 0058-1 elution test and the Environment Agency's Notice No. 13 elution test

To investigate radiocaesium concentrations and the elution properties of radiocaesium and heavy metals in treated fly ash sampled during the chemical mixture addition test period, tests were performed using the methods shown in Table 11.

5.4.1.3.2.3. Repetitive elution tests (JIS K 0058-1)

The average of radiocaesium concentrations in the treated fly ash sampled during the chemical mixture addition test period was calculated. A sample that indicated a radiocaesium concentration closest to the average value was subjected to four JIS K 0058-1 repetitive elution tests, shown in Table 11, (a sample having been subjected to an elution test was immersed into a new solvent and this operation was repeated four times). An eluate obtained from each test was examined for radiocaesium concentration, heavy metal concentrations, pH and EC. Tests using artificial seawater as a solvent were also carried out.

5.4.1.3.3. Tests on zeolite addition to the mixture of fly ash and chelate agent by kneading at actual facilities

At the municipal waste incineration facilities mentioned in 5.4.1.3.1., heavy metal elution suppression treatment in which zeolite was added to a chelate agent kneader for suppressing heavy metal elution from incineration ash was performed for five consecutive days. During the heavy metal elution suppression treatment period, the treated fly ash was sampled at 14:00 each day and tested to determine radiocaesium concentrations and elution property.

5.4.1.3.3.1. Germanium semiconductor detector test, JIS K 0058-1 elution test and the Environment Agency's Notice No. 13 elution test

Tests were conducted using the method shown in Table 11 to examine the radiocaesium concentrations and the elution properties of radiocaesium and heavy metals in the treated fly ash sampled during the mixing addition test period.

5.4.1.3.3.2. Repetitive elution tests (JIS K 0058-1)

The average of radiocaesium concentrations in the treated fly ash sampled during the mixing addition test period was calculated. A sample that showed a radiocaesium concentration closest to the average value was subjected to four JIS K 0058-1 repetitive elution tests (a sample having been subjected to an elution test was immersed into a new solvent, and this operation was repeated four times). An eluate obtained from each test was examined for radiocaesium concentration, heavy metal concentrations, pH and EC. Tests using artificial seawater as a solvent were also carried out.

5.4.2. Results

5.4.2.1. Radiocaesium elution tests from ashes

5.4.2.1.1. Data acquisition of radiocaesium leaching characteristics

We sampled bottom ash and fly ash from 15 MSW incineration facilities in Fukushima Prefecture and performed radiocaesium leaching tests using these samples. The test results indicate that radiocaesium leaching from bottom ash was limited (below 1% to 16%), but leaching from fly ash was extremely high (35% to 94%), as is generally expected (Tables 12-1, 2, 3, and 4). Please note that 'BA' and 'FA' in the tables are the abbreviations of 'bottom ash' and 'fly ash' respectively.

Table 12-1. Radiocaesium leaching test results (1).

Facility		A				B										C		D		E	
Samplimg date		2014				2015										2014		2014		2015	
		6/23		7/2		9/7		9/8		9/9		9/10		9/11		7/28		11/25		10/26	
Sample type		BA	FA	BA	FA	BA	FA	BA	FA	BA	FA	BA	FA	BA	FA	BA	FA	BA	FA	BA	FA
Radiocaesium concentration in solid [Bq/kg]	Cs-134	400	2,100	300	3,900	45	380	43	320	25	280	65	250	24	190	300	1,700	92	390	56	300
	Cs-137	1,400	6,100	760	11,000	220	1,600	230	1,500	180	1,100	230	1,100	130	960	790	5,500	350	1,100	210	1,100
	Total	1,800	8,200	1,060	14,900	265	1,980	273	1,820	205	1,380	295	1,350	154	1,150	1,090	7,200	442	1,490	266	1,400
【Leaching test】 Radiocaesium concentration in liquid [Bq/L]	Cs-134	0.1	130	0.1	230	0.1	31	0.1	28	0.1	20	0.1	15	0.1	18	0.1	130	2	16	0.1	22
	Cs-137	1	360	3	670	1	130	0.1	110	0.1	94	0.1	70	0.1	77	2	380	5	54	0.1	92
	Total	1	490	3	900	1	161	0.2	138	0.2	114	0.2	85	0.2	95	2	510	7	70	0.2	114
Leaching rate	[%]	0.6	59	3.6	61	3.8	81	0	76	0.0	83	0	63	0	83	2.2	65	16	47	0	81

Table 12-2. Radiocaesium leaching test results (2).

Facility		F										G			H		I		
Samplimg date		2015										2016			2016		2016		
		10/13	10/12	10/14	10/13	10/15	10/14	10/16	10/15	10/17	10/16	3/11			3/1		3/17		
Sample type		BA	FA	BA	FA	BA	FA	BA	FA	BA	FA	BA	FA	FA-t	BA	FA-t	BA	FA	FA-t
Radiocaesium concentration in solid [Bq/kg]	Cs-134	550	4,100	1,000	6,300	700	5,500	930	4,700	580	4,300	42	310	300	9	50	200	2,300	840
	Cs-137	2,300	17,000	4,500	27,000	3,100	23,000	3,900	20,000	2,500	18,000	220	1,600	1,500	40	260	1,200	11,000	4,200
	Total	2,850	21,100	5,500	33,300	3,800	28,500	4,830	24,700	3,080	22,300	260	1,900	1,800	49	310	1,400	13,000	5,000
【Leaching test】 Radiocaesium concentration in liquid [Bq/L]	Cs-134	3	290	3	350	2	330	1	310	2	300	<0.1	21	24	<0.1	5	1	75	80
	Cs-137	12	1,200	11	1,500	8	1,400	6	1,300	10	1,300	0.2	100	120	0.1	24	6	270	390
	Total	15	1,490	14	1,850	10	1,730	7	1,610	12	1,600	<0.3	120	140	<0.2	29	7	450	470
Leaching rate	[%]	5	71	3	56	3	61	1	65	4	72	<1	63	78	<4	94	5	35	94

Table 12-3. Radiocaesium leaching test results (3).

Facility		J				K								L			
Sampiling date(2016 fy)		8/24	2/10	8/24	2/10	8/24	2/10	8/24	2/10	8/24	2/10	8/24	2/10	8/25	2/9	8/25	2/9
Sample type		BA		FA		BA		FA		Boiler ash		FA-t		BA		FA	
		S	W	S	W	S	W	S	W	S	W	S	W	S	W	S	W
Radiocaesium concentration in solid [Bq/kg]	Cs-134	<6	10	48.3	81	74	10	340	129	553	298	274	103	31	16	244	232
	Cs-137	44	67	315	560	404	67	2,010	841	3,110	1,960	1,640	718	174	105	1,480	1,570
	Total	<50	77	363	641	478	77	2,350	970	3,660	2,260	1,910	821	205	121	1,720	1,800
【Leaching test】 Radiocaesium concentration in liquid [Bq/L]	Cs-134	<0.6	<0.4	3.9	6	<0.8	<0.4	29	10.2	19.6	11.5	26	9.2	<0.9	<0.4	19	19.5
	Cs-137	<0.7	<0.4	24.6	42	0.8	<0.4	157	66.7	117	76.3	138	62.1	<0.7	0.5	113	134
	Total	<1.3	<0.8	28.5	48	<1.6	<0.8	186	76.9	137	87.8	164	71.3	<1.6	<0.9	132	154
Leaching rate[%]	Cs-134+ Cs-137	<26.0	<10.4	78.5	74.9	<3.3	<10.4	79.1	79.3	37.4	38.8	85.9	86.8	<7.8	<7.4	76.7	85.6
	CS-137	<15.9	<6.0	78.1	75	2	<6.0	78.1	79.3	37.6	38.9	84.1	86.5	<4.0	4.8	76.4	85.4

Table 12-4. Radiocaesium leaching test results (4).

Facility		M								N				O					
Sampiling date(2016 fy)		8/25	1/20	8/25	1/30	9/6	2/8	8/25	1/30	9/30	2/9	9/30	2/9	9/30	2/10	9/30	2/10	9/30	2/10
Sample type		BA		FA		Boiler ash		FA-t		BA		FA		BA		FA		FA-t	
		S	W	S	W	S	W	S	W	S	W	S	W	S	W	S	W	S	W
Radiocaesium concentration in solid [Bq/kg]	Cs-134	452	438	1,290	1,460	1,530	893	815	908	76	69	836	450	28	15	219	170	171	111
	Cs-137	2,460	2,780	6,960	9,150	8,570	5,720	4,710	5,860	409	464	4,750	3,040	187	103	1,190	1,120	995	754
	Total	2,910	3,220	8,250	10,600	10,100	6,610	5,530	6,770	485	533	5,590	3,490	215	118	1,410	1,290	1,170	865
【Leaching test】 Radiocaesium concentration in liquid [Bq/L]	Cs-134	<0.9	<0.5	51	82	46	17.7	48	56.9	<0.6	<0.6	59	35.8	<0.7	<0.4	11	7.5	7.8	5.3
	Cs-137	1	<0.7	284	521	270	117	271	365	0.9	2.2	344	235	<0.8	<0.4	64	51.5	44.5	35.3
	Total	<1.9	<1.2	335	603	316	135	319	422	<1.5	<2.8	403	271	<1.5	<0.8	75	59	52.3	40.6
Leaching rate[%]	Cs-134+ Cs-137	<0.7	<0.4	40.6	56.9	31.3	20.4	57.7	62.3	<3.1	<5.3	72.1	77.7	<7.0	<6.8	52.9	45.7	44.7	46.9
	CS-137	0.4	<0.3	40.8	56.9	31.5	20.4	57.5	62.3	2.2	4.7	72.4	77.2	<4.3	<3.9	53.4	46	44.7	46.8

In contrast to most Facilities, for ash from Facilities D and M, we should note that the radiocaesium leaching rate was low for fly ash but high for bottom ash. In addition, the radiocaesium concentration in incinerated ash may differ greatly among facilities. We saw no clear seasonal trends in the radiocaesium leaching rates when comparing summer and winter (Figures 13 and 14).

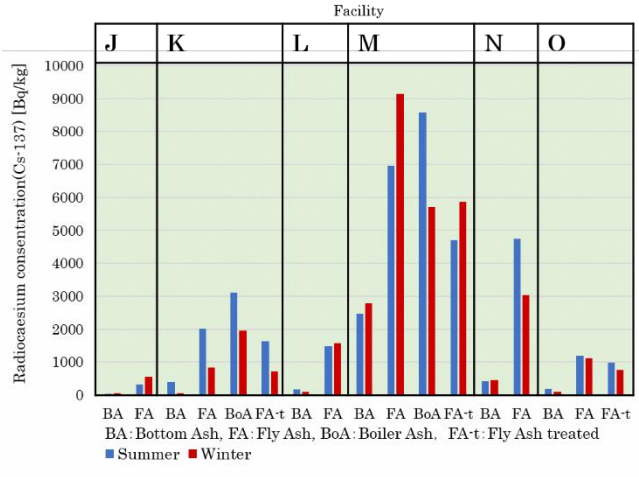

Figure 13. Facility-by-facility radiocaesium concentration in summer and winter samples.

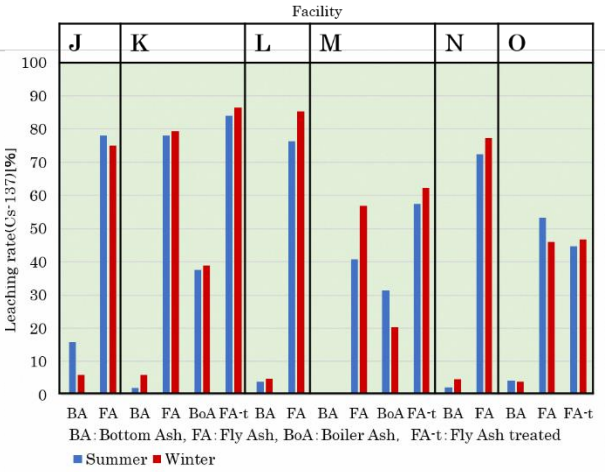

Figure 14. Facility-by-facility radiocaesium leaching rate from summer and winter incineration ash.

In Figures 13 and 14, fly ash refers to crude ash captured by a bag filter not yet treated by chelating agent addition or other methods. Treated fly ash is described as FA-t. If possible, we also sampled and measured boiler ash whose generation is small and is indicated as “BoA”. Radiocaesium concentration of BoA is closer to FA and radiocaesium leaching rate shows an intermediate value between BA and FA.

5.4.2.1.2. Laboratory radiocaesium immobilisation test

Table 13 and Figure 15 show relationships between test specimen conditions (ash type, additive material type, addition rate, curing temperature and curing time) and the radiocaesium leaching rate.

Table 13. Laboratory radiocaesium immobilisation test.

Ash type	Added chemicals	Addition ratio	Curing temperature[℃]	Curing period	Cs leaching rate [%]
Fly ash	Chemicals not added				79.1
	Zeolite	5%	25	1week	13
				1month	18.3
			80	1week	51.2
				1month	57.8
		20%	25	1week	4.3
				1month	4.8
			80	1week	17.3
				1month	24.2
	Bentonite	5%	25	1week	41.9
				1month	45.5
			80	1week	53.4
				1month	67.2
		20%	25	1week	14.1
				1month	14.8
			80	1week	17.2
				1month	28.7
	Sewage sludge	5%	25	1week	71.5
				1month	79.2
			80	1week	81.7
				1month	87.9
		20%	25	1week	66.2
				1month	61
			80	1week	66.5
				1month	67.9

Ash type	Added chemicals	Addition ratio	Curing temperature[℃]	Curing period	Cs leaching rate [%]
Treated fly ash	Chemicals not added				85.9
	Zeolite	20%	80	1month	24.8
	Bentonite				14.7
	Sewage sludge				59.4
Bottom ash	Chemicals not added				2
	Zeolite	5%	25	1week	<0.9
				1month	<1.1
			80	1week	<0.9
				1month	<1.1
		20%	25	1week	<1.0
				1month	<1.0
			80	1week	<1.1
				1month	<1.0
	Bentonite	5%	25	1week	<1.0
				1month	1
			80	1week	<1.0
				1month	<0.9
		20%	25	1week	<1.1
				1month	<1.1
			80	1week	<1.2
				1month	<1.0

Black numerals indicate elution rates calculated from caesium-134 and caesium-137, and red and blue numerals indicate elution rates calculated from caesium-137 (Red indicates the most immobilized case).

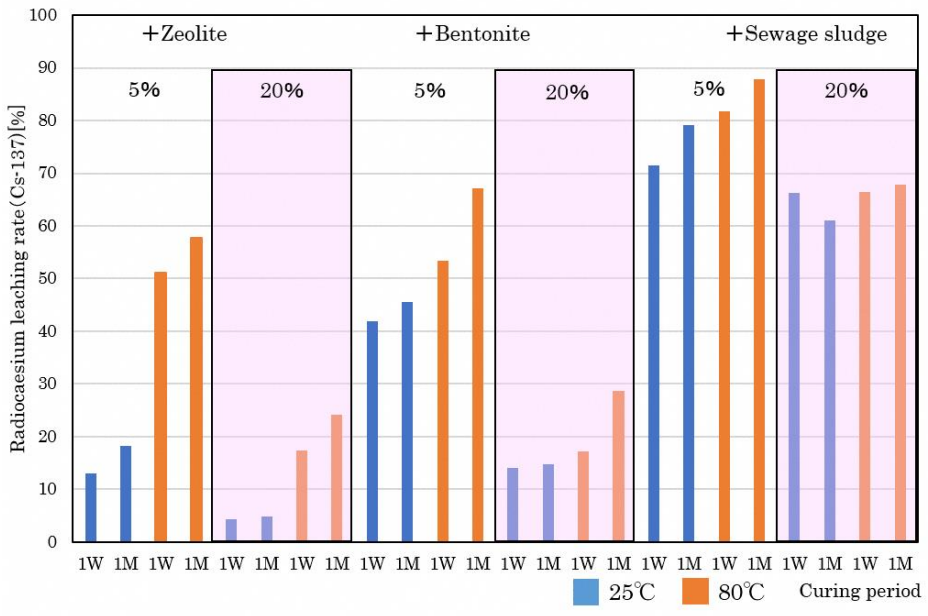

Figure 15. Relationship between leaching rate and additive, rate of addition, cure temperature and cure duration (Fly ash).

A very obvious reduction of radiocaesium leaching rate was observed for fly ash. The addition of 20% zeolite and 1 week of curing at 25°C resulted in the greatest reduction in the radiocaesium leaching rate, from 79.1% to less than 5%.

The materials added to fly ash showed leaching rate reduction in decreasing order as follows: zeolite, bentonite and sewage sludge. Both zeolite and bentonite showed 1/3 lower leaching rates for the addition of 20% than for 5%. Zeolite was not effective at a higher cure temperature (80°C) compared with bentonite. For both zeolite and bentonite, longer (one month) curing duration had slightly adverse effects on the leaching rate reduction

5.4.2.2. Radiocaesium elution suppression test

5.4.2.2.1. Germanium semiconductor detector and as-is agitation tests

Table 14 summarizes test results regarding solid phase radiocaesium concentrations, liquid phase radiocaesium concentrations (as-is agitation test), radiocaesium elution rates and others.

The results of radiocaesium concentrations in solid phase sample showed a tendency in which radiocaesium concentrations were higher in fly ash and treated fly ash than in the bottom ash and treated bottom ash.

Facility	Sample	Solid Phase Sample		Liquid Phase Sample			
		Cs134+137 (Bq/kg)	Moisture content (%)	Cs134+137 (Bq/kg)	Elution rate (%)	pH	EC (mS/m)
Facility 1	Bottom Ash	1,400	0.3	7.2	5.1	12.5	820
	Fly Ash	13,000	2.0	450	34.6	8.6	2,470
	Treated Fly Ash	5,000	23.8	470	94.0	12.0	5,480
Facility 2	Bottom Ash	210	0.5	2.1	10.0	12.6	1,436
	Fly Ash	1,300	3.9	43	33.1	12.2	3,900
Facility 3	Treated Bottom Ash	49	32.0	0.1	2.0	11.5	244
	Treated Fly Ash	310	23.6	29	93.5	12.2	3,900
Facility 4	Treated Bottom Ash	550	26.2	1.1	2.0	12.1	385
	Treated Fly Ash	3,700	23.0	310	83.8	12.2	3,730
Facility 5	Treated Bottom Ash	260	29.0	0.2	0.8	11.6	235
	Fly Ash	1,900	2.1	120	63.2	12.4	4,110
	Treated Fly Ash	1,800	13.8	140	77.8	11.7	3,050
Facility 6	Treated Bottom Ash	150	26.2	0.5	3.3	12.2	460
	Fly Ash	1,500	0.9	81	54.0	12.2	4,230
	Treated Fly Ash	1,000	19.3	85	85.0	12.1	3,800
Facility 7	Bottom Ash	1,300	0.2	8.6	6.6	12.7	1,201
	Fly Ash	12,000	1.3	680	56.7	12.3	3,690
	Treated Fly Ash	6,100	17.5	390	63.9	11.7	2,650
Facility 8	Treated Bottom Ash	51	28.6	ND	ND	11.4	188
	Fly Ash	620	1.4	48	77.4	12.3	6,140
	Treated Fly Ash	350	19.2	33	94.3	12.2	3,610

Table 14. Results of germanium semiconductor detector and as-is agitation tests

Regarding solid phase samples in the same facility, radiocaesium concentrations were lower in treated fly ash than in fly ash. This is probably because of the effect of water added during chelate

agent treatment to suppress heavy metal elution from fly ash. Similarly to the test results of the solid phase samples, the test results of radiocaesium concentrations in liquid phase samples suggested that radiocaesium concentrations tend to be higher in fly ash and treated fly ash than in bottom ash and treated bottom ash. The comparison of radiocaesium concentrations in bottom ash and treated bottom ash indicated a tendency in which the radiocaesium concentrations in treated bottom ash were lower in general, whereas the comparison of those in fly ash and treated fly ash did not show a similar tendency. The results of calculating radiocaesium elution rates indicated a tendency in which those of fly ash and treated fly ash were generally higher than those of bottom ash and treated bottom ash.

5.4.2.2.2. A test on radiocaesium elution suppression (long-term as-is agitation test)

Figure 16 summarizes the results (radiocaesium elution rates) of radiocaesium elution suppression tests by mixing an acid clay into treated fly ash by 5% in weight at facilities 1, 3, 4, 5, 6 and 7.

These results have confirmed that the mixture of an acid clay into any treated fly ash by 5% in weight suppresses radiocaesium elution rate to 30% or lower, in other words, an acid clay is effective in the suppression of radiocaesium elution. This is probably because a clay mineral, which is the major component of a clay, captures radiocaesium into its structure and suppresses its elution. The maximum duration of these tests were 30 days, during which no radiocaesium elution rate exceeded 30%.

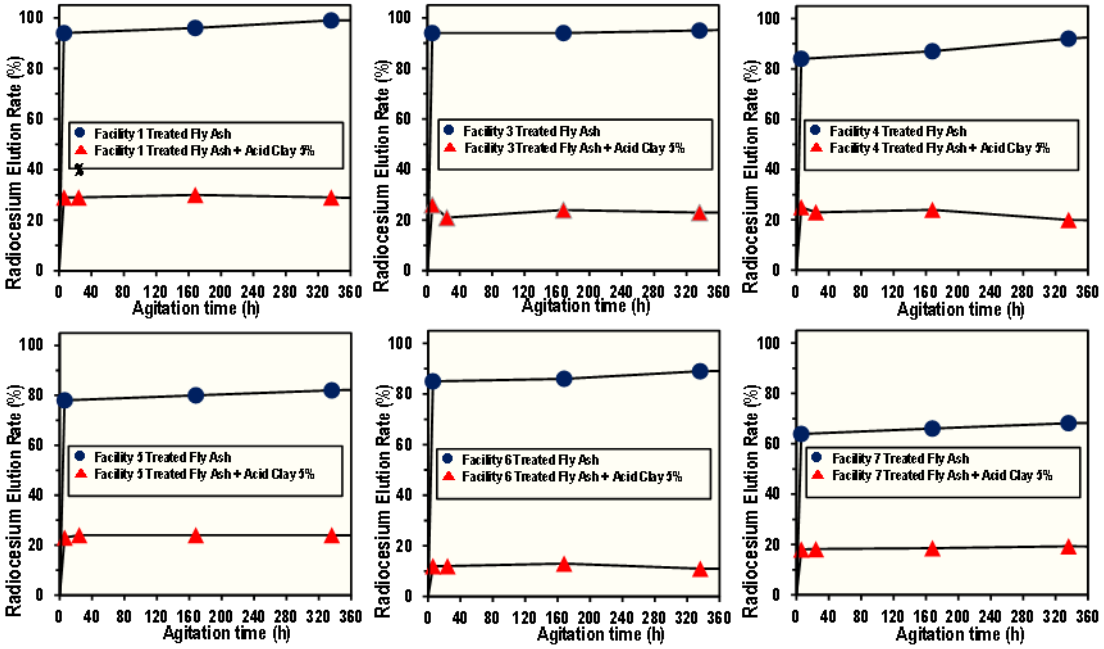

Figure 16. Results of radiocaesium elution suppression tests (radiocaesium elution rates)

5.4.2.2.3. Radiocaesium elution suppression tests (MP-AES / ion chromatography test)

Table 15 summarizes the concentrations of metals and others in the eluate. As a result of mixing an acid clay into treated fly ash by 5% in weight and agitating the mixture for six hours or 30 days, it was found that the long-term agitation did not result in significant differences in the concentrations of metals and others. As a result of comparing 30-day agitation without mixing an acid clay and 30-day agitation after mixing an acid clay, some cases were observed in which acid clay mixture resulted in low concentrations, but generally the obtained concentrations showed a similar tendency and suggested that the mixing of an acid clay does not block the effect of chelate.

Table 15. Results of radiocaesium elution suppression test (concentrations of metals and others in eluates) * mg/L **g/L

Facility	Sample	Metal									Anion			pH	EC (mS/m)
		Zn^{*}	Sr^{*}	Cu^{*}	Pb^{*}	Ba^{*}	Li^{*}	Ca^{**}	Na^{**}	K^{**}	Cl^{-**}	Br^{-*}	SO_4^{2-*}		
Facility 1	Treated fly ash + Acid clay 5%, Stirred for 6 hours	1.3	14.1	0.6	27.1	1.9	0.9	5.9	1.5	2.4	19	53	1240	12.3	4,580
	Treated fly ash + Acid clay 5%, Stirred for 30 days	0.7	13.5	0.4	11.1	1.9	0.6	5.2	1.3	1.9	17	52	990	12.2	4,260
	Treated fly ash, Agitated for 30 days	2.1	15	0.4	55.2	1.2	1	7	1.8	2.8	25	85	940	12.2	5,440
Facility 3	Treated fly ash + Acid clay 5%, Stirred for 6 hours	0.1	11.6	0.4	0.7	2.7	1.3	2.1	3.5	2.8	12	24	170	12.4	3,570
	Treated fly ash + Acid clay 5%, Stirred for 30 days	0.1	12.6	0.4	0.6	18.2	1.7	1.8	3.3	2.5	13	41	10	12.1	2,820
	Treated fly ash, Agitated for 30 days	0.1	12.8	0.4	0.8	13.3	2.6	2.3	4.1	3.2	15	50	10	12.3	4,350
Facility 4	Treated fly ash + Acid clay 5%, Stirred for 6 hours	0.1	10.4	0.4	0.8	1	1.1	2.5	2.1	2.2	11	30	440	12.4	3,110
	Treated fly ash + Acid clay 5%, Stirred for 30 days	0.2	11.4	0.3	0.6	2.7	1.8	2.2	2	2	11	43	80	11.9	2,920
	Treated fly ash, Agitated for 30 days	0.1	11.9	0.4	0.3	3.1	2.6	2.5	2.3	2.5	13	63	10	11.9	3,920
Facility 5	Treated fly ash + Acid clay 5%, Stirred for 6 hours	0.1	8.8	0.4	0.7	6.4	1	0.8	2.5	2.2	8	12	20	11.5	2,150
	Treated fly ash + Acid clay 5%, Stirred for 30 days	0.2	9.3	0.3	0.7	8.7	1.3	0.9	2.5	2	8	16	10	10.9	2,260
	Treated fly ash, Agitated for 30 days	0.1	10.2	0.5	0.6	6	1.9	1.2	3.3	2.8	11	32	40	10.6	3,110
Facility 6	Treated fly ash + Acid clay 5%, Stirred for 6 hours	0	11.8	0.4	0.4	2.7	1.3	2.6	2.7	2.4	11	57	380	12.3	3,320
	Treated fly ash + Acid clay 5%, Stirred for 30 days	0.1	13.3	0.3	0.5	10.7	1.6	2.2	2.6	2.2	12	73	40	11.7	3,130
	Treated fly ash, Agitated for 30 days	0.1	13.8	0.4	0.3	6.6	2.4	2.5	3	2.7	16	91	30	11.7	3,910
Facility 7	Treated fly ash + Acid clay 5%, Stirred for 6 hours	0.1	13.2	0.4	1.7	2.4	1.1	0.6	2.4	2.4	6	38	730	11.3	1,910
	Treated fly ash + Acid clay 5%, Stirred for 30 days	0.2	14.5	0.3	0.6	3.4	1.7	0.5	2.5	2.3	7	46	190	10.6	2,060
	Treated fly ash, Agitated for 30 days	0.1	16	0.4	0.4	9	2.5	0.8	3.2	3.3	10	63	1060	9.4	2,950
Facility 8	Treated fly ash + Acid clay 5%, Stirred for 6 hours	0	7.6	0.3	0.7	0.9	1.1	1.5	2.8	2.3	10	26	900	12.3	2,940
	Treated fly ash + Acid clay 5%, Stirred for 30 days	0.3	9.2	0.3	0.7	1.1	1.3	1.3	3	2.4	11	58	70	11.2	2,840
	Treated fly ash, Agitated for 30 days	0.1	10.5	0.4	0.6	0.6	2.2	1.3	3.2	2.8	14	68	70	11.2	3,650

5.4.2.3. Tests on radiocaesium elution suppression in incineration ash at municipal waste incineration facilities

5.4.2.3.1. Tests during a normal operation

5.4.2.3.1.1. Germanium semiconductor detector test, JIS K 0058-1 elution test and the Environment Agency's Notice No. 13 elution test

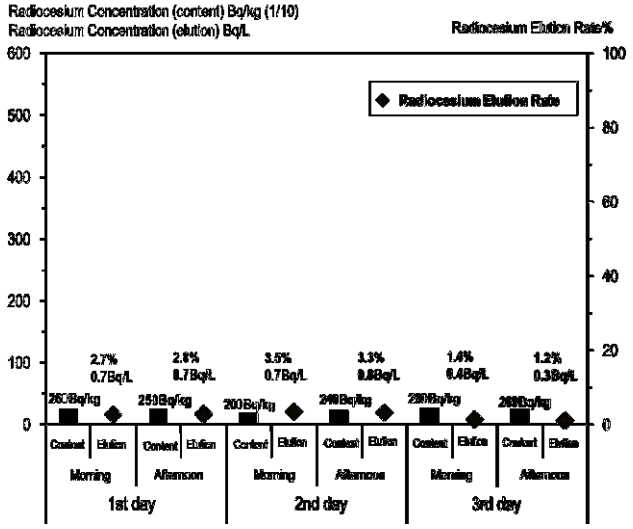

Figure 17. Daily fluctuations of radiocaesium concentrations in bottom ash (normal operation)

Figures 17 to 19 show the daily fluctuations of radiocaesium concentrations (contained or elution radiocaesium) and elution rates in the bottom ash, fly ash and treated fly ash sampled in normal operation tests. These results indicate a tendency in which fly ash and treated fly ash rather than bottom ash showed higher radiocaesium contents, elution quantities and elution rates.

Radiocaesium contents were 200 to 280 Bq/kg (248 Bq/kg on average) for bottom ash, 2,300 to 5,200 Bq/kg (3,517 Bq/kg on average) for fly ash, and 1,500 to 2,000 Bq/kg (1,650 Bq/kg on average) for treated fly ash. The quantities of radiocaesium elution were 0.3 to 0.8 Bq/L (0.6 Bq/L on average) for bottom ash, 150 to 360 Bq/L (240 Bq/L on average) for fly ash, and 97 to 160 Bq/L (121 Bq/L on average) for treated fly ash.

Radiocaesium elution rates were 1.2 to 3.3% (2.5% on average) for bottom ash, 64.3 to 73.9% (68.2% on average) for fly ash, and 64.7 to 81.3% (73.0% on average) for treated fly ash, and therefore the results of the Environment Agency's Notice No. 13 elution test generally satisfied the basic requirements for heavy metals and others.

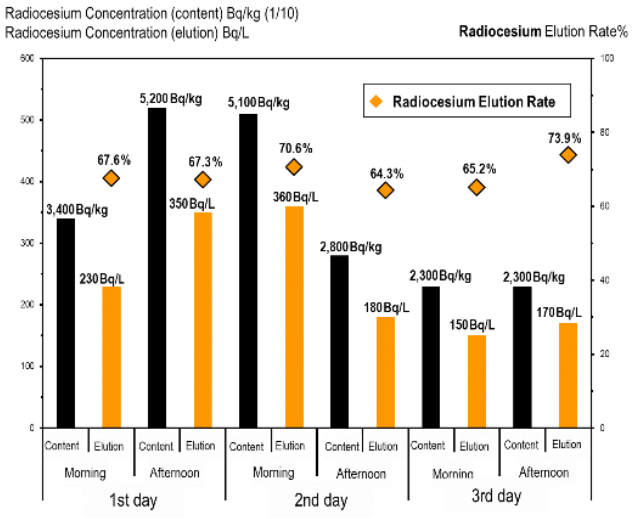

Figure 18. Daily fluctuations of radiocaesium concentrations in fly ash (normal operation)

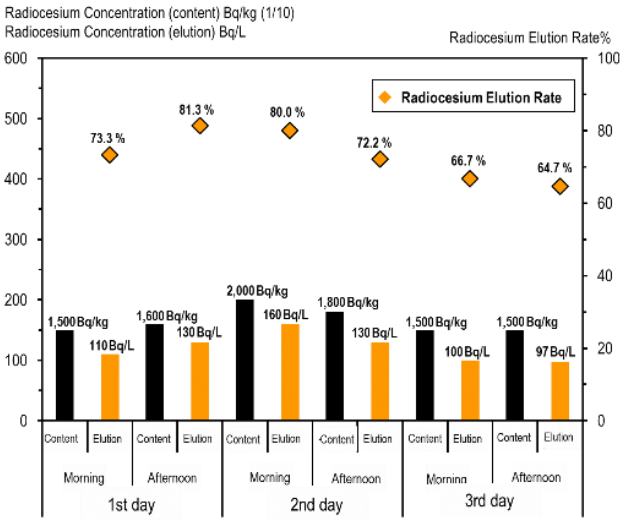

Figure 19. Daily fluctuations of radiocaesium concentrations in chelated fly ash (normal operation)

5.4.2.3.1.2. Repetitive elution tests (JIS K 0058-1)

Table 16 (bottom ash) and Table 17 (treated fly ash) show the results of repetitive elution tests. This time, samples taken in the afternoon (14:00) of the first day were used. Radiocaesium elution property indicated by each sample and also the results of the repetitive elution tests showed a tendency in which radiocaesium elution rates were higher in the case of treated fly ash than bottom ash. The cumulative rate of radiocaesium elution from bottom ash was 3.2% and that from treated fly ash was 81.9% in the four tests. The samples of the first test showed the highest amount and rate of radiocaesium elution, which gradually decreased as the number of tests increased.

Table 16. Results of repetitive elution tests using bottom ash (normal operation)

Item		Unit	Bottom Ash (1st day afternoon)			
			1st	2nd	3rd	4th
JISK0058-1	Radiocesium Concentration (elution)*1	Bq/L	0.5	0.3	0	0
	pH	-	11.7	11.3	10.8	10.9
	EC	mS/m	420	109	55.0	42.9
	Radiocesium Elution Rate*2	%	2.0	1.2	0	0
	Hg	mg/L	<0.0005	<0.0005	<0.0005	<0.0005
	Cd		<0.009	<0.009	<0.009	<0.009
	Pb		<0.03	<0.03	<0.03	<0.03
	As		<0.01	<0.01	<0.01	<0.01
	Se		<0.01	<0.01	<0.01	<0.01
	Cr		<0.02	<0.02	<0.02	<0.02
	Cl-		1,010	136	46.0	14.7

* Each value is calculated with its radiocesium concentration (content) as of 250 Bq/kg.

Table 17. Radiocaesium concentration in flue gas during bag filter cloth co-incineration tests

Item		Unit	Chelated Fly Ash (1st day afternoon)			
			1st	2nd	3rd	4th
JISK0058-1	Radiocesium Concentration (elution)*1	Bq/L	120	10	1	0
	pH	-	12.4	12.5	12.6	12.6
	EC	mS/m	3,380	1,150	911	871
	Radiocesium Elution Rate*2	%	75.0	6.3	0.6	0
	Hg	mg/L	0.0006	<0.0005	<0.0005	<0.0005
	Cd		<0.009	<0.009	<0.009	<0.009
	Pb		0.16	0.10	0.14	0.14
	As		<0.01	<0.01	<0.01	<0.01
	Se		<0.01	<0.01	<0.01	<0.01
	Cr		0.07	<0.02	<0.02	<0.02
	Cl-		10,400	1,200	256	88.6

* Each value is calculated with its radiocesium concentration (content) as of 1,600 Bq/kg.

The values of EC also tended to decrease as the number of elution tests increased. Results regarding heavy metals and others did not show any anomalous value and suggested a trend in which their values decreased as the number of elution tests increased similarly to the EC results.

From the results of the test described in 5.4.2.3.1.1. and the repetitive elution tests, it was found that the radiocaesium concentrations (of contained or eluted radiocaesium) in treated fly ash and the rates of radiocaesium elution from it were higher compared with bottom ash. The suppression of radiocaesium elution by means of chelate agent treatment is difficult to achieve, as the elution rate was high even before the earthquake and FDNPP accident. Therefore, it is particularly important to study the methods of suppressing radiocaesium elution from the treated fly ash in municipal waste incineration ash.

5.4.2.3.1.3. Zeolite addition test in laboratory

In order to investigate the presence or absence of a zeolite addition effect on heavy metals and others in the test of adding zeolite to fly ash, zeolite was added by different amount (5%, 10%, 15%, 20%) to the treated fly ash (chelate agent addition: 2% across the board) before the test.

Tables 18 (fly ash) and 19 (treated fly ash) show test results.

Table 18. Results of adding zeolite to fly ash in laboratory

Item		Unit	Fly Ash (1st day afternoon)	Fly Ash (1st day afternoon) + Chelate Agent 2%			
			Not added	5% added	10% added	15% added	20% added
Radiocesium Concentration (content)*1		Bq/kg	5,200	3,100	3,000	2,900	2,700
Moisture content		%	-	28.9	29.6	29.8	29.8
JISK0058-1	Radiocesium Concentration (elution)*1	Bq/L	350	98	56	40	28
	pH	-	12.4	12.4	12.4	12.4	12.4
	EC	mS/m	5,490	3,860	3,720	3,630	3,560
Radiocesium Elution Rate		%	67.3	31.6	18.7	13.8	10.4
Notice No. 13	Hg	mg/L	<0.0005*2	<0.0005	<0.0005	<0.0005	<0.0005
	Cd		<0.009*2	<0.009	<0.009	<0.009	<0.009
	Pb		9.2*2	<0.03	<0.03	<0.03	<0.03
	As		<0.01*2	<0.01	<0.01	<0.01	<0.01
	Se		0.02*2	<0.01	<0.01	<0.01	<0.01
	Cr		0.14*2	0.13	0.11	0.09	0.07
	Cl-		20,000*2	12,000	9,980	11,000	10,700

* Value without chelate addition

Table 19. Results of adding zeolite to chelated ash in laboratory

Item		Unit	Chelated Fly Ash (2nd day morning)				
			Not added	5% added	10% added	15% added	20% added
Radiocesium Concentration (content)*1		Bq/kg	2,000	1,300	1,300	1,200	1,100
Moisture content		%	-	29.0	29.4	29.5	29.6
JISK0058-1	Radiocesium Concentration (elution)*1	Bq/L	160	29	15	10	7
	pH	-	12.2	12.4	12.4	12.4	12.4
	EC	mS/m	3,740	2,820	2,720	2,620	2,550
Radiocesium Elution Rate		%	80.0	22.3	11.5	8.3	6.4
Notice No. 13	Hg	mg/L	<0.0005	<0.0005	<0.0005	<0.0005	<0.0005
	Cd		<0.009	<0.009	<0.009	<0.009	<0.009
	Pb		0.06	0.13	0.08	0.06	0.04
	As		<0.01	<0.01	<0.01	<0.01	<0.01
	Se		<0.01	<0.01	<0.01	<0.01	<0.01
	Cr		0.16	0.02	<0.02	<0.02	<0.02
	Cl-		11,200	7,770	7,060	6,840	6,490

The comparison of the test results indicated that the addition of zeolite to fly ash and treated fly ash suppresses radiocaesium elution. A tendency in which an increase in zeolite addition increased a radiocaesium elution suppression effect was also observed. The test results concerning heavy metal elution indicated that the addition of zeolite does not block the effect of chelate agent.

In chemical mixture addition and mixing addition tests at actual facilities, a goal of suppressing the total elution of caesium 134 and 137 from the finally generated treated ash to 10 Bq/L was set, and the test results revealed that zeolite must be added by at least 15% with each method to achieve the goal. Therefore, while taking into account the results of daily radiocaesium concentration fluctuations, each addition test at actual facilities was performed by mixing (kneading) zeolite and the chemical mixture so that zeolite is added by about 20%.

5.4.2.3.2. Tests on zeolite addition to an exhaust gas treatment agent at actual facilities

5.4.2.3.2.1. Exhaust gas composition analysis tests

Table 20 shows the results of exhaust gas composition analysis tests. A comparison with the results obtained during normal operation revealed that the injection of a chemical mixture

(containing zeolite) did not result in any anomalous values of the basic items, with the standard values satisfied.

Table 20. Results of analyzing exhaust gas Composition

	Sample	Unit	Normal	Blowing-in
Field measurement	Exhaust gas temperature	°C	141	155
	Flow velocity	m/s	17.2	16
	Wet exhaust gas volume	m^3(N)/h	34,000	30,400
	Dry exhaust gas volume	m^3(N)/h	24,200	18,700
	Moisture content	vol%	28.7	38.3
	Carbon dioxide	vol%	9	9.2
	Oxygen	vol%	11	10.8
	Carbon monoxide	vol%	<0.2	<0.2
	Nitrogen	vol%	80	80
	Air ratio	-	2.07	2.03
Laboratory measurement	Dust (dust concentration)	g/m^3(N)	0.039	0.014
	Dust (12% conversion ratio)	g/m^3(N)	0.036	0.013
	Sulfur oxides	ppm	9	7
	Sulfur oxide emissions	m^3(N)/h	0.21	0.13
	Nitrogen oxide	ppm	57	110
	Nitrogen oxide (12% conversion ratio)	ppm	51	100
	Nitrogen oxide emissions	m^3(N)/h	1.3	2
	Hydrogen chloride	mg/m^3(N)	16	39
	Hydrogen chloride (12% conversion ratio)	mg/m^3(N)	15	35
	Hydrogen chloride	ppm	10	23
	Hydrogen chloride (12% conversion ratio)	ppm	9	21
	Cs-134	Bq/m^3(N)	Less than the lower limit of detection	Less than the lower limit of detection
	Cs-137	Bq/m^3(N)	Less than the lower limit of detection	Less than the lower limit of detection
	Cs-134+137	Bq/m^3(N)	Not detected	Not detected

5.4.2.3.2.2. Germanium semiconductor detector test, JIS K 0058-1 elution test and the Environment Agency's Notice No. 13 elution test

Table 21 shows the concentrations of radiocaesium, heavy metals and others in sampled treated fly ash. Figure 20 shows the daily fluctuations of radiocaesium concentrations (of contained or eluted radiocaesium) and the summarized radiocaesium elution rates based on the results of Table 21. First, radiocaesium contents were 2,200 to 4,100 Bq/kg (2,800 Bq/kg on average), the quantities of radiocaesium elution were 8 to 16 Bq/L (11 Bq/L on average) and radiocaesium elution rates were 3.1 to 5.5% (4.1% on average).

Table 21. Results regarding chelated fly ash (blow injection)

Item		Unit	Chelated Fly Ash				
			1st day	2nd day	3rd day	4th day	5th day
Radiocesium Concentration (content)*		Bq/kg	2,200	2,300	2,800	4,100	2,600
JISK0058-1	Radiocesium Concentration (elution)*	Bq/L	12	9	12	16	8
	pH	-	12.3	12.3	12.3	12.3	12.4
	EC	mS/m	3,440	3,060	2,710	2,800	2,250
Radiocesium Elution Rate		%	5.5	3.9	4.3	3.9	3.1
Notice No. 13	Hg	mg/L	<0.0005	<0.0005	<0.0005	<0.0005	<0.0005
	Cd		<0.009	<0.009	<0.009	<0.009	<0.009
	Pb		<0.03	0.09	<0.03	<0.03	<0.03
	As		<0.01	<0.01	<0.01	<0.01	<0.01
	Se		<0.01	<0.01	<0.01	<0.01	<0.01
	Cr		0.16	0.05	0.03	0.05	0.07
	Cl-		10,400	9,520	7,890	8,140	6,310

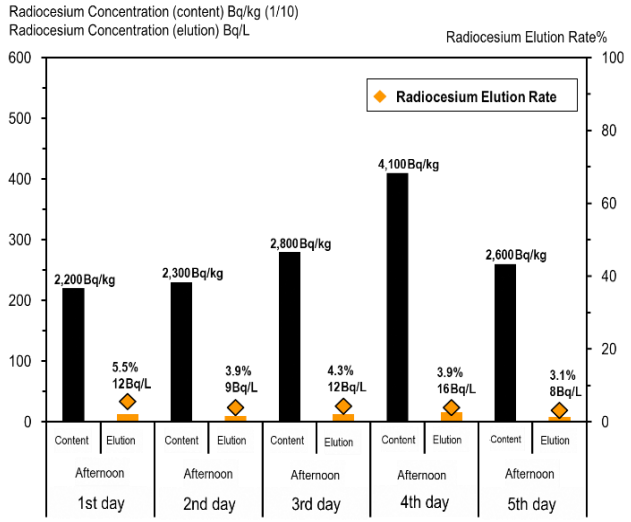

Figure 20. Daily fluctuations of chelated fly ash concentrations (after blow injection)

The comparison of each average value of radiocaesium in treated ash obtained from normal operation tests and each average value of radiocaesium obtained from chemical mixture addition tests performed this time indicated that the injection of zeolite significantly reduced quantities of radiocaesium elution (normal operation: 121 Bq/L → after chemical mixture addition: 11 Bq/L) and radiocaesium elution rate (normal operation: 73.0% → after chemical mixture addition: 4.1%). The results of the Environment Agency's Notice No. 13 elution test indicated that, as with the results of zeolite addition test in laboratory, the blow injection of the mixture of hydrated lime and zeolite at an actual facility also did not block the effect of a chelate agent.

5.4.2.3.2.3. Repetitive elution tests (JIS K 0058-1)

Tables 22 (solvent: ultrapure water) and 23 (solvent: artificial seawater) show the results of repetitive elution tests. This time, treated fly ash sampled on the third day, whose radiocaesium concentration was closest to the average value of treated fly ash sampled during chemical mixture addition test period, was used.

Table 22. Results of repetitive elution tests on chelated fly ash (solvent: ultrapure water)

Item		Unit	Chelated Fly Ash (3rd day afternoon), Ultra Pure Water			
			1st	2nd	3rd	4th
JISK0058-1	Radiocesium Concentration (elution)*1	Bq/L	35	3	0.7	0.3
	pH	-	11.6	11.8	11.9	11.9
	EC	mS/m	2,270	437	214	155
	Radiocesium Elution Rate*2	%	12.5	1.1	0.3	0.1
	Hg	mg/L	<0.0005	<0.0005	<0.0005	<0.0005
	Cd		<0.001	<0.001	<0.001	<0.001
	Pb		<0.01	<0.01	<0.01	<0.01
	As		<0.01	<0.01	<0.01	<0.01
	Se		<0.01	<0.01	<0.01	<0.01
	Cr		0.05	<0.02	<0.02	<0.02
	Cl-		7,970	1,110	254	78

Table 23. Results of repetitive elution tests on the elution of chelated fly ash (solvent: artificial seawater)

Item		Unit	Chelated Fly Ash (3rd day afternoon), Artificial seawater			
			1st	2nd	3rd	4th
JISK0058-1	Radiocesium Concentration (elution)*1	Bq/L	80	33	25	19
	pH	-	10.8	9.8	9.2	9.1
	EC	mS/m	6,910	5,770	5,720	5,660
	Radiocesium Elution Rate*2	%	28.6	11.8	8.9	6.8
	Hg	mg/L	<0.0005	<0.0005	<0.0005	<0.0005
	Cd		<0.001	<0.001	<0.001	<0.001
	Pb		<0.01	<0.01	<0.01	<0.01
	As		<0.01	<0.01	<0.01	<0.01
	Se		<0.01	<0.01	<0.01	<0.01
	Cr		0.09	0.12	0.07	0.04
	Cl-		28,000	22,800	22,900	22,900

With regard to radiocaesium elution properties, when four tests were performed using ultrapure water as a solvent, 14% of radiocaesium eluted in total. When this was compared with the results of treated fly ash not added with zeolite shown in Table 17, zeolite was found to significantly suppress radiocaesium elution (total elution rate of the four-time tests: 81.9% → four-time total elution rate after chemical mixture addition: 14%).

However, when artificial seawater was used as a solvent, the total radiocaesium elution rate increased (total elution rate using ultrapure water 4 times: 14% → artificial seawater 4 times: 56.1%). It was found that regardless of the use of the either solvent, treated fly ash added with zeolite showed a certain radiocaesium elution suppression effect compared with not adding zeolite to treated fly ash. The heavy metal elution when ultrapure water or artificial seawater was used also did not result in any anomalous values.

5.4.2.3.3. Tests regarding zeolite addition to the mixture of fly ash and chelate agent (mixture using a kneader) at actual facilities

5.4.2.3.3.1. Germanium semiconductor detector test, JIS K 0058-1 elution test and the Environment Agency's Notice No. 13 elution test

Table 24 shows the results of the concentrations of radiocaesium, heavy metals and others in sampled treated fly ash. Figure 21 shows the daily fluctuations of radiocaesium concentrations (contained and eluted radiocaesium) and radiocaesium elution rates based on the results of Table 24. First, radiocaesium contents were 1,200 to 1,400 Bq/kg (1,280 Bq/kg on average), quantities of radiocaesium elution were 6 to 11 Bq/L (8 Bq/L on average) and radiocaesium elution rates were 4.6 to 7.9% (5.9% on average).

The comparison of radiocaesium average values in treated fly ash sampled in chemical mixture addition tests and mixing addition tests indicated that the quantities of radiocaesium elution were similar in both cases (11 Bq/L for chemical mixture addition, 8 Bq/L for mixing addition, and 121 Bq/L for normal operation) and radiocaesium elution rates (4.1% for chemical mixture addition, 5.9% for mixing addition, and 73% for normal operation). Thus, it was concluded that, regardless of zeolite addition method (the blow injection or mixing of zeolite), its addition itself has the effect of suppressing the elution of radiocaesium. The results of the Environment Agency's Notice No. 13 elution tests indicate that similar to the results obtained from zeolite addition tests and chemical mixture addition tests in the laboratory, the simultaneous mixing of fly ash, a chelate agent and zeolite at actual facilities did not block the effect of the chelate agent.

Table 24. Results regarding chelated fly ash (mixed with zeolite)

Item		Unit	Chelated Fly Ash (afternoon)				
			1st	2nd	3rd	4th	5th
Radiocesium Concentration (content)*		Bq/kg	1,400	1,200	1,200	1,300	1,300
JISK0058-1	Radiocesium Concentration (elution)*	Bq/L	11	8	6	7	6
	pH	-	12.5	12.5	12.5	12.4	11.8
	EC	mS/m	3,370	2,980	2,840	2,350	2,170
Radiocesium Elution Rate		%	7.9	6.7	5.0	5.4	4.6
Environment Agency Notice No. 13	Hg	mg/L	<0.0005	<0.0005	<0.0005	<0.0005	<0.0005
	Cd		<0.009	<0.009	<0.009	<0.009	<0.009
	Pb		<0.03	<0.03	<0.03	<0.03	<0.03
	As		<0.01	<0.01	<0.01	<0.01	<0.01
	Se		<0.01	<0.01	<0.01	<0.01	<0.01
	Cr		0.11	0.13	0.04	0.06	0.05
	Cl-		10,000	8,930	8,080	6,970	7,290

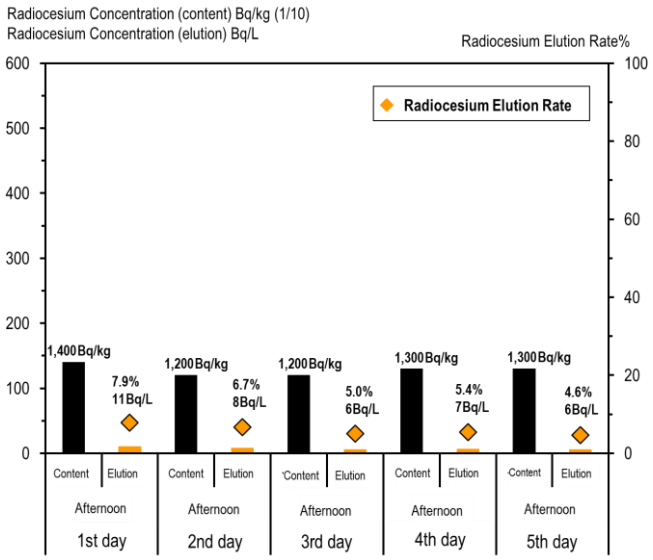

Figure 21. Daily fluctuation of chelated fly ash (mixed with zeolite)

5.4.2.3.3.2. Repetitive elution tests (JIS K 0058-1)

Tables 25 (solvent: ultrapure water) and 26 (solvent: artificial seawater) show the results of repetitive elution tests. This time, treated fly ash sampled on the fourth day of the zeolite-mixing test period, whose radiocaesium concentration was closest to the average value, was used.

Table 25. Results of repetitive elution tests on elution from chelated fly ash (ultrapure water)

Item		Unit	Chelated Fly Ash (4th day afternoon), Ultra Pure Water			
			1st	2nd	3rd	4th
JISK0058-1	Radiocesium Concentration (elution)*1	Bq/L	12	1	0.4	0
	pH	-	12.0	12.1	12.0	12.0
	EC	mS/m	2,240	664	316	235
	Radiocesium Elution Rate*2	%	9.2	0.8	0.3	0
	Hg	mg/L	<0.0005	<0.0005	<0.0005	<0.0005
	Cd		<0.001	<0.001	<0.001	<0.001
	Pb		<0.01	<0.01	<0.01	<0.01
	As		<0.01	<0.01	<0.01	<0.01
	Se		<0.01	<0.01	<0.01	<0.01
	Cr		0.05	<0.02	<0.02	<0.02
	Cl-		6,660	1,140	340	108

* Each value is calculated with its radiocesium concentration (content) as of 1,300 Bq/kg.

Table 26. Results of repetitive elution tests on elution from chelated fly ash (artificial seawater)

Item		Unit	Chelated Fly Ash (4th day afternoon), Artificial Seawater			
			1st	2nd	3rd	4th
	Radiocesium Concentration (elution)*1	Bq/L	26	12	10	8
	pH	-	11.4	11.0	9.9	9.2
	EC	mS/m	6,820	5,920	5,740	5,680
	Radiocesium Elution Rate*2	%	20.0	9.2	7.7	6.2
JISK0058-1	Hg	mg/L	<0.0005	<0.0005	<0.0005	<0.0005
	Cd		<0.001	<0.001	<0.001	<0.001
	Pb		<0.01	<0.01	<0.01	<0.01
	As		<0.01	<0.01	<0.01	<0.01
	Se		<0.01	<0.01	<0.01	<0.01
	Cr		0.11	0.21	0.29	0.18
	Cl-		27,400	23,900	22,300	22,400

* Each value is calculated with its radiocesium concentration (content) as of 1,300 Bq/kg.

First, regarding radiocaesium elution properties, when four tests were carried out using ultrapure water as a solvent, radiocaesium was eluted by 10.3% in total. The results (81.9% radiocaesium elution in total in four tests during normal operation → 14% radiocaesium elution in total in four tests with the addition of chemical mixture, and 10.3% elution in total in four tests using a mixing method) were broadly similar to the results of treated fly ash sampled in the chemical mixture addition tests shown in Table 22.

Secondly, when four tests were carried out using artificial seawater as a solvent, similar results were obtained (56.1% elution in total for artificial seawater added with chemical mixture and 43.1% elution in total for artificial seawater mixed with chemical mixture). Results regarding heavy metal elution also did not show any anomalous value regardless of whether ultrapure water or artificial seawater was used as a solvent.

Given the effect of zeolite in suppressing radiocaesium elution shown in the zeolite mixing addition tests and the results of laboratory tests on zeolite addition to treated fly ash, the addition and mixing of zeolite into the treated fly ash before the repacking of ash (whose treatment is difficult because of its high radiocaesium concentration) to a new container, seems to be one of effective means of enhancing safety.

While both the zeolite addition methods (the method using the chemical mixture and the zeolite mixing method) were found effective in suppressing radiocaesium elution, when it comes to the burial of ash at a landfill disposal site, the excessive addition of zeolite to the ash may increase the total landfill volume, so the addition of zeolite by a maximum of 20% of total volume at a maximum is deemed appropriate.

In applying a zeolite addition method, either by using chemical mixture or by the mixing addition of zeolite, the modification of the facility may be necessary.

In the case of the chemical mixture addition method, an existing hydrated lime silo can be used and all of the hydrated lime needs can be replaced with the chemical mixture for radiocaesium elution suppression. However, unlike the blow addition of hydrated lime alone during a periodical

inspection, this method may cause pipe abrasion or may clog the bag filter, so careful measures in details may have to be taken.

In the case of adopting a mixing addition method, a silo equipped with a chelate agent kneading machine and a mechanism capable of adding zeolite may need to be newly built, and in such a case, periodical inspections may be needed to carefully check the abrasion of such a machine. Therefore, an optimal addition method and quantity of zeolite should be selected according to the characteristics of disposal facility to ensure applicability to it.

5.4.3. Conclusions

Radiocaesium elution tests were conducted for fly ash and bottom ash (64 samples in total) at 15 facilities in Fukushima Prefecture to obtain caesium elution data. At facility K, zeolite or bentonite, both of which are expected to be effective in caesium elution suppression, was added to and kneaded with incineration ash and then a radiocaesium elution test was performed. The results showed the excellent effects of zeolite and bentonite in the suppression of radiocaesium elution from the fly ash, and the effect of zeolite was particularly remarkable.

As a result of testing radiocaesium elution from incineration ash (bottom ash, treated bottom ash, fly ash and treated fly ash), which seems to be the cause of radiocaesium detected from leachate (seeping water) at the landfill disposal sites, radiocaesium concentrations in and radiocaesium elution from the fly ash (including treated fly ash) were higher compared with bottom ash (including treated bottom ash) at each site. When an acid clay was added to and mixed with treated fly ash having a high radiocaesium elution property, the radiocaesium elution decreased and the acid clay did not block the heavy metal elution prevention effect of chelate.

Tests were performed at actual facilities in which fly ash was added with zeolite, whose radiocaesium elution suppression effect had been recognized in the final report of the previous project. The results of the tests confirmed that both the methods of mixing zeolite into a blow-in chemical such as hydrated lime and the method of adding zeolite immediately before adding and mixing a chelate agent significantly suppress radiocaesium elution and does not block the heavy metal elution prevention effect of the chelate agent. Based on these results combined with laboratory results, these methods are effective in suppressing radiocaesium elution not only for fly ash to be generated at incineration facilities in the future but also for incineration ash temporarily stored at present. However, the application of these methods to actual disposal facilities requires the consideration of the characteristics of each incineration facility and landfill disposal site, including consideration of an increase in the amount of landfill disposal due to zeolite addition as well as facility structure and capacity.

5.5. Situations of landfill and radiocaesium elution

The relationship between the landfill status of incineration ash and the concentration of radiocaesium in leachate was investigated on the waste landfill sites in Fukushima Prefecture where incinerated waste ash was landfilled after the nuclear power plant accident. As a result, periodic water sampling of leachate at a repository where radiocaesium was detected in leachate

was conducted, and the concentration of radiocaesium in the leachate and the relationship between various elements in the leachate and the status of radiocaesium leaching were investigated.

5.5.1. Investigations

5.5.1.1. Situations of landfill and radiocaesium elution

5.5.1.1.1. FY 2015

The investigations regarding the landfill situation of incineration ash (bottom ash and fly ash) were conducted at seven landfill disposal sites in Fukushima Prefecture. From January until March 2016, leachate (seeping water), discharged water, water-treated sludge and nearby underground water were sampled once a month at the sites. Then their radiocaesium concentrations were measured to investigate a correlation between landfill situation and radiocaesium elution. In addition, radiocaesium concentrations in leachate and discharged water were compared to check the radiocaesium treatment situations at leachate treatment facilities. The situations of incineration ash landfill at the seven landfill disposal sites are shown in Table 27. Their incineration ash landfill situations fell under the following four types: “landfill in the same way as before the accident,” “landfill of only fly ash without contact with rainwater,” “landfill of only bottom ash,” and “no landfill of incineration ash.” Landfill disposal sites D and E prevent contact between fly ash and rainwater by burying fly ash in sandbags.

Table 27. Situations of the landfill of incineration ash

	Disposal Site A	Disposal Site B	Disposal Site C	Disposal Site D	Disposal Site E	Disposal Site F	Disposal Site G
Bottom Ash	○	○	×	○	○	○	○
Fly Ash	○	○	×	△	△	×	×

○: Landfill is done in the same way as before the accident.
△: Landfill is conducted so as not to contact rainwater.
×: Not landfilled.

5.5.1.1.2. FY 2016

In November and February, leachate (seeping water), discharged water, water-treated sludge, and nearby underground water were sampled from six landfill disposal sites in total (Table 28, namely four landfill disposal sites C, E, F and G among seven landfill disposal sites surveyed in FY 2015, landfill disposal site H where incineration ash was buried in the same method used before the accident, and landfill disposal site I where only bottom ash was buried), and their radiocaesium was analyzed.

Table 28. The list of landfill disposal sites

	Disposal Site C	Disposal Site E	Disposal Site F	Disposal Site G	Disposal Site H	Disposal Site I
Bottom Ash	×	○	○	○	○	○
Fly Ash	×	△	×	×	○	×

○: Landfill is done in the same way as before the accident.
△: Landfill is conducted as not to contact rainwater.
×: Not landfilled.

5.5.1.2. Correlation between the annual elution situation of radiocaesium and other elements

In four landfills (A, B, D, and H) from FY2017 to FY2021 and in five landfills including landfill J from FY2019, leachate, effluent, water treatment sludge and surrounding groundwater were sampled and radiocaesium concentrations were measured. Water-treated sludge was sampled only in FY 2017. Among the five landfill disposal sites, four landfill disposal sites A, B, H and J were burying fly ash in the same methods they used before the nuclear power station accident, and landfill disposal site D was burying fly ash after putting it in large sandbags. However, during a certain period immediately after the accident, site D buried part of fly ash without putting it in large sandbags (Table 29). In FY 2017, concentrations of elements and others shown in Table 30 in addition to radiocaesium were measured. Furthermore, with regard to the two landfill sites B and J, an interview was conducted with two landfill site managers on self-measured data of radiocaesium concentrations in leachate since FY2011.

Table 29. Situations of incineration ash landfill at five disposal sites

	Disposal Site A	Disposal Site B	Disposal Site D	Disposal Site H	Disposal Site J
Bottom Ash	○	○	○	○	○
Fly Ash	○	○	△	○	○

○： Landfilling is done in the same way as before the accident.

△： Landfilling is conducted so as not to contact rainwater.

Table 30. Analyzed elements and others

Elements to be analyzed
sodium, magnesium, sulfur, potassium, calcium, rubidium, barium, antimony, nickel, cobalt, molybdenum, selenium, caesium, strontium, chloride ion, nitrous acid, nitric acid

5.5.2. Results

5.5.2.1. Situations of landfill and radiocaesium elution

Table 31 shows radiocaesium analysis results in FY 2015. Radiocaesium was detected in leachate (seeping water) and discharged water from disposal sites A and B, where incineration ash was buried, and from disposal site D, where fly ash was buried without contact with rainwater. On the other hand, radiocaesium in leachate and discharged water was below the lower detection limit (about 1 Bq/L) for disposal site C, where no incineration ash was buried, disposal site E, where incineration ash was buried by preventing its contact with rainwater, and disposal sites F and G, where only bottom ash was buried. None of these disposal sites exceeded the lower detection limit (about 1 Bq/L) in terms of radiocaesium concentration in nearby underground water.

Table 31. Results of analyzing radiocaesium in leachate and others in FY 2015

Units: Bq/L for leachate and discharged water, Bq/kg for sludge

Lower detection limit: 1 Bq/L or Bq/kg

	Disposal Site A			Disposal Site B			Disposal Site C			Disposal Site D			Disposal Site E			Disposal Site F			Disposal Site G		
	Leachate (Bq/L)	Discharged water (Bq/L)	Sludge (Bq/kg)	Leachate (Bq/L)	Discharged water (Bq/L)	Sludge (Bq/kg)	Leachate (Bq/L)	Discharged water (Bq/L)	Sludge (Bq/kg)	Leachate (Bq/L)	Discharged water (Bq/L)	Sludge (Bq/kg)	Leachate (Bq/L)	Discharged water (Bq/L)	Sludge (Bq/kg)	Leachate (Bq/L)	Discharged water (Bq/L)	Sludge (Bq/kg)	Leachate (Bq/L)	Discharged water (Bq/L)	Sludge (Bq/kg)
Jan	2.6	1.9	1.9	10.9	11.2	8.4	N.D.	N.D.	N.D.	2.4	1.6	5.3	N.D.	N.D.	N.D.	N.D.	N.D.	N.D.	N.D.	N.D.	N.D.
Feb	1.8	1.6	3.1	10	10.3	6.6	N.D.	N.D.	N.D.	1.7	N.D.	2.5	N.D.	N.D.	N.D.	N.D.	N.D.	N.D.	N.D.	N.D.	1.0
Mar	2.2	1.7	1.8	9.7	10.7	6.0	N.D.	N.D.	N.D.	2.2	1.6	1.5	N.D.	N.D.	1.1	N.D.	N.D.	N.D.	N.D.	N.D.	N.D.

Table 32 shows radiocaesium analysis results in FY 2016. Radiocaesium was detected in leachate (seeping water) and discharged water from the disposal site H only, where fly ash had been buried as it is. Radiocaesium concentrations in underground water at all the landfill disposal sites shown in Table 32 were below the lower detection limit (0.1 Bq/L).

Table 32. Results of analyzing radiocaesium in leachate and others in FY 2016

Units: Bq/L for leachate and discharged water, Bq/kg for sludge

Lower detection limit: 1 Bq/L or Bq/kg

	Disposal Site C			Disposal Site E			Disposal Site F			Disposal Site G			Disposal Site H			Disposal Site I		
	Leachate (Bq/L)	Discharged water (Bq/L)	Sludge (Bq/kg)	Leachate (Bq/L)	Discharged water (Bq/L)	Sludge (Bq/kg)	Leachate (Bq/L)	Discharged water (Bq/L)	Sludge (Bq/kg)	Leachate (Bq/L)	Discharged water (Bq/L)	Sludge (Bq/kg)	Leachate (Bq/L)	Discharged water (Bq/L)	Sludge (Bq/kg)	Leachate (Bq/L)	Discharged water (Bq/L)	Sludge (Bq/kg)
Nov	<0.1	<0.1	—	<0.1	<0.1	0.42	<0.1	<0.1	0.24	<0.1	<0.1	0.38	7.1	6.7	4.9	<0.1	<0.1	0.87
Feb	<0.1	<0.1	—	<0.1	<0.1	0.17	<0.1	<0.1	0.26	<0.1	<0.1	0.11	3.9	4.5	6.0	<0.1	<0.1	0.19

Based on the results in FYs 2015 and 2016, it was likely that radiocaesium was detected in leachate and discharged water only at landfill disposal sites having buried radiocaesium-containing fly ash without preventing its contact with rainwater. Regarding disposal site D, where radiocaesium was detected in leachate although the site had buried fly ash while preventing its contact with rainwater, a detailed on-site hearing concerning the landfill situation revealed that a part of the fly ash had been buried without a rainwater contact prevention measure during a period immediately after the Fukushima accident, namely from the period of reconstructing the incineration facility until the Ministry of the Environment's notice ordering the halt of

incineration ash burial. It is likely that radiocaesium continuously eluted from the incineration fly ash in question and leached from the disposal site D through discharged water.

5.5.2.2. Correlation between the annual elution situation of radiocaesium and other elements

Figures 22 through 26 show concentration of radiocaesium in leachate that have been measured so far, as well as that in leachate measured voluntarily at B and J disposal sites by each disposal site.

5.5.2.2.1. Disposal site A

The maximum concentration of radiocaesium in the leachate of disposal site A was about 5 Bq/L. No seasonal trend was observed in leaching conditions, and radiocaesium concentrations are gradually decreasing. Because radiocaesium concentrations in landfill waste, especially in incineration ash, are also low, that in leachate is also expected to be less than the detection limit.

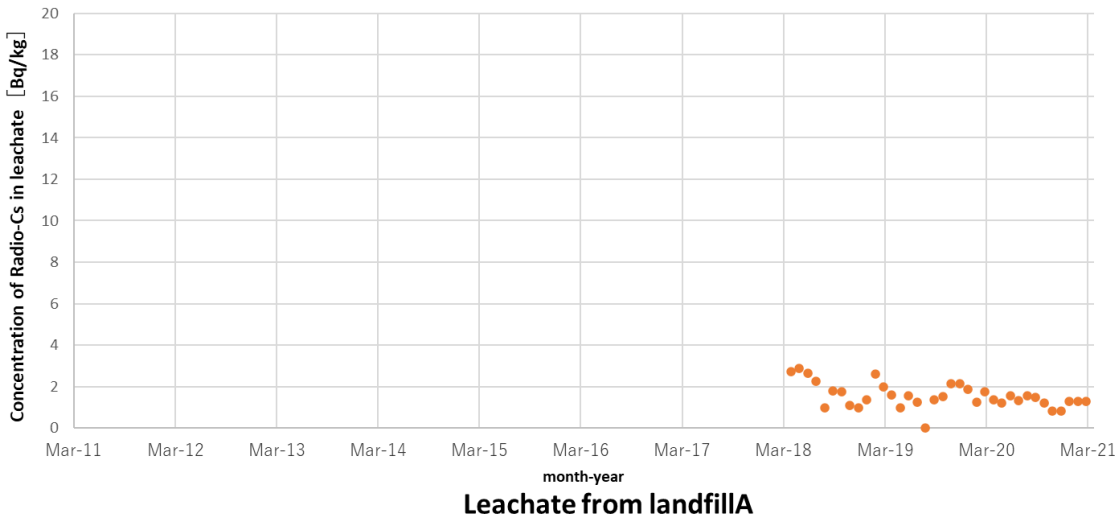

Figure 22. Radiocaesium concentrations in leachate at disposal site A

5.5.2.2.2. Disposal site B

The maximum concentration of radiocaesium in the leachate from the disposal site B was about 15 Bq/L. No seasonal trend was observed in changes of radiocaesium concentrations in the leachate. Radiocaesium concentrations increased from 2011 to March 2015 and gradually decreased until January 2018, but they began to increase again, peaking in October 2019 and began to decrease again. It is thought that the construction work to raise the height of the disposal site underway at that time may have had an impact on the results.

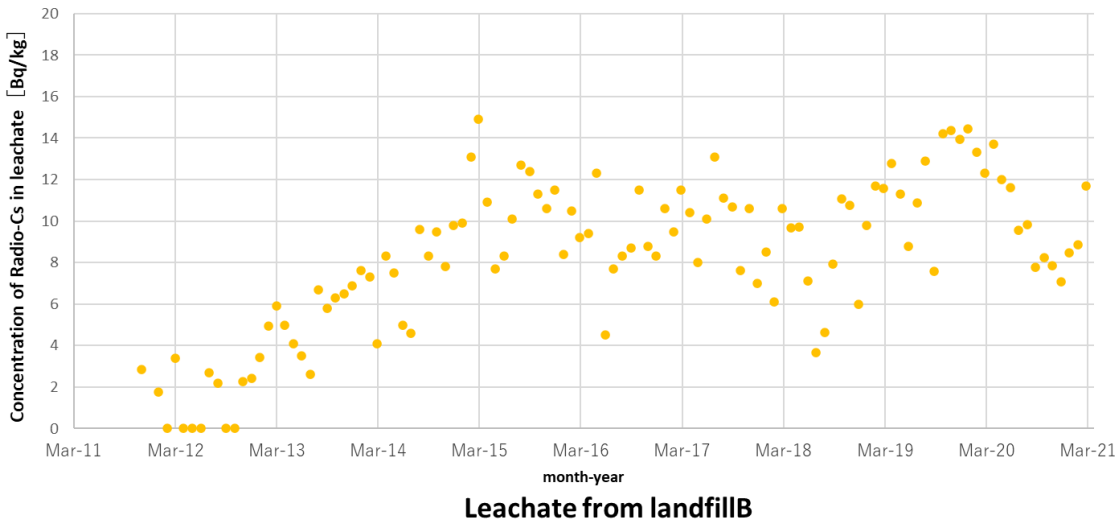

Figure 23. Radiocaesium concentrations in leachate at disposal site B

5.5.2.2.3. Disposal site D

The highest radiocaesium concentration in leachate at disposal site D was about 3 Bq/L. The concentrations were generally low, often below the lower detection limit, thus a seasonality was not confirmed. This is thought to be because the fly ash was placed in large sandbags and landfilled, preventing them from coming into contact with water.

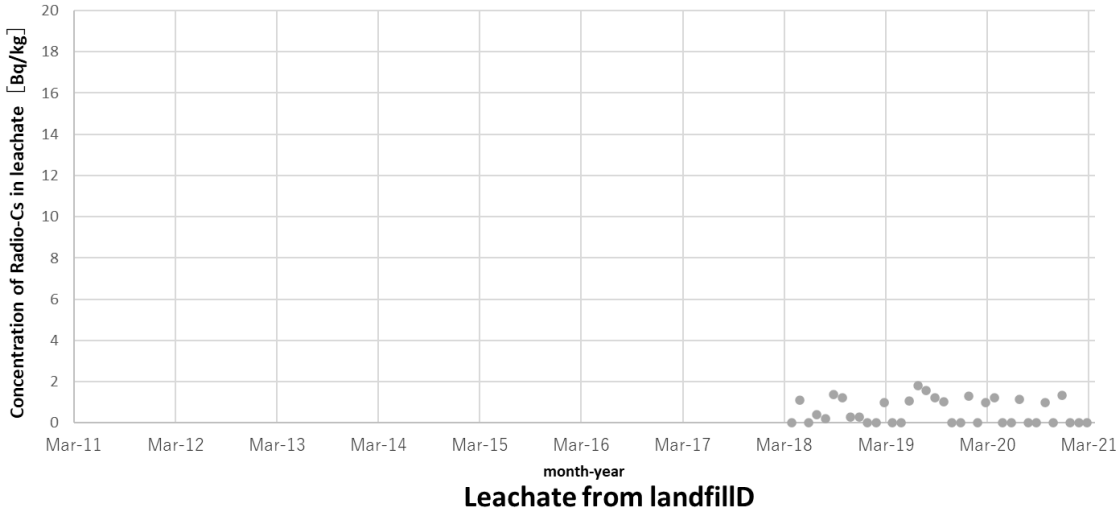

Figure 24. Radiocaesium concentrations in leachate at disposal site D

5.5.2.2.4. Disposal site H

The maximum concentration of radiocaesium in the leachate from disposal site H was about 8 Bq/L. Although there were some increases and decreases in radiocaesium concentrations, no seasonal trend was observed. The concentration of radiocaesium in the incinerated fly ash that had been landfilled was similar to that of B disposal site, but since the concentration of radioactive caesium in leachate was low, it is necessary to compare the structure of the disposal site and the caesium adsorption capacity of the soil lining material with those of

disposal site B to understand the differences.

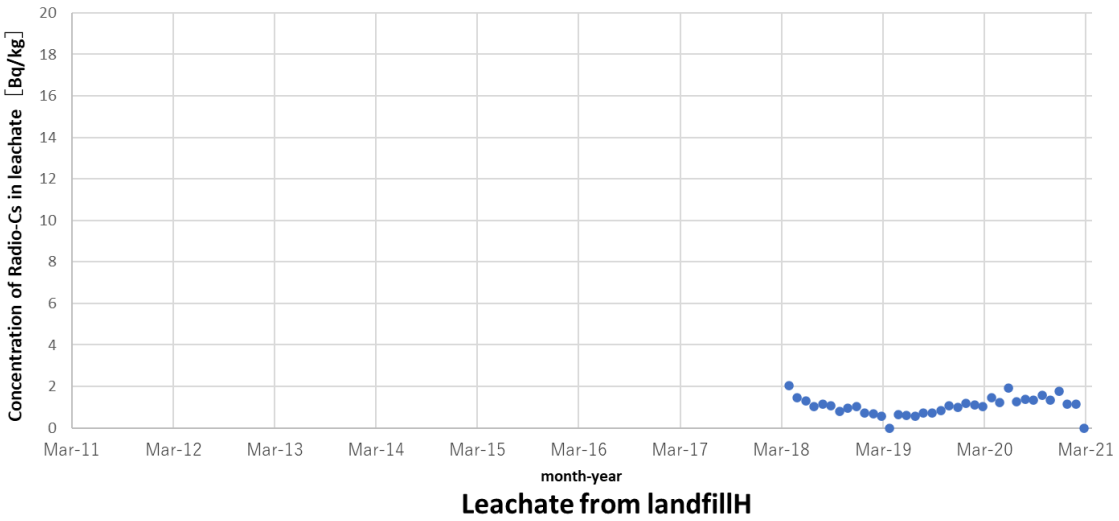

Figure 25. Radiocaesium concentrations in leachate at disposal site H

5.5.2.2.5. Disposal site J

The maximum concentration of radiocaesium in the leachate from disposal site J was about 11 Bq/L. As of 2018, the concentration of radiocaesium in the leachate was the second highest following disposal site B. It was expected to maintain a concentration of about 5 Bq/L, but the concentration of radiocaesium has decreased since the final covering of the soil in July 2019. It is thought that the cause may be the reduction in volume of infiltration water due to the final soil cover, and so continued investigation and research on the cause are necessary.

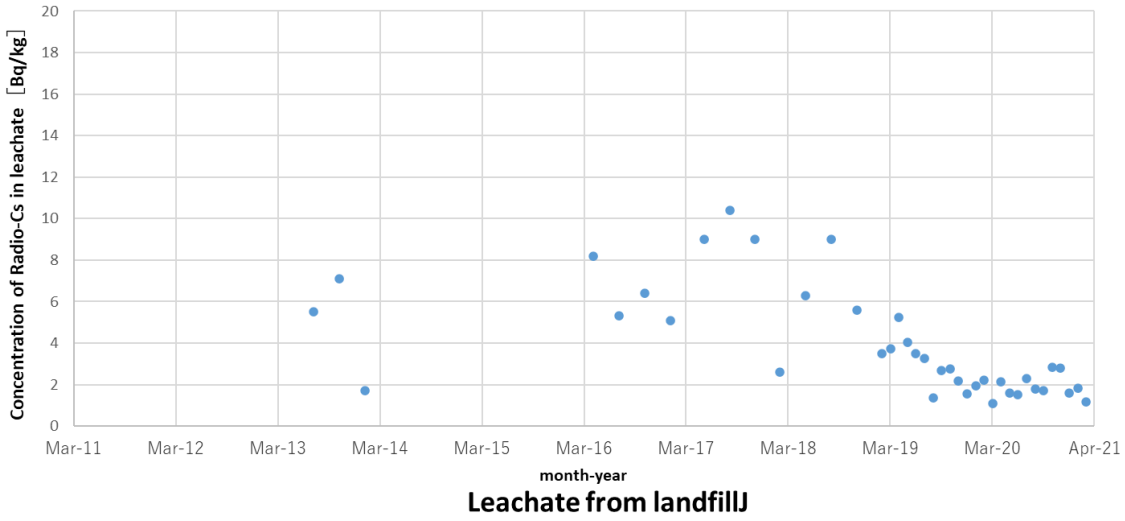

Figure 26. Radiocaesium concentrations in leachate at disposal site J

Table 33 shows the results of analyzing elements in leachate at landfill disposal sites in FY 2017, namely radiocaesium and chloride ion concentrations. A possibility was suggested that the higher the chloride ion concentration, the higher the radiocaesium concentration becomes. A correlation diagram (Figure 27) was developed by plotting radiocaesium concentrations on the vertical axis

and chloride ion concentrations on the horizontal axis. The diagram indicated a positive correlation between them.

Table 33. Radiocaesium and chloride ion concentrations

	Disposal Site A		Disposal Site B		Disposal Site D		Disposal Site H	
	Leachate (Bq/L)	Chloride ion (mg/L)	Leachate (Bq/L)	Chloride ion (mg/L)	Leachate (Bq/L)	Chloride ion (mg/L)	Leachate (Bq/L)	Chloride ion (mg/L)
Apr	0	83	8	13000	1	1400	8	4800
May	1	2000	8	12000	2	1800	1	5200
Jun	3	5100	10	12000	0	310	0	3900
Jul	3	5700	13	13000	2	2300	0	3600
Aug	4	7800	11	13000	3	1600	0	3000
Sep	4	7600	10	13000	2	1900	0	4000
Oct	4	7300	10	12000	0	1000	0	3900
Nov	5	7600	11	12000	0	1000	0	2800
Dec	4	7500	9	11000	2	1800	1	3700
Jan	4	7500	8	12000	1	980	2	7200
Feb	5	7800	10	12000	1	2100	3	8000
Mar	5	8700	12	12000	2	1800	2	6400

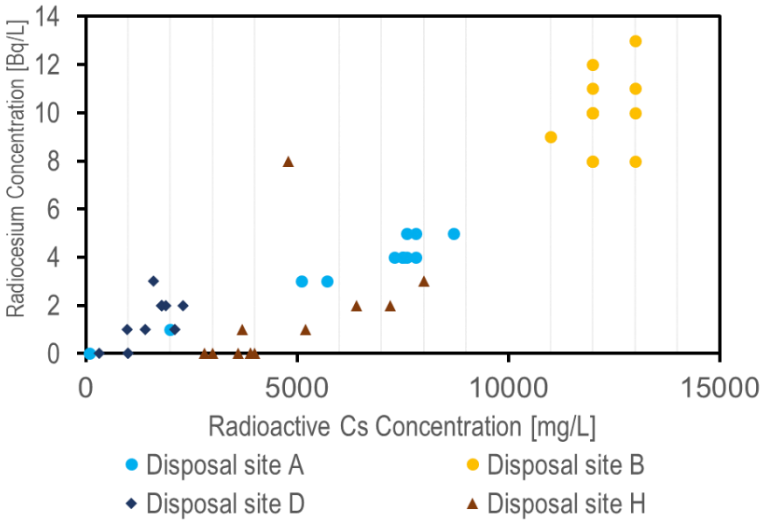

Figure 27. Correlation between radiocaesium and chloride ion concentrations

5.5.3. Conclusions

The surveys conducted this time have confirmed that the burial of fly ash at landfill disposal sites without elution-preventing measures such as water shielding results in the elution of radiocaesium. Regarding elution situations at the disposal sites, it is presumed that neither seasonality is common to them nor seasonality at each of them is present. Moreover, a positive correlation was observed between radiocaesium concentration and chloride ion concentration suggested a possibility that chloride ions in incineration ash are affecting radiocaesium elution.

It is thought that the concentration of radiocaesium in the leachate can be reduced by the structure of the disposal site, the soil cover and the condition of the soil cover, and so it is necessary to keep on investigating this topic moving forward.

5.6. Radiation safety assessment using landfill assessment tool

As stated earlier, municipal waste landfills in the Fukushima Prefecture have accepted wastes containing radioactive caesium since the Fukushima Daiichi Nuclear Power Plant Accident. Even though the concentration of the radioactive caesium is below the governmental limit (8000 Bq/kg), the Prefecture as well as the citizens, had certain concerns on the long-term safety of the disposal. The Prefecture therefore started to develop its own safety assessment of these municipal landfills.

IAEA has developed a landfill clearance tool which supports the assessment of safety by calculating the radionuclide concentrations in materials that can safely be disposed of in a landfill. The clearance tool implements a methodology for derivation of specific clearance levels (Bq/g) for disposal of different contaminated materials in different types of landfills. The methodology includes definition of exposure scenarios, assessment models and required input data for the models.

For the current project, the Prefecture, with the support of the IAEA, modified the IAEA clearance tool into an assessment tool for use in this safety assessment, that reflects the situation in Fukushima Prefecture. The modification included the use of scenarios that are representative of the situation and environment in Fukushima Prefecture, and parameters measured at, or suitable for, the actual disposal site.

The assessment model was calibrated using measured radiocaesium concentrations in the seepage (leachate) water from one of the landfills (landfill B). Landfill B was selected because this site has long-term data on radiocaesium concentrations in both waste and seepage water. Deterministic and probabilistic estimates of the radiation doses that the residents could potentially receive were calculated, and compared with the relevant dose criteria.

5.6.1. Safety assessment approach

The safety assessment approach adopted in this study was based on the IAEA recommendations for development of a safety case and safety assessment for disposal of radioactive waste (IAEA 2012)[1]. It consists of the following main steps:

(1) Assessment context
(2) System description
(3) Description of scenarios
(4) Description of the models
(5) Dose assessment and analysis of compliance

These different steps are described in the sections below.

5.6.1.1. Assessment context

5.6.1.1.1. Purpose and scope

For landfills that accept waste containing radiocaesium, a reference level of 8,000 Bq/kg has been established under the "Assessment of the Effects of Radioactive Substances on the Treatment and Disposal of Disaster Waste in the Hamadori and Nakadori Areas of Fukushima Prefecture (excluding evacuation zones and planned evacuation zones)" conducted by the JAEA. However, the safety assessment by JAEA was conducted for an inert waste disposal site and did not consider the leaching of radiocaesium from the waste. In fact, the leachability of radiocaesium in fly ash was found to be high, and waste-related guidelines have started to require fly ash to be buried to avoid contact with water. Nevertheless, there can be situations where radiocaesium is leached (including from the properly buried fly ash) by rainwater in the actual landfills. Therefore, Fukushima Prefecture has started to develop, using the modified IAEA clearance tool a safety assessment of the municipal landfills in the Prefecture considering the leaching and elution of radiocaesium from the waste.

The purpose of the safety assessment was to evaluate the safety of disposal of fly ash containing radiocaesium, originating from the nuclear accident at the Fukushima Daichi NPP, in conventional municipal landfills of Fukushima Prefecture.

In this study, the scope has been limited to an assessment for one municipal landfill (Landfill B). Future studies may extend the scope to other municipal landfills existing in Fukushima Prefecture.

5.6.1.1.2. Regulatory criteria

The radiological criteria that have been used in this study are those applied in GSR Part 3 (IAEA 2014)[2] as basis for calculation of Specific Clearance Levels (SCLs) for recycling and landfill disposal of radioactive materials:

For scenarios likely to occur, the assessed annual potential effective doses to members of the public shall not exceed 10 μSv/year, when using realistic parameter values in the calculations.

Additionally, in IAEA (2005 and 2021)[3][4] it is required that doses calculated for unlikely scenarios or using conservative low-probability parameter values should not exceed 1 mSv/year. A scenario unlikely to occur is defined by two cases: 1) The event causing the exposure to non-radiation workers and/or the population occurs with a low probability, 2) the values assigned to one or more parameters are conservative and unlikely to be observed.

A summary of the radiological criteria to derive the SCLs is given in Table 34.

Table 34. Radiological criteria for the public and landfill non-radiation workers for scenarios likely to occur and for scenarios unlikely to occur.

Group considered	Scenario likely to occur	Scenario unlikely to occur
Public (both age groups, i.e., adults and infants)	Dose less than 10 μSv/year	Dose less than 1 mSv/year
Non-radiation worker	Dose less than 10 μSv/year	Dose less than 1 mSv/year

These criteria are the same that has been used in the IAEA Basic Safety Standards GSR Part 3 (IAEA, 2014)[2] and IAEA SRS-44 (IAEA, 2005)[3] to derive General Clearance Levels (GCLs). They are considered "sufficiently low as not to warrant regulatory control" (IAEA 2014)[2], since such control of the cleared material would yield no net benefit.

5.6.1.1.3. Assessment endpoints

Consistent with the approach used for the derivation of GCLs (IAEA 2005)[3], doses were calculated for two age groups: adults >17 years old) and infant children (1-2 years old).

5.6.1.1.4. Assessment timeframes

The assessment considered three main phases of the landfill evolution in time:

- The Operational period – when materials are being disposed of in the landfill.
- The period of active institutional control – from the moment when the disposal operations have ended until the end of the institutional control period, assumed to be 30 years.
- The period after the end of the active institutional control period.

5.6.1.1.5. Treatment of uncertainties

The assessment of doses arising during disposal of waste is associated with several sources of uncertainties. One type of uncertainty is associated with the lack of knowledge about future exposure pathways. This type of uncertainty has been addressed by considering several exposure scenarios in the assessments. The mathematical models used in the assessment also have an associated uncertainty - this has been addressed in this study by applying models from the IAEA assessment tool which are considered fit for this specific assessment purpose. Another type of uncertainty comes from the limited data available on the parameter values that are used when estimating the dose. In this work, a probabilistic approach (IAEA 2003a, b)[5][6] has been adopted for evaluation of parameter uncertainties.

In the probabilistic approach, a Probability Distribution Function (PDF) is assigned to uncertain parameters. PDFs were either obtained from published data, for parameters with existing statistical data, or they were assigned by expert judgement, taking care that they were consistent with the values selected for the deterministic approach. The Monte Carlo method (Vose, 1996)[7] was then used to propagate the uncertainties through the model, allowing us to obtain different statistics of the calculated doses. This method provides a more holistic consideration of the uncertainties, as it explores all possible combinations of parameter values, balanced by their relative likelihoods. It also comes with the added advantage that it also enables parameter sensitivity analyses.

5.6.1.2. System description

Landfill B is a controlled type landfill which has accepted incineration ash containing radiocaesium (at concentrations less than 8,000 Bq/ kg). The caesium in this incineration ash derives from the Fukushima Daiichi Nuclear Power Plant accident and was deposited from the atmosphere on various environmental media some of which were managed by incineration.

Disposal of radiocaesium-containing ash was conducted in the period following the accident. Landfill B is a mountain-area landfill and, along with the incineration ash, sludge containing some organic matter was also landfilled. Information on the characteristics of leachate from the landfill is given in section 5.5.2..

5.6.1.3. Description of the scenarios

An important step in the assessment was the identification of exposure scenarios. These scenarios include all relevant activities and potential exposure situations related to the landfill disposal of the contaminated ash that may cause radiation exposure to the public.

The exposure scenarios in IAEA (2021)[4] have been adopted in this study. The scenarios in IAEA (2021)[4] were the basis of the calculations performed for the derivation of the GCLs recommended in the IAEA Basic Safety Standards GSR Part 3 (2014)[2] and IAEA SRS-44 (2005)[3]. Also, other IAEA work on disposal of radioactive waste in near surface disposal facilities has been considered (IAEA 2003b)[6].

The scenarios consider exposures to members of the public that may be directly or indirectly exposed to radionuclides in the disposed radioactive waste. The exposure of members of the public may occur at or near the landfill sites.

Some of the exposure scenarios are expected to occur (likely exposure scenarios), while others may occur only with a small probability (exposure scenarios unlikely to occur). A schematic view depicting the scenario is given in Figure 28.

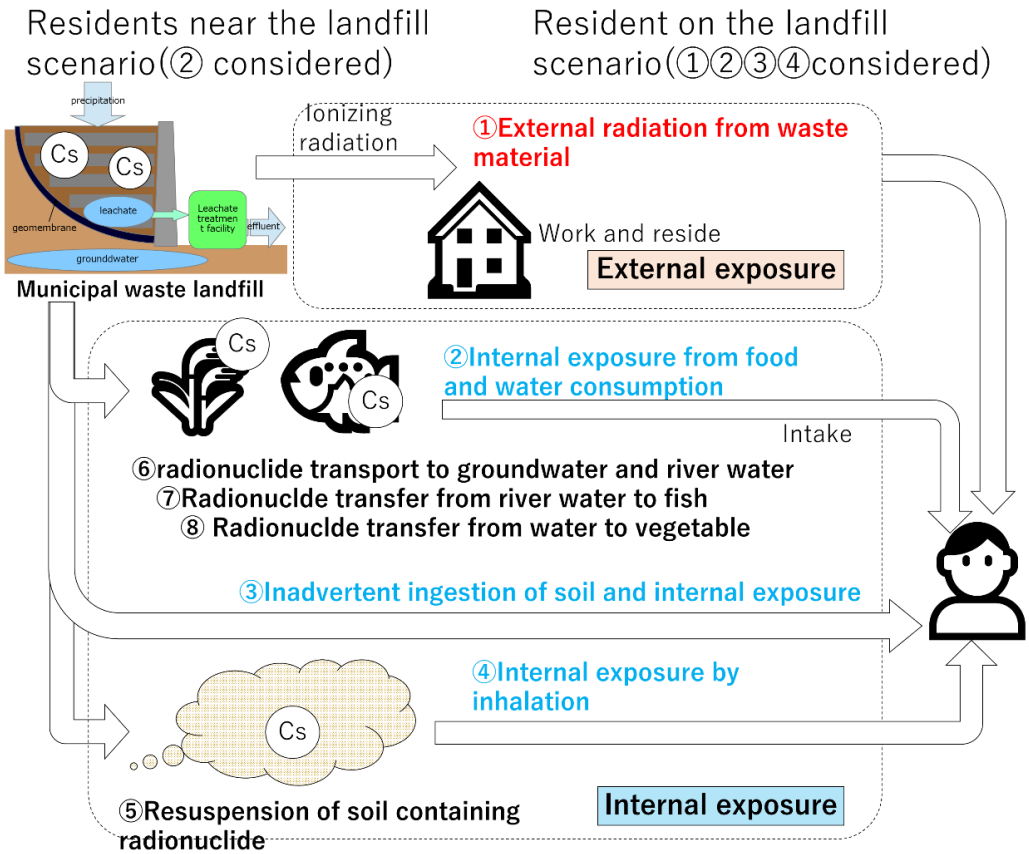

Figure 28. A schematic view depicting the scenarios considered in the safety assessment

The scenarios that were used for evaluating doses to the public in the safety assessment are presented in Table 35. The assessment model used includes generic values for some parameters, such as the half-life of radioactive nuclides, and dose conversion factors. For other parameters site-specific values for landfill B were selected by the Prefecture and used in the simulations. The results of the simulations such as radiocaesium concentrations in seepage water (leachate) were compared with measured values (calibration step). The doses calculated for residents under different scenarios were compared with relevant regulatory criteria (evaluation step).

Table 35. Safety assessment scenarios assuming leaching of radiocaesium from fly ash

Short name	Name of the scenario	Landfill phase	Exposed groups	Exposure pathways
RL_OP	Resident near the landfill	Operational Period	Resident near the landfill (adult and child)	· Ingestion of river water · Ingestion of vegetables irrigated with river water · Ingestion of river fish
RL_PO	Resident near the Landfill	Active Institutional Control Period	Resident near the landfill (adult and child)	· Ingestion of river water · Ingestion of vegetables irrigated with river water · Ingestion of river fish
RL_IC	Resident near the landfill	Period after the End of Active Institutional Control	Resident near the landfill (adult and child)	· Ingestion of well water · Ingestion of vegetables irrigated with well water · Ingestion of river fish
RO	Resident On the landfill	Period after the End of Active Institutional Control	Resident on the landfill (adult and child)	· Ingestion of seepage water (leachate) · Ingestion of vegetables grown onsite · External irradiation from the ground · Inhalation of resuspended dust · Inadvertent soil ingestion (for children only)
SE	Small excavation on the landfill	Period after the End of Active Institutional Control	Worker doing the excavation (adult and child)	· External irradiation from the excavated material · Inhalation of resuspended dust

The scenarios RL-OP, RL-PO, RL-IC and SE are classified as high probability, since the exposure situations covered by these scenarios are likely to occur. For these scenarios the dose criteria of 10 μSv/year applies.

Long term exposure situations may result from a loss of knowledge at some point in the future about the previous use of the site as a landfill. After the end of active institutional control, the site may be used for purposes that cause exposure to the public. If knowledge about the site is lost, buildings (e.g., residential houses) may be constructed on top of the covered landfill. During the construction of houses, the cover would be disturbed, and waste material would become accessible to a limited extent on the surface. Such situations are addressed by the RO scenario. A complete loss of knowledge about the site is considered not very likely; therefore, it is assumed that during major construction activities the special nature of the site would be re-discovered, and the residential use of the site is considered as an unlikely scenario (IAEA 2005, 2021)[3)4)]. In this case, the dose criterion of 1 mSv/y applies.

The construction of a road through the landfill and the subsequent use of this road is also possible in the long term. However, previous studies (IAEA 2003b) [6)] have shown that this scenario causes lower doses than residence on site scenario due to considerably shorter exposure times. The consequences of this scenario are thus covered by the scenario estimating doses to residents on the site.

The classification of scenarios by their likelihood in this study is consistent with the one adopted in IAEA (2005, 2021)[3)4)] for derivation of General and Specific Clearance Levels.

5.6.1.4. Description of the models

5.6.1.4.1. Models

Mathematical models were used for calculating the annual doses (Sv/y) arising from the different scenarios for a given radiocaesium concentration (Bq/g) in the disposed waste.

The IAEA assessment tool that has been used consists of models implemented in the modelling and simulation software Ecolego (www.ecolego.se). The models are either identical to those described in IAEA SRS-44 (2005)[3)] or have been derived by modifying some of the SRS-44 models.

The purpose of the original clearance tool was to use it for generic assessment, and to determine limits for radionuclide concentrations in the waste that can be landfilled while satisfying the dose criteria. The clearance tool consists of a set of models of radionuclide transport from landfills to and in the environment, as well as dosimetric models to calculate doses to the public (Figure 29). The tool includes a database of input parameters required by the models, such as groundwater flow, food consumption, and solid-liquid distribution coefficients (K_d hereafter) for radionuclides. Since the default values for model parameters used in this tool are generic, the Prefecture applied modifications to those values to reflect the site-specific conditions in Fukushima Prefecture.

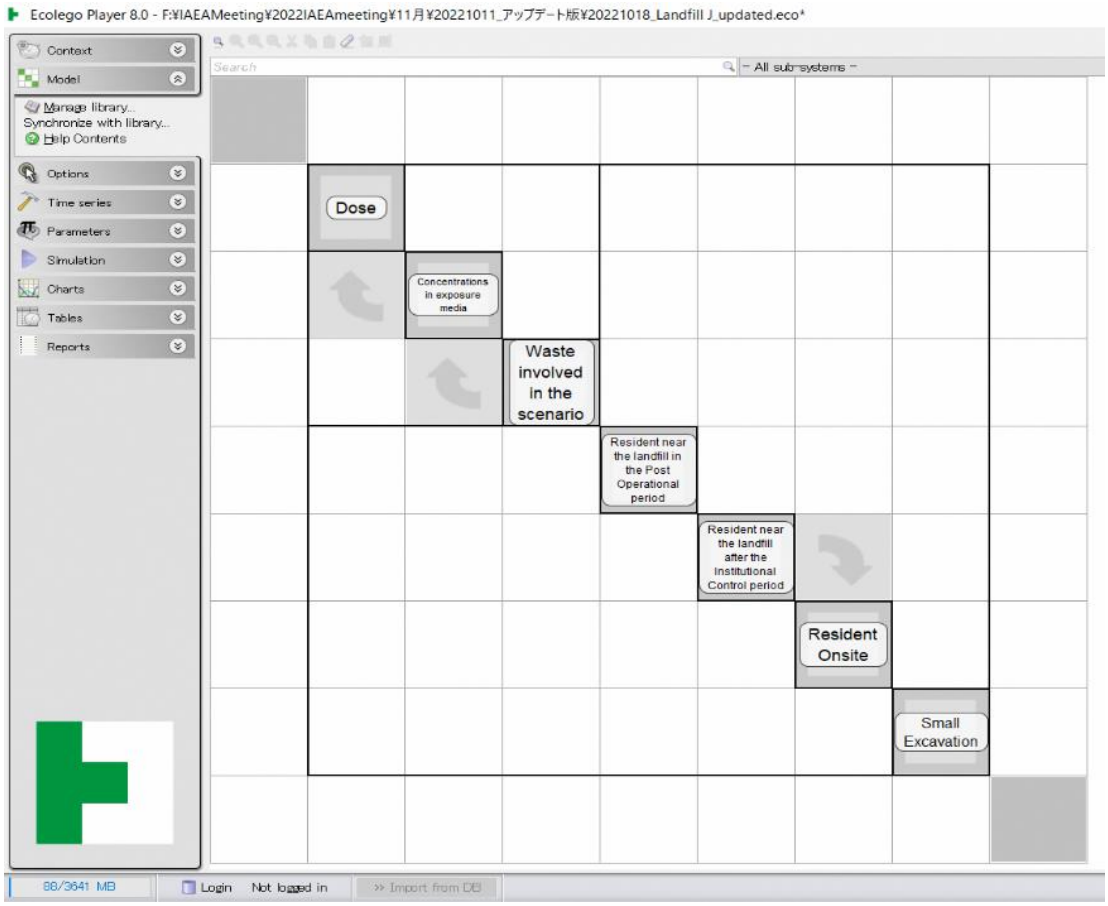

Figure 29. The assessment tool as implemented in Ecolego

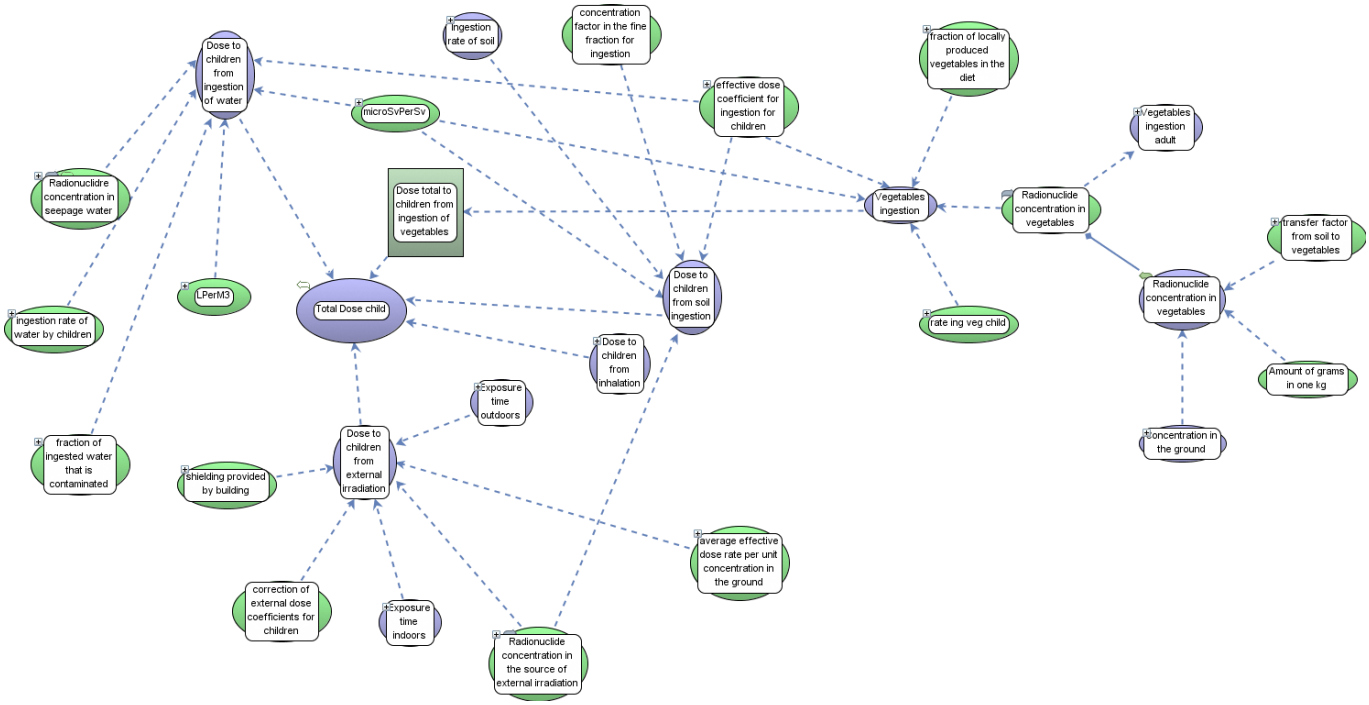

Figure 30. Influence diagram of the processes corresponding to the total dose to a child for the RO scenario

Radionuclide transport is expressed as transfers between components; an example influence diagram representing components is shown in Figure 30. The major components of the biosphere,

such as surface soil and river water, are included. Figure 30 shows how the components interact with each other in the calculation of total doses to a child by different exposure pathways (ingestion of water, ingestion of vegetables, external irradiation, inhalation and inadvertent soil ingestion) for the RO scenario.

5.6.1.4.2. Model parameters

Key parameters used in the simulation are tabulated in Table 36. For other model parameters, default values in the IAEA clearance tool were used.

Exposure pathways are defined according to assumptions about how radiocaesium may lead to external exposure of humans and/or may migrate in water from the landfill and move through various biosphere media. Human characteristics and behaviors, such as jobs and lifestyles, are determined to identify how humans may interact with these biosphere media. The model the Prefecture used considers features and processes concerning radiocaesium transport in the landfill, aquifer and other surface water systems (river and water wells), together with radiocaesium transport into environmental components that are accessible to human beings.

Waste disposed of in the landfill B principally consists of incineration ash, inert waste, soil, and sludge. The radiocaesium concentration in incineration ashes were obtained from the data collected monthly after July 2011. The radiocaesium concentrations in seepage water are governed by the radiocaesium concentration in the disposed waste, K_d values, the weight and density of the waste, the height of the landfill, and the infiltration rate of water into the landfill. Data on groundwater hydraulic gradients after the landfill was constructed at landfill B were scarce, but data from before landfill construction was available. The Prefecture decided to estimate hydraulic gradients using the data from before the construction. The bulk density of waste was estimated by dividing the total amount of waste in the landfill by the volume of the landfill. Databases of K_d values derived from batch sorption experiments and column experiments have been developed from literature studies. Databases were also developed for transfer factors between soil and various agricultural products, as well as for transfer factors between water and aquatic organisms. The databases were used in probabilistic simulations made the assessment tool.

The final stage of safety assessment concerns radionuclide transport in the biosphere and the exposure pathways giving rise to radiation doses to humans. Though future change are probable e.g. in lifestyles, climate, and farming and fishing practices, the present lifestyle was assumed in the safety assessment.

Potentially exposed groups (e.g. farming, freshwater fishing) were defined based on their habits and expected intakes of local products (crops, livestock, and freshwater fishes). Parameters deemed specific for Japan, such as food consumption, were determined based on average Japanese conditions, using statistics provided by the Japanese government.

Table 36. Values for key parameters used in the simulations

Parameter	Units (FW: Fresh Weight, DW: Dry Weight,)	Arithmetic Mean	Arithmetic Standard Deviation
Radiocaesium concentration in the waste	Bq/g	1	n.a.
Groundwater flow velocity	m/year	112.2	125
K_d of waste *1	cm^3/g	50	n.a.
K_d of soil*1	cm^3/g	370	n.a.
Ingestion rate of rice	kg FW/year	108.6 (69.5) *2	64 (33) *2
Ingestion rate of freshwater fish	kg FW/year	1.97 (1.68) *2	7.85 (5.66) *2
Ingestion rate of cabbage	kg FW/year	11.9 (4.38) *2	19.4 (7.99) *2
Ingestion rate of onion	kg FW/year	11.6 (7.77) *2	15 (7.63) *2
Institutional control period	years	30	n.a.
Operational period	years	13	n.a.
Transfer factor from soil to rice	kg FW/kg DW	0.03 *3	0.006 *3
Transfer factor from soil to cabbage	Kg FW/kg DW	0.3 *3	1.5 *3
Transfer factor from soil to onion	kg FW/kg DW	0.05 *3	0.14 *3
Transfer factor from fresh water to fish	L/kg FW	3667*3	3937*3

*1 Optimized in the calibration step

*2 Values in parentheses are for the children of age 1 to 6. The values for adults are for ages above 20 years. These values are the most representative of available statistical data for the age groups considered in the dose calculations: >17 years old adult and 1-2 years old child.

*3 Values of the mean E[X] and variance V[X] of the log normal distribution from IAEA database are given. Relationships between geometric mean μ and standard deviation σ are $E[X]= e^{(\mu+2\sigma^2)}$ and $V[X]= (e^{\sigma^2}-1)\, e^{(2\mu+\sigma^2)}$.

5.6.2. Dose assessment and analysis of compliance

The dose assessment was carried out by performing simulations with the assessment tool for each scenario. Two types of simulations were performed: deterministic and probabilistic. The

deterministic approach consisted of performing one simulation using realistic expected values for all model parameters. When statistical data was available for a parameter, the mean was used as realistic value. When statistical data was not available the realistic values were selected by expert judgement.

In the probabilistic approach, a Probability Distribution Function (PDF) was assigned to uncertain parameters, whereas for certain parameters realistic estimates were used. The Monte Carlo method (Vose, 1996)[7] was then used by performing 3000 iterations of the model simulation and the results were used to obtain different statistics of the calculated doses.

5.6.2.1. Results of the calibration step

K_d values for the waste were optimized in the calibration step using a trial-and-error approach to fit the measured radiocaesium concentration in the seepage from landfill B (8.7 Bq/L in average). The optimum K_d value was 50 cm^3/g. This K_d value was used throughout the deterministic simulations in the evaluation step.

After 10,000 runs assuming that the K_d for waste had a log-normal distribution, the concentration of radiocaesium in seepage water was obtained as shown in the histogram below (Figure 31). The figure shows that the radiocaesium concentration can vary between 1 Bq/L to 40 Bq/L, indicating that the K_d for waste is one of the important parameters governing the elution of radiocaesium from the landfill.

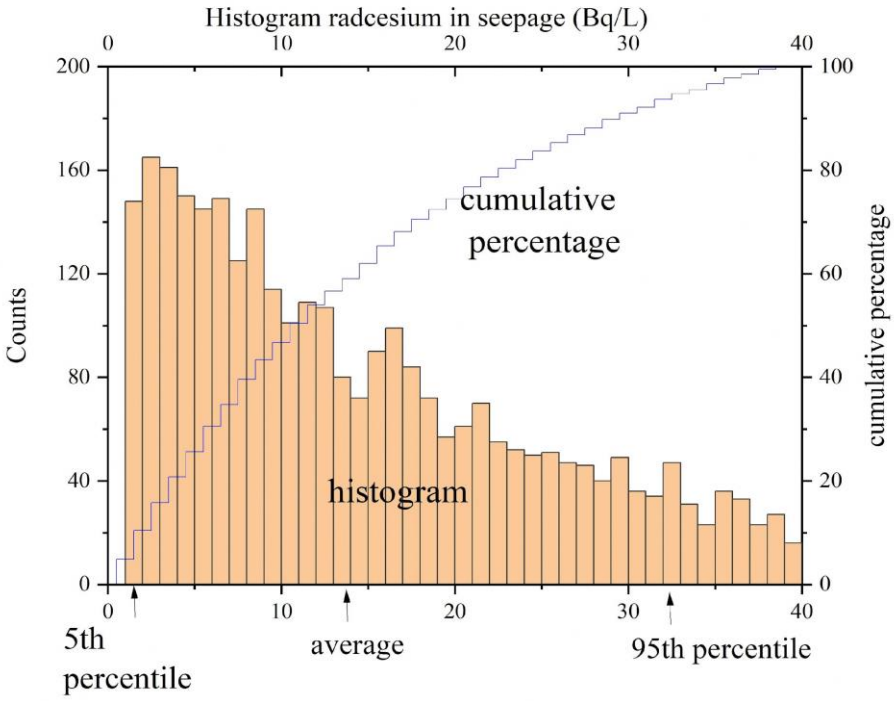

Figure 31. Histogram of radiocaesium concentration in seepage water when K_d values were varied in the simulations with the model

5.6.2.2. Results of the evaluation step

Doses to residents under different scenarios were calculated with the assessment tool. For each scenario, probabilistic as well as deterministic results of the dose calculations are presented in

Table 37. For the probabilistic simulations 3000 runs were conducted and mean, standard deviation, 5th percentile, and 95th percentile of the dose estimates were tabulated, along with the deterministic estimate of the dose (Table 37). The results are also shown in Figures 32 and 33.

As shown in the results summarized in Table 37, the highest dose estimate was obtained for the RO scenario, which assumes that the potentially exposed group resides on the landfill lacking a cover soil (unlikely scenario, low probability scenario). Detailed inspection of the simulation results for the RO scenario, shown in Table 37(d), revealed that the highest doses were caused by ingestion of seepage water (leachate) and external exposure from the waste. The potential dose estimates for other scenarios were in the order of RL_OP ≅ RL_IC > RL_PO for the mean dose obtained in the probabilistic simulation and for the dose estimates obtained in the deterministic simulations.

Table 37. Dose estimate under each scenario

(a) RL_OP: Resident near the Landfill during the Operational Period

Exposure pathway	Age group	Mean µSv/y	Std. Deviation µSv/y	5% µSv/y	Median µSv/y	95% µSv/y	Deterministic µSv/y
Ingestion of fish	adult	2.9E-03	2.1E-02	1.1E-05	3.2E-04	9.2E-03	1.6E-03
Ingestion of river water	adult	8.2E-04	6.3E-04	1.1E-04	6.6E-04	2.1E-03	4.4E-04
Ingestion of vegetables	adult	3.7E-05	4.0E-05	3.4E-06	2.4E-05	1.1E-04	2.0E-05
All pathways	adult	3.7E-03	2.1E-02	1.8E-04	1.2E-03	1.1E-02	2.1E-03
Ingestion of fish	child	2.1E-03	7.8E-03	8.9E-06	3.2E-04	8.2E-03	1.3E-03
Ingestion of river water	child	3.0E-04	2.3E-04	4.0E-05	2.4E-04	7.6E-04	1.6E-04
Ingestion of vegetables	child	2.0E-05	2.1E-05	1.8E-06	1.3E-05	6.1E-05	1.1E-05
All pathways	child	2.4E-03	7.8E-03	8.3E-05	6.7E-04	8.7E-03	1.4E-03

(b) RL_PO: Resident near the Landfill during the Active Institutional Control period

Exposure pathway	Age group	Mean µSv/y	Std. Deviation µSv/y	5% µSv/y	Median µSv/y	95% µSv/y	Deterministic µSv/y
Ingestion of fish	adult	1.7E-03	1.3E-02	5.7E-06	1.9E-04	5.4E-03	9.5E-04
Ingestion of river water	adult	4.8E-04	3.8E-04	6.6E-05	3.9E-04	1.2E-03	2.6E-04
Ingestion of vegetables	adult	2.2E-05	2.5E-05	1.9E-06	1.5E-05	6.6E-05	1.2E-05
All pathways	adult	2.2E-03	1.3E-02	1.1E-04	7.4E-04	6.3E-03	1.2E-03
Ingestion of fish	child	1.2E-03	4.4E-03	5.3E-06	1.9E-04	4.9E-03	7.5E-04
Ingestion of river water	child	1.8E-04	1.4E-04	2.4E-05	1.4E-04	4.4E-04	9.6E-05
Ingestion of vegetables	child	1.2E-05	1.3E-05	1.1E-06	7.8E-06	3.5E-05	6.3E-06
All pathways	child	1.4E-03	4.5E-03	4.9E-05	4.1E-04	5.1E-03	8.5E-04

(c) RL_IC: Resident near the Landfill during the Period after the End of Active Institutional Control

Exposure pathway	Age group	Mean µSv/y	Std. Deviation µSv/y	5% µSv/y	Median µSv/y	95% µSv/y	Deterministic µSv/y
Ingestion of fish	adult	5.0E-07	1.1E-05	<1.0E-10	<1.0E-10	4.3E-08	<1.0E-10
Ingestion of well water	adult	3.2E-03	8.0E-02	<1.0E-10	<1.0E-10	5.6E-04	<1.0E-10
Ingestion of vegetables	adult	2.0E-04	3.7E-03	<1.0E-10	<1.0E-10	4.7E-05	<1.0E-10
All pathways	adult	3.4E-03	8.3E-02	<1.0E-10	<1.0E-10	6.1E-04	<1.0E-10
Ingestion of fish	child	6.3E-07	1.4E-05	<1.0E-10	<1.0E-10	4.0E-08	<1.0E-10
Ingestion of well water	child	1.2E-03	3.0E-02	<1.0E-10	<1.0E-10	2.1E-04	<1.0E-10
Ingestion of vegetables	child	1.0E-04	1.7E-03	<1.0E-10	<1.0E-10	2.7E-05	<1.0E-10
All pathways	child	1.3E-03	3.1E-02	<1.0E-10	<1.0E-10	2.4E-04	<1.0E-10

(d) RO: Resident On the landfill during the Period after the End of Active Institutional Control

Exposure pathway	Age group	Mean µSv/y	Std. Deviation µSv/y	5% µSv/y	Median µSv/y	95% µSv/y	Deterministic µSv/y
External irradiation	adult	1.1E+01	4.3E+00	5.7E+00	1.0E+01	2.0E+01	1.1E+01
Inhalation	adult	1.3E-04	1.3E-04	2.5E-05	9.6E-05	3.6E-04	1.3E-04
Ingestion of seepage water	adult	3.5E+01	2.9E+01	4.2E+00	2.7E+01	9.4E+01	1.9E+01
Ingestion of vegetables	adult	1.2E+00	7.1E+00	3.6E-02	2.5E-01	3.5E+00	9.2E-01
All pathways	adult	4.7E+01	3.0E+01	1.4E+01	3.9E+01	1.1E+02	3.1E+01
External irradiation	child	1.3E+01	5.2E+00	6.8E+00	1.2E+01	2.4E+01	1.3E+01
Inhalation	child	2.9E-05	2.7E-05	5.4E-06	2.1E-05	7.8E-05	2.8E-05
Ingestion of seepage water	child	1.3E+01	1.1E+01	1.5E+00	1.0E+01	3.5E+01	7.1E+00
Ingestion of vegetables	child	4.5E-01	2.5E+00	1.8E-02	1.2E-01	1.2E+00	3.6E-01
Ingestion of soil	child	1.1E-01	4.1E-02	5.5E-02	9.9E-02	1.9E-01	1.0E-01
All pathways	child	2.7E+01	1.2E+01	1.2E+01	2.4E+01	5.1E+01	2.0E+01

(e) SE: Small Excavation on the landfill during the Period after the End of Active Institutional Control

Exposure pathway	Age group	Mean µSv/y	Std. Deviation µSv/y	5% µSv/y	Median µSv/y	95% µSv/y	Deterministic µSv/y
External irradiation	adult	8.3E-02	3.8E-02	3.4E-02	7.4E-02	1.6E-01	8.3E-02
Inhalation	adult	4.0E-05	2.6E-05	1.2E-05	3.3E-05	9.3E-05	4.1E-05
All pathways	adult	8.3E-02	3.8E-02	3.4E-02	7.4E-02	1.6E-01	8.3E-02

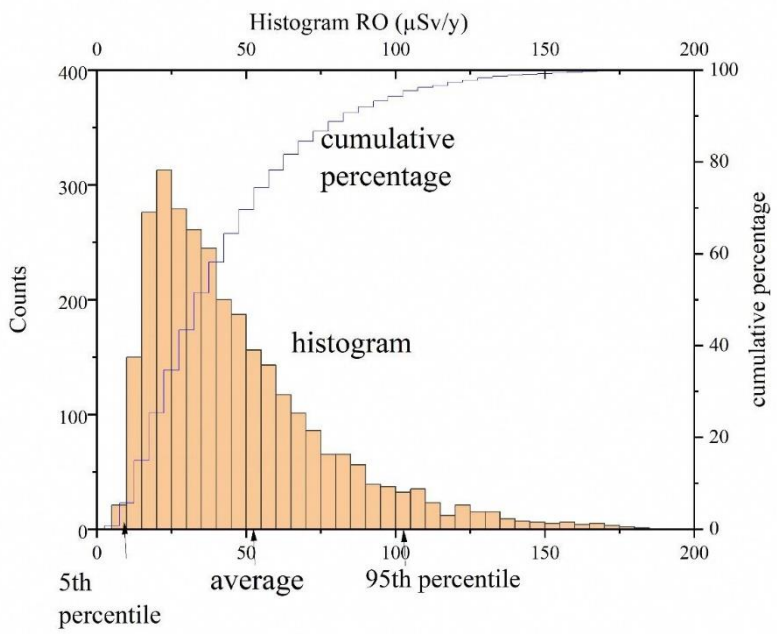

Figure 32. Histogram of individual dose in RO scenario when a combination of the parameters was varied

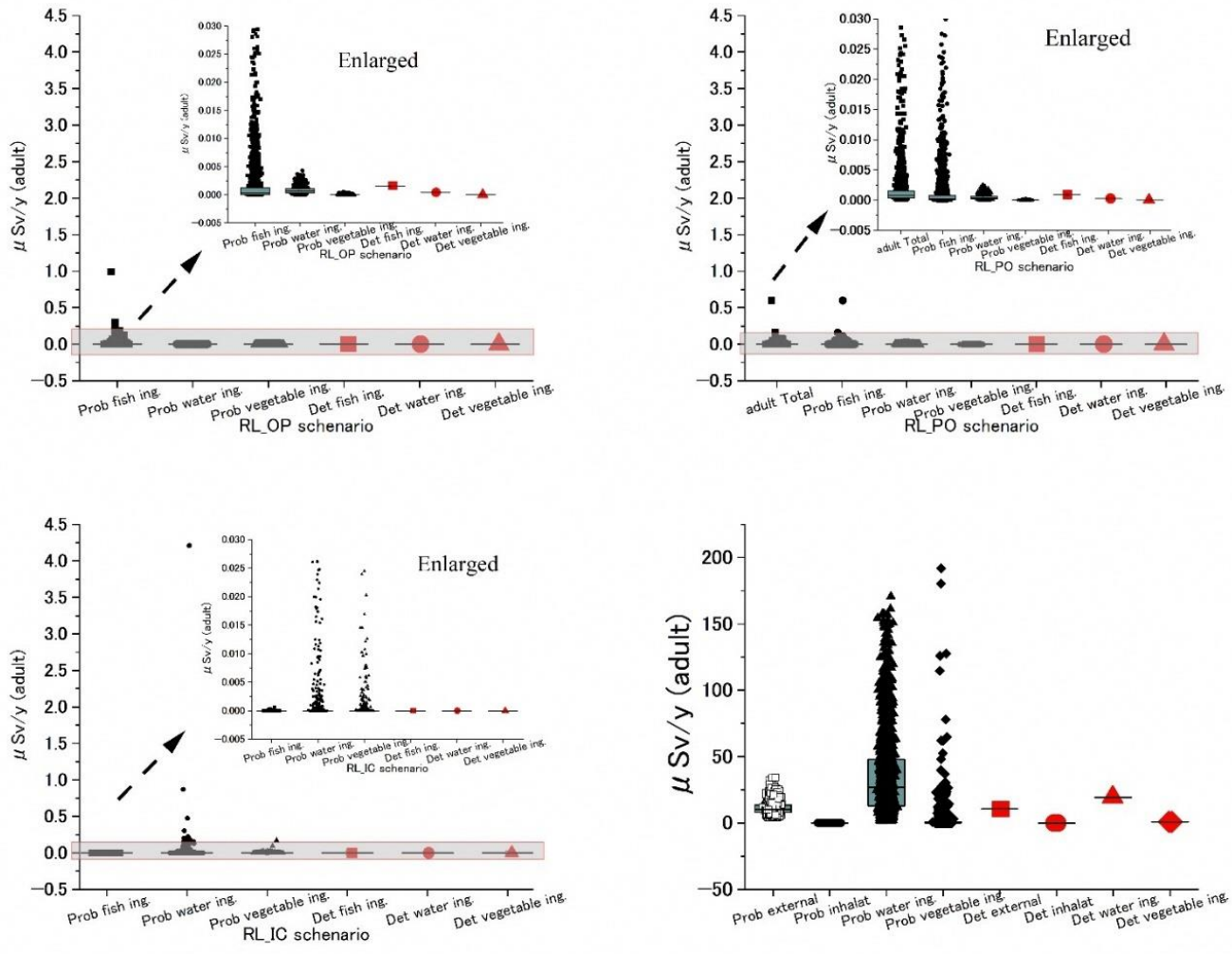

Figure 33. Probabilistic and deterministic estimate of the dose

The dots in the graph show the doses given by each run, though the runs giving similar results are overlapped in the Figure. The box in the graph shows the 25th percentile and 75th percentile values of the dose estimate in the runs.

5.6.2.3. Sensitivity analysis

The results of the probabilistic simulations were used for performing parameter sensitivity analyses. The parameter sensitivity analysis allows apportioning of the relative effect, of the parameters on the uncertainty of the simulation endpoints.

The effect of the model parameters on a simulation endpoint (for example the total annual dose) can be positive (i.e., when a model parameter increases or decreases, the dose also increases or decreases, respectively) or negative (i.e., when the parameter increases the dose decreases and when the parameter decreases the dose increases). To illustrate this, Standardized Rank Regression Coefficients (SRRC) were calculated. The SRRCs are a measure of the effect of varying each parameter on the value of a model output. The SRRC is obtained by fitting the model predictions for the output to a linear first order polynomial dependency with the studied input parameters (Saltelli et al. 2004)[8].

The SRRCs can be presented as tornado plots, such as those in Figure 34, showing the parameters with the highest absolute SRRCs values for the RO scenario.

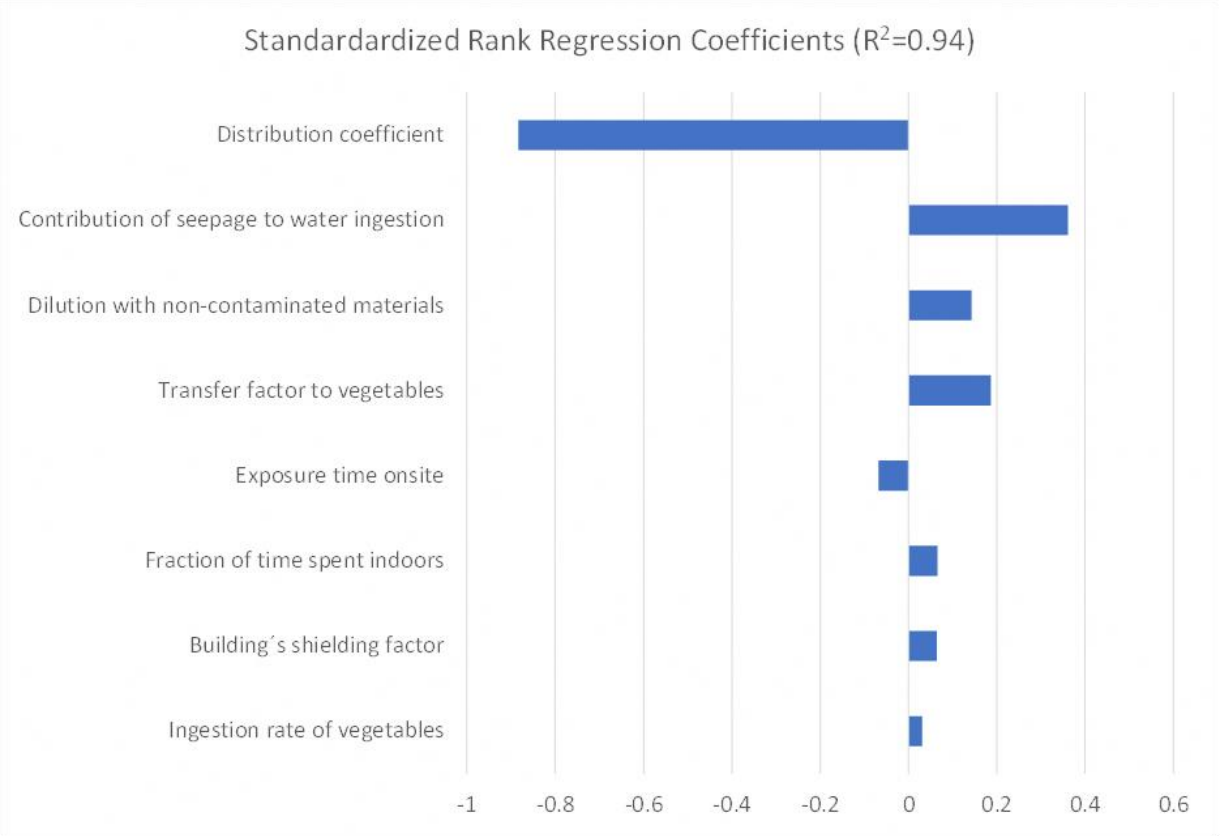

Figure 34. Importance of the parameters to the final dose estimate

5.6.2.4. Analysis of compliance with the radiological criteria

For the high probability scenarios (RL-OP, RL-PO, RL-IC and SE), the results of the deterministic and probabilistic simulations (the mean and even the 95th percentile) are well below the applicable regulatory criterion (10 μSv/year). This is true even if the concentrations in the waste are increased from 1 Bq/g (estimated value for Landfill B) to 8 Bq/g (current landfill standard).

For the low probability scenario (RO), the results of the deterministic and probabilistic simulations (the mean and even the 95th percentile) are also well below the applicable regulatory criterion (1 mSv/year). This is also true even if the concentrations in the waste are increased from 1 Bq/g (estimated value for Landfill B) to 8 Bq/g (current landfill standard).

5.6.3. Conclusions

A safety assessment was conducted for a landfill site containing a proportion of Radiocaesium-contaminated incineration ash using a safety assessment tool provided by the IAEA with modifications to reflect the actual situation in Fukushima Prefecture. The results of the safety assessment using this modified tool for landfill site B, taking account of the amount of ash disposed of in the landfill, indicate that the additional exposure dose for residents living near the facilities in the future is very low for the scenarios considered, the models developed, and the parameters used. Furthermore, even for the unlikely scenario of people living on the landfill site and drinking landfill water (leachate) more than 30 years after the disposal facilities are closed, the estimated dose was found to be less than 1 mSv/y. In the future, the scope of the safety assessment should be expanded to include additional landfill sites in Fukushima Prefecture. If necessary, the assessment tool should be modified according to each site and scenario, more detailed dynamic simulations of radiocaesium flow should be performed, and observations should be continued to confirm that the behavior of radiocaesium in the landfill is consistent with the simulation results.

5.7. Landfill site management after the completion of landfill of waste

In order to consider future maintenance and management standards, including monitoring of landfill sites where waste containing radioactive caesium has been landfilled in the Fukushima Prefecture, the IAEA shared information on cases of radioactive waste being landfilled at industrial waste sites overseas. We compared the monitoring items and frequency for the overseas landfill sites with the monitoring standards imposed on landfill sites for waste containing radioactive caesium in Japan.

5.7.1. Implementation of monitoring plan

Landfill disposal locations in Japan have been managed under the Waste Disposal and Public Cleansing Law (hereinafter referred to as “Waste Disposal Law”), in addition to related laws and regulations. Those laws and regulations relate to non-radioactive materials and so were based on the assumption that radioactive materials would not be present in the waste. Additional standards by national government were imposed for the management of waste containing radioactive materials under the Act on Special Measures Concerning Handling of Radioactive Pollution after the Fukushima accident. These laws mostly stipulate matters related to the management of waste containing radiocaesium during operational period, and there is no description regarding the confirmation of radioactive materials during the post operational period and the post Institutional Control period. Therefore, in order to examine the method of management regarding disposal locations by the time of decommissioning and the method of confirmation regarding radiocaesium at the time of decommissioning, information was provided by the IAEA on examples of landfill for radiocaesium in foreign industrial waste disposal locations, which will be referenced in order to investigate to which extent experience in other countries could be applied to waste disposal in Japan.

5.7.2. Results

Guidelines provided by the Ministry of the Environment include additional standards for the management and monitoring of waste containing radiocaesium after landfill under the Act on Special Measures Concerning Handling of Radioactive Pollution, as shown in the table below. However, there are no national decommissioning standards for radiocaesium concentrations (as of December, 2022), although there are national maintenance management standards at the time of landfill and by the time of decommissioning (when landfill is completed), as shown in the table 38 below.

Table 38. Additional criteria for landfill maintenance and management according to waste-related guidelines

	Items	Waste Disposal Law	Additional Standards
Maintenance Management Standards	Groundwater Measurement	Inspection items (such as groundwater, etc.) and dioxins should be measured before starting landfill and at least once a year during landfill. The rate of electrical conductivity, or chloride ion should be measured before starting landfill and at least once a month during landfill.	Radiocaesium concentrations should be measured before starting landfill and at least once a month during landfill.
	Discharged Water Measurement	Items included in the discharge standards and dioxins should be measured at least once a year. pH, BOD, COD, SS and T-N should be measured at least once a month.	Radiocaesium concentrations should be measured at least once a month.
	Spatial Dose Rate Measurement	—	Radiation doses at the boundary of the landfill site should be measured at least once every 7 days.
	Record	The type and amount of landfill materials, the content of inspections under the maintenance management, and details of tests and implementation should be recorded. (If municipal waste containing asbestos is reclaimed, drawings of the landfill locations should be recorded as well.)	The type and amount of landfill materials, the date of the landfill disposal, the content of inspections under the maintenance management, details of tests and implementation, and drawings of landfill locations should be recorded.
	Record Keeping	Keep until decommissioning.	Keep until decommissioning.

On the other hand, at foreign industrial waste disposal locations where waste containing radiocaesium is reclaimed, safety cases (safety management standards) for radioactive waste have been developed and managed in addition to the original method of disposal location management.

One example of such disposal location is the ENRMF (East Northants Resource Management Facility) operated by Augean PLC. This disposal location is subject to standards for approval of disposal locations concerning low level polluted waste known as GRA. In order to meet those standards, the ENRMF accepts radioactive waste under specific methods and standards for management in addition to the original standards for management. These standards are not uniform standards for any and all cases, but detailed standards which are tailored to each disposal location, taking into consideration the location, structure, landfill methods, and waste which has been reclaimed in the past. In particular, a detailed monitoring program has been established for safety, and the measurement locations and frequency of ambient dose rates, gases, leachate, dust concentrations, surrounding rivers, and observation pits are described in the ESCs. The measurement frequency for each item is defined as follows: air dose rates are measured constantly,

the volume of gases generated, leachate, dust concentration and water from observation wells are measured once a month, and water from the surrounding rivers is measured once a year.

Figure 35. ENRMF (East Northants Resource Management Facility)

Waste to managed in those foreign disposal facilities is generally contained in drums or double-packed, since the waste is generated from experimental facilities and the vicinity of nuclear power plants. Waste containing radioactive caesium generated in Fukushima Prefecture is not bagged and therefore differs from these treatment. With this in mind, while the guidelines stipulate that landfill methods that prevent water intrusion should be applied, water would likely eventually intrude when taking caesium half-life into account. This implies that appropriate monitoring and countermeasures be anticipated.

5.7.3. Conclusions

The IAEA shared examples of monitoring and management methods of radioactive waste after disposal in landfill facilities in different countries in the world. In foreign cases, the same monitoring approaches as those stipulated in the Waste Disposal Law in Japan, such as peripheral groundwater and discharged water, are implemented. Therefore, the monitoring standards of legislation in Japan were confirmed to be adequate. On the other hand, in foreign cases, the monitoring frequency and the method of management up to decommissioning were determined prior to the acceptance of radioactive waste in the facility, taking into account the structure of the individual disposal locations and its past management, as well as its future handling. In light of this, in the case of the Fukushima Prefecture, it is considered necessary to consider the method of handling and monitoring frequency up to decommissioning for each characteristic of the disposal facilities.

5.8. Conclusions

Fukushima Prefecture, with advice from the IAEA, has conducted studies and tests on waste incineration, especially on radioactive caesium in incineration ash, and found (1) that it is difficult to control the distribution of radioactive caesium in bottom ash/fly ash during waste incineration, (2) that radioactive caesium in fly ash emitted from municipal waste incineration facilities in Fukushima Prefecture is soluble in water, and (3) that the elution of radiocaesium from fly ash

can be suppressed by adding zeolite and other materials, which demonstrates satisfactory results in actual waste incineration facilities.

The study was also conducted on landfill disposal of waste, and showed (1) that when incineration fly ash is landfilled while in contact with water, radiocaesium leaches out, but the concentration is sufficiently low compared to the standard concentration of radiocaesium in public waters, (2) that there is no seasonal regularity in the leached concentration, and (3) that there is a positive correlation between radiocaesium concentration and chloride ion concentration.

The IAEA provided us with a safety assessment tool for landfill disposal, the scenarios in the assessment tool were modified to suit the situation in Fukushima Prefecture, and a safety assessment was conducted by using actual data from landfill sites in the prefecture, which clarified that the current landfill standards are sufficiently on the safe side.

In addition, the monitoring items and frequency related to the additional standards for maintenance and management at landfill sites, which are indicated by the Ministry of the Environment of Japan, it was confirmed that it is necessary to consider the monitoring items and frequency according to the disposal site in advance for the abolition of landfill disposal sites in the future by comparing with landfill sites overseas where radioactive waste are buried.

References

1) IAEA (2012). The Safety Case and Safety Assessment for the Disposal of Radioactive Waste. IAEA Specific Safety Guide SGG-23, Vienna 2012.
2) IAEA (2014). Radiation Protection and Safety of Radiation Sources: International Basic Safety Standards, General Safety Requirements Part 3, GSR Part 3, Vienna, Austria
3) IAEA (2005). Derivation of activity concentration values for exclusion, exemption and clearance. IAEA Safety Reports Series No 44. International Atomic Energy Agency, Vienna, Austria
4) IAEA (2021). Derivation of specific clearance levels in materials being suitable for recycling, reuse, or for disposal in landfills. IAEA Safety Report Series, (IN PRESS)
5) IAEA (2003a) Evaluating the reliability of predictions made using environmental transfer models, Safety Series No. 100, IAEA, Vienna (1989)
6) IAEA (2003b). Derivation of activity limits for the disposal of radioactive waste in near surface disposal facilities. TECDOC-1380. International Atomic Energy Agency, Vienna, Austria
7) Vose, D. (1996). Quantitative Risk Analysis – A guide to Monte Carlo Simulation Modelling, John Wiley and Sons, New York
8) Saltelli, A, Tarantola, E, Campolongo, F and Ratto, M. (2004). Sensitivity analysis in practice – A guide to assessing scientific models. John Wiley & Sons Ltd., Chichester

Report summary

Except for FIP4, this report covers activities from FY2013, focusing on activities from FY2018 and FY2019. Since FIP4 was completed in FY2015, we report on the activities from FY2013 to FY2015 with some wordings revised and update added since the theme ended in FY2015. The reports on each theme are summarized as follows.

FIP1: Survey, and evaluation of the effect of radiocaesium dynamics in the aquatic systems

Monitoring of suspended and dissolved radiocaesium concentrations in river water in Fukushima Prefecture were carried out. The results showed that the trends to decrease with time was maintained regardless of the forms. Simulations of radiocaesium concentrations in river water during base and high water flow were carried out and generally reproduced the measured values.

FIP2: Survey of radionuclide movement with wildlife

Comparisons of the activity concentration s of caesium-137 in the muscle tissues of wild boars and Asian black bears revealed higher activity concentration s in wild boars, while comparisons between copper pheasant and green pheasants revealed higher levels in copper pheasant, revealing that trends differed depending on the species.

The activity concentration of caesium-137 in the muscle tissues of wild boars was confirmed to be strongly affected by diet. As a result of confirming the seasonal change of caesium-137 activity concentration s in the muscles of wild boar and Asian black bear, even in recent years, individuals with high activity concentration s that exceeded 10 times the standard limit of radioactive caesium activity concentration in general foods were captured. The long-term fluctuation of caesium-137 activity concentration in the muscles of wild boar and Asian black bear showed a decrease over time during the entire period, both the low activity concentration period and the high activity concentration period. The model now needs to be reconsidered to provide a better estimate of the long-term fluctuations of radio caesium in the animals, particularly during the high activity concentration period.

Compared to wild boars living outside the areas under evacuation orders, those living in the areas under evacuation orders tended to have wider home ranges that tended to shift to farmlands. In addition, wild boars in Fukushima Prefecture are genetically divided into two strain groups, suggesting that their movement may be restricted from east to west with the Abukuma River and around as the boundary.

FIP3: Sustainable countermeasures for radioactive materials in terrestrial and aquatic areas

In this project, decontamination demonstration tests were carried out on riverbanks to investigate the effectiveness of decontamination methods based on the spatial distribution of radiocaesium. Continuous measurements of gamma dose rates and activity levels in sediments were conducted on the riverbanks after decontamination; the results showed that the air dose rate continuously decreased and the decontamination effect persisted. In addition, investigations in river parks and

other areas before and after the floods caused by the passage of Typhoon Hagibis in 2019 showed that air dose rates in general did not increase and re-contamination due to the flooding was not detected. The results of these studies were provided to the relevant sections in Fukushima Prefecture, and the methods for the decontamination of riverbeds were subsequently utilised as river maintenance measures.

FIP4: Development of environmental mapping technology using GPS walking surveys

A GPS-linked dose rate measurement device, KURAMA from Kyoto University, was used as a basis and the configuration was made more suitable for walking surveys. Then, the GIS data processing system was prepared on the assumption that it would be linked with the analysis of the obtained data and the monitoring of aircraft surveys by UAV. In addition, it has become possible to measure the dose rate in a walking survey by collecting data necessary for measurement such as directional characteristics and calibration constants. We conducted walking surveys at several points and confirmed that it was possible to measure dose rates and create contour maps using a GIS data processing system. A manual was prepared so that even inexperienced people can use the system. Since fiscal 2016, it has been used for conducting walking surveys and has been rented out at the request of municipalities. In recent years, walking surveys have been utilized in the public projects for monitoring of the air dose rates (e.g., Satoyama Restration Model Project).

FIP5: Study of proper treatment of waste containing radioactive material

Surveys and tests were conducted at landfill sites and waste incinerators to examine treatment, disposal and management methods for waste containing radiocaesium generated in the prefecture. A survey of leachate at the landfill site confirmed that when the incinerated fly ash was buried in contact with rainwater, radiocaesium was eluted from the incinerated fly ash and was detected in the leachate. In order to suppress the elution of radiocaesium from this incinerated fly ash, various incineration ash elution tests and incineration ash sparingly soluble tests were conducted in laboratories and facilities. As a result, it was found that the addition of zeolite into the incineration ash has a remarkable effect of suppressing the elution of radiocaesium However, in the application to the implementation facility, it is added according to the target incineration facility or landfill site, and so it is considered necessary to further study the method and the amount of zeolite added.

In addition, the safety assessment tool provided by the IAEA was modified to suit the conditions in Fukushima Prefecture, and a safety assessment of the actual deposit location in Fukushima Prefecture was conducted. As a result of the safety assessment, it was confirmed that currently landfilling of the landfill site B is a fairly safe value, and future confirmations will be conducted so that this assessment tool can be applied to other disposal locations in the future. Also, as a reference for the future management of disposal locations in Fukushima Prefecture, information was provided on the management of disposal locations overseas where radioactive waste will be buried. In overseas cases, the waste conditions and dose control methods were defined in advance, and not all disposal locations could be used as a reference. However, information from these overseas disposal locations that can be utilized in the management of individual disposal locations

in Fukushima Prefecture was obtained, including methods of management depending on the structure of disposal locations and the frequency of monitoring after the end of landfill operations.